THE MATHEMATICAL MODELLING AND SIMULATION OF A MONOETHANOLAMINE-CARBON DIOXIDE PLANT

by

Richard Joseph Burkett B.Sc.(Eng),ACGI

A thesis submitted for the degree of Doctor of Philosophy of the University of London and for the Diploma of Imperial College.

Department of Chemical Engineering
and Chemical Technology
Imperial College of Science and Technology
London, England.

November, 1977

BIBL.
LONDIN.
UNIV.

ABSTRACT

Comprehensive and simple models are derived to represent the steady state and dynamics of a monoethanolamine plant which separates carbon dioxide from nitrogen. The comprehensive models are generally applicable but the simpler ones are particular to the pilot plant at Imperial College.

Various expressions are examined for representing the absorption rate which is assisted by a second order chemical reaction. For the conditions in the pilot plant it is shown that the absorption rate is approximately pseudo-first order and using this assumption a simple steady state model is developed together with a technique to estimate the parameters from plant measurements. A comprehensive dynamic model capable of accepting any absorption rate expression is presented. The column dynamics are dominated by the liquid phase and the resulting equations are solved by the method of characteristics. The gas phase hold up is negligible and a time instantaneous solution incorporating dispersion is used. Simplifications to the model are described and the model is compared with other representations. The model is used to investigate the dynamics of the column and the problem of controlling the column against inlet composition disturbances.

A steady state model for the desorption column is proposed and shown to give a feasible behaviour. A general dynamic model incorporating the reboiler and condenser is also described together with methods of simplification.

Model responses are investigated and compared with those of a simpler model. Due to the rapid desorption near the top of the column the model equations are stiff and special techniques for the rapid integration of such systems are evaluated. A new method suitable for on-line use is proposed.

The problem of selecting the best set of measurements to estimate model parameters when using a Kalman filter is considered in general terms. A novel solution is proposed and shown to improve the estimation of parameters in the desorption column model.

TO MY PARENTS

ACKNOWLEDGEMENTS

I would like to thank Professor Sargent for his encouragement and guidance during the research and preparation of this work. I wish also to thank my colleagues in the Department for many useful discussions. I gratefully acknowledge the financial support of an S.R.C. Grant during my research. I am very grateful for the continual support and encouragement which I received from my parents throughout the course of my studies. Finally, I thank my wife, Marilyn, for her love and patience during the preparation of this work.

CONTENTS

		Page
CHAPTER 1	INTRODUCTION	
1.1.	Introduction	8
1.2.	Description of the MEA - carbon dioxide absorption-desorption system	10
1.3.	Purpose of this study	13
CHAPTER 2	MODELLING OF THE ABSORPTION COLUMN	
2.1.	Introduction and literature survey	15
2.2.	Representation of the absorption rate	22
2.3.	Equations for the liquid phase hold up	28
2.4.	Statement of model equations	32
2.5.	Solution of model equations	34
2.6.	Steady state behaviour	44
2.7.	Dynamic behaviour	73
2.8.	Model development and simplification	82
2.9.	Conclusions	95
2.10.	Nomenclature for Chapter 2	99
CHAPTER 3	MODELLING OF THE DESORPTION COLUMN	
3.1.	Introduction and literature survey	102
3.2.	General approach	106
3.3.	Solution for the steady state	111
3.4.	Equations for the comprehensive dynamic model	124
3.5.	Responses of the full model	141
3.6.	Statement of simple dynamic model	145
3.7.	Comparison of the comprehensive and simple models	149
3.8.	Conclusions	158
3.9.	Nomenclature for Chapter 3	159

		Page
CHAPTER 4	NUMERICAL INTEGRATION METHODS	
4.1.	Introduction and literature survey.	164
4.2.	Integration methods	167
4.3.	Definition of sample problem	179
4.4.	Performance of methods: results and discussion	179
4.5.	Conclusions	191
4.6.	Nomenclature for Chapter 4	193
CHAPTER 5	PARAMETER ESTIMATION	
5.1.	Introduction and literature survey	194
5.2.	Statement of equations for extended and iterated filters	197
5.3.	Concept of an optimal measurement set	199
5.4.	Application to the estimation of the parameters in the desorption column model	206
5.5.	Conclusions	219
5.6.	Nomenclature for Chapter 5	231
CHAPTER 6	CONCLUSIONS	232
	References	235
Appendix 1	Parameters for the absorption column model	245
Appendix 2	Computational procedures for the absorption column model	251
Appendix 3	Procedure for on-line estimation of the absorption rate parameters	264
Appendix 4	Parameters for the desorption column model	271

CHAPTER ONE

INTRODUCTION

The chemical industry has always been confronted with the problem of controlling physical and chemical processes. Good control has always been desirable for a variety of reasons but over the past decade a number of factors have greatly accentuated this need. With the increasing cost of fuel and feedstocks it is becoming more important to use the minimum of energy and to meet product specifications as closely as possible. At the same time, the duty of control systems is becoming more difficult as modern plants increase in complexity and interaction.

There are indications that the control and operation of processes can be significantly improved by replacing classical control systems with modern ones which could involve using a computer. Advanced control and computer techniques have been used successfully in the aerospace industry and their use in the chemical process industries is now increasing. However, over the last decade, far more techniques have appeared than have been tested and examined in detail on actual chemical plant. The pilot plants at Imperial College have, therefore, been constructed to provide an opportunity to study the dynamics of some typical unit operations and to evaluate new concepts and their practical implementation.

Many of the new techniques arise from the theory for linear systems which has advanced rapidly with many elegant

solutions to simple problems, for example the optimal feedback control of a linear system. A useful feature is that the solutions are often found in a closed form which is suitable for use in a computer. Other techniques, not all of which necessitate the use of a computer, include non-interacting[75], modal[74], feed forward[57] and adaptive control[28] to mention a few. Linear control system theory represents an advance because it accounts for the multi-variable nature of the process and can, as a consequence, successfully counteract process and control loop interaction, a common example of which is the control of both ends of a distillation column.

The theory for non-linear systems is, not surprisingly, less well developed, although in the area of optimal control some interesting results have been found which suggest new approaches to the operation and control of processes. Pollard and Sargent[79] have shown that the optimal control policy for the start up and shut down of a distillation column can show appreciable economic savings over a more traditional approach. Unfortunately, these control policies cannot always be implemented in an on-line computer without simplifications which sacrifice some of the advantages gained.

A vitally important role in modern control theory is played by mathematical models which represent the dynamic and steady state properties of the plant. The model state vector summarises all the information about the plant and consquently the size of it, the choice of elements and their relationship ultimately determine the control or results

obtained from the model. The complexity and the number of parameters have to be balanced against the required accuracy of the model and the ease of using it to fit plant data and make predictions. How this balance is reached is dependent upon the situation and the purpose of the model. For general simulation off-line relatively large and complex models may be used, but simplicity is very important when a model is used on-line for control.

The model may take the form of a black box type with an arbitrarily defined algebraic structure, or a set of differential equations derived from physical reasoning. This latter form may often be more complex and less suitable for direct use in a control system but is far more convenient for simulating the physical processes involved and leading to an understanding of them. This is the technique adopted in this work.

1.2. Description of the Carbon Dioxide Absorption Plant

The line diagram of the pilot plant is shown in Fig.1.1. Carbon dioxide is separated from nitrogen by contact with a solution of monoethanolamine (MEA) in the packed absorption column. The absorption of the carbon dioxide is assisted by a chemical reaction with the MEA and the column is operated under pressure. The MEA rich in carbon dioxide, obtained from the base of the absorption column, is heated and passed to the desorption column where the carbon dioxide is stripped from the solution by steam at atmospheric pressure. The desorption, or stripping, column consists of twenty one sieve plates and a natural circulation reboiler to supply the stripping steam. The lean MEA from the bottom of the

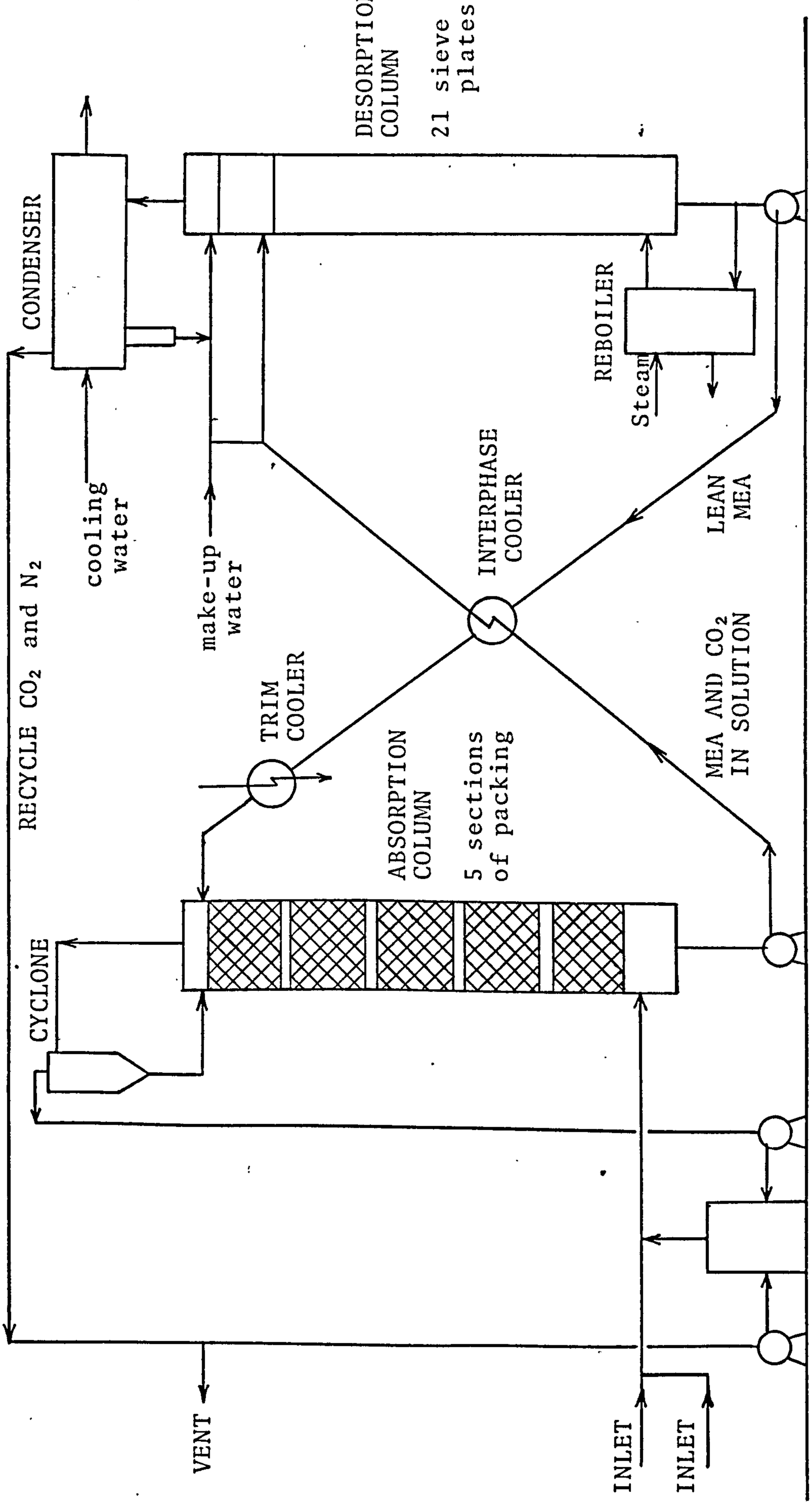


FIG. 1.1. Line Diagram of MEA - Carbon Dioxide Plant

stripping column exchanges heat with the carbon dioxide rich MEA and is water cooled before entering the absorption column to complete the circulation loop. The carbon dioxide stripped from the MEA is normally sent to further gas processing equipment but on this particular plant is recycled to form part of the feed to the absorption column, therefore making it a closed system.

The pilot plant is linked to an on-line computing system which is used for logging and control purposes; a description of the system is given elsewhere[12]. The computer can accept programmes to run in the background, so that on-line simulation, estimation and optimisation can be performed. In addition, the standard control package can be replaced to allow the testing of new control schemes and techniques.

Industrial applications of the MEA process include the removal of carbon dioxide and hydrogen sulphide from fuel gases, recovery and purification in carbon dioxide production, and the cleaning of synthesis gas for ammonia production[19,47]. The synthesis gas is often made from steam reforming followed by a shift reaction and the amount of carbon dioxide to be removed varies according to the carbon/hydrogen ratio of the feedstock. The typical problem for this plant is therefore to control the concentration of carbon dioxide in the gas leaving the absorption column in face of disturbances in the inlet concentration or flow rate of carbon dioxide. The cost of operation of this gas sweetening unit is dominated by the cost of the stripping steam employed, and there is, therefore, the problem of how to control the unit to minimise energy consumption.

1.3. Purpose of this Study

The purpose of this work is to produce suitable models for simulating the pilot plant and to use them in identifying the general behaviour of the columns. Comprehensive models for the dynamic and steady states of both columns are derived and then simplified whilst retaining the significant features of their behaviour. Simplifications are made by physical assumptions, the use of mathematical approximations and in the particular case of the absorption column different modelling techniques are examined. The mathematical techniques used for the solution of the models are described and are adapted or developed for the particular case. In addition the parameters associated with the significant effects are identified together with the plant measurements which determine their magnitude. The work on the absorption column is described in Chapter 2 and that on the desorption column in Chapter 3.

An ultimate aim is to use models in the on-line computer for either estimation or control purposes and, therefore, integration techniques which use a minimum of computation time are clearly of importance. Furthermore, these techniques have to be robust and very economic in the use of storage. Some modern techniques are examined in Chapter 4 and a very simple technique suitable for on-line use is developed.

With the form of the models specified, the next problem is the estimation of their parameters. A Kalman filtering approach is envisaged and the particular problem of

selecting which measurements should be used to fit the desorption column model is considered in Chapter 5. The aim is to find a policy for the selection from a large number of measurements those which will give the best estimate of the model parameters.

This work should form the basis for future research work on the pilot plant by the provision of an understanding of the principal behaviour of the plant, suitable models and techniques for their efficient solution.

A literature survey is given in the introduction to each chapter and the mathematical notation employed is explained by a nomenclature at the end of each chapter.

CHAPTER TWO

ABSORPTION COLUMN

2.1. Introduction and Literature Survey

This Chapter considers the problem of constructing suitable steady state and dynamic models for the carbon dioxide absorption column. The aim is to look at various methods for simulating the column and finally to produce some relatively simple models which can be fitted easily from plant data.

Jaswon and Smith[40] were among the first to consider the problem of countercurrent unsteady state transfer of either mass or heat and derived the partial differential equations describing the phase compositions or temperatures. They assumed plug flow for each of the phases, a simple linear transport equation, and were able to solve the equations analytically for flow and composition disturbances. Since this initial theoretical work there have been a number of papers reporting experimental work, and in almost all cases a linear transport equation was used to enable analytic solution of the model equations.

Gray and Prados[36] investigated by frequency response techniques the dynamics of a column absorbing carbon dioxide into water when subjected to inlet gas composition disturbances. Assuming isothermal conditions and a linear equilibrium line they obtained analytic solutions for the plug flow, mixing cell and dispersion models, each of which gives a different representation of the mixing in the two

phases. A frequency response analysis showed that all the models could adequately predict the phase shift but that none of them could fit the attenuation over a large frequency range.

A more detailed study of absorber dynamics was made by Lees[55] who considered the absorption of hydrogen chloride and ammonia in water. Assuming isothermal conditions, a linear equilibrium line and using a plug flow model he obtained a matrix of transfer functions between the outlet and inlet compositions and flow rates. Experimental responses on both laboratory and plant columns to changes in inlet gas and liquid flow rates were fitted well by the model in terms of frequency responses. However, the more interesting response to a change in inlet gas concentration was not considered experimentally.

One of the first investigations to consider the role of the liquid phase reaction in the dynamics of a packed absorption column was made by Prados and Sakata[71] who analysed the absorption of carbon dioxide by a solution of sodium hydroxide. They represented the absorption rate as irreversible pseudo-first order where the absorption is proportional to the gas phase partial pressure, and consequently were able to find transfer functions between the outlet compositions and the gas inlet composition for each of the plug flow, mixing cell and dispersion models. They analysed the experimental data as before, in terms of phase shift and attenuation, and concluded that the mixing cell and dispersion models could both satisfactorily reproduce the data throughout the frequency range considered.

They found that the two models gave virtually identical predictions provided the relationship found by Kramers and Alberda[50] was satisfied, and that the measurements indicated a mixing cell size comparable to the packing size. In addition they found that although the plug flow model could satisfactorily predict the phase shift and attenuation for the liquid phase it could not predict the attenuation for the gas phase at high frequencies where mixing effects are of significance.

The papers reviewed so far show that the principal dynamics of an absorption column with linear transport equation can be reproduced by simple models which can be solved analytically. As a consequence of moving away from cases with a linear transport equation the models are likely to become more specialised and require greater insight into the underlying physical processes. As an example, Shulman, Mellish and Lyman[89] studied the absorption of ammonia into both sulphuric acid and water and then proposed a model with a novel liquid distribution system in order to explain the unusual behaviour of the overall gas phase mass transfer coefficient. Initially, with uncontaminated absorbent the mass transfer is high, but this decreases with time to a steady state value. The explanation is that initially all the liquid in the column is able to absorb, but as time progresses the relatively stagnant liquid becomes saturated and ineffective, and consequently the apparent transfer coefficient based upon the total area decreases. The absorption is gas phase controlled and the authors propose a number of cells in parallel to represent the liquid phase,

the liquid distribution to each being adjusted to reproduce the steady state exit concentrations. They proceed to show how the model explains the change in mass transfer coefficient during the start up period and how the mean absorption rate in the column can be increased by cyclic variation of the liquid flow rate.

In this chapter the previous work in the field of absorption is extended by considering the absorption of carbon dioxide by MEA where the absorption rate is non-linear and developing suitable techniques for the solution of the dynamic equations. The basic techniques developed can be applied generally to any system with a non-linear absorption expression, although obviously the final models proposed here are specific to the carbon dioxide MEA system and to the pilot plant in particular. In addition to the normal responses to change in inlet flow and compositions the response to a change in total pressure is also considered.

The modelling of a packed absorption column requires a representation of each phase in addition to the representation of the mass transfer process. There are two facets to this problem for each phase: the quantity within the column, how it is distributed and varies with the operating conditions, and secondly how the flow propagates through this hold up.

Shulman, Ulrich and Wells[88] investigated liquid hold up and interfacial area on different packing types and sizes. They identified the static hold up, which is the hold up of liquid at zero flow rate and consists of the liquid held in the interstices of the packing, and the operating hold up, which consists of the liquid film flowing over the packing.

Under normal operating conditions the static hold up is usually only a small portion of the total liquid hold up and is virtually stagnant in comparison with the operating hold up. The static hold up is dependent upon the size, type and the type of surface of the packing whereas the operating hold up depends upon the size and type of the packing and the liquid flow rate, and provided the column is below the loading point is independent of the gas rate. The gas phase hold up is easily calculated having taken into consideration the column pressure and the fraction of the total volume occupied by the packing and liquid.

The responses to a change in inlet liquid and gas flows have been investigated experimentally by Gilath[35] and compared with those of a theoretical model based upon the correlation of film thickness with liquid flow rate on an inclined surface. The column acts principally as a simple delay in the response of the outlet flow to a change in the inlet liquid flow, although responses to large positive and negative changes were found to be slightly assymetric. As may be expected the response of the outlet liquid flow to a change in the gas flow depends upon the sensitivity of the liquid hold up to the gas rate, and consequently upon the proximity to the loading point.

The distribution and mixing processes of the liquid flow have received considerable attention because of the relevance to interfacial area and mass transfer rates. Important aspects in column design are the radial distribution of the liquid flow, particularly the column length to establish a uniform distribution, the magnitude of the wall flow and

the significance of the axial dispersion. Porter and Templeman[68] drew attention to the significance of the wall flow particularly for small laboratory columns where it can become almost half the total flow. The evolution of the radial flow distribution has generally been studied in association with the diffusion equation, although Porter[65] introduced the rivulet flow model which treats the problem in a more fundamental manner. This model describes the flow as rivulets which break up and coalesce at random, and as a consequence of its fundamental nature is an attractive model to consider for the purpose of predicting liquid interfacial areas, the distribution of liquid residence times and mass transfer coefficients. However, it is too complex to be considered as the basis of a general dynamic model for predicting composition responses.

Porter and Jones[67] and Dutkai and Ruckenstein[27] have studied experimentally the flow distribution on various packings and their results show that pall rings, which are used in the pilot plant, offer the possibility of obtaining the most uniform flow distribution with a small wall flow. In absorption column and reactor studies the radial distribution and mixing effects have generally been assumed negligible; therefore with the knowledge of the comparatively good distribution given by pall rings this assumption is made in this work.

The uniformity of the gas phase flow has not been studied and is probably less important because the interfacial area between the two phases is determined essentially by the liquid flow. Furthermore, the gas phase

constitutes the major volume of the column and because it flows rapidly the distribution is likely to be close to uniform with little chance of the formation of stagnant regions.

The random flow of both phases over the packing and the composition gradients give an inherent mixing process in both the axial and radial directions, although the latter is assumed perfect. The two well known descriptions of the mixing process are the mixing cell model introduced by Kramers and Alberda[50] and the turbulent or dispersion model of Aris and Amundson[3]. The relation between the two descriptions is well known, and was used by Amundson[2] to transform partial differential equations to a set of ordinary differential equations. Aris and Amundson considered both models for describing axial dispersion in gas flow through a bed packed with spheres, and concluded that the Peclet number should approach a limiting value of 2 for high Reynolds numbers; this was verified experimentally by McHenry and Wilhelm[60]. For a column packed with raschig rings, this limiting value was again confirmed by De Maria and White[23], who investigated the effect of liquid flow rate on gas phase mixing. They showed that gas phase mixing increases with increasing liquid flow rate and decreasing packing size. The general trend of these results has been confirmed by Sater and Levenspiel[81] who present data on mixing for both phases. As may be expected by comparing the momentum of both phases, the interaction between the phases affects the gas phase considerably more than the liquid phase.

A modern approach to the problem of flow and mixing processes has been to envisage them as random, or stochastic processes; Schmalzer and Hoelscher[84] have considered the comparison of such models with experimental results. However, as with the rivulet flow model, this rather complex approach to the description of just the hold up and mixing could not feasibly form the basis of a general column model.

The literature associated with the absorption of carbon dioxide by MEA is reviewed in the next section together with a description of the absorption rate and equilibrium conditions.

2.2. Representation of the Absorption Rate

The rate of absorption of carbon dioxide by monoethanolamine (MEA) is increased by the chemical reaction between the carbon dioxide and the amine. The reaction mechanism has been studied by a number of investigators and references are given by Danckwerts[18]. The reactions, equilibria and the effects of arsenite as catalyst are discussed by Danckwerts and McNeil[20]. The most significant reaction is second order, forming the carbamate salt:

$$2HOC_2H_4NH_2 + CO_2 \rightleftharpoons HOC_2H_4NHCOO^- + HOC_2H_4NH_3^+ \qquad (2.1)$$

The reaction rate is defined by

$$r = k_c [CO_2][M'] \qquad (2.2)$$

where $[CO_2] = c$ = local concentration of carbon dioxide

$[M'] = c_o$ = local concentration of free amine

$= M_m - 2c$

and M_m is the molar concentration of MEA before absorption of carbon dioxide.

The quantity of carbon dioxide in solution is expressed as the carbonation ratio, defined by

$$\alpha = \frac{\text{total moles of carbon dioxide per unit volume}}{\text{total moles of amine per unit volume}}$$

$$= \frac{C}{M_m} \qquad (2.3)$$

It is clear that if (2.1) were the only reaction possible, the carbonation ratio could never exceed 0.5. However, a slower secondary reaction leading to the bicarbonate is also possible:-

$$HOC_2H_4NHCOO^- + H_2O \rightleftharpoons HOC_2H_4NH_2 + HCO_3^- \qquad (2.4)$$

For carbonation ratios approaching 0.5 equation (2.1) cannot be considered completely irreversible. However, the value of the equilibrium constant shows that the concentration of free carbon dioxide can be neglected for carbonation ratios up to about 0.47. The absorption equations are derived here with the assumption that (2.1) is irreversible, and the extension to include the effect of reversibility is given in Appendix 1.

Prediction of the local absorption rate with second order reaction has been considered using the film model[51] or the Higbie surface renewal model[10] to represent the absorption of carbon dioxide at the interface. The Higbie model offers a better representation of the experimental data, and further support for choice of this model is given by the known existence of interfacial turbulence accompanying the absorption[11]. The fundamental equations for the absorption rate cannot be solved analytically and so Brian, Hurley and Hasseltine[10] have solved the equations numerically. They

present the solution in terms of an enhancement factor ψ which is defined by

$$\psi = \frac{\text{rate of absorption with chemical reaction}}{\text{rate of physical absorption}} = \frac{R}{k_L c^*} \quad (2.5)$$

which is then correlated with the dimensionless groups

ψ_i = limiting value of ψ for instantaneous reaction

$$= 1 + \frac{c_0}{2c^*}\sqrt{\frac{D_M}{D_c}} \quad (2.6)$$

$$\text{and } \sqrt{M} = \frac{\sqrt{D_c k_c c_0}}{k_L} \equiv \frac{\text{reaction rate}}{\text{diffusion rate}} \quad (2.7)$$

The correlation proposed by Brian et al is

$$\psi = \frac{\sqrt{M(\psi_i-\psi)/(\psi_i-1)}}{\tanh\{\sqrt{M(\psi_i-\psi)/(\psi_i-1)}\}} \quad (2.8)$$

A similar function, but which is far more convenient to use because it is explicit has been proposed by Porter [65]:-

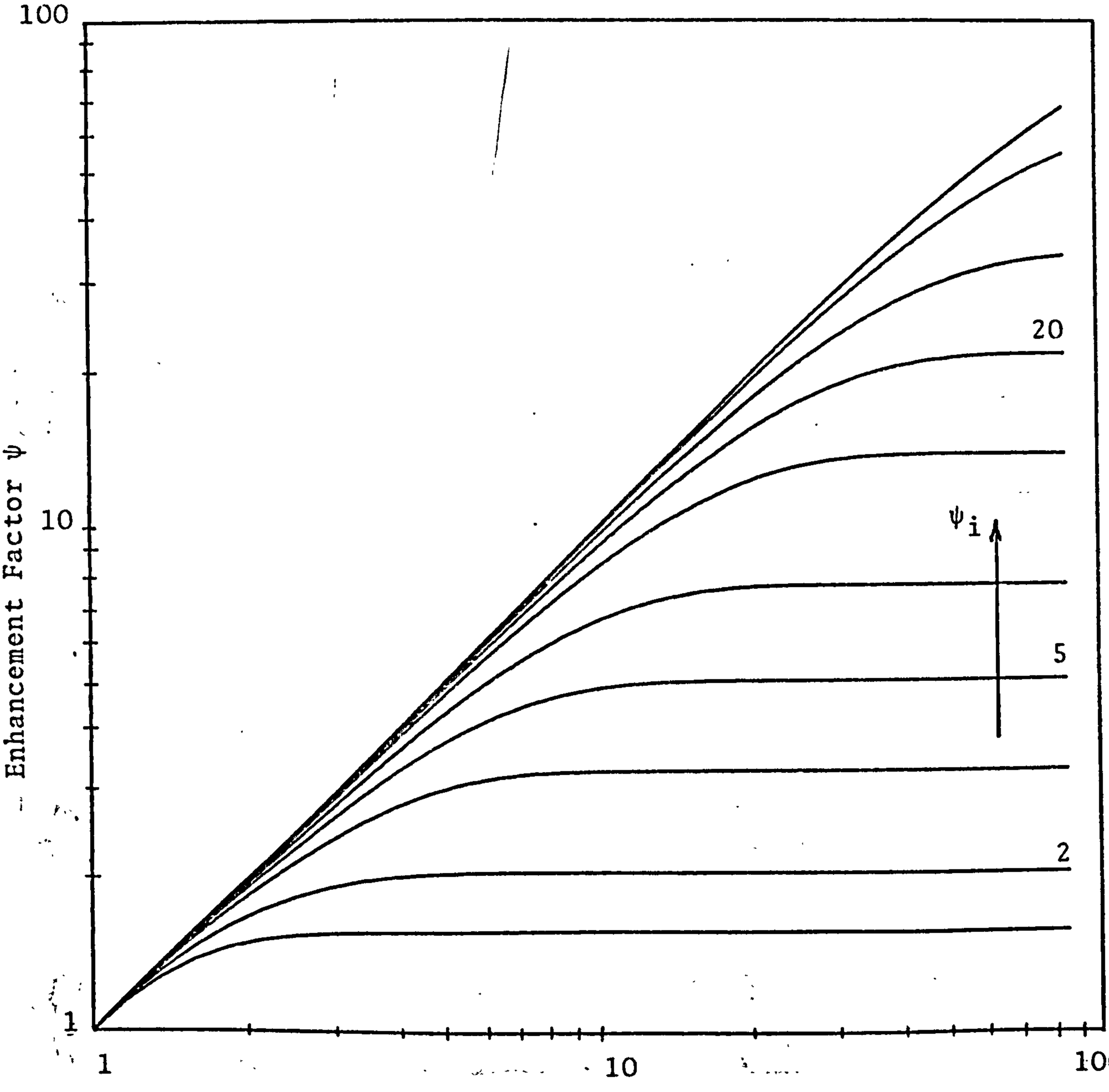
$$(\psi-1) = (\psi_i-1)\{1 - \exp[-\frac{\sqrt{M}-1}{(\psi_i-1)}]\} \quad (2.9)$$

Equation (2.9) agrees well with the function given by Brian et al and is shown in Fig. 2.1. Some important asymptotes can be recognised. If

$$\sqrt{M} \geq 10\psi_i \quad (2.10)$$

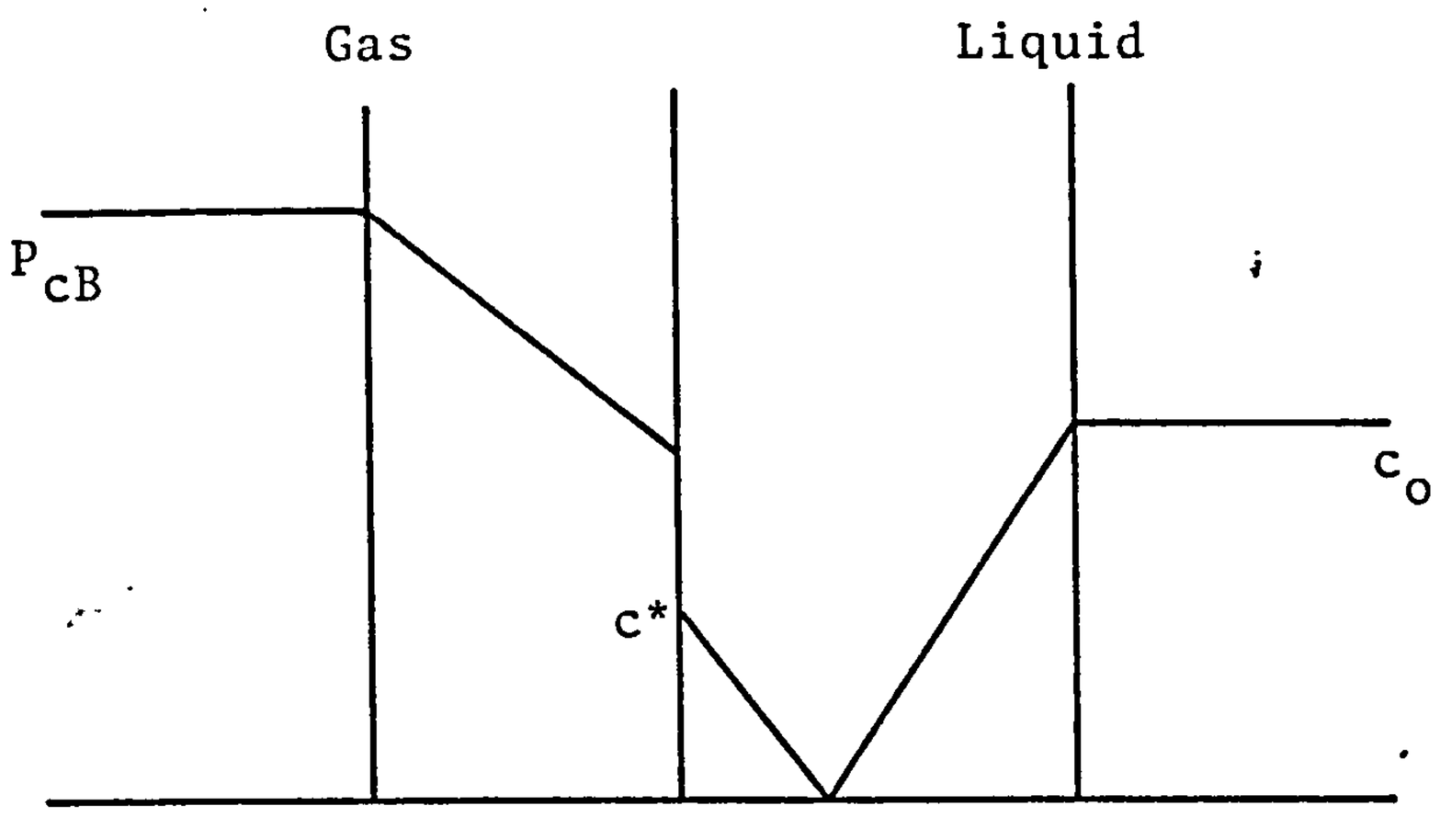
then the reaction is sufficiently fast for the absorption rate to be limited by the rate of diffusion of reactants to the reaction zone as shown in Fig. 2.2(a). The enhancement factor is then given by equation (2.6).

Another important condition exists when the reaction does not significantly reduce the concentration of free amine in the reaction zone as shown in Fig. 2.2(b). The reaction is then pseudo-first order and this condition

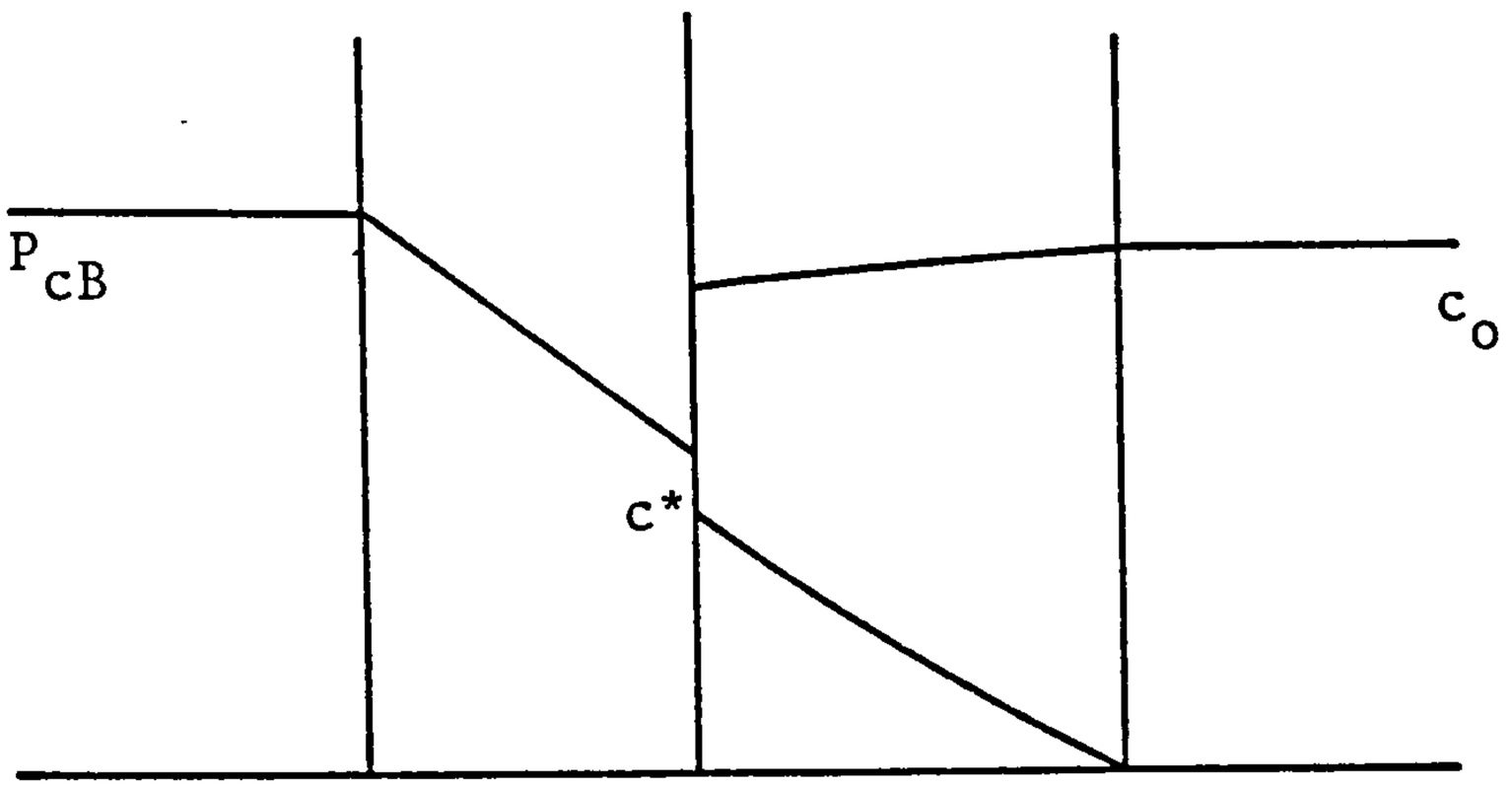


$$\sqrt{M} = \frac{\sqrt{D_c k_c c_0}}{k_L}$$

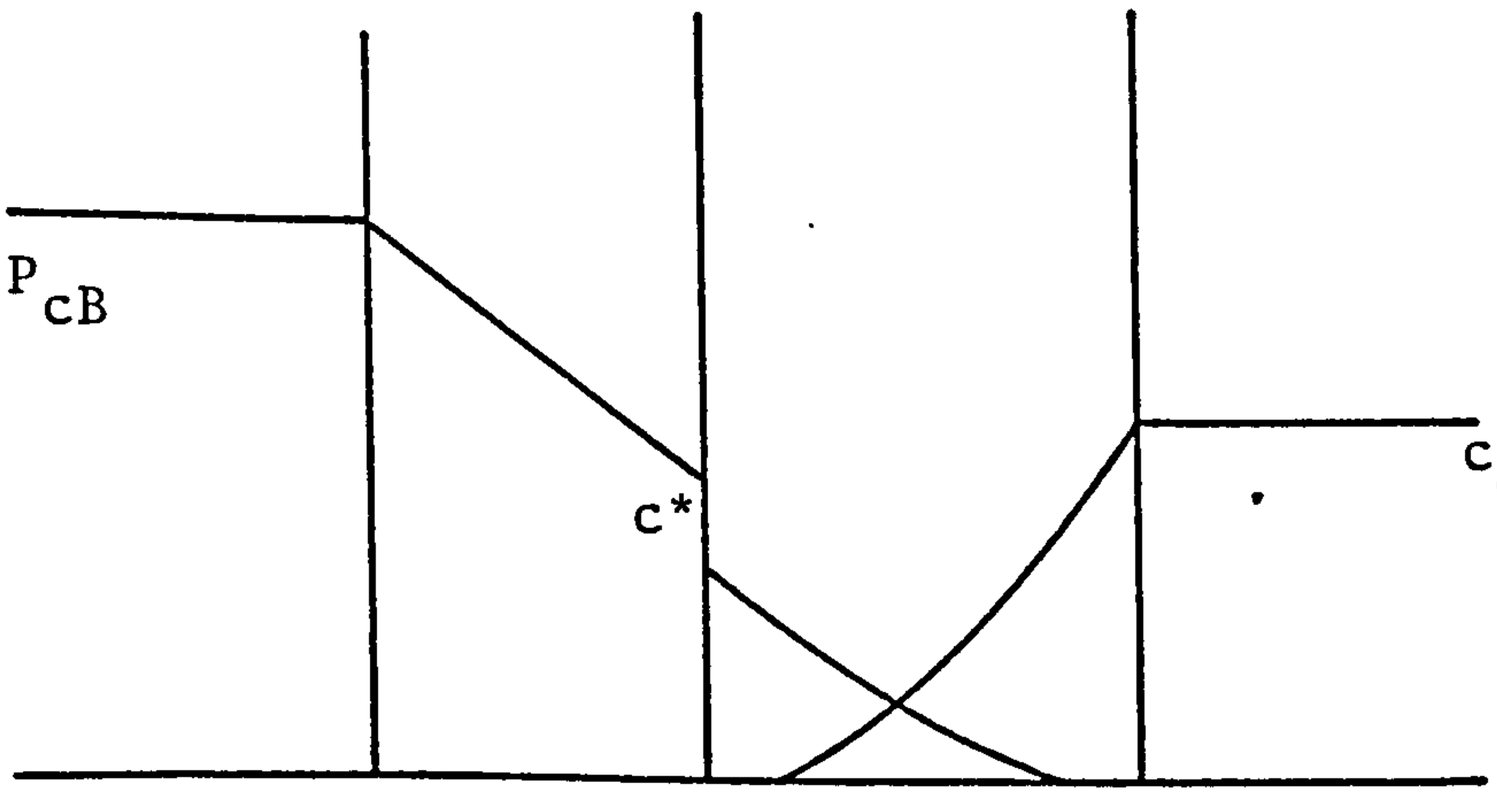
FIG. 2.1. RELATIONSHIP BETWEEN ENHANCEMENT FACTOR AND DIMENSIONLESS GROUPS $\sqrt{M}$ AND ψ_i



(a) Instantaneous



(b) Pseudo-first order



(c) General case

FIG. 2.2. Concentration profiles of carbon dioxide and unreacted MEA

exists if:

$$\sqrt{M} \leq \tfrac{1}{2}(\psi_i - 1) \tag{2.11}$$

The absorption rate is then given by

$$R = c^* \sqrt{k_L^2 + D_c k_c c_0} = k_L c^* \sqrt{1+M} \tag{2.12}$$

and if $\sqrt{M} \geq 5$ then equation (2.12) can be written with only a very small error, as

$$\left.\begin{aligned} R &= c^* \sqrt{D_c k_c c_0} \\ \text{or} \quad \psi &= \sqrt{M} \end{aligned}\right) \tag{2.13}$$

and the absorption rate is independent of the liquid phase mass transfer coefficient.

The carbon dioxide is only one component in the gas phase, and so a general model for the absorption rate includes a gas phase mass transfer coefficient k_G:-

$$R = k_G(p_c - p_i) = \psi k_L c^* \tag{2.14}$$

The interfacial compositions are related by a solubility coefficient H:

$$c^* = Hp_i \tag{2.15}$$

so that the general expression for the local absorption rate can be written as

$$R = \frac{\psi(\psi_i, M) \cdot k_L H p_c}{1+(\psi(\psi_i, M) k_L H / k_G)} \tag{2.16}$$

The absorption rate R is therefore computed iteratively because of the dependence of ψ on the interfacial compositions. However, this presents very little problem, and is generally solved very quickly.

For the special case of pseudo-first order reaction, this reduces to

$$R = \frac{Hp_c\sqrt{D_c k_c c_0}}{1 + (H\sqrt{D_c k_c c_0}/k_G)} \qquad (2.17)$$

The solubility coefficient, diffusivities and reaction rate are all temperature dependent; the correlations used in this study are given in Appendix I.

An empirical approach to the correlation and prediction of the absorption rate has been made by Kohl and Riesenfold[48] who analysed data from industrial columns to obtain a correlation for the overall gas phase mass transfer coefficient:

$$(K_G a) = f(\frac{L}{\mu})^{2/3} [1+5.7(.5-\alpha)M_m \exp(.214+.0121T-3.4p_c)] \qquad (2.18)$$

where f is a correlation parameter dependent upon packing size and type.

The absorption rate is then computed from:

$$Ra = (K_G a)[p_c - p_c^*(\alpha)] \qquad (2.19)$$

where $p(\alpha)$ is the equilibrium partial pressure.
Data for the equilibrium partial pressure of carbon dioxide over MEA has been given by a number of workers[42,59].

2.3. Equations for liquid phase hold up

Before discussion of the full model equations for composition the problem of the liquid phase hold up is considered, and particularly how liquid flow transients should be represented in a general model. Assuming that the liquid phase can be treated as uniformly distributed across the column cross section area the partial differential equation describing the time variation of hold up is:

$$\frac{\partial L}{\partial z} = A\frac{\partial \phi_L}{\partial t} \tag{2.20}$$

where ϕ_L = fractional volume liquid hold up

L = liquid volume flow rate

z = height measured vertically upwards

To relate hold up and liquid flow rate Shulman et al[88] used a relation of the form

$$L = K' \phi_L^m \tag{2.21}$$

with $1.5 < m < 2.0$

If equation (2.21) is used there can be the problem of the development of a shock wave due to the variation of propagation rate with hold up. Substituting (2.21) into (2.20) gives

$$mK' \phi_L^{m-1} \frac{\partial \phi_L}{\partial z} = A\frac{\partial \phi_L}{\partial t} \tag{2.22}$$

Consider the problem of a steady increase in the entry flow rate so that the initial and boundary conditions are.

$$\left.\begin{aligned} \phi_L(z,t) &= \phi^* \quad 0 \leq z \leq Z \quad t \leq 0 \\ \phi_L(Z,t) &= \phi^* + gt \qquad\qquad t > 0 \end{aligned}\right\} \tag{2.23}$$

The solution to (2.22) for these conditions is:

$$1 - \left(\frac{z}{Z}\right) = \phi_L^{m-1}\left[t\left(\frac{ZA}{mK'}\right) - \frac{\phi_L - \phi^*}{g}\right] \tag{2.24}$$

The solution is shown graphically in Fig. 2.3. Lines of constant hold up in the (z,t) plane are defined by

$$d\phi_L = 0 = \frac{\partial \phi_L}{\partial z}\, dz + \frac{\partial \phi_L}{\partial t}\, dt$$

$$\text{so} \quad \frac{dz}{dt} = -m\, K' \phi_L^{m-1}/A \tag{2.25}$$

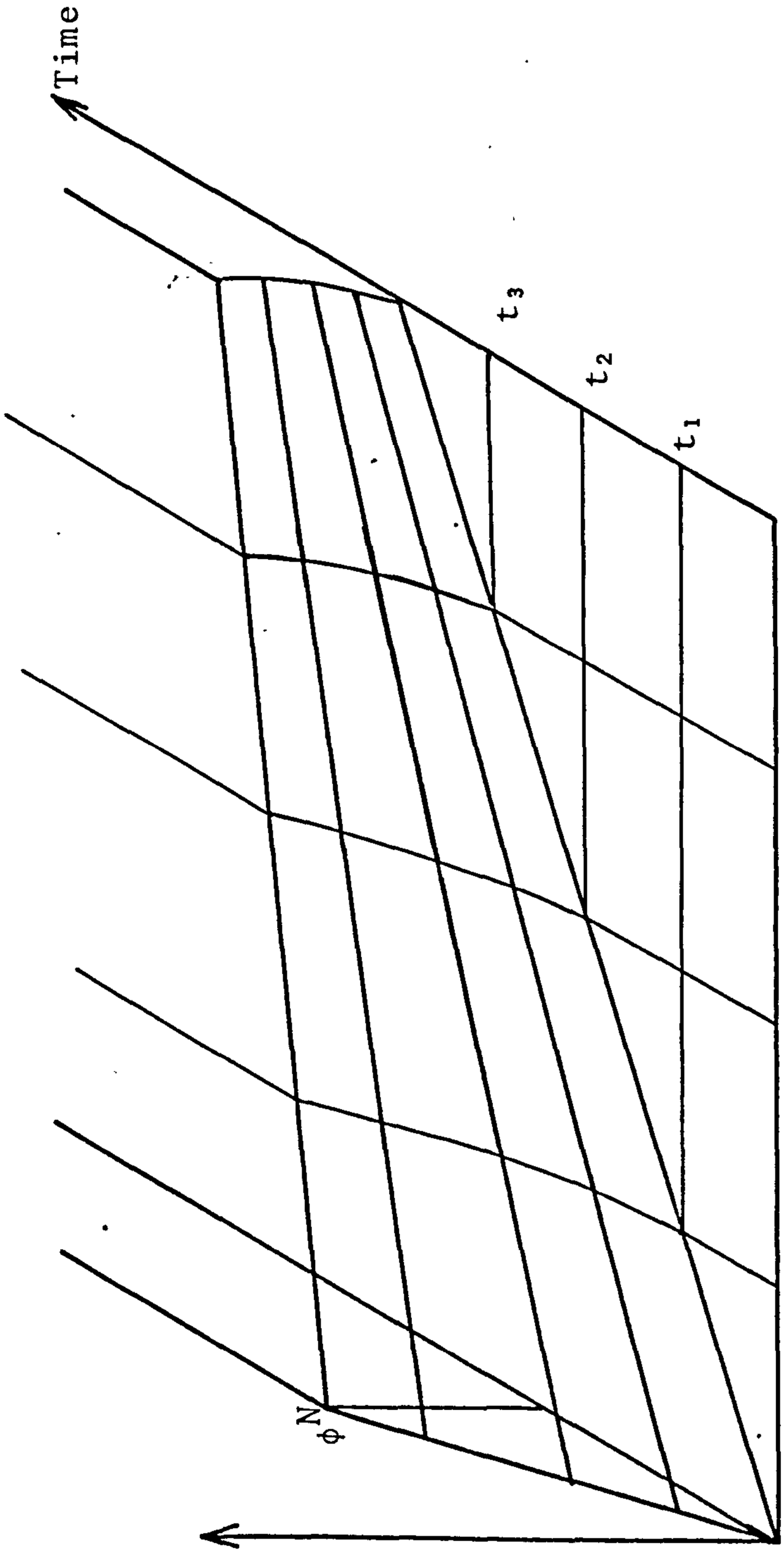


FIG.2.3. PROPAGATION OF CHANGE IN HOLD UP ACCORDING TO EQUATION (2.20)

This equation shows that the local rate of propagation increases with hold up and explains why the front becomes steeper as it passes down the column. If the column were sufficiently long, or the rate of rise g sufficiently large the front would become vertical to produce a shock wave. This will not occur provided:

$$\phi_L^{m+1} > m\ g\ [1 - (z/Z)] \qquad (2.26)$$

For low values of m this condition will be satisfied in practice except for large increases in the inlet liquid flow rate. For a decrease in the entry flow rate there is no problem, and clearly this model will predict assymetric responses similar to those reported by Gilath[35].

The use of a linear flow hold up relationship considerably simplifies the computation of the column response and because the primary aim of the model developed in this chapter is to predict composition responses a linear relationship is reasonable:

$$L = k_1 + k_2\phi_L \qquad (2.27)$$

The solution of (2.20) is then a trivial problem:

$$\left.\begin{aligned} \phi_L &= \phi^* && t < (zA/k_2) \\ \phi_L &= \phi^* + g(t - (zA/k_2)) && t \geq (zA/k_2) \end{aligned}\right\} \qquad (2.28)$$

and the propagation rate of a disturbance is independent of hold up

$$\frac{dz}{dt} = -\frac{k_2}{A} \qquad (2.29)$$

The parameter k_2 can be estimated by observing the delay in the response of the bottom flow or level to a change in the inlet liquid flow rate. Initial experience

from the plant indicates that this form of model should be adequate.

2.4. Statement of Model Equations

The three basic types of model that can be proposed differ in their representation of the mixing processes of the gas and liquid phases. The models are:-

1) dispersion model,
2) cell model,
3) plug flow model.

The assumptions made for all the models are that:

a) both phases can be treated as homogeneous in the plane perpendicular to the flow direction
b) the radial and end effects can be neglected
c) there is perfect heat transfer between the phases so that they are at the same temperature; because the gas flow and specific heat are small compared with those of the liquid the heat transfer between phases is not represented
d) the gas phase is saturated with water vapour
e) liquid hold up and flow rate are linearly related as described in the previous section
f) the total pressure remains constant throughout the column.

The dispersion model, which represents the mixing processes by dispersion coefficients, can be written:-

$$+\frac{AD_G}{R'T_G}\frac{\partial^2 p_c}{\partial z^2} - \frac{\partial v_c}{\partial z} - N(p_c,c,T) = \frac{A\phi_G}{R'T_G}\frac{\partial p_c}{\partial t} \qquad (2.30)$$

$$- D_L A \frac{\partial^2 c}{\partial z^2} + \frac{\partial}{\partial z} Lc + N(p_c,c,T) = A \frac{\partial}{\partial t} \phi_L c \qquad (2.31)$$

$$-D_H A \frac{\partial^2 T}{\partial z^2} + \frac{\partial}{\partial z} LT + \frac{N\Delta E}{\rho c_p} = A\frac{\partial}{\partial t} \phi_L T \qquad (2.32)$$

$$\frac{\partial L}{\partial z} = A\frac{\partial \phi}{\partial t}L \qquad (2.20)$$

where $L = k_1 + k_2\phi_L$ (2.27)

and $N(p_c,c,T) = RaA$ (2.33)

The specific absorption rate R may be computed from either the theoretical reaction model or the correlation due to Kohl and Riesenfeld as described in section 2.2.

$$\frac{p_c}{p_T} = \frac{v_c}{v_c+v_l} \qquad (2.34)$$

The cell model assumes that each phase in the column is made up of a finite number of perfectly mixed cells, their size determining the degree of mixing. The equations for the cells are derived by mass and energy balances:-

$$\frac{d}{dt} U_{Gn}\left(\frac{p_{cn}}{p_T}\right) = v_{cn-1} - v_{cn} - N_n(p_{cn},c_n) \qquad (2.35)$$

$$\frac{d}{dt} U_{Ln}c_n = L_{n+1}c_{n+1} - L_n c_n + N_n(p_{cn},c_n) \qquad (2.36)$$

$$\frac{d}{dt} U_{Ln}T_n = (L_{n+1}T_{n+1} - L_n T_n) + (N_n\Delta E/\rho c_p) \qquad (2.37)$$

$$\frac{d}{dt} U_{Ln} = L_{n+1} - L_n(U_{Ln}) \qquad (2.38)$$

where $L_n = k_3 + k_4 U_{Ln}$)
)
or more generally $L_n = L(U_{Ln})$) (2.39)

Aris and Amundson[3] show that the cell and dispersion models are identical to second order if the cell size is correctly related to the dispersion coefficient. For the liquid phase, the relationship is:

$$\Delta z = \frac{2D_L A}{L} \quad (2.40)$$

Or, if a Peclet Number is defined

$$Pe_L = \frac{(L/A).d_p}{D_L} \quad (2.41)$$

then (2.40) can be written as:

$$\Delta z = 2d_p/Pe_L \quad (2.42)$$

The work of De Maria and White[23] showed that the Peclet Number for the liquid phase is about 2; therefore, the cell size that should be used for the liquid is of the same order as the packing size.

The final model considered, the plug flow model, assumes that there is no mixing in either phase. The model equations are simply those of the dispersion model with the diffusion coefficients set to zero.

2.5. Solution of Model Equations

2.5.1. Introduction

The absorption rate is generally non-linear and therefore analytical solutions of the model equations are not possible.

The mixing cell model has the advantage of being a set of ordinary differential equations and is therefore in a

convenient form for simulation. However, as the dispersion decreases, the number of cells increases, so not only is the dimension of the model increased, but the equations become stiffer.

The dispersion model equations are parabolic, and therefore require solution by a method such as Crank-Nicholson. A Crank-Nicholson solution was attempted, but problems with convergence of the implicit equations prevented this method from being very efficient. Furthermore, for the particular column considered, the ratio of the column height to packing size is about 200, and consequently the mixing process suggested by equations (2.35) to (2.37) may not be very significant. For this reason, the behaviour of the column was initially investigated using the plug flow model, which can be solved easily for both the dynamic and steady states.

2.5.2 Unsteady State Solution by Method of Characteristics

With no dispersive terms (2.30) to (2.32) form a set of simultaneous hyperbolic equations:

$$\frac{\partial v_c}{\partial z} + \frac{A\phi_G}{R' T_G} \frac{\partial p_c}{\partial t} = -N \qquad (2.43)$$

$$\frac{\partial}{\partial z} Lc - A\frac{\partial}{\partial t} \phi_L c = -N \qquad (2.44)$$

$$\frac{\partial}{\partial z} LT - A\frac{\partial}{\partial t} \phi_L T = -N\Delta E/\rho c_p \qquad (2.45)$$

$$\frac{\partial L}{\partial z} = A \frac{\partial \phi_L}{\partial t} \qquad (2.20)$$

$$L = k_1 + k_2 \phi_L \qquad (2.27)$$

Using (2.27) with (2.44) and (2.45)

$$L\frac{\partial c}{\partial z} - A\phi_L\frac{\partial c}{\partial t} = -N \qquad (2.46)$$

and $$L\frac{\partial T}{\partial z} - A\phi_L\frac{\partial T}{\partial t} = -N\Delta E/\rho c_p \qquad (2.47)$$

Now if v_c is replaced by use of (2.34):

$$\frac{-v_I p_T}{(p_T-p_c)^2}\frac{\partial p_c}{\partial z} - \frac{A\phi_G}{R' T_G}\frac{\partial p_c}{\partial t} = N \qquad (2.48)$$

A convenient method of solution is to use the method of characteristics, the theory of which is well presented by Abbot[1].

The method of characteristics transforms the partial differential equations (2.46) to (2.48) by defining a set of characteristic directions in the (z,t) plane along which the variation of the dependent variables can be expressed by ordinary differential equations. In the case of the packed column these directions represent the rate at which the two phases move through the column. For the equations given, these directions are defined by

$$\left.\frac{dz}{dt}\right)_I = \frac{-L}{A\phi_L} \qquad (2.49)$$

$$\left.\frac{dz}{dt}\right)_{II} = \frac{v_I p_T R' T_G}{(p_T-p_c)^2 A\phi_G} \qquad (2.50)$$

for the liquid and gas phases respectively.

The characteristic directions for the liquid composition and temperature are identical, and the gas phase characteristic is curved due to the decrease in the total gas flow rate as a result of the absorption. The assumption of a constant gas flow rate leads to an error of less than 10% in the top

partial pressure for inlet carbon dioxide compositions up to 15%, and is therefore a reasonable assumption to make. Equation (2.34) therefore becomes

$$\frac{p_c}{p_T} = \frac{v_c}{v_I} \tag{2.51}$$

and as a result the gas phase characteristic is then linear

$$\left.\frac{dz}{dt}\right)_{II} = \frac{v_I R' T_G}{A\phi_G p_T} \tag{2.52}$$

A characteristic grid with constant gas and liquid flow rates is shown in Fig. 2.4. The more complex case where the liquid flow rate and hold up vary with time is described in Appendix 2. Generally the grid has to be altered in a reasonably simple manner to account for flow changes. However, a very simple situation exists when the static hold up is zero as then flow and composition disturbances propagate at the same rate and the grid can then be left unaltered.

The ordinary differential equations for the dependent variables along the characteristic directions can be written in terms of height:

$$\left.\frac{dc}{dz}\right)_I = -\frac{N}{L} \tag{2.53}$$

$$\left.\frac{dT}{dz}\right)_I = -\frac{N\Delta E}{\rho c_p L} \tag{2.54}$$

$$\left.\frac{dp_c}{dz}\right)_{II} = -\frac{Np_T}{v_I} \tag{2.55}$$

or, equivalently in terms of time:

$$\left.\frac{dc}{dt}\right)_I = \frac{N}{A\phi_L} \tag{2.56}$$

$$\left.\frac{dT}{dt}\right)_I = \frac{N\Delta E}{\rho c_p A\phi_L} \tag{2.57}$$

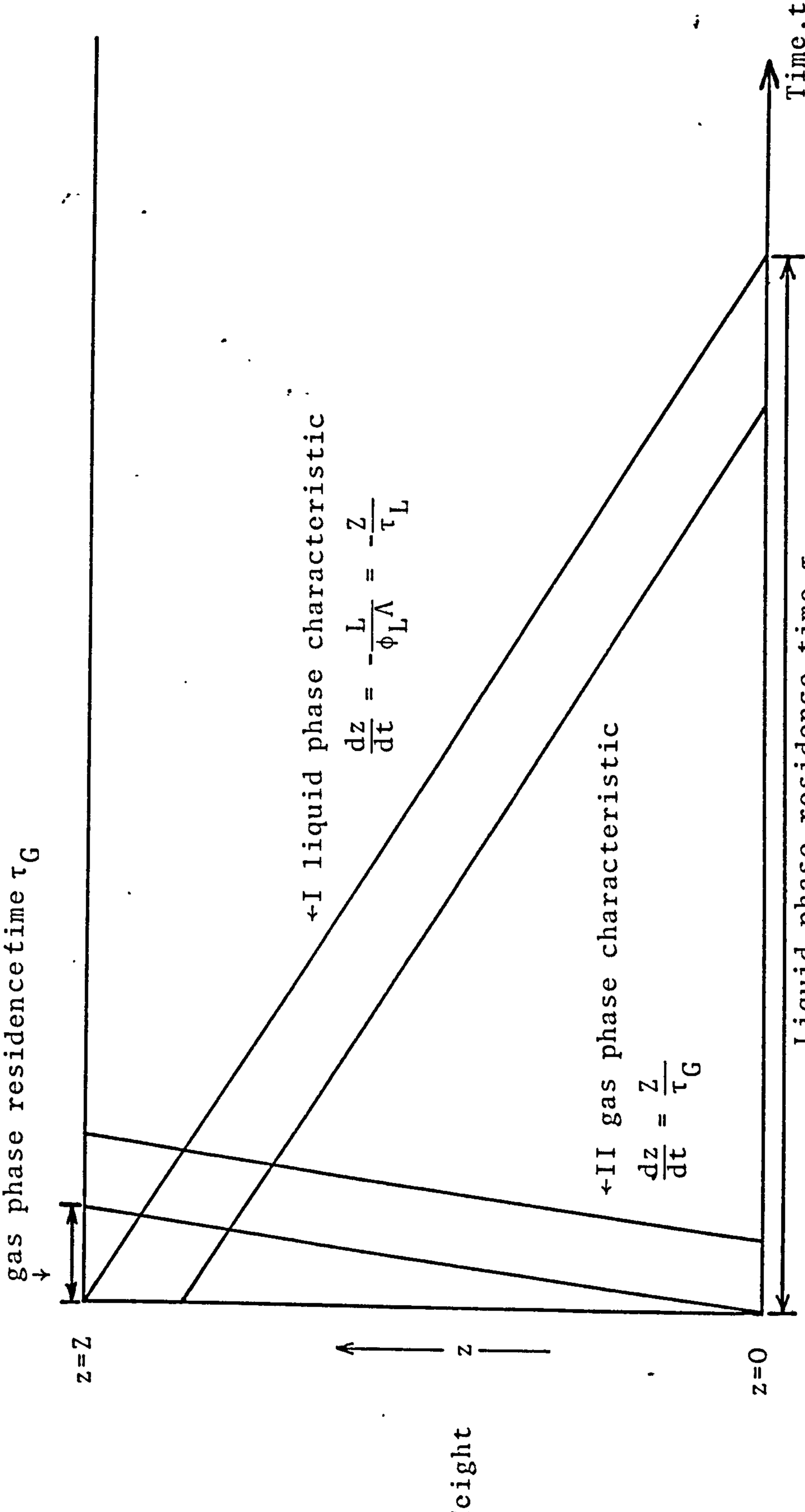


FIG.2.4. CHARACTERISTIC

$$\left(\frac{dp_c}{dt}\right)_{II} = -\frac{NR' T_G}{A\phi_G} \quad ; \qquad (2.58)$$

Either of these two forms can be used in a particular case, whichever is the more convenient.

The initial conditions for these equations are obtained from the initial and boundary conditions for the partial differential equations:

$$\left.\begin{aligned} c(z,0) &= c^0(z) \\ p_c(z,0) &= p^0(z) \\ T(z,0) &= T^0(z) \\ \phi_L(z,0) &= \phi_L^0(z) \end{aligned}\right\} \quad t = 0 \quad 0 \leq z \leq Z \qquad (2.59)$$

$$\left.\begin{aligned} c(Z,t) &= c_T(t) \\ p_c(0,t) &= p_{cB}(t) \\ T(Z,t) &= T_T(t) \\ \phi_L(Z,t) &= \phi_{LT}(t) \end{aligned}\right\} \quad t > 0 \qquad (2.60)$$

It is clear that the solutions for the liquid composition and temperature are linearly related so that it is not necessary to compute the temperature solution by integration of a differential equation. The temperature can be obtained from the linear relationship:

$$T(z,t) = T(Z,t') + \frac{\Delta E}{\rho c_p} \{c(z,t) - c(Z,t')\} \qquad (2.61)$$

where (Z,t') denotes the initial point of the characteristic passing through the point (z,t).

2.5.3. Transformation of Equations

The first programme written used values of p_c,c, stored along the current and previous gas phase characteristics,

so that Simpson integration could be used for integration along both the characteristics.

Initial experience with the programme showed that the integration of equation (2.55) along the gas phase characteristic often became unstable, even with the use of as many as 40 points along a line, see Table 2.1. The instabilities occur near the top of the column where the absorption is approximately pseudo-first order:

$$N = \frac{a\ AH\sqrt{D_c k_c c_0}}{1+\frac{H\sqrt{D_c k_c c_0}}{k_G}}\ p_c \qquad (2.62)$$

The cause of this instability was attributed to the fact that near the top of the column the free amine concentration c_0 is at its largest so that the eigenvalue associated with (2.55) is large even though the absorption rate is low. The problem was overcome by introducing the transformation

$$\left(\frac{1}{p_c}\ \frac{dp_c}{dz}\right)_{II} = \frac{d}{dz}\ \ell n\ p_c = \frac{N}{p_c} \qquad (2.63)$$

This type of transformation can be adopted for any of the absorption rate models considered, and can be applied in both the steady and unsteady states. Furthermore, a similar equation can be written for the steady state non-dilute gas phase model:-

$$\frac{1}{v_c}\ \frac{dv_c}{dz} = \frac{d}{dz}\ \ell n\ v_c = (N/v_c) \qquad (2.64)$$

For convenience the improvement given by the transformation was investigated by considering the steady state as opposed to the dynamic model, and the results are given in Table 2.2. The comparison was made by integrating the two

equations from a boundary condition specified at the base of the column. It is clearly seen that the transformation permits a stable and accurate solution to be obtained with the use of only 10 steps whereas the original equation is unstable with the use of even 40 steps.

TABLE 2.1 INSTABILITY OF THE GAS PHASE SOLUTION USING EQUATION (2.55) FOR A START UP SIMULATION

Height from base, z	Point No.	p_c (bars)	c (kmole/m^3)
0.149	1	.1646	.4479
0.895	6	.6253E-01	.4519
1.640	11	.2361E-01	.4541
2.386	16	.9169E-02	.4563
3.132	21	.3220E-02	.4586
3.877	26	.1597E-02	.4613
4.623	31	.9894E-03	.4639
4.772	32	.8376E-03	.4646
4.921	33	-.1150E-03	.4650
5.070	34	.7643E-03	.4658
5.219	35	-.2855E-03	.4661
5.368	36	.7410E-03	.4669
5.517	37	-.4296E-03	.4672
5.666	38	.7553E-03	.4680
5.816	39	-.5598E-03	.4683
5.965	40	.7990E-03	.4692

Note: .6253E-01 $\equiv$ $.6253\times10^{-1}$

The points in the characteristic grid are numbered upwards from the base as described in Appendix 2.

Conditions: $L = .35\times10^{-3}\,m^3/s$

$p_{cB} = .20$ bars

$p_T = 3.32$ bars

$v_I = 2.99\times10^{-3}$ kmole/s

$c_T = .4464,\ \alpha_T = .18$

at $t = 0$ $\quad \begin{cases} c(z) = .4464 \\ p_c(z) = 10^{-7} \end{cases} \quad 0 < z < Z$

Absorption rate calculated from the theoretical reaction model.

TABLE 2.2. COMPARISON OF INTEGRATION OF ORIGINAL EQUATION (2.55) AND TRANSFORMED EQUATION (2.64)

40 step solution, Δz = 0.1525m

Height from base z	Original Equation			Transformed Equation	
	p_c	α	Derivative	p_c	α
1.22	.6344E-01	.2470	.6960E-04	.6334E-01	.2469
2.44	.1402E-01	.1945	.1625E-04	.1401E-01	.1945
3.66	.2893E-02	.1829	.3386E-05	.2906E-02	.1829
4.88	.5655E-03	.1805	.6632E-06	.5951E-03	.1805
5.337	.3659E-03	.1802	.4292E-06		
5.490	.2296E-03	.1801	.2692E-06		
5.642	.2634E-03	.1801	.3090E-06		
5.795	.1356E-03	.1800	.1591E-06		
5.947	.1970E-03	.1801	.2311E-06		
6.100	.6983E-03	.1799	.8192E-07	.1215E-03	.1800

20 step solution, Δz = 0.305m.

Height from base, z	Original Equation			Transformed Equation	
	p_c	α	Derivative	p_c	α
1.22	.6297E-01	.2464	.6914E-04	.6329E-01	.2468
2.44	.1317E-01	.1936	.1528E-04	.1399E-01	.1945
3.66	.1454E-02	.1814	.1703E-05	.2904E-02	.1829
3.965	.3627E-02	.1836	.4242E-05		
4.88	INTEGRATION FAILURE			.5945E-03	.1805
6.10				.1214E-03	.1800

10 step solution, Δz = 0.61m

Height from base, z	Original Equation			Transformed Equation	
	p_c	α	Derivative	p_c	α
1.22	INTEGRATION FAILS			.6347E-01	.2470
2.44				.1404E-01	.1945
3.66				.2912E-02	.1829
4.88				.5964E-03	.1805
6.10				.1217E-03	.1800

Note: .6344E-01 ≡ $.6344 \times 10^{-1}$

Aborption rate calculated from theoretical absorption model.

Conditions: $L = .35 \times 10^{-3} m^3/sec.$

$p_{cB} = .2003$ bars

$c_B = .9947$ kmole/m^3, $\alpha_B = .4011$

2.6. Steady State Behaviour

2.6.1. The Steady State Solution

To assess the general performance of the column and also the difference between the Kohl and reaction models, a number of steady state concentration and temperature profiles were computed. For simplicity, the plug flow model was used; dispersion effects were investigated separately and are presented later. The equations for solution are formulated from the dynamic model equations:-

$$\frac{d}{dz} v_c = - R(c, p_c, T)a A$$

or $$\frac{d}{dz} \ell n\, v_c = - RaA/v_c \qquad (2.65)$$

together with material and energy balance equations

$$c(z) = c_T + (v_c(z) - v_{cT})/L \qquad (2.66)$$

$$T(z) = T_T + \frac{\Delta E}{\rho c_p} (c(z) - c_T) \qquad (2.67)$$

where the specific absorption rate R may be given by either the Kohl or reaction models.

The inlet concentrations are specified at opposite ends of the column:

$$\left.\begin{aligned} v_c(0) &= v_{cB} \\ c(Z) &= c_T \end{aligned}\right\} \qquad (2.68)$$

The inlet liquid temperature is specified at the top of the column

$$T(Z) = T_T \qquad (2.69)$$

Because initially both stream concentrations are not known at either end an iterative procedure is required. The

procedure adopted was to update an estimate of the top partial pressure until the boundary condition at the column base was met. Equation (2.65) was employed for the computation of the profiles because it was found to be very stable with relatively few steps of a Runge Kutta integration procedure.

2.6.2. Solutions using the Reaction Model

A set of possible plant operating conditions was defined and the resulting column profiles computed. As may be expected, the majority of the absorption occurs in the lower third of the column; the enhancement factor due to chemical reaction is shown in Fig. 2.5 and Table 2.3 for two typical cases. In both cases the majority of the absorption occurs in the lower third of the column and the absorption in the top of the column is very close to the pseudo-first order asymptote. For the second case the absorption conditions are close to pseudo-first order throughout the column length, but for the first case there is significant departure from the asymptote in the lower part of the column. Departure from this asymptote increases with increasing gas and liquid concentrations; for the conditions studied the departure was generally insignificant provided the exit carbonation ratio was less than 0.4 and the inlet gas composition less than 6% (0.2 bars for the chosen conditions). The variation of exit concentrations with inlet gas partial pressure and liquid flow rate is shown in Fig. 2.6. In assessing column performance a comparison of the top partial pressures is the most critical measure because almost all the CO_2 is absorbed. At

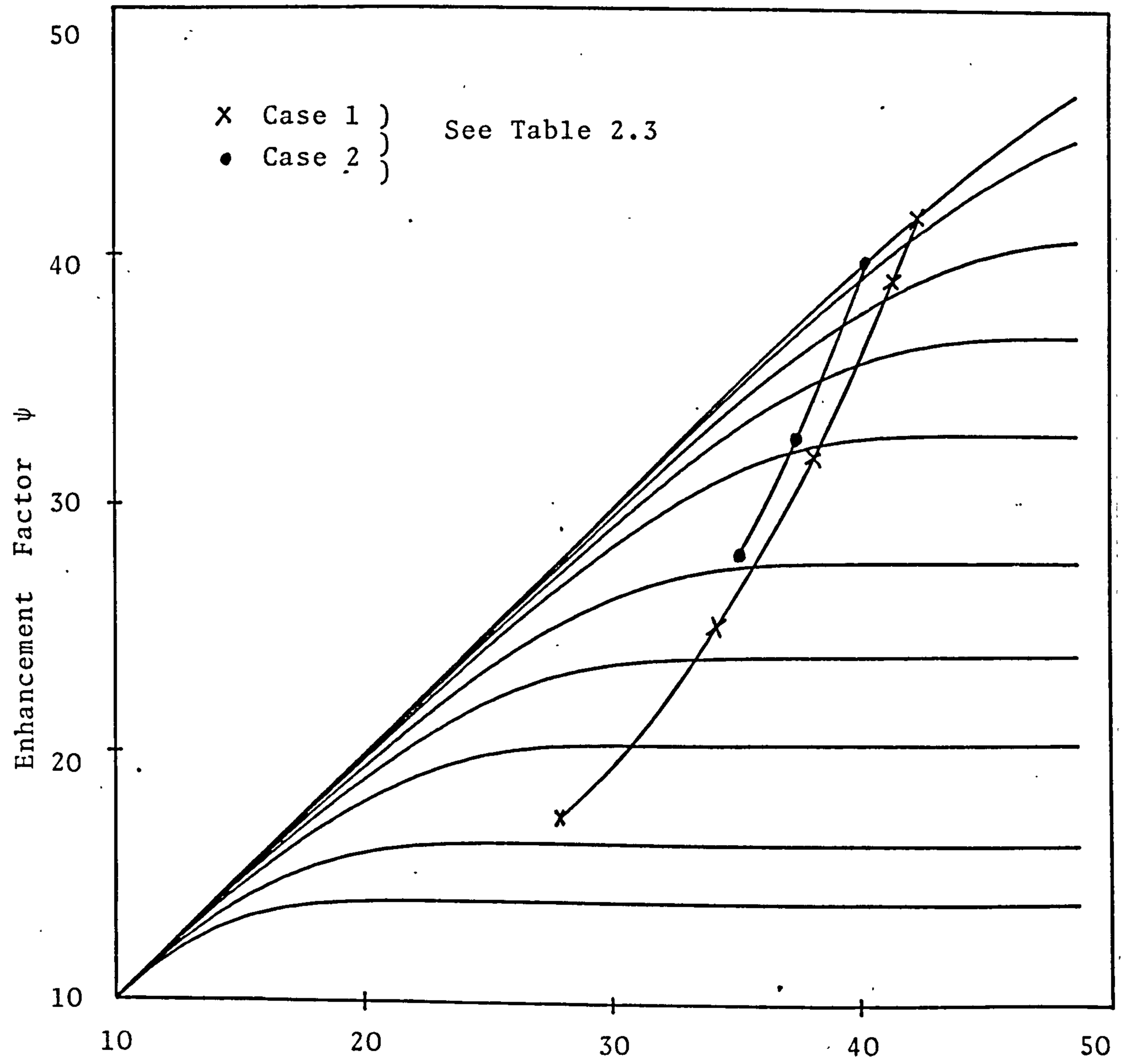


FIG. 2.5. INCREASE IN ABSORPTION RATE DUE TO CHEMICAL REACTION

TABLE 2.3. VARIATION OF THE ENHANCEMENT FACTOR AND ABSORPTION CONDITIONS (DATA FOR FIG. 2.5.)

Case 1 $L = .3 \times 10^{-3}$; $p_{cB} = .20$

Height from base z	p_c (bars)	α	% CO_2 Absorbed from base	$\sqrt{M}$	ψ
Top 6.10	.1556E-03	.1800	100.0	42.34	42.34
4.88	.7620E-03	.1807	99.73	42.34	42.34
3.66	.3717E-03	.1843	98.33	42.36	42.36
2.44	.1780E-01	.2015	91.65	42.42	42.42
1.22	.7733E-01	.2756	62.86	41.65	38.61
0.61	.1373	.3532	32.71	38.20	31.64
0.30	.1706	.3975	15.50	34.22	25.47
Base 0.0	.2000	.4374	0.0	28.40	17.59

Case 2 $L = .375 \times 10^{-3}$; $p_{cB} = .175$

Height from base z	p_c (bars)	α	% CO_2 Absorbed from base	$\sqrt{M}$	ψ
Top 6.10	.9437E-04	.1801	100.0	39.37	39.37
4.88	.4622E-03	.1804	99.83	39.37	39.37
3.66	.2260E-02	.1821	98.88	39.38	39.38
2.44	.1094E-01	.1905	94.18	39.43	39.43
1.22	.5047E-01	.2295	72.35	39.38	39.38
0.61	.1013	.2811	42.92	38.60	35.16
.0.30	.1359	.3171	23.30	37.42	32.57
Base 0.0	.1750	.3588	0.0	35.15	28.10

Other conditions : $p_T = 3.32$ bars

$c_T = .4464$, $\alpha_T = .18$

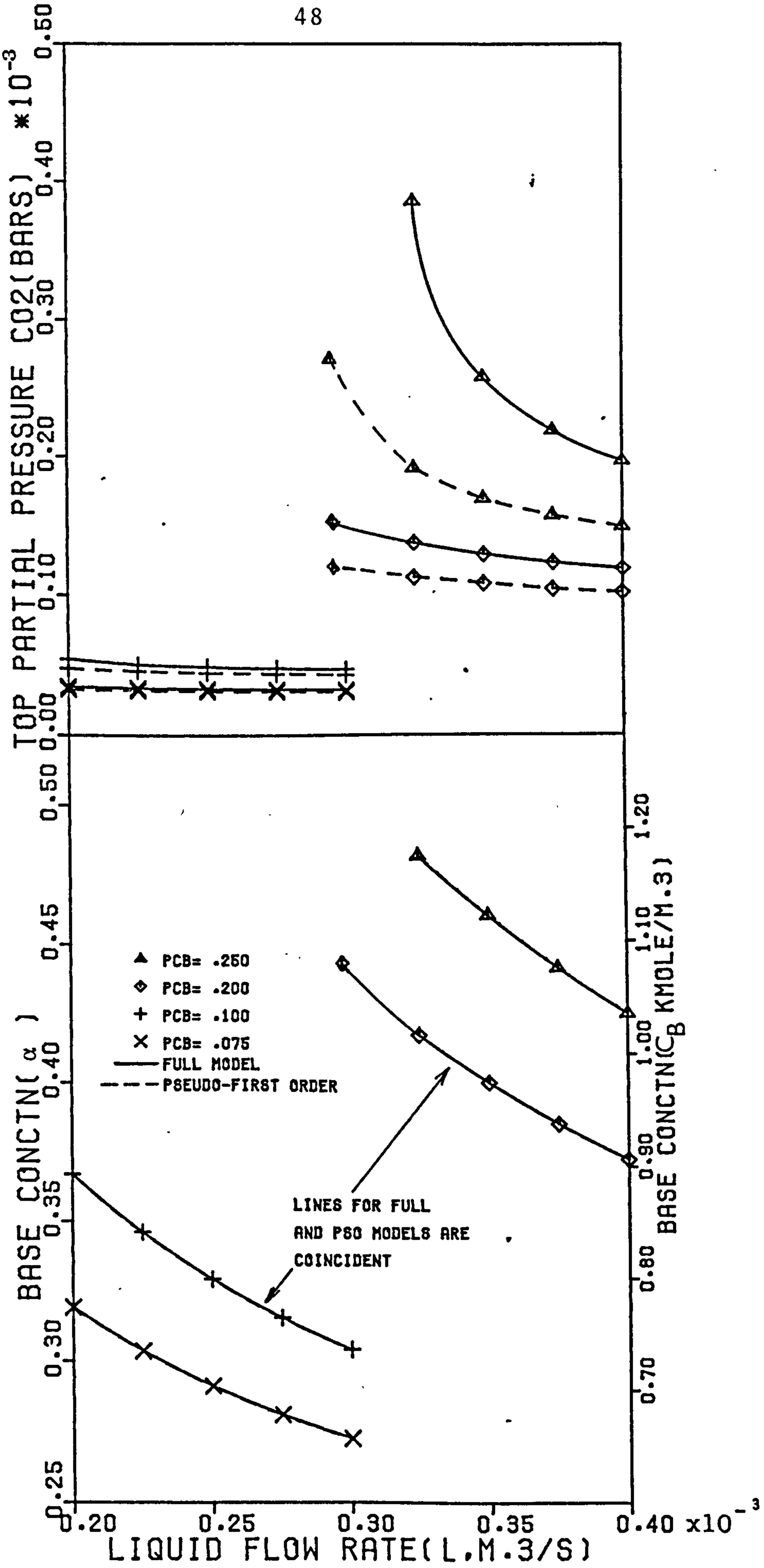


FIG.2.6. NON ISO-THERMAL REACTION MODEL:
VARIATION OF EXIT CONCENTRATIONS

low gas concentrations, the top partial pressure is nearly independent of liquid flow rate and the absorption rate is then very close to pseudo-first order.

For cases with very high exit carbonation ratios, the absorption rate passes through a maximum on descending the column, with a final value close to the physical absorption rate at the column base. This prompted the question of the significance of the secondary hydration reaction and the build up of free carbon dioxide in solution.

Calculation of the quantity of free carbon dioxide in solution showed it to be small and for most cases significantly less than the interfacial concentration of carbon dioxide (see Appendix 1). Generally the decrease in the enhancement factor has a greater effect than the reduction due to approaching the equilibrium of reaction (2.1).

Absorption rates were calculated for conditions near to the base of the column with the assumption that the absorption rate was physically controlled, followed by a slow reaction in the liquid. This showed the absorption rate to be very low, and also that the secondary reaction did not significantly alter the carbonation ratio because of the small amount of free carbon dioxide in solution. It was concluded that this could lead to only a very small change in the carbonation ratio in the column bottoms where the exposure time is longer, and that the effect on the absorption rate on the packing is negligible.

Returning to the case of second order reaction, which was found to be far more likely, the absorption regime is dependent upon the dimensionless groups M, ψ_i and

consequently their constituent physical parameters. For a specific column and set of operating conditions the two parameters which are most difficult to estimate a priori are the liquid phase mass transfer coefficient and the interfacial area. The latter is important in defining the overall absorption, but not in defining the regime of the absorption which is mainly dependent upon the liquid phase mass transfer coefficient, interfacial carbon dioxide concentration and free amine concentration.

The parameter values in this study are taken from the measurements and results of Danckwerts et al[19], see Appendix 1. Together with the nominal operating conditions for the plant these measurements indicate a liquid mass transfer coefficient sufficiently large to give absorption close to pseudo-first order conditions in the majority of cases. The work of Brian et al[11] shows that a considerable increase in the liquid phase mass transfer coefficient is possible due to the presence of interfacial turbulence, and this would further increase the likelihood of absorption close to pseudo-first order conditions.

The variation in the top partial pressure with liquid phase mass transfer coefficient is shown in Fig. 2.7. At the lower inlet partial pressure the absorption conditions must be close to pseudo-first order as the mass transfer coefficient has negligible effect. The higher inlet partial pressure favours a departure from pseudo-first order and this is achieved with the lower value of the mass transfer coefficient. The correlation by Danckwerts (see Appendix 1) gives a value for the mass transfer coefficient closer to the higher value selected.

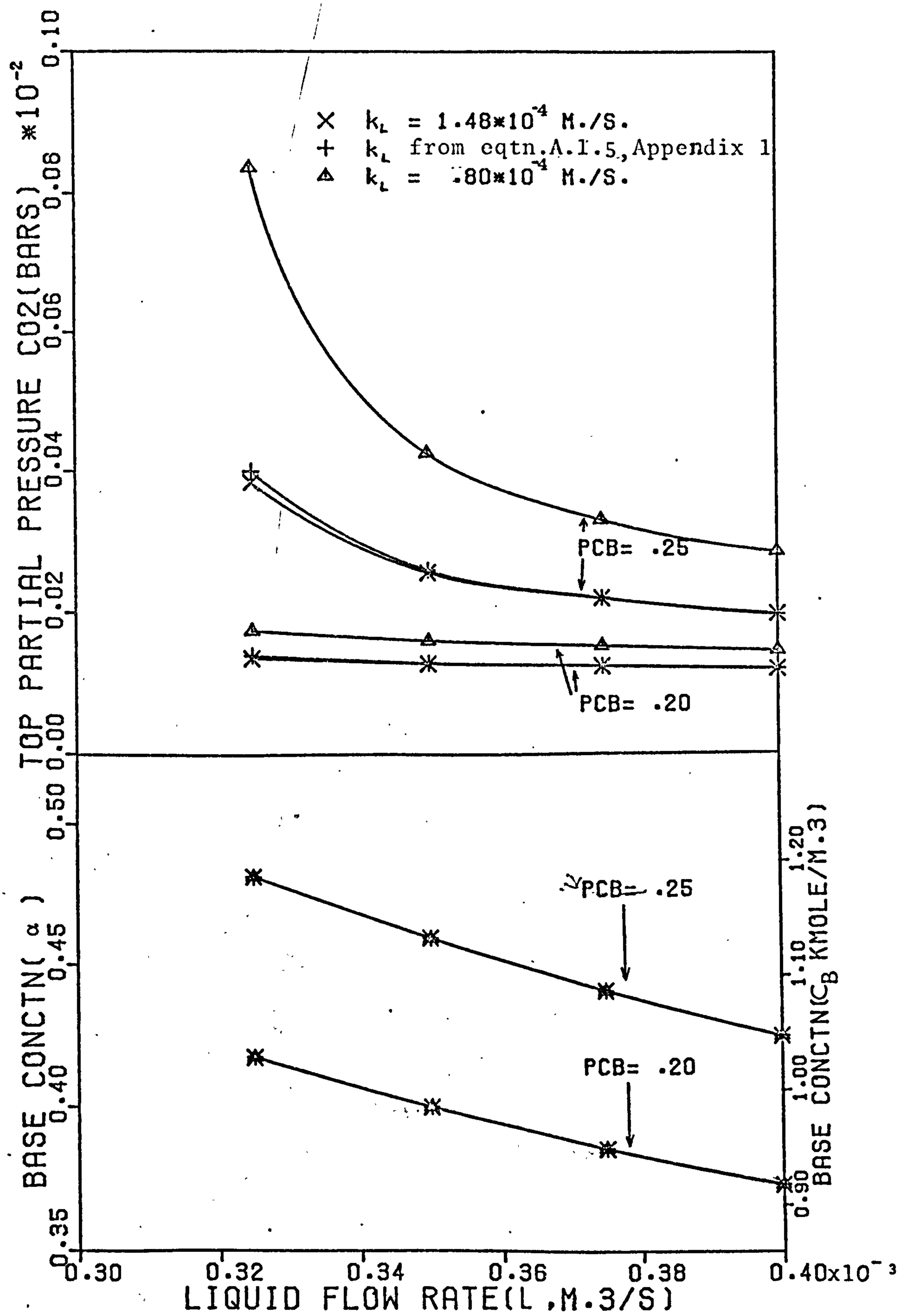


FIG. 2.7. REACTION MODEL: VARIATION OF EXIT CONCENTRATION WITH LIQUID PHASE MASS TRANSFER COEFFICIENT

In summary, the reaction model has a general applicability to any of the likely regimes of absorption. The parameters used in this study show that for the particular column and operating conditions concerned, behaviour close to pseudo-first order is likely.

2.6.3. Solution using Kohl Model

The alternative absorption rate model is the Kohl correlation, equation (2.18). The parameter f has been empirically correlated with packing size and operating conditions in the literature, so that a priori estimates of its magnitude cannot be made reliably for packings which were not considered. A value of f was therefore chosen which gave an approximate fit to one of the profiles computed with the reaction model. From Table 2.4 and Fig. 2.8. it is clear that the absorption rate and concentration profiles given by the Kohl model are different from those given by the reaction model. Computation of exit stream concentrations over the same range of operating conditions revealed a significant difference between the two models, see Figs. 2.6 and 2.9. The Kohl and reaction models predict practically the same variation in base liquid concentration because the carbon dioxide is almost totally absorbed. It is therefore the behaviour of the top partial pressure which reveals the difference between the two models, the Kohl model generally showing a greater variation with the liquid flow rate than the reaction model.

This difference in prediction can be rationalised by reference to the data upon which the Kohl correlation is

TABLE 2.4 COMPARISON OF THEORETICAL REACTION MODEL WITH KOHL CORRELATION

Conditions : $L = .4 \times 10^{-3}$ m^3/s

$p_{cB} = .20$ bars

$P_T = 3.32$ bars

$v_I = 2.99 \times 10^{-3}$ kmole/s

$c_T = .4464$; $\alpha_T = .18$

Theoretical Reaction Model					Kohl Correlation, f = 2.8			
height, z m	p_c bars	$^\circ\alpha$	T °C	Absptn Rate kmole/m^4	p_c bars	α	T °C	Absptn Rate kmole/m^4
6.10	$.1111 \times 10^{-3}$	.1800	30.00	$.4250 \times 10^{-3}$	$.1006 \times 10^{-3}$	.1800	30.00	$.4734 \times 10^{-3}$
4.88	$.5446 \times 10^{-3}$	.1804	30.02	$.1597 \times 10^{-2}$	$.6496 \times 10^{-3}$	.1805	30.02	$.2230 \times 10^{-2}$
3.66	$.2661 \times 10^{-2}$	.1823	30.10	$.7789 \times 10^{-2}$	$.4116 \times 10^{-2}$	.1837	30.16	$.1388 \times 10^{-1}$
2.44	$.1286 \times 10^{-1}$	.1916	30.66	$.3734 \times 10^{-1}$	$.2366 \times 10^{-1}$	.2015	30.94	$.7210 \times 10^{-1}$
1.22	$.5886 \times 10^{-1}$	.2343	32.38	.1638	$.9338 \times 10^{-1}$	.2671	33.82	.1942
.000	.200	.3725	38.44	.3505	.2000	.3731	38.47	.2124

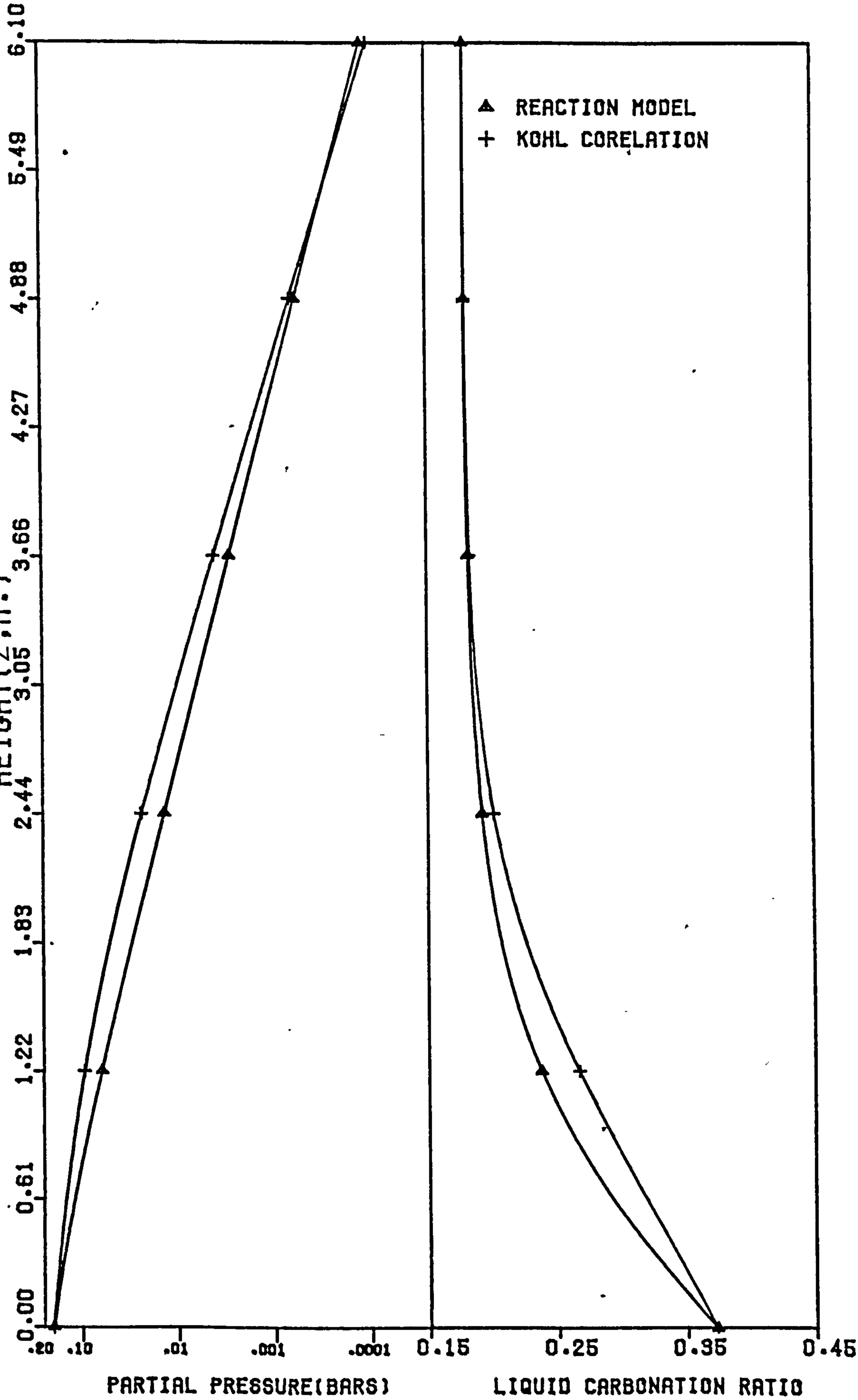


FIG. 2.8. COMPARISON OF ABSORPTION PROFILES

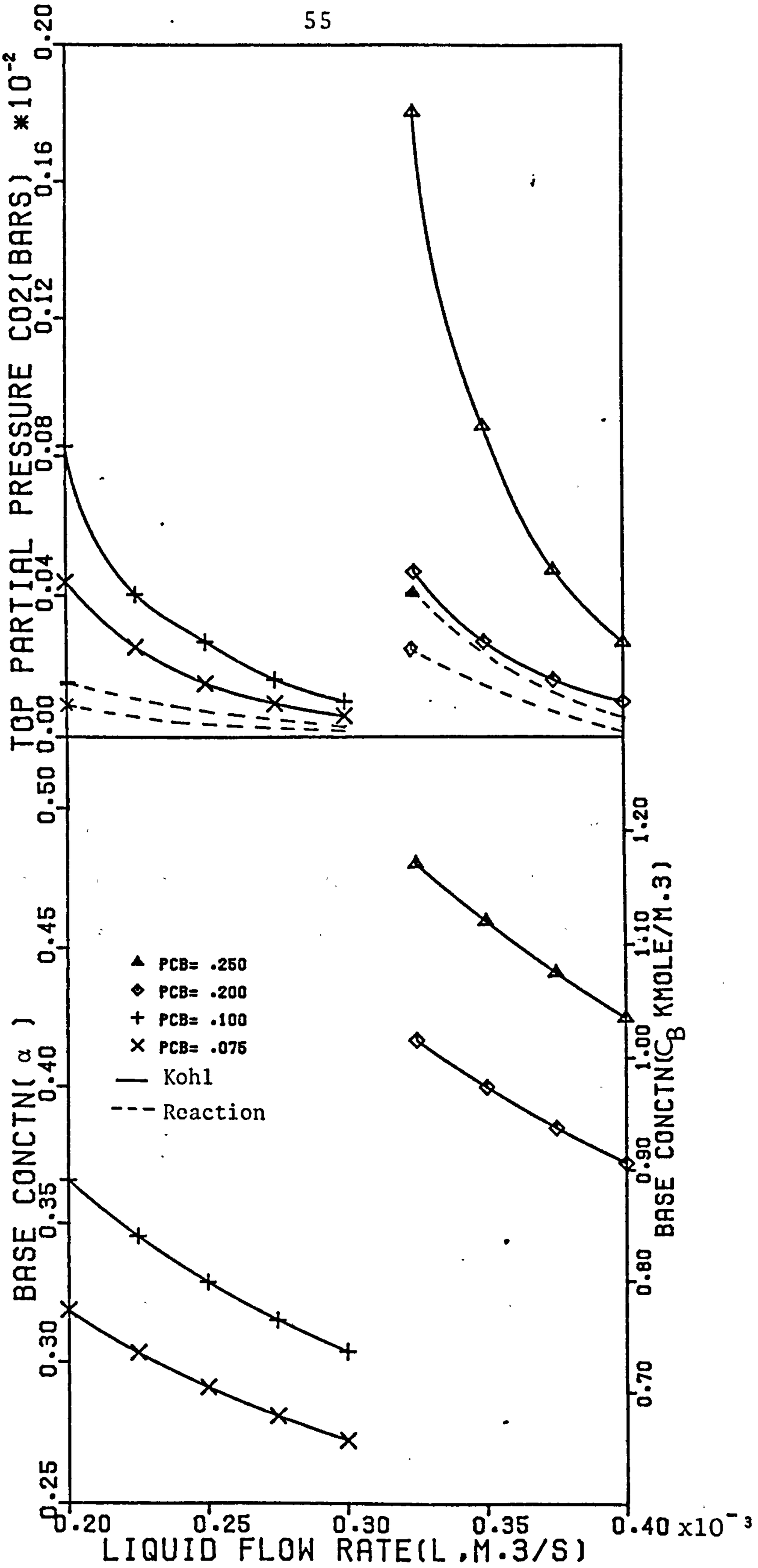


FIG. 2.9. KOHL MODEL: VARIATION OF EXIT CONCENTRATIONS (REACTION MODEL SHOWN SUPERIMPOSED)

based. In many cases, the exit stream concentrations were used to compute a mean overall gas phase mass transfer coefficient: this is inaccurate, and also implies that the correlation includes, in some sense, the effects of dispersion in both liquid and gas phases. Furthermore, different operating pressures, column and packing sizes were used, the inlet gas concentrations were generally between 8% and 12%, and the packings used were almost exclusively Raschig rings or Berl saddles. These operating conditions are likely to result in absorption closer to instantaneous reaction conditions, for which the enhancement factor is:

$$\psi_i = 1 + \frac{c_0}{2c^*}\sqrt{\frac{D_M}{D_c}} \qquad (2.70)$$

The similarity of the Kohl correlation to this expression can be shown: for zero amine concentration, the Kohl correlation gives an expression for the physical mass transfer coefficient, and hence an enhancement factor based on the Kohl correlation can be written:-

$$\psi_i^K = 1 + 5.7(.5-\alpha)M \exp(.214 + .0121T - 3.4p_c) \qquad (2.71)$$

In both equations (2.70) and (2.71) the enhancement factor is directly proportional to the free amine concentration, although the dependence upon the partial pressure is not exactly the same. In contrast, for the pseudo-first order regime, the absorption rate is proportional to the partial pressure and the square root of the free amine concentration.

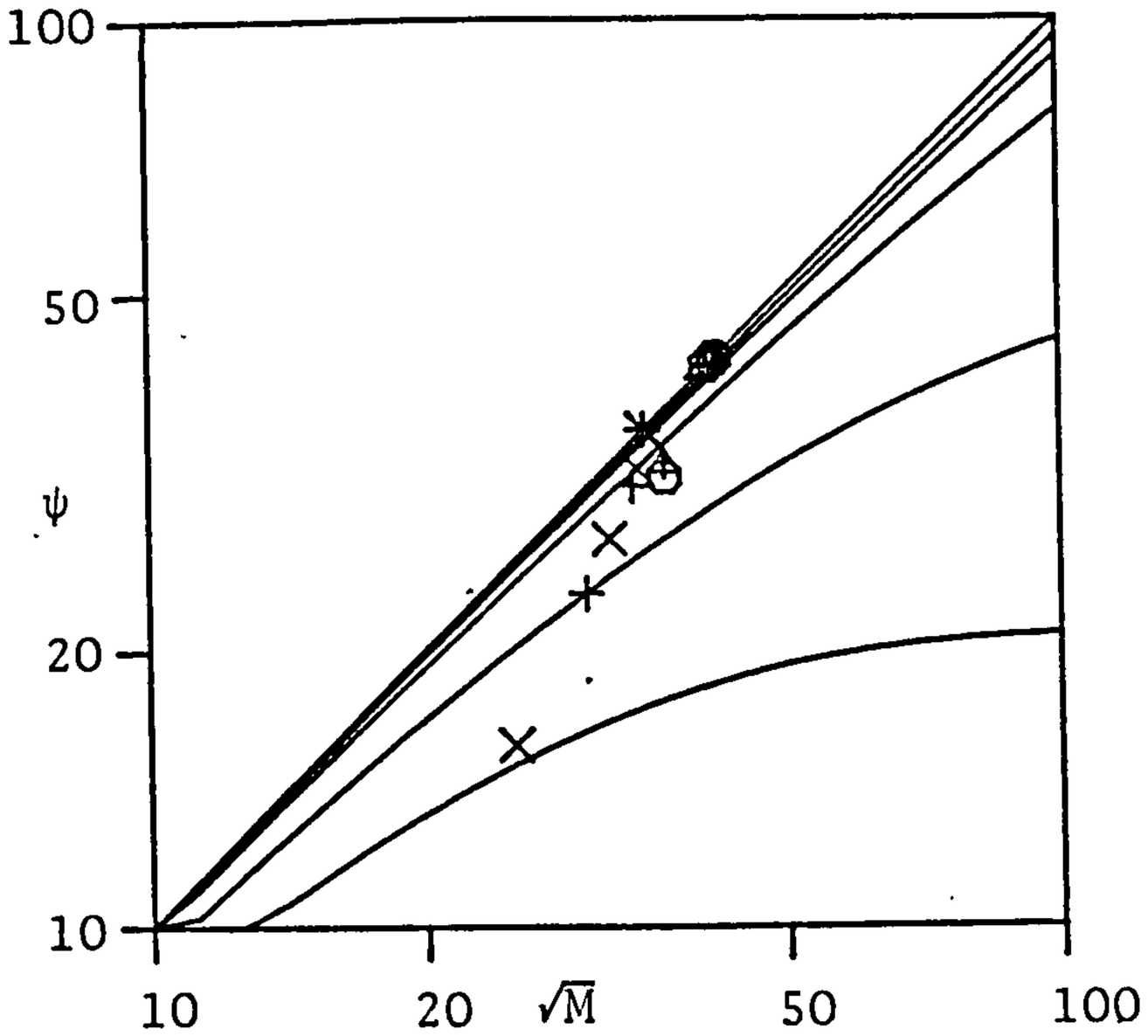
To provide further insight an attempt was made to represent the Kohl absorption predictions in terms of the dimensionless groups used for the reaction model and then

plot typical cases on a diagram similar to Fig. 2.5. Some column profiles predicted by the Kohl model were fitted by considering the liquid phase mass transfer coefficient, interfacial area and the group $H\sqrt{D_c k_c}$ as parameters in the reaction model, the parameters being estimated by comparing the partial pressure profiles at 5 points, see Table 2.5(a) for the values obtained. The selected cases are shown plotted in Fig. 2.10, together with some typical profiles for the reaction model; in each case the absorption conditions are shown at selected points in the column. The Kohl correlation shows a behaviour which is more typical of the instantaneous regime: the values of the enhancement factor are generally higher at the top of the column than for the equivalent case with the reaction model, and the decrease in the enhancement factor is far greater. The profiles therefore tend to be closer to a vertical line as opposed to the pseudo-first order asymptote which is followed more closely by the reaction model. It is apparent that this type of behaviour for the Kohl correlation will be true regardless of the value of the parameter f.

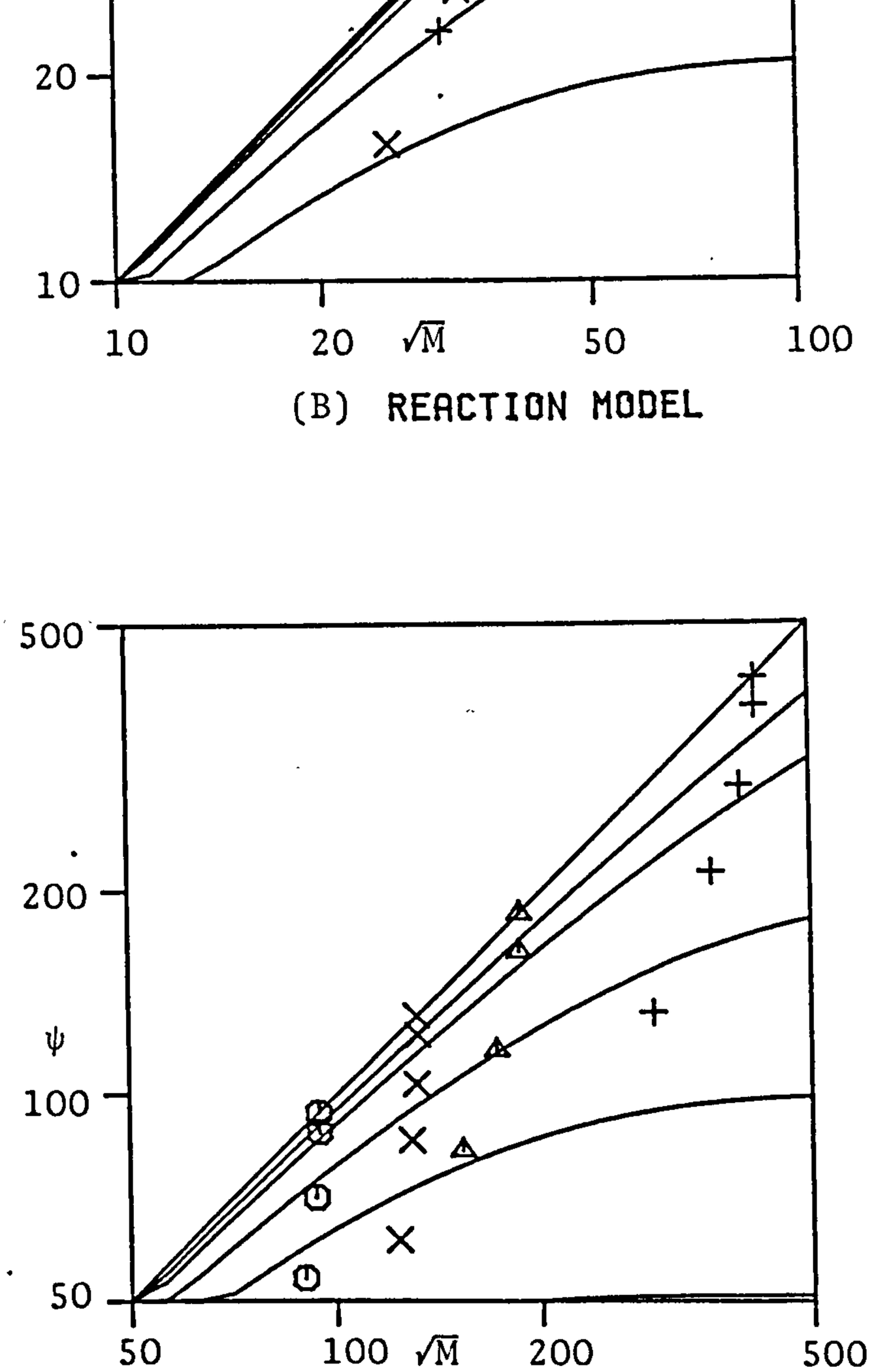
The application of the Kohl model is therefore restricted to conditions close to absorption with instantaneous reaction and hence attempts to use the model outside this region will be unsuccessful. By contrast, the reaction model can, by suitable choice of the parameters, be applied in any of the possible absorption-reaction regimes.

2.6.4. General Column Performance

The variation of exit concentrations with inlet liquid



(B) REACTION MODEL



(A) KOHL MODEL

FIG. 2.10. COMPARISON OF KOHL AND REACTION MODELS IN TERMS OF DIMENSIONLESS GROUPS OF REACTION MODEL

TABLE 2.5(A) FITTING OF KOHL MODEL VALUES PLOTTED IN FIG.2.10

Case	L	P_{CB}(bars)	P_T(bars)	α_B	Values from model fitting		
					k_L	a	b
1	.40E-03	.20	3.32	.3728	.0047	1.41	8.18
2	.30E-03	.20	3.32	.4362	.0028	2.81	8.63
3	.40E-03	.250	3.32	.4252	.0012	8.89	9.14
4	.25E-03	..10	3.32	.32937	$.39x10^{-2}$	.94	8.045

b is the parameter in log $H\sqrt{D_c K_c}$ = b + (c/T) where c is fixed and k_L,a,b are expressed in gm.mole.,cm.,sec.units

Case		Height above base (metres)				
		0	.61	1.22	2.44	6.10
1	$\sqrt{M}$		101.1	105.1	106.5	106.3
	ψ_i		87.4	176.1	760.8	70,930
	ψ		60.55	79.6	99.5	106.2
2	$\sqrt{M}$	152.0	172.7	194.4	210.0	210.6
	ψ_i	82.0	123.3	230.4	785.	37,140
	ψ	68.5	93.68	131.9	184.5	210.1
3	$\sqrt{M}$	330	402.4	443.8	468.2	468.1
	ψ_i	180.0	356.6	664.8	2363	$.154x10^{6}$
	ψ	150	241.9	324.3	424.9	467.4
4	$\sqrt{M}$	139.0	145.5	148.1	148.9	148.6
	ψ_i	82.0	163.3	302.7	1053	$.45x10^{5}$
	ψ	69.0	96.89	117.5	139.0	148.4

TABLE 2.5(B) REACTION MODEL VALUES PLOTTED IN FIG.2.10

Case	L	p_{cB}	p_T	α_B
1	.20E-03	.10	3.32	.367
2	.20E-03	.075	2.5	.367
3	.40E-03	.20	3.32	.3731
4	.40E-03	.25	3.32	.4253

Case		Height above base (metres)				
		0	.61	1.22	2.44	6.10
1	$\sqrt{M}$	41.36	46.09	47.08	47.13	47.07
	ψ	34.80	46.09	47.08	47.13	47.07
2	$\sqrt{M}$	41.33	45.60	47.15	47.13	47.07
	ψ	35.94	45.60	47.15	47.13	47.07
3	$\sqrt{M}$	33.90	38.16	39.21	39.32	39.26
	ψ	25.90	34.05	39.21	39.32	39.26
4	$\sqrt{M}$	28.30	36.01	38.73	39.34	39.26
	ψ	17.68	29.77	35.50	39.34	39.26

carbonation ratio as predicted by both models is shown in Table 2.6. As before, the Kohl model predicts a far greater variation of top partial pressure than does the reaction model. The variation of exit concentrations with inlet liquid temperature, shown in Table 2.7, is perhaps not as large as may be expected. Although an increase in liquid temperature increases the reaction rate constant, this is offset by a decrease in the solubility coefficient. The liquid temperature increases throughout the column, although the temperature difference between the top and bottom remains practically constant. The possible variation of top partial pressure with inlet liquid temperature is comparable to the variation with inlet concentrations, and hence is an effect which should be accounted for in the model.

The difference between the assumptions of isothermal and non-isothermal reactions is shown in Table 2.8. Apart from the obvious difference in the liquid phase temperature the two assumptions lead to very similar results, and this small difference may again be attributed to the opposing variations of the reaction rate and solubility with temperature.

The models considered above have assumed constant total pressure throughout the column. Spatial variation in total pressure can be introduced by the equation:-

$$\frac{dp_T}{dz} = - K_p \qquad (2.72)$$

$$p_T(0) = p_{TB} \qquad (2.73)$$

The parameter K_p was estimated from an empirical

TABLE 2.6 VARIATION OF EXIT CONCENTRATIONS WITH INLET CONCENTRATIONS

Reaction Model

	Inlet liquid concentration α_T		
	.16	.18	.20
p_{cT}	$.102 \times 10^{-3}$	$.129 \times 10^{-3}$	$.171 \times 10^{-3}$
α_B	.38071	.40068	.42064
T_B	39.67	39.67	39.67

Kohl Model

	Inlet liquid concentration α_T		
	.16	.18	.20
p_{cT}	$.156 \times 10^{-3}$	$.272 \times 10^{-3}$	$.483 \times 10^{-3}$
α_B	.38065	.40053	.42031
T_B	39.67	39.67	39.67

TABLE 2.7 VARIATION OF EXIT CONCENTRATIONS WITH INLET LIQUID TEMPERATURE

Reaction Model

	Inlet liquid temperature T_T		
	30	35	40
p_{cT}	$.129 \times 10^{-3}$	$.959 \times 10^{-4}$	$.727 \times 10^{-4}$
α_B	.40068	.40071	.40074
T_B	39.67	44.67	49.68
ΔT	9.67	9.67	9.68

Kohl Model

	Inlet liquid temperature T_T		
	30	35	40
p_{cT}	$.272 \times 10^{-3}$	$.175 \times 10^{-3}$	$.109 \times 10^{-3}$
α_B	.40053	.40062	.40070
T_B	39.67	44.67	49.67
ΔT	9.67	9.67	9.67

Conditions for both Tables: $L = .35 \times 10^{-3} m^3/s$ $p_{cB} = .20$ bars, $p_T = 3.32$ bars $v_I = 2.99 \times 10^{-3}$ kmole/s

TABLE 2.8 COMPARISON OF ISOTHERMAL AND NON-ISOTHERMAL ASSUMPTIONS: THEORETICAL REACTION MODEL

Conditions: $L = .35 \times 10^{-3}$ m^3/s

$V_I = 2.99 \times 10^{-3}$ kmole/s

Isothermal results computed using T = 30°C

$P_{cB} = .20$

Height z m	ISOTHERMAL	NON-ISOTHERMAL	
	Partial pressure p_c, bars	Partial pressure p_c, bars	Temperature T C
6.10	.1221E-03	.1110E-03	30.00
4.88	.5979E-03	.5437E-03	30.02
3.66	.2918E-02	.2656E-02	30.12
2.44	.1401E-01	.1283E-01	30.58
1.22	.6229E-01	.5841E-01	32.65
.000	.2000	.2000	39.09

$P_{cB} = .25$

6.10	.2035E-03	.1785E-03	30.00
4.88	.9962E-03	.8741E-03	30.03
3.66	.4849E-02	.4263E-02	30.19
2.44	.2298E-01	.2040E-01	30.92
1.22	.9603E-01	.8881E-01	34.03
.000	.2500	.2500	41.36

Note: .9603E-01 $\equiv .9603 \times 10^{-1}$

TABLE 2.9 VARIATION OF EXIT CONCENTRATIONS WITH COLUMN PRESSURE DROP

Conditions : $L = .350 \times 10^{-3}$ m^3/sec.

$P_{cB} = .20$ bars

$\alpha_T = .18$

$T_T = 30.0°C$

$P_T = 3.32$ bars

Reaction Model

Overall column pressure drop (bars)	Top partial pressure (bars)	Equivalent Molar flow rate (kmoles/s)	α_B
0	$.1210 \times 10^{-3}$	$.1090 \times 10^{-3}$	.4007
.05	$.1248 \times 10^{-3}$	$.1141 \times 10^{-3}$	.4007
.10	$.1286 \times 10^{-3}$	$.1194 \times 10^{-3}$	.4007

Kohl Model

Overall column pressure drop (bars)	Top partial pressure (bars)	Equivalent Molar flow rate (kmoles/s)	α_B
0	$.2724 \times 10^{-3}$	$.2453 \times 10^{-3}$	.4005
.05	$.2850 \times 10^{-3}$	$.2606 \times 10^{-3}$	.4005
.10	$.2979 \times 10^{-3}$	$.2767 \times 10^{-3}$	.4005

correlation given by Eckert[29] for the pressure drop with pall rings. At the nominal design gas flow rate the correlation predicts an overall pressure drop of .07 bars, see Appendix 1, a value in accordance with those observed on the plant. The effect of the pressure drop on the overall absorption predicted by both models is shown in Table 2.9. For a pressure drop of 0.1 bar, the increase in the molar flow rate of the exit carbon dioxide is predicted by both models to be about 10%. This change is small compared with the possible variation with either inlet liquid or gas concentrations, and therefore it is justifiable to neglect pressure variation within the column.

2.6.5. Development of a Simplified Approximate Model

The two absorption models described are both complex in structure. The reaction model is generally applicable but requires estimation of six parameters: $\sqrt{D_C k_C}$, k_L, H $\sqrt{D_M/D_C}$, k_G and a. The Kohl model has one basic parameter, f, and four additional parameters which could be considered for fitting. It would be both difficult and time consuming to evaluate all these parameters for either model, and so a simpler model is required to enable fitting with greater ease and confidence. In addition, a simple model is more convenient to use in the prediction of steady state operating conditions and control policies.

The region of operating conditions for which a simple model provides an adequate plant description is generally smaller than that for a more complex model; the region over which predictions can be made is likewise limited, although

in on-line applications this problem can be alleviated by updating the model parameters so that an accurate local description is always achieved about the current operating conditions. To ensure that the size of the region of local description is reasonably large, a model form should be chosen which is valid for all possible plant operating conditions. From this aspect, a simplification of the Kohl model cannot be considered because it is valid only for conditions close to instantaneous reaction. The reaction model is general in its applicability, and therefore it is logical to look for a means of simplifying the complex dependence of the enhancement factor upon the other two dimensionless groups.

The general absorption rate expression is

$$N = \frac{\psi(M,c)\,k_L\,aHA}{1+\frac{\psi(M,c)\,k_L aH}{k_G a}}\,p_c \qquad (2.74)$$

where $\sqrt{M} = \sqrt{D_c k_c c_0}/k_L$ and $c = \frac{c_0}{2c^*}\sqrt{\frac{D_M}{D_c}}$

The pseudo-first order model assumes

$$\psi = \sqrt{M}$$

so that (2.74) becomes:

$$N = \frac{a\,AH\sqrt{D_c k_c c_0}}{1+\frac{aH\sqrt{D_c k_c c_0}}{k_G a}}\,p_c \qquad (2.75)$$

Analysis of the results from the full non-isothermal reaction model showed that an approximate relationship is

$$\psi = k''\sqrt{M} \qquad (2.76)$$

The model is therefore of pseudo-first order form:

$$N = \frac{aAk''H\sqrt{D_c k_c c_0}}{1 + \frac{ak''H\sqrt{D_c k_c c_0}}{k_G a}} \; p_c \qquad (2.77)$$

with parameters $(ak''H\sqrt{D_c k_c})$ and $(k_G a)$.

For the parameter values used in the full model the variable term in the denominator is not very significant in determining the absorption rate. This was confirmed in an attempted fitting of the model; the gas phase coefficient assumed widely ranging values without significantly affecting the column profile predicted. The model was therefore simplified to:

$$N = aAk''H\sqrt{D_c k_c} \; \sqrt{c_0} \; p_c \qquad (2.78)$$

The single parameter was estimated by fitting a particular column profile computed by the full non-isothermal model, see Table 2.10. The fitting process was by minimisation of the sum of squared fractional errors in the predicted partial pressure at five points in the column.

The exit concentrations predicted by the full and simple models are compared in Fig. 2.11 over a range of operating conditions. The top partial pressures predicted by both models are in good agreement over a wide range of inlet gas concentration and liquid flow rate. Deviation between the two models can be expected at high exit liquid carbonation ratios because of the very rapid decrease in absorption rate predicted by the full model. However, the results show that the simple model provides an adequate representation of the exit concentrations even for conditions departing from pseudo-first order. Furthermore, the simple

TABLE 2.10 FITTING OF SIMPLE ONE PARAMETER MODEL

Simple model used $H\sqrt{D_c k_c} = 1.842 \times 10^{-4}$

Height z	Full Model		Simple Model	
	p_c	α	p_c	α
Top 6.10	$.1556 \times 10^{-3}$	.1800	$.1559 \times 10^{-3}$	.1800
4.88	$.762 \times 10^{-3}$	.1807	$.765 \times 10^{-3}$	.1807
3.66	$.372 \times 10^{-2}$	.1843	$.373 \times 10^{-2}$	.1843
2.44	$.178 \times 10^{-1}$	.2015	$.177 \times 10^{-1}$	.2014
1.22	$.773 \times 10^{-1}$	.2757	$.739 \times 10^{-1}$	.2713
0.0	.200	.4374	.200	.4374

Conditions: $L = .3 \times 10^{-3}$ m³/s

$p_T = 3.32$ bars

$T_T = 30°C$

$\alpha_T = .18$

$p_{cB} = .20$ bars

TABLE 2.11 COMPARISON OF TOP PARTIAL PRESSURE PREDICTED BY FULL AND SIMPLE MODEL AT $p_T = 3$ bars

Entry Partial Pressure p_{cB}	Liquid flow rate, L		
	$.3 \times 10^{-3}$	$.35 \times 10^{-3}$	$.40 \times 10^{-3}$
.15	.202E-03 (.160E-03)	.184E-03 (.148E-03)	.170E-03 (.140E-03)
.20	.407E-03 (.380E-03)	.320E-03 (.270E-03)	.281E-03 (.245E-03)

The predictions of the simple model are shown in brackets.

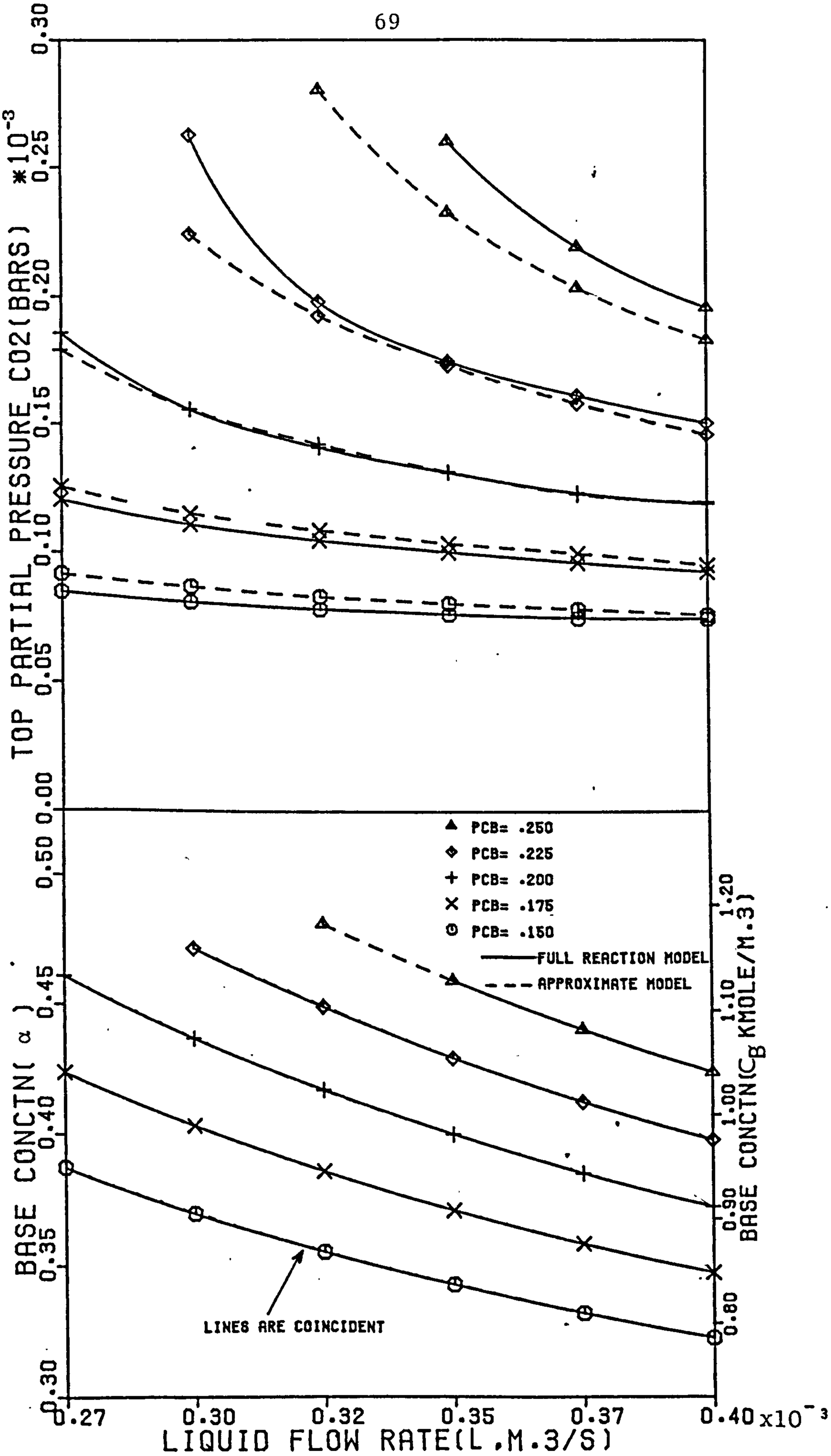


FIG. 2.11. APPROXIMATION TO FULL REACTION MODEL BY FITTED MODEL WITH PSEUDO-FIRST ORDER FORM

model still gives a good approximation to the column composition profiles. In addition the simple model gives a good approximation when the total pressure is varied, see Table 2.11., and clearly the fit could be improved by refitting the parameter.

The model parameters can be fitted from measurements of the liquid and vapour flow rates, either the entry or the exit liquid concentration, and the partial pressure profile. Also available are the temperatures of the liquid leaving each of the packing sections and because the absorption reaction is exothermic this temperature profile can be used in estimating the model parameters. Because only one gas analyser is available to sample the partial pressures, use of the temperature profile is likely to give a more rapid indication of changes in absorption in the column. However, the accuracy of corrections to parameters or model based predictions that can be expected from the temperature profile is dependent upon the magnitude of the heat of reaction. A recursive least squares estimator or Kalman filter is proposed for the on-line estimation of the model parameters and the techniques used to obtain the matrices required for the filter are given in Appendix 3.

The model proposed contains only a single parameter and consequently cannot predict all the responses that could possibly occur. Perhaps the most important of these is the response to a change in the inlet liquid temperature, and for this purpose the correct way of extending the model is to write:

$$\ell n\ (ak'' H\sqrt{D_C k_C}\ ) = k_5 + \frac{k_6}{T} \qquad (2.79)$$

where k_5 and k_6 are parameters to be determined. Obviously the way in which the single parameter model is extended will depend upon experience gained on the plant.

In summary, the simple model has the capability of approximating over a wide range of operating conditions the exit concentrations and profiles given by the full model. The form of the model is sufficiently simple that computation of column profiles is rapid and the parameters are easily updated from plant measurements.

2.6.6. A Special Solution for the Gas Phase for the case of pseudo-first order reaction

If the absorption rate is proportional to the gas phase partial pressure, as it is for pseudo-first order conditions, then a simple analytical approximation can be made to the partial pressure profile, or alternatively the molar flow rate. This approximation can be used to replace the cell description of the gas phase, equation (2.35), in the cell model and it will be shown later how it can be generalised for use in a dynamic model which is fairly complex but also computationally rapid.

The assumption made is that the temperature and free amine concentration remain constant over a certain height of packing, which is conveniently chosen as the cell height if a cell description of the liquid phase is used. The equation

$$\frac{\partial v_c}{\partial z} = -N = -\frac{a\ A\ p_T\ H\sqrt{D_c k_c c_0}}{(1+\frac{H\sqrt{D_c k_c c_0}}{k_G})(1+\frac{v_I}{v_c})} \qquad (2.80)$$

can then be integrated analytically to give

$$(v_{cj-1}-v_{cj})+v_I \ln(\frac{v_{cj-1}}{v_{cj}}) = \frac{aAp_T\sqrt{D_c k_c c_0}}{1+\frac{H\sqrt{D_c k_c c_0}}{k_G}} \cdot \Delta z \qquad (2.81)$$

Where Δz is the cell height,

v_{cj} = molar flow rate of CO_2 at height $j\Delta z$

and $v_{cj} = v_{cB}$ for $j = 0$.

Equation (2.81) has to be solved recursively for v_{cj} and the following expression was found to be numerically very stable, seldom requiring more than two iterations:-

$$v_{cj} = v_{cj-1}\ \exp\{(v_{cj-1}-v_{cj}-k^*)/v_I\} \qquad (2.82)$$

where $k^* = \frac{a\ A\ p_T\ H\sqrt{D_c k_c c_0}}{1+\frac{H\sqrt{D_c k_c c_0}}{k_G}} \cdot \Delta z$

The free amine concentration is known, and the absorption rate parameters are evaluated at the appropriate liquid phase temperature.

Starting from the bottom, equation (2.82) can be applied sequentially up the column to find the molar flow rate of carbon dioxide at heights $j\Delta z$ corresponding to liquid cell boundaries. The transfer of carbon dioxide into cell j is easily calculated from

$$N_j = (v_{cj-1}-v_{cj}) \qquad (2.83)$$

If a dilute gas phase description is used then equation (2.82) is replaced by the following, which does not require iteration:-

$$p_{cj} = p_{cj-1} \exp\left(-\frac{k^*}{v_I}\right) \qquad (2.84)$$

2.7.1. Simulation of the dynamics of column start up

A simulation of a typical column start up was used for studying the dynamic responses and computational requirements of the various models. The operating, initial and boundary conditions chosen are given in Table 2.12. At initial conditions the liquid flowing through the column contains a residual amount of carbon dioxide due to incomplete liquid stripping on the previous occasion that the plant was operated. The simulation is started at time zero with the introduction of carbon dioxide at the base of the column.

2.7.2 Simulation of start up using the cell model

The cell representation was used to consider the effects of liquid and gas phase mixing on the dynamics and steady state behaviour of the column. Two models were employed so that the effects of liquid and gas phase mixing could be assessed separately and in all cases the reaction model for the absorption rate was used. The first model consisted of a cell representation for the liquid phase and, assuming negligible gas phase hold up and dispersion, the analytic solution for the gas phase described in Section 2.6.6. Shown in Fig. 2.12 are exit concentration responses computed using different cell sizes, and it is clear that

TABLE 2.12. INITIAL AND BOUNDARY CONDITIONS FOR START UP PROBLEMS

Liquid flow rate L = $.35 \times 10^{-3}$ m^3/s

Total pressure p_T = 3.32 bars

Entry liquid temperature = 30°C

At t = 0 $c(z) = .4464$ kmoles/m^3) $0 \leq z \leq Z$

$p_c(z) = 10^{-7}$bars)

Entry gas flow rate

$v_I = 2.99 \times 10^{-3}$ kmole/s

(carbon dioxide free)

t > 0 $c(Z) = .4464$ kmoles/m^3

$p_c(0) = p_{cB} = .20$ bars

Total molar flow rate of

entry gas = $v_c + v_I = 3.18$ gmole/s

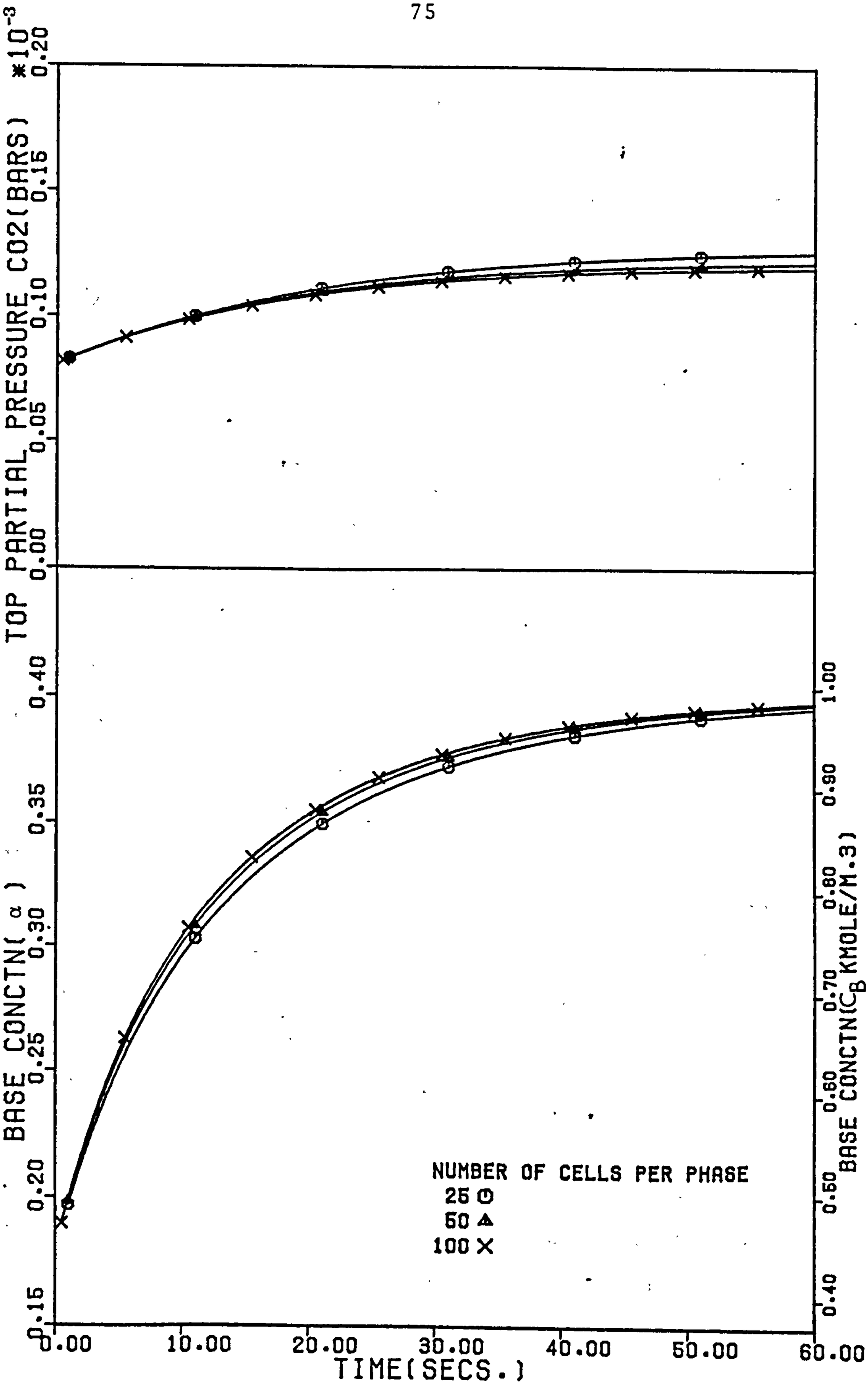


FIG. 2.12. SIMULATION OF START UP USING CELL MODEL FOR LIQUID PHASE

over the range chosen, variation in cell size has negligible effect on either of the two concentrations. The final steady state values are given in Table 2.13 and compared with those of the plug flow model which represents the limit of no dispersion. From the work of De Maria and White[23] a Peclet number of approximately two can be expected, and in this case would correspond to a model with about 200 cells. For normal operating conditions, up to the column loading and flooding limits, it is reasonable to expect that liquid mixing will not be greatly influenced by the gas flow. Therefore, it is reasonable to employ a plug flow description for the liquid phase.

In the second model the analytic gas phase solution was replaced by a cell description to permit an assessment of the gas phase mixing. Because the gas phase residence time is relatively small the use of a cell representation for the gas phase imparts considerable stiffness to the model equations, even if only a few cells are used: step lengths of 0.5 second or less were required for integration by a Runge Kutta procedure, compared with about 1 or 2 seconds for the previous model. However, the model was used to show that gas phase dispersion effects are not negligible for the gas phase, although the effect on the liquid concentration profile is practically insignificant. Steady state values of the top partial pressure and exit liquid concentration are given in Table 2.14 for different cell sizes. From the work in the literature it is expected that gas phase mixing, dependent upon packing type and flow rate, would be represented by Peclet numbers between .1 and 1 which would

TABLE 2.13 STEADY STATE FOR LIQUID PHASE CELL MODEL WITH PLUG FLOW FOR GAS PHASE

Number of liquid cells	Top partial pressure (bars)	Exit liquid concentration α_B
25	$.128 \times 10^{-3}$	.3994
50	$.123 \times 10^{-3}$	.3999
100	$.121 \times 10^{-3}$	.4003
Plug flow for both phases	$.120 \times 10^{-3}$	.4007

TABLE 2.14 STEADY STATE FOR CELL MODEL FOR BOTH PHASES

Number of cells in each phase	Top partial pressure (bars)	Exit liquid concentration α_B	Time step for Runge Kutta integration (sec.)
25	$.336 \times 10^{-3}$	.4003	1
50	$.206 \times 10^{-3}$	.4003	0.5
.100	$.154 \times 10^{-3}$	.4003	0.25

Time steps given are approximate limiting step rises for a gas phase residence time of 8 seconds.

correspond approximately to 10 and 100 cells in the cell model. As a consequence gas phase mixing could be significant and should be represented in a general model, although the very severe restriction on step length prevents the cell representation from being used.

2.7.3. Simulation of start up by characteristics

The same problem of start up was solved by use of the method of characteristics, and having made the transformation for the gas phase equation as described in Section 2.5.3., the solution could be found to an adequate accuracy by use of a grid containing twenty lines. The computation time for the same period of simulation was found to be appreciably less than that with the cell model. Further computational savings were found to be possible with the assumption of zero gas phase hold up, which simplifies the characteristic grid, and in addition permits the use of the analytical gas phase solution in place of an integration procedure. A model employing characteristics for solution together with the assumption of negligible gas phase hold up appeared to offer the potential of a computationally rapid model. Furthermore, the assumption of negligible gas phase hold up allows a time instantaneous solution for this phase to be used, and dispersion effects can be included in such a solution.

2.7.4. Comparison of the dynamics of the Kohl and reaction models

Analysis of the steady state predicted by the reaction and Kohl absorption rate models has already shown a

difference between the two, and in this section the analysis is carried further by considering dynamic responses. The method of characteristics was used to compute the responses, shown in Fig. 2.13, given by the two absorption rate models to a sequence of disturbances shown in Table 2.15. The column is at steady state shortly after 100 seconds and is then subjected to an increase and then a decrease in the entry carbon dioxide partial pressure. The liquid responses given by the two models are similar, which may be expected as virtually all the carbon dioxide is absorbed, and in both cases the reaction model is seen to respond slightly more rapidly. The top partial pressure responses exhibit a greater difference; the Kohl model shows a far greater variation than the reaction model, and furthermore the responses to a change in inlet partial pressure take longer to achieve a steady state.

The greater variation in the exit partial pressure predicted by the Kohl model is partly explained by the fact that, as a consequence of being empirical, the Kohl expression must represent the effect of gas phase dispersion which increases the variation in the exit partial pressure. It is shown later that the response predicted by the reaction model is increased in magnitude and becomes slower when gas phase dispersion is introduced and this will tend to make the response of the reaction model more like that of the Kohl model. For a change in inlet liquid composition the responses are similar in the time taken to reach the new steady state. The final part of the simulation is a steady decrease in the inlet partial pressure, to which both models respond similarly.

TABLE 2.15 INITIAL CONDITIONS AND SEQUENCE OF DISTURBANCES FOR COMPARISON OF REACTION AND KOHL MODELS SHOWN IN FIG.2.13

Liquid flow rate $.4 \times 10^{-3}$ m³/s.

Total pressure = 3.32 bars

Fractional liquid hold up ϕ_L = .10

Gas phase residence time τ_G = 4 seconds

Entry gas flow rate v_I = 2.99×10^{-3} kmole/s

at t=0 c(z) = .4464 kmole/m³) $0 < z < Z$

$p_c(z) = 10^{-7}$bars)

Time	Disturbance
0	$p_{cB} = p_c(0) = .20$ bars
	$c(Z) = .4464$
150	$p_{cB} = .25$ bars
250	$p_{cB} = .20$ bars
300	$c(Z) = .496$ or $\alpha_T = .20$
400	$c(Z) = .4464$ or $\alpha_T = .18$
500 to 700	$p_{cB} = .20$ {1-(t-500)/200}

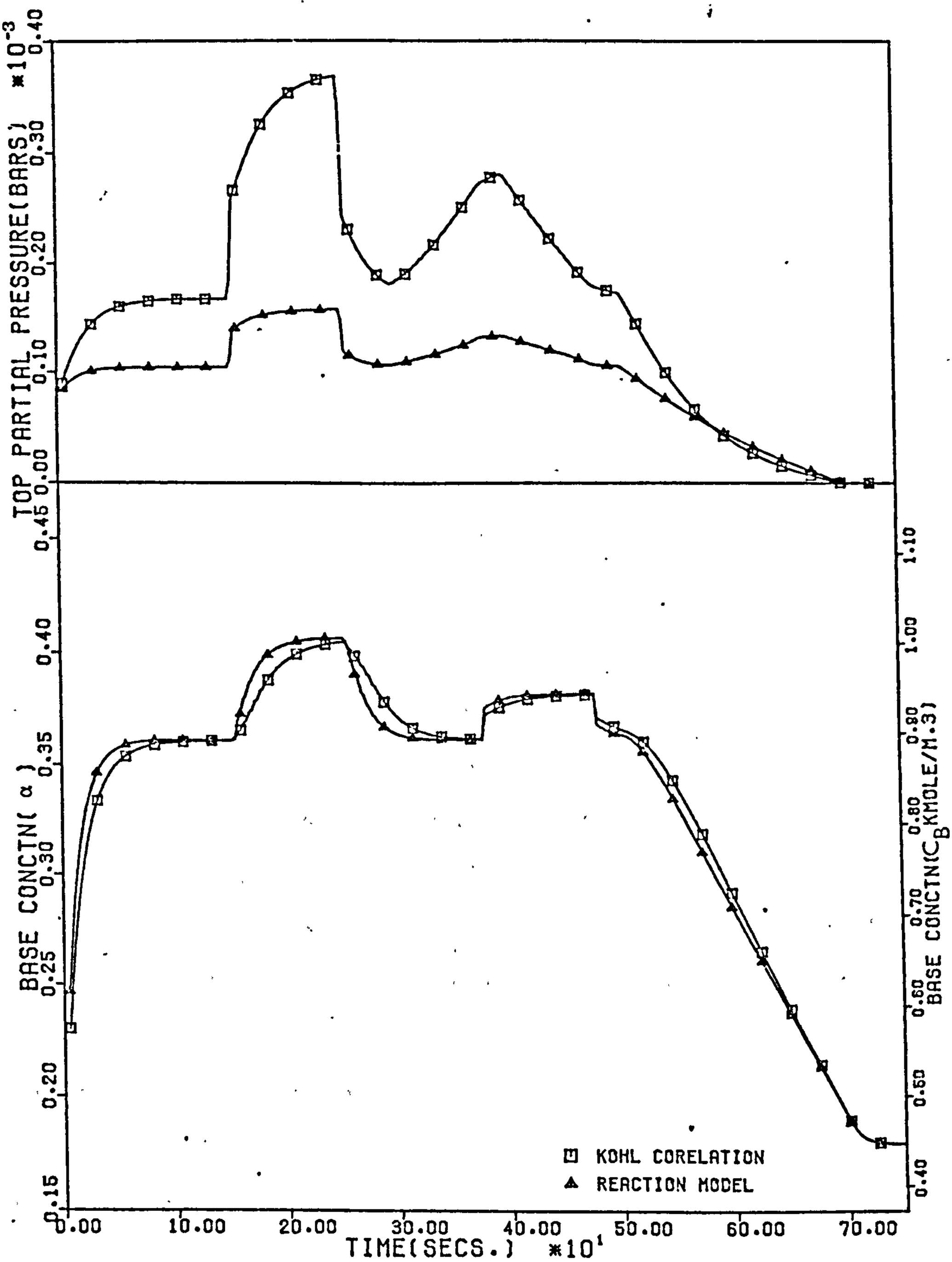


FIG. 2.13. COMPARISON OF DYNAMICS OF KOHL AND REACTION MODELS

2.8.1. Model Development and Simplification

The simulations described in the preceding sections have shown the general form of the responses that can be expected, and of greater importance, the factors which are of significance and some of those which can be neglected. In addition, simulations have been carried out with various models so that their numerical requirements and computation times can be compared, and typical values for the models considered are given in Table 2.16. It is clear that a cell description for either the gas or liquid phase requires a considerable amount of computation in comparison to the other models. This is undoubtedly due to the low gas phase hold up and for the liquid phase the use of a cell description where mixing is relatively small. As a consequence, a plug flow description of the liquid phase, leading to a solution by characteristics is far more efficient. A considerable time saving for the methods employing characteristics was made by assuming negligible gas phase hold up and replacing the integration procedure for the partial pressure profile by the algebraic solution described in section 2.6.6.

The main step in the simplification process is taken by assuming negligible gas phase hold-up as in practice the residence time for the gas phase is about 8 seconds, compared with 60 seconds or more for the liquid phase. The dynamics of the column are therefore dominated by those of the liquid phase. As a consequence of this assumption the dispersion term can be retained in the gas phase equation

without much difficulty, and this, therefore, overcomes the principal problem with the use of a plug flow description. The following equations therefore should offer an adequate description of the column together with the possibility of an efficient solution:-

$$-\frac{D_G A}{\acute{R}T_G}\frac{d^2p_c}{dz^2} + \frac{dv_c}{dz} + N(p_c,c,T) = 0 \qquad (2.85)$$

$$\frac{\partial Lc}{\partial z} + N(p_c,c,T) = A\frac{\partial}{\partial t}\phi_L c \qquad (2.44)$$

$$\rho c_p \frac{\partial}{\partial z} LT + N(p_c,c,T)\Delta E = A\rho c_p \frac{\partial}{\partial t}\phi_L T \qquad (2.45)$$

$$\frac{\partial L}{\partial z} = A\frac{\partial \phi_L}{\partial t} \qquad (2.20)$$

$$L = k_1 + k_2\phi_L \qquad (2.27)$$

This set of equations can be conveniently solved by using a characteristics solution for the liquid phase, and for the gas phase a development of the analytic solution described previously. The solutions for liquid composition and temperature are linearly dependent so that it is only necessary to solve (2.44) for the composition and then the temperature can be obtained from the linear relationship (2.61). At each time instant the liquid composition profile is specified by the current values in the solution of the ordinary differential equations used in the characteristic grid. The derivatives of these equations contain the absorption rate and so this has to be computed at each grid point in the column from the composition and temperature profiles together with the corresponding instantaneous

solution for the gas phase. The grid used for the characteristic solution can easily be extended to include the case of varying liquid flow rate and hold up; the construction of the grid and the differential equations employed are described in detail in Appendix 2.

The solution of equation (2.85) at each time step is based upon the assumption presented in 2.6.6.: that over a small height increment, which will be specified by the characteristic grid, the temperature and free amine concentration remain constant. The inclusion of the dispersion coefficient requires slightly more computation than the plug flow solution because of the split boundary value problem. Similar to the case with reactors the iteration procedure is most stable if the partial pressure profile is computed from an estimated exit boundary condition which is adjusted until the entry conditions are satisfied.

New spatial co-ordinates are therefore defined:

$$s = Z - z \tag{2.86}$$

and equation (2.85) is re-written as:

$$-\frac{D_G A}{R' T_G}\frac{d^2 p_c}{ds^2} - \frac{dv_c}{ds} + N(p_c, c, T) = 0 \tag{2.87}$$

and the relevant boundary conditions are:

$$\left.\begin{aligned} \frac{dp_c}{ds} &= 0 \quad \text{and } p_c = p_{cT} \quad \text{at } s = 0 \\ v_{cB} &= v_c + \left(\frac{D_G A}{R' T_G}\right)\frac{dp_c}{ds} \quad \text{at } s = S \end{aligned}\right\} \tag{2.88}$$

Starting from the top of the column, with an estimate of the top partial pressure, equation (2.87) is used sequentially

to compute the partial pressure and its first derivative at all heights $j\Delta s$ from the top of the column, where s is the height increment used for the liquid composition profile. Equation (2.87) is written as

$$-\left(\frac{D_G A}{R' T_G}\right)\frac{d^2}{ds^2} p_c - \frac{v_I p_T}{(p_T - p_{cj-1})^2}\frac{dp_c}{ds} + k_j p_c = 0 \qquad (2.89)$$

where

$$k_j = \frac{aAp_T H\sqrt{D_c k_c c_0}}{1+(H\sqrt{D_c k_c c_0}/k_G)} \cdot \Delta s \qquad (2.90)$$

with $c_0 = M_m - (c_{j-1}+c_j)$

and the absorption parameters evaluated at the mean of the temperatures at the points j-1 and j.

Equation (2.89) can be solved analytically, and the solution used to compute the partial pressure and its first derivative at $j\Delta s$ from those at $(j-1)\Delta s$:

$$p_c(j\Delta s) = A_1 \exp(m_1 \Delta s) + A_2 \exp(m_2 \Delta s) \qquad (2.91)$$

where m_1, m_2 are the roots of the characteristic equation of (2.89):

$$-\frac{D_G A}{R' T_G} m^2 - \frac{v_I p_T m}{(p_T - p_{cj-1})^2} + k_j = 0 \qquad (2.92)$$

The coefficients A_1, A_2 are defined by the conditions at $(j-1)\Delta s$:-

$$p_c((j-1)\Delta s) = A_1 + A_2 \qquad (2.93)$$

$$\frac{d}{ds} p_c((j-1)\Delta s) = m_1 A_1 + m_2 A_2 \qquad (2.94)$$

These equations are applied sequentially down the column until the bottom is reached, where the following is computed:

$$F = -v_{cB} + \frac{v_I}{p_T} p_c(S) + \frac{D_G A}{R' T_G} \frac{d}{ds} p_c(S) \qquad (2.95)$$

If the top partial pressure has been chosen correctly F is zero and the boundary condition in equation (2.88) is satisfied. Generally this is not true, so a Newton Raphson technique is used to update the top partial pressure $p_c(0)$ until F is less than a specified value. It was found in practice that this iteration converged very rapidly indeed, usually after one or at the most two corrections.

The Kohl absorption rate equation can also be employed in which case equation (2.90) is changed to

$$k_j = (K_G a)\, A[1 - (p_c^*/p_{cj-1})] \qquad (2.96)$$

where p_c^* and $(K_G a)$ are evaluated using the appropriate liquid phase conditions.

The gas phase solution is conveniently combined with the dynamic solution for the liquid phase to give a model which is comprehensive and computationally rapid, as may be seen from Table 2.16. It was found that a characteristic grid using 20 lines at any time instant gave solutions which were sufficiently accurate for normal purposes.

In order to assess the error caused by the assumption of negligible gas phase hold up a comparison was made with the cell model. The results computed, shown in Fig. 2.14, consist of the simulation of a start up followed by the response to an increase in the inlet partial pressure, and at a later time a decrease in the inlet liquid concentration. The disturbances used are given in Table 2.17, and values of the Peclet number were selected to give reasonable agreement between the two models. There is good agreement between the dynamics of the two models at both the levels

TABLE 2.16 APPROXIMATE COMPUTATIONAL SPEEDS OF THE MODELS

Model	Computation time in seconds (CDC 6400) for 100 seconds of simulation
Full non-isothermal model Characteristic grid including gas phase hold up (30 lines)	10
Isothermal model characteristic grid including gas phase hold up (30 lines)	7
Isothermal model Cell model: 50 cells per phase	11
Isothermal model Characteristics for liquid phase + integration for gas phase (hold up assumed negligible)	6.5
Isothermal model Characteristics for liquid phase + analytic solution for gas phase (40 lines)	2.3
As above, but with 20 lines	0.8
Full model described in 2.8.1 Non-isothermal model Characteristics for liquid phase with variable grid (20 lines) Analytic solution for gas phase with dispersion	0.9

TABLE 2.17 CONDITIONS AND DISTURBANCES USED FOR COMPARISON OF FULL DISPERSION MODEL WITH CELL MODEL IN FIG. 2.14

Gas phase residence time 8 seconds

ϕ_L = .10

L = .35 x 10^{-3} m^3/s

p_T = 3.32 bars

v_I = 2.99 x 10^{-3} kmole/s

α_T = .18

Initial conditions:

c(z) = .4464 (α= .18) $0 \leq z \leq Z$

p_{cB} = 0

then: $0 < t < 75$ p_{cB} = .20

$t > 75$ p_{cB} = .25

$t > 150$ L = .40 x 10^{-3} m^3/s

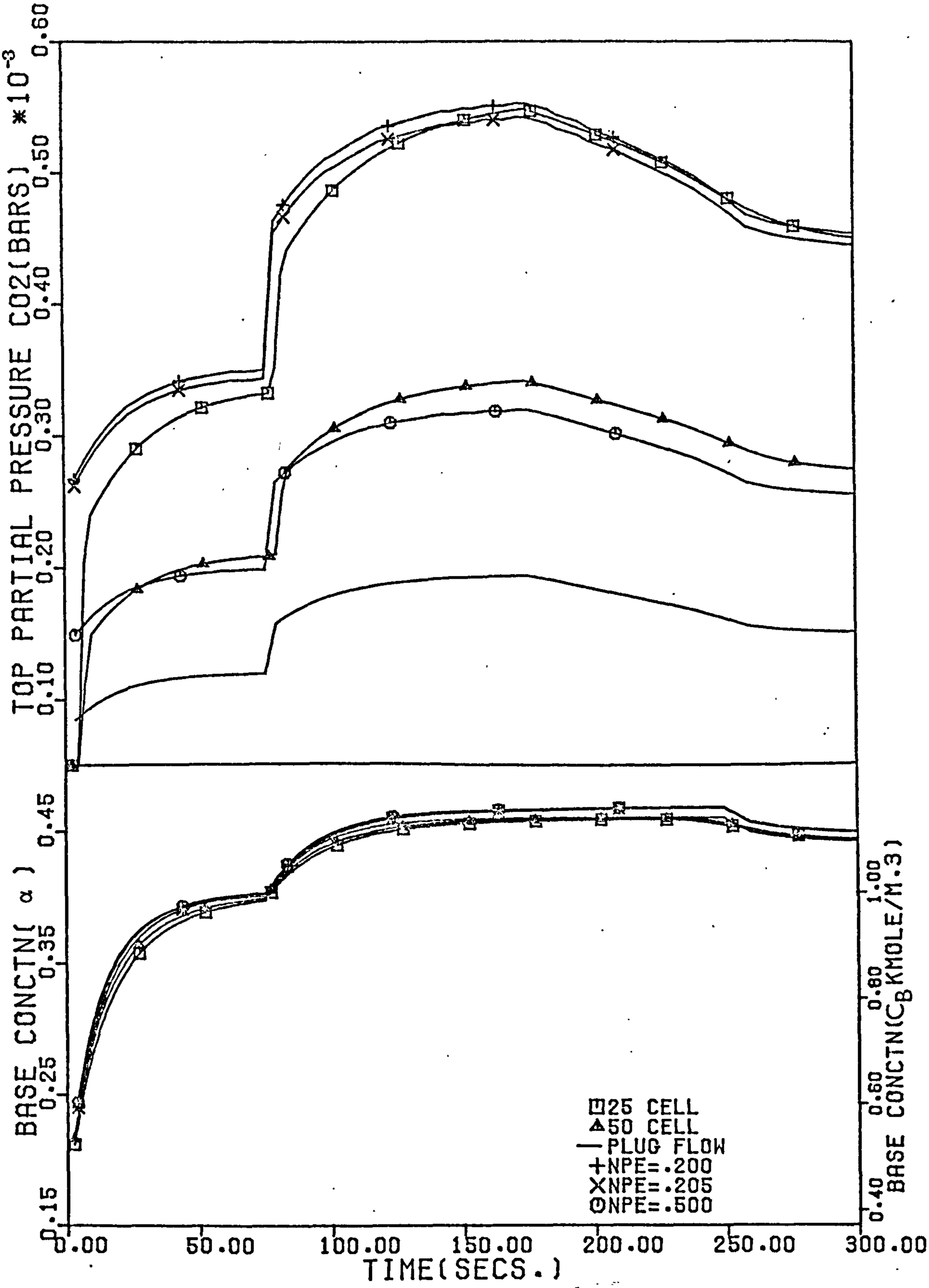


FIG. 2.14. COMPARISON OF RESPONSES USING CELL MODEL AND MODELS ASSUMING NEGLIGIBLE GAS PHASE HOLD UP

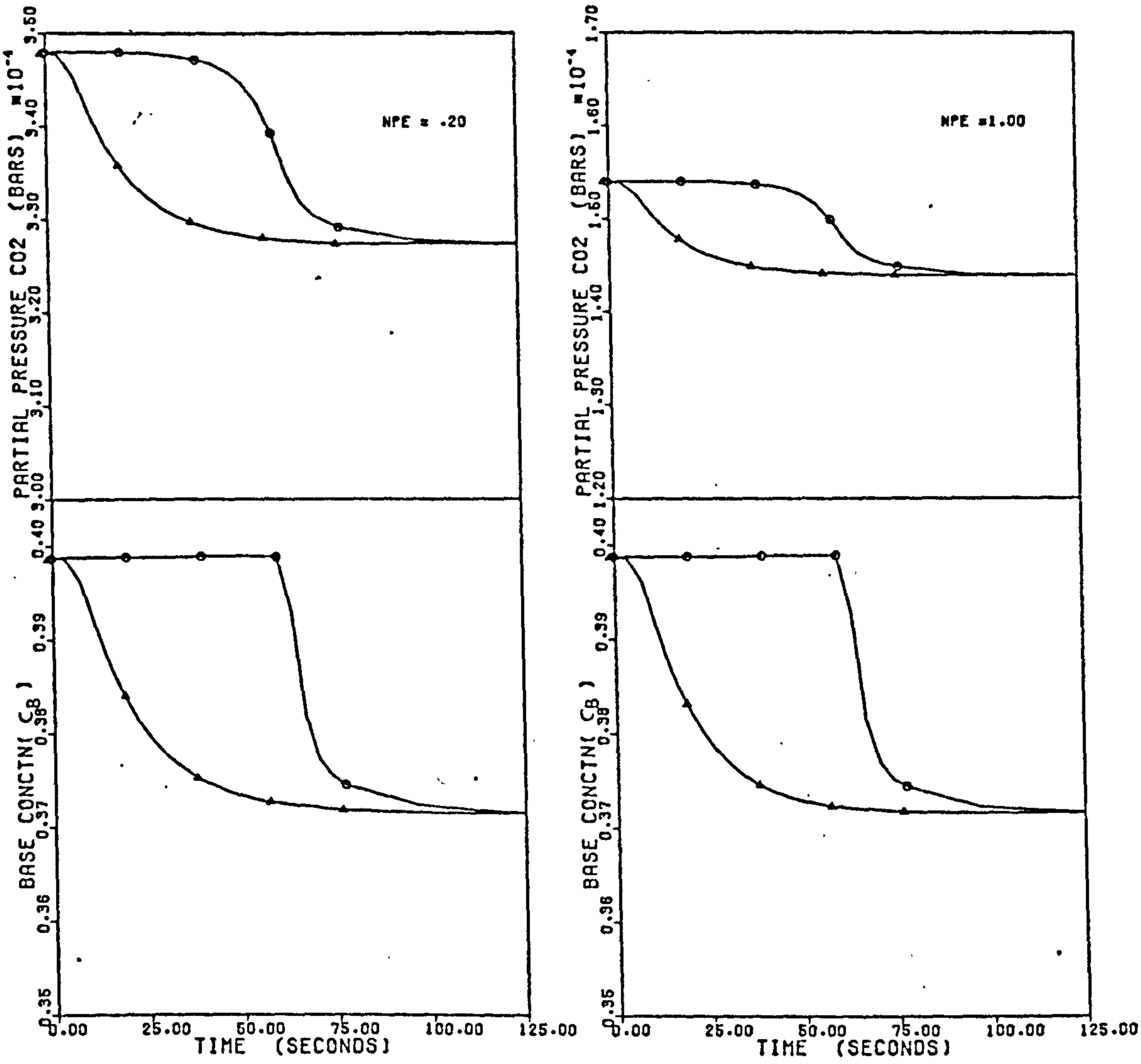
of dispersion considered, and as a consequence the assumption of negligible gas phase hold up is justified. It is also interesting to note, as may be expected, that the magnitude of the partial pressure responses increases as the dispersion increases, and also that the exit liquid response becomes slightly slower. It is difficult to say a priori the precise magnitude of dispersion that can be expected because this is dependent upon the packing characteristics and the loading of both the phases. However, it is clear that dispersion effects will be present.

The proposed model introduces only two more parameters to describe the dynamic state and as a consequence should be fairly simple to fit from experimental data.

2.8.2. Simulation of Column Response to change in inlet liquid flow rate

The response of the column to a change in inlet liquid flow rate was computed using the general model described previously. Comparative simulations were made using the alternative assumptions that the change in liquid flow rate transmits: (i) immediately throughout the column; (ii) according to the flow hold up model described in section 2.3.

The responses were computed for both the absorption models and at different Peclet numbers to assess any possible difference in behaviour. In all the responses, examples of which are shown in Figs. 2.15 and 2.16, the significantly different behaviour arising from the two assumptions is clearly evident. Repetition of the responses using the cell model showed, as expected, that the liquid phase dispersion has only negligible affect on the dynamics.

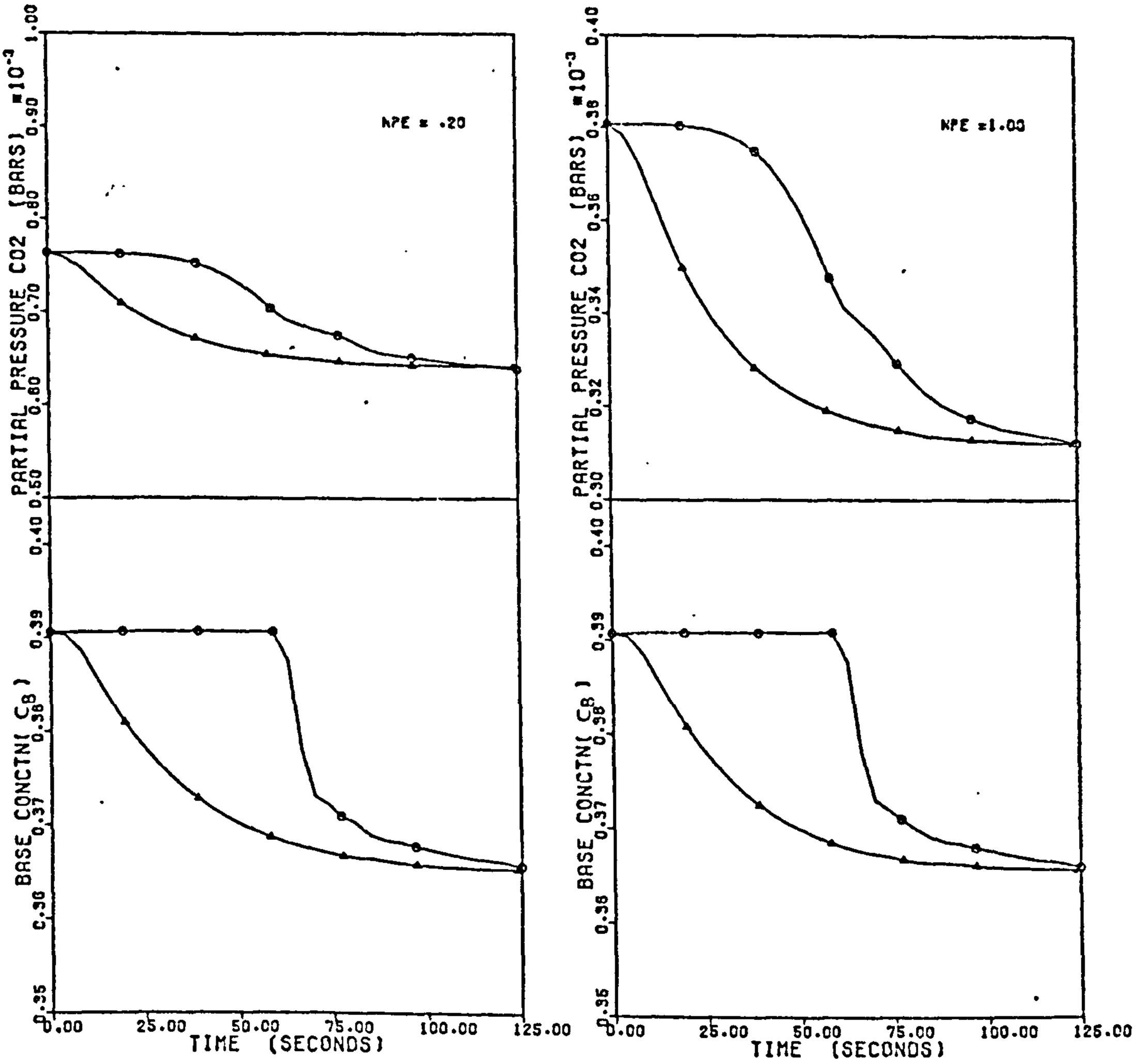


$L = (-.115+5.15\phi)x10^{-3}$

L changed from .35 to $.40x10^{-3}$ at t=0

⊙ FLOW TRANSIENT COMPUTED
▲ FLOW TRANSMITS IMMEDIATELY

FIG. 2.15 RESPONSE TO CHANGE IN INLET LIQUID FLOW RATE: REACTION MODEL



Data as for FIG.2.15

○ FLOW TRANSIENT COMPUTED
▲ FLOW TRANSMITS IMMEDIATELY

FIG. 2.16. RESPONSE TO CHANGE IN INLET LIQUID FLOW RATE: KOHL MODEL

The appreciable delay in the response of the exit concentrations is due to the time required for the liquid transient to reach the lower section of the column where the majority of the absorption occurs. The rate at which liquid transients propagate down the column depends upon the variation of liquid hold up with flow rate, as expressed by the coefficient k_2 in equation (2.27). This is dependent upon the packing used, and the operating conditions, which are assumed here to be below the loading and flooding limits. The parameter values selected are considered to be realistic: the coefficient k_2 is in accordance with liquid propagation rates observed on the real column, and k_1 was chosen to give a realistic value for the liquid hold up.

There is no striking difference between the dynamic responses of the Kohl and reaction models, except that the Kohl model predicts a greater change in top partial pressure, which is in accordance with the steady state behaviour. Similarly, the Peclet number has the greatest influence upon the difference between the initial and final top partial pressures rather than on the dynamic response itself.

The simulations therefore show that the liquid dynamics can be of considerable significance in any form of absorption column where the majority of the absorption is near the base, as is generally the case. The significance is accentuated by a slow rate of propagation of liquid transients, or a long column length.

2.8.3. Response to changes in total pressure

The total pressure within the column may vary with time due to changes in operating conditions, and consequently

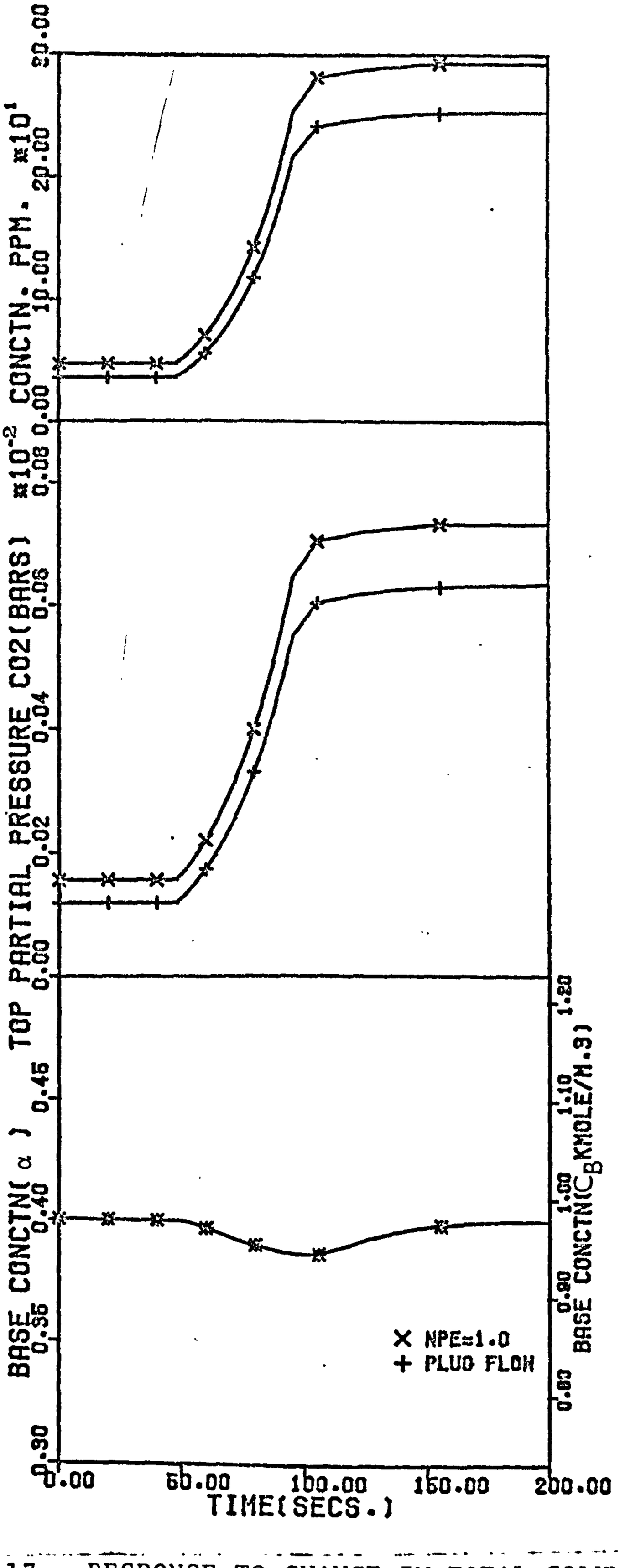


FIG. 2.17. RESPONSE TO CHANGE IN TOTAL COLUMN PRESSURE FROM 3.32 to 2.5 BARS

this will affect the amount of carbon dioxide absorbed. The total pressure influences the absorption rate and also the gas phase hold up; however, because the latter is small, changes in pressure pass very rapidly through the column. The assumption is therefore made that the total pressure remains uniform throughout the column even though it may be changing with time.

The column response to a decrease in pressure was computed using the plug flow and general models. The responses according to both models are very similar, as shown in Fig. 2.17, and it is interesting to note that whilst the top partial pressure increases monotonically with time, the liquid concentration exhibits an underdamped response. Similar responses were obtained for an increase in total pressure. The explanation is that initially in the lower part of the column, the absorption rate, and consequently the liquid concentration, decrease with the decrease in total pressure, but this is offset at a later time by the arrival of liquid containing an increased concentration of carbon dioxide due to the general increase in partial pressure throughout the column. At the new steady state the absorption rate in the upper parts of the column shows an increase over the initial state, but the net effect is a reduction in the total absorption because the majority of the absorption is achieved in the lower part of the column, where the absorption rate has decreased.

2.9. Conclusions

To represent the absorption of carbon dioxide by MEA

the reaction model has been shown to be preferable to the empirical Kohl expression which is restricted to the instantaneous reaction absorption regime. Furthermore, for the particular column considered it is likely that the absorption rate is approximately pseudo-first order, and under such conditions a very simple model can be proposed. This expression is also valid for small deviations from pseudo-first order conditions and since it contains only very few parameters it should be quite easy to fit from experimental data. A procedure employing the column temperature profile and some composition measurements has been suggested for the on-line estimation of the parameters in this simple model.

From an analysis of mixing cell models it can be expected that dispersion is significant in the gas phase but negligible in the liquid phase. In addition it has been shown that the gas phase hold up has only a small effect on the dynamic responses of the column compositions, and as a consequence the dynamics are dominated by those of the liquid phase. This enables a comprehensive yet computationally rapid model to be written, employing characteristics for solution of the liquid phase compositions combined with an algebraic solution for the carbon dioxide partial pressure profile. The dynamic model proposed uses the simple absorption rate model and introduces only two more parameters to define the dynamics for the liquid phase.

The model has been used to show the importance of the liquid dynamics: there is an appreciable delay in the response to a change in the liquid flow rate due to the time

required for the flow change to penetrate to the lower parts of the column where the majority of the absorption takes place. However, as may be expected, both ends of the column respond almost immediately to a change in column pressure.

It is interesting to consider, as a consequence of the results obtained in this chapter, the problem of controlling the top partial pressure of carbon dioxide. This has to be controlled to be less than a specified limit, and the principal disturbances entering the column will be changes in the inlet molar flow rate of carbon dioxide. At low liquid outlet concentrations the top partial pressure is relatively insensitive to the liquid flow rate, so that even a moderate increase in the inlet carbon dioxide flow rate would require a large increase in liquid flow rate to restore the top partial pressure to its original value. Under such circumstances control could be poor and it may be necessary to use some control in addition to the absorbent circulation rate. The controls that could be considered include the column pressure, inlet liquid temperature and residual carbon dioxide concentration. Although the top partial pressure is sensitive and responds rapidly to the total column pressure it is probably impractical to consider the pressure as a control. The inlet liquid temperature could be considered and the range of control achieved will depend upon the capacity and operation of the absorbent cooler. It is likely that the range of control achieved will be small and as a consequence it will be necessary to consider the inlet liquid concentration. Because of the delay between changes in the steam rate

and the inlet liquid concentration it would be worthwhile to consider the use of feedforward control. There is therefore an interesting problem of selecting the steady state operating conditions for maximum energy economy together with the control system to maintain the specified top partial pressure.

For the purpose of specifying the absorbent recirculation rate and stripper duty for a given absorption duty it is necessary to have some representation of the desorption column. Furthermore, to consider the control of the complete MEA gas cleaning process it is necessary to have a dynamic model of the desorption column, particularly in the light of the problem discussed above. Both the dynamic and steady state aspects of the desorption column are considered in the next chapter.

2.10. Nomenclature for Chapter 2.

a	interfacial area per unit volume of packing	m^{-1}
A	column cross section area	m^2
A_1, A_2	coefficients in partial pressure solution, eqtn. (2.91)	
c	concentration of CO_2 in liquid solution	$kmole/m^3$
c_0	concentration of free amine	$kmole/m^3$
c_p	specific heat of liquid	$kJ/kg°C$
c*	concentration of CO_2 at interface	$kmole/m^3$
d_p	packing size	m
D_C	diffusivity of CO_2	m^2/s
D_G	gas phase dispersion coefficient	m^2/s
D_H	thermal diffusivity	m^2/s
D_L	liquid phase dispersion coefficient	m^2/s
D_M	diffusivity of MEA	m^2/s
f	parameter in Kohl absorption expression (2.18)	
H	solubility coefficient for carbon dioxide	$kmole/m^3bar$
k_1, k_2	parameters in linear liquid flow hold up relationship (2.27)	
k_3, k_4	parameters in linear liquid flow hold up relationship (2.39)	
k_c	second order reaction rate constant	$m^3/kmole.s$
k_G	gas phase mass transfer coefficient	$kmole/m^2s.bar$
k_L	liquid phase mass transfer coefficient	m/s
K′	constant in non-linear liquid hold up flow relationship (2.21)	m^3/s

k''	parameter defined by equation (2.76)	
K_G	overall gas phase mass transfer coefficient	kmole/m^2s.bar
L	volume liquid flow rate	m^3/s
m	index in non-linear liquid hold up flow relationship (2.21)	
m_1, m_2	characteristic roots of equation (2.89) which defines the partial pressure profile	
M	dimensionless group defined by equation (2.7)	
M_m	molarity of MEA	kmole/m^3
M'	local concentration of free amine	kmole/m^3
N	absorption rate/unit height	kmole/m.s
N_n	absorption rate per cell, in equations (2.35) to (2.37)	kmole/s
p_c	bulk partial pressure of CO_2	bars
p_i	interfacial partial pressure of CO_2	bars
p^*	equilibrium partial pressure of CO_2	bars
Pe_L	Peclet No. based on packing size	
p_T	total column pressure	bars
R	specific absorption rate	kmole/m^2sec
R'	gas constant	m^3bar/kmole°K
s	spatial co-ordinate defined by (2.86)	m
t	time	sec
T	liquid temperature	°C
T_G	gas temperature	°K
U_G	gas phase hold up for cell model	kmole
U_L	liquid phase hold up for cell model	m^3

v_c	molar flow rate of CO_2	kmole/sec
v_I	molar flow rate of inert gas	kmole/sec
z	column height positive upwards unless otherwise indicated	m
Z	total column height	m
α	carbon ratio	
ΔE	heat of reaction	kJ/kmole
ρ	liquid density	kg/m^3
ϕ_G	fractional gas hold up	
ϕ_L	fractional liquid hold up	
ϕ^*	boundary condition	
ψ	enhancement factor for absorption with reaction, defined by equation (2.5)	
ψ_i	enhancement factor for absorption with instantaneous reaction	
ψ_i^K	enhancement factor derived from Kohl correlation	

CHAPTER THREE

THE PLATE DESORPTION COLUMN

3.1. Introduction and Literature Survey

There are many papers in the literature about both the theoretical and operational aspects of the absorption process but comparatively few on the complementary desorption process. Shah and Sharma[85] have recently reviewed the available literature on desorption and explain the application of the film and penetration equations in different situations. Fundamental work has been hindered by the difficulties of the gas-liquid interface which is in a violent state of agitation due to gas evolution in contrast to absorption where it is stable and laminar. It is therefore difficult to measure the interfacial area and estimate the individual mass transfer coefficients.

Neglecting the problems of the interface Porter et al[70] have studied theoretically the penetration theory equations for both absorption and desorption for a general reversible reaction. From numerical solutions of the equations they concluded that the rate of desorption is generally less than that for absorption, equality holding only for pseudo-first order or infinite reaction rates. These calculations were made assuming that the physical parameters remain the same for the two processes, which is unlikely.

The importance of the state of the gas-liquid interface was shown experimentally by Langley and Haselden[53] who found that the desorption rate of carbon dioxide from potassium carbonate solution was significantly influenced by

the degree of agitation induced by a stirrer. The desorption rate on a sieve plate can therefore be expected to be dependent upon the degree of agitation of the liquid and consequently upon the liquid and vapour rates. This was shown to be true when Danckwerts et al[21] successfully predicted carbon dioxide desorption rates from potash solutions on a sieve plate using data obtained from a stirred cell.

Benson et al[6,7] presented data for both absorption and desorption rates using hot potassium carbonate and MEA solutions. The rates are expressed in terms of overall gas phase mass transfer coefficients and are given with other results which indicate the relative merits of the two processes for the cleaning of synthesis gas. They found the potassium carbonate process to be the most economical in their case, although if a lower contamination of carbon dioxide in the synthesis gas were specified the MEA process would be preferable. Weiland and Trass[95] studied the absorption of carbon dioxide by ethylenediamine (EDA) and also the desorption process which was found to be dominantly gas phase controlled, the liquid phase offering appreciable resistance only for high liquid concentrations. They examined the economics of the entire gas cleaning process and found in agreement with Benson et al that the overall operating cost is dominated by the regeneration process.

The dynamics of plate columns have generally been studied with distillation as the mass transfer process. However, a brief literature review is justifiable because

the dynamics of a unit are determined not only by the mass transfer process, but also by the manner in which the liquid and vapour streams are brought into contact. A good summary of the current state of distillation technology has recently been published by Rijnsdorp et al[72]. The work includes a comprehensive survey of the literature from both the modelling and control viewpoints.

The general principle of plate column simulation by solving the differential equations for the dynamic material and component balances was verified experimentally by Armstrong and Wilkinson[4], and Lamb[52]. In an extensive study Luyben et al[58] went on to show that simple linearised equations can adequately predict most simple responses of a binary distillation column.

With the advent of digital computers, larger and more complex models were written and studied. Pieser and Grover[64] formulated a column model incorporating mass and energy balance equations for the trays, as well as separate equations for the reboiler and condenser. However, they did not explain their procedure for solving the equations, which needs care as the equations are not all independent. Holland et al[38] describe a very complex column model which includes tray mixing and channelling effects, as well as equations for component,material and energy balances. They describe the solution procedure, which is rather complex, together with some examples of the application of the model.

The effects dominating the dynamics of a column responding to a simultaneous feed flow and composition disturbance vary with time after the disturbance entered;

this is because flow and composition disturbances propagate through the column at different rates, as described by Rosenbrock[75]. During the period immediately after the disturbance the dynamics are dominated by flow changes, whilst the longer term dynamics are determined by the composition responses on each plate. Some of the complex effects which can dominate the short term dynamics have been investigated: a notable example being the inverse response[73] of the composition at the bottom of a column to a change in the reboiler heat load. The conditions under which vapour and liquid come into contact, and the manner in which these change is clearly of importance in determining the short term dynamics. The work of Sargent and Bernard[77] on the hydrodynamics of a sieve plate generally supports the equations that have been used to model pressure drop, hold up and flow rates associated with a plate.

The reboiler and condenser also contribute to the dynamics of the column. Day[22] examined the dynamics of a natural circulation reboiler which are complicated by the presence of two phase flow in association with the heat transfer process. However, he showed that the dynamics can be represented approximately by a first order relationship between the vapour produced and the applied heat load. In another study Stafford[93] shows that a similar simple representation is acceptable. The dynamics of condensers have not been so widely investigated, possibly because in many cases they do not influence the column dynamics significantly.

The aim of the work described in this chapter is to develop a reasonably general model for the desorption column

and then to consider a comparatively simple model which may be used for general simulation purposes and which may be fitted easily from plant data.

3.2. General Approach

The carbon dioxide to be desorbed exists in a chemically combined form with the monoethanolamine as the carbamate, possibly with some as bicarbonate which is the product of the secondary and slower reaction. This slow reaction is of no significance on the packing in the absorption column, but may exist to a small extent in the bottom of the absorption column and the downstream pipework. In addition, there may be a small quantity of free carbon dioxide in solution which will flash off on entering the desorption column. This quantity is neglected as it is small compared with the amount of carbon dioxide produced from decomposition of the carbamate. The desorption column is operated at a lower pressure and higher temperature than the absorption column to favour the decomposition of the carbamate and subsequent desorption. The reboiler produces steam which rises up the column and condenses to provide the heat of decomposition.

There is no data in the literature about the equilibrium between carbon dioxide, carbamate, bicarbonate and monoethanolamine or the associated reaction rates, under the conditions of desorption. However, there have been a number of investigations into the equilibrium partial pressure of carbon dioxide over MEA and the original data are shown together with some fitted curves in Fig.3.1. In

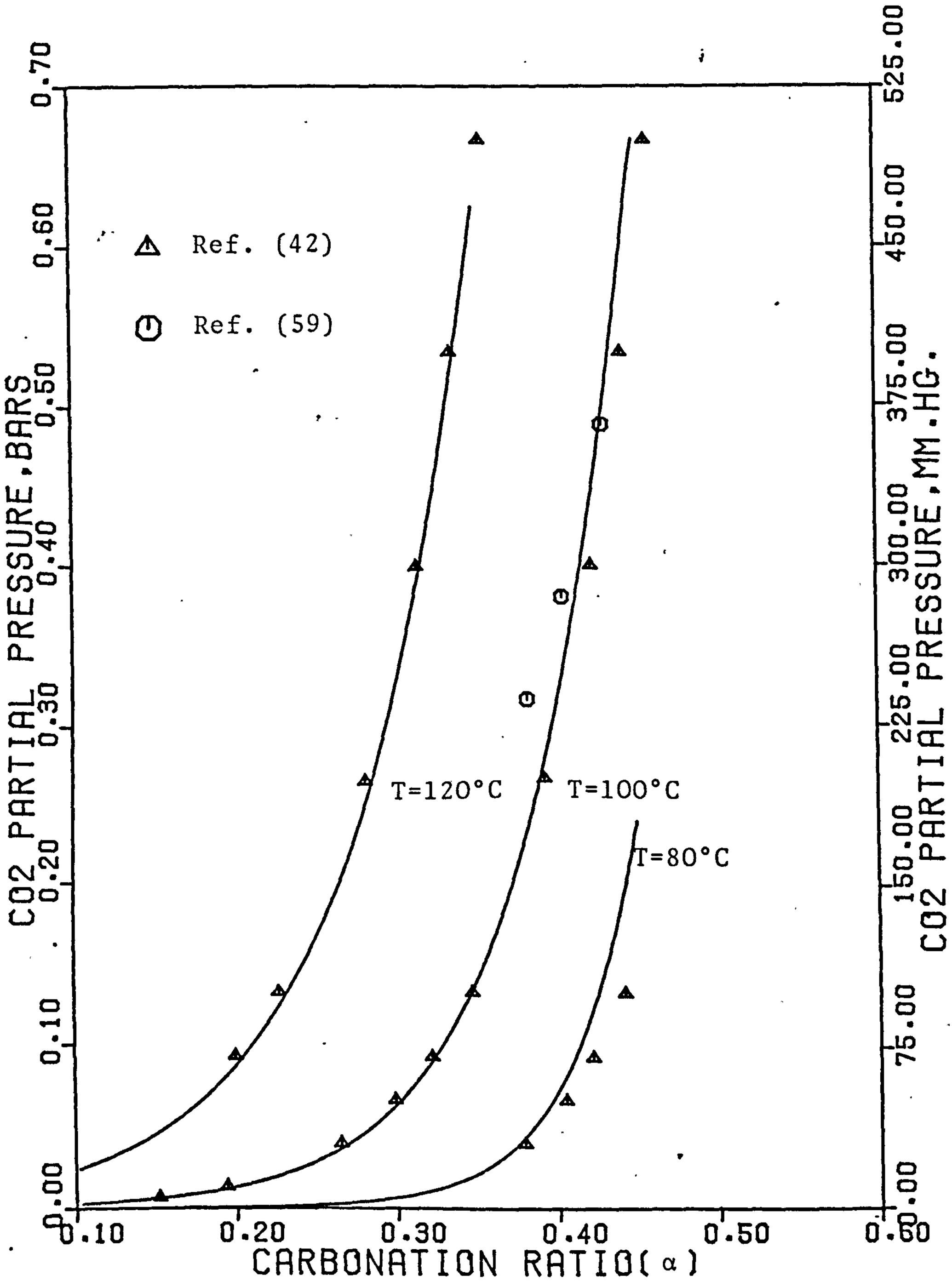


FIG. 3.1. EQUILIBRIUM PARTIAL PRESSURE OF CARBON DIOXIDE OVER MEA

order to obtain a model of reasonable simplicity it was assumed that only the carbamate decomposition reaction is of significance. An analysis of the desorption equations is made to derive a simple model which includes an expression for the partial pressure curves shown in Fig. 3.1. and a type of plate efficiency which can be related to the physical parameters involved.

The principal decomposition reaction is that of the carbamate to carbon dioxide and monoethanolamine:

$$HO\ C_2H_4NHCOO^- + HOC_2H_4NH_3^+ \rightleftharpoons CO_2 + 2HOC_2H_4NH_3 \qquad (3.1)$$

The solution of the surface renewal model for this reversible reaction gives the following expression for the specific desorption rate

$$R = -(c_i - c^*)\sqrt{Dk_r c_o + k_L^2} \qquad (3.2)$$

where c^* is the equilibrium concentration of free carbon dioxide in solution,

c_i is the interfacial concentration of carbon dioxide

and c_o is the concentration of carbamate in the bulk.

In addition a gas phase resistance is assumed:

$$R = -k_G(p - p_i) \qquad (3.3)$$

The equilibrium and interfacial liquid compositions can be related to the gas phase partial pressures by use of the solubility coefficient H:

$$c^* = Hp^* \qquad (3.4)$$

$$c_i = Hp_i \qquad (3.5)$$

From equations (3.2) to (3.5) the following expression for the specific desorption rate can be derived:

$$R = \frac{(p^*-p)\ H\sqrt{Dk_r c_o + k_L^2}}{1 + \frac{H\sqrt{Dk_r c_o + k_L^2}}{k_G}} \qquad (3.6)$$

which can be rewritten as:

$$R = K_{oG}\ (p^*-p)$$

$$\text{where } K_{oG} = \frac{H\sqrt{Dk_r c_o + k_L^2}}{1 + \frac{H\sqrt{Dk_r c_o + k_L^2}}{k_G}} \qquad (3.7)$$

The total desorption over a plate is obtained by integrating (3.6) over the depth of the liquid foam on the tray; over a differential height dz_L:

$$V\frac{dp}{\pi} = K_{oG}\ a\ (p^*-p)\ dz_L \qquad (3.8)$$

where V is the molar flow rate of vapour

π is the total pressure in mm. of mercury

and a is the interfacial area per unit volume of hold up.

The liquid on the tray is assumed perfectly mixed so that c_o, p* and the overall gas phase mass transfer coefficient remain constant. The vapour is assumed to be in plug flow so that equation (3.8) can be integrated to give the relationship between the entry and exit partial pressures p_{cj-1} and p_{cj} around plate j:

$$\frac{p^*-p_{cj}}{p^*-p_{cj-1}} = \exp\ \left[-\ \frac{K_{oG}\ a\ \pi\ z_L}{V}\ \right] \qquad (3.9)$$

The partial pressure leaving the plate can be written as

$$p_{cj} = Ep^* + (1-E)p_{cj-1} \qquad (3.10)$$

where the stage efficiency E is given by:

$$E = 1 - \exp\left[-\frac{K_{oG}\, a\pi z_L}{V}\right] \qquad (3.11)$$

Equation (3.11) shows that the stage efficiency is dependent upon the liquid phase composition and therefore will vary from plate to plate. However, a mean value is used for all plates in the column.

The separation in the column is therefore specified by the parameters for the equilibrium line and the stage efficiency E. These parameters can be estimated from plant measurements and it is not necessary to estimate the individual parameters in equation (3.11). The general aim of this work is to produce a model which will represent the column adequately rather than a complex model which could be used to distinguish the significance of the various decomposition reactions and the influence of the physical parameters.

The composition of the vapour phase and the plate temperature are calculated in a manner analogous to a bubble point calculation for distillation by considering the partial pressures of the carbon dioxide and water vapour.

The equilibrium partial pressure of carbon dioxide, shown in Fig. 3.1. was fitted by the following equation:

$$p^*(\alpha,T) = \exp\left[c_1 + c_2T + c_3T^2\right] \qquad (3.12)$$

where p^* is the equilibrium partial pressure in mm of mercury

T is the temperature in degrees centrigrade

α is the carbonation ratio of the liquid and has the same definition as in the previous chapter,

$$\left.\begin{aligned} \text{and } c_1 &= -47.91 + 112.8\alpha \\ c_2 &= .7615 - 1.668\alpha \\ c_3 &= -.0029 + .0070\alpha \end{aligned}\right\} \qquad (3.13)$$

The partial pressure of water vapour in mm. of mercury is given by the Antoine expression:

$$p_H = \exp\left[a_H - \frac{b_H}{T+c_H}\right] \qquad (3.14)$$

where T is the temperature in degrees centigrade

and $a_H = 18.379$, $b_H = 3880.1$ and $c_H = 230$

The plate temperature is found by Newton Raphson solution of the equation:

$$p^*(\alpha,T) + p_H(T) = \pi \qquad (3.15)$$

The actual partial pressure of carbon dioxide is then found from equation (3.10) and the partial pressure of water vapour is obtained by difference from the total pressure.

3.3. Steady State Solution

3.3.1. Introduction

A procedure for calculating the total desorption rate and the plate compositions given the desorption model and process conditions is required to predict the general performance of the column. This procedure will be used to estimate the model parameters and should therefore be robust and efficient.

3.3.2. Computational Technique

The equations to be solved for the steady state of the desorption column are similar to those for distillation and therefore it appeared sensible to adapt a standard distillation programme. The method of Murtagh and Sargent[78] was therefore selected. The monoethanolamine was assumed non-volatile and the concentrations on the plates could then be calculated immediately the internal liquid flow rates were known, so this did not present a problem. However, the calculation of the condenser had to be considered separately from the remainder of the column because the carbon dioxide is non-condensable and this made the overall programme more complex than originally hoped. Furthermore, the non-linearity of the carbon dioxide partial pressure curve caused severe convergence problems and solutions were generally achieved only if a good initial estimate was given. This matrix method was therefore rejected in favour of developing a more robust method of solution.

The equations which have to be satisfied for the overall material and energy balances are:

$$F_F = L_1 + (V_T M_T/\rho_L) \tag{3.16}$$

$$F_F c_{cF} = \frac{V_T p_{cT}(T_c)}{\pi} + L_1 c_{c_1} \tag{3.17}$$

$$F_F h_F + Q_R = L_1 h_1 + V_T H_T(T_c) + Q_c \tag{3.18}$$

$$F_F c_{MF} = L_1 c_{M_1} \tag{3.19}$$

where the variables are defined in Fig. 3.2 and the liquid flows are expressed in m^3/s and vapour flows in kmole/s.

The equations which have to be satisfied within the column are:

$$L_{j+1} = L_1 + (V_j M_j/\rho_L) \qquad 1 \leq j \leq N-1 \qquad (3.20)$$

$$L_{J+1}c_{cj+1} = L_1 c_{c_1} + V_j p_{cj}/\pi \qquad 1 \leq j \leq N-1 \qquad (3.21)$$

$$L_{j+1}h_{j+1} = L_1 h_1 + V_j H_j - Q_R \qquad 1 \leq j \leq N-1 \qquad (3.22)$$

$$L_{j+1}c_{Mj+1} = L_1 c_{M_1} = F_F c_{MF} \qquad 1 \leq j \leq N-1 \qquad (3.23)$$

$$p_{cj}^* = p^*(c_{cj}/c_{Mj}, T_j) \qquad 1 \leq j \leq N \qquad (3.24)$$

$$p_{cj+1} = (1-E)p_{cj} + Ep^*_{cj+1} \qquad 1 \leq j \leq N-1 \qquad (3.25)$$

where N is the number of plates in the column.

For the condenser the following equations have to be satisfied:

$$V_N = V_T + (F_R\rho_L/18.01) \qquad (3.26)$$

$$V_N H_N = V_T H_T + Q_c + F_R h_R(T_c) \qquad (3.27)$$

$$V_N p_{cN} = V_T p_{cT} \qquad (3.28)$$

The procedure adopted is to specify the feed rate, composition and enthalpy together with the reboiler heat load and the top vapour rate V_T. The equations are solved by the procedure shown in Fig. 3.4. An estimate of the carbon dioxide content of the stripped MEA is made and used together with heat and material balances to compute up the column plate by plate. When using the energy balance equation (3.22) and the material balance equation (3.20) to predict the vapour rate leaving plate j and the liquid rate from plate j+1 the enthalpy of the liquid on plate j+1 is

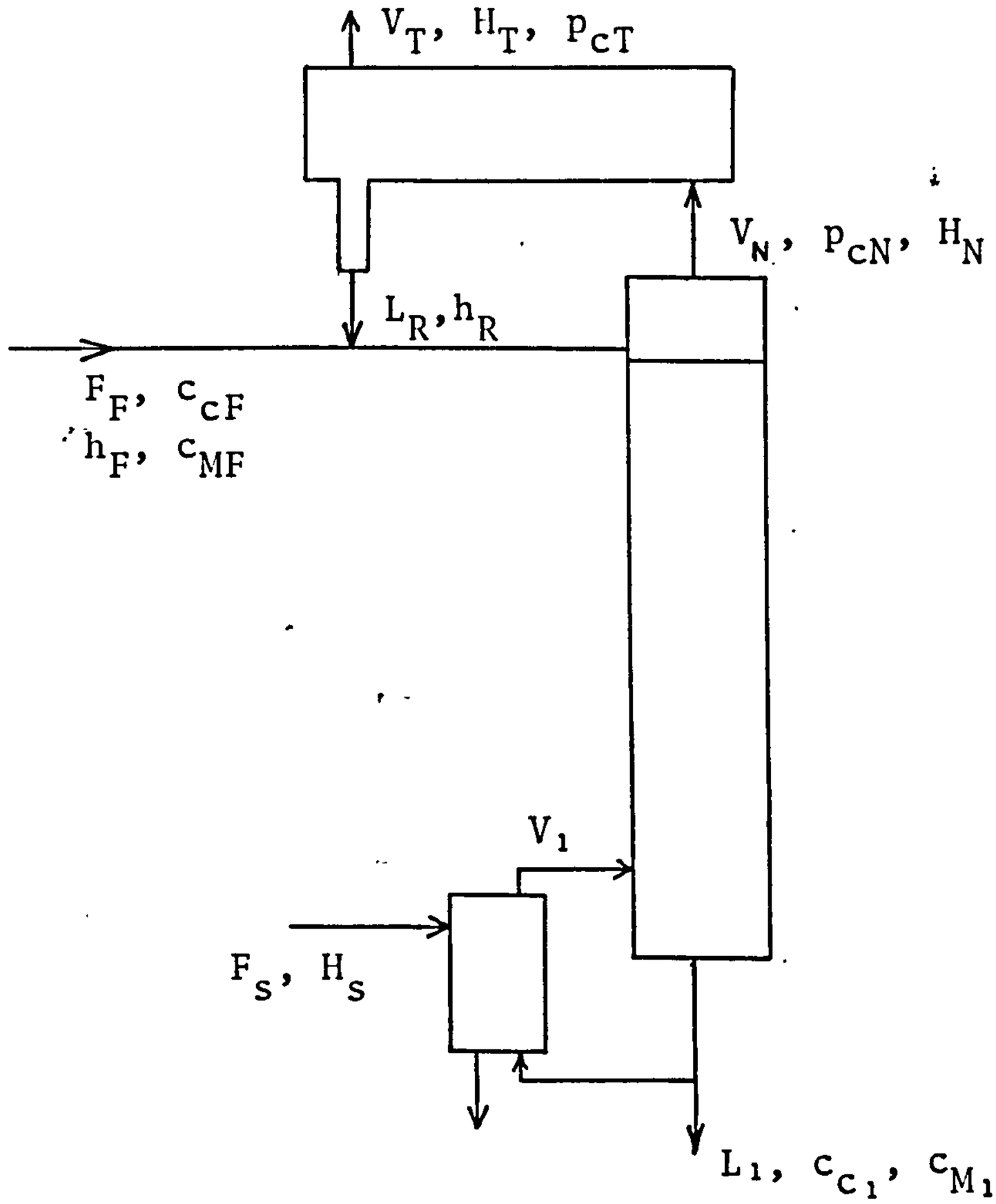


FIG. 3.2. DEFINITION OF COLUMN VARIABLES

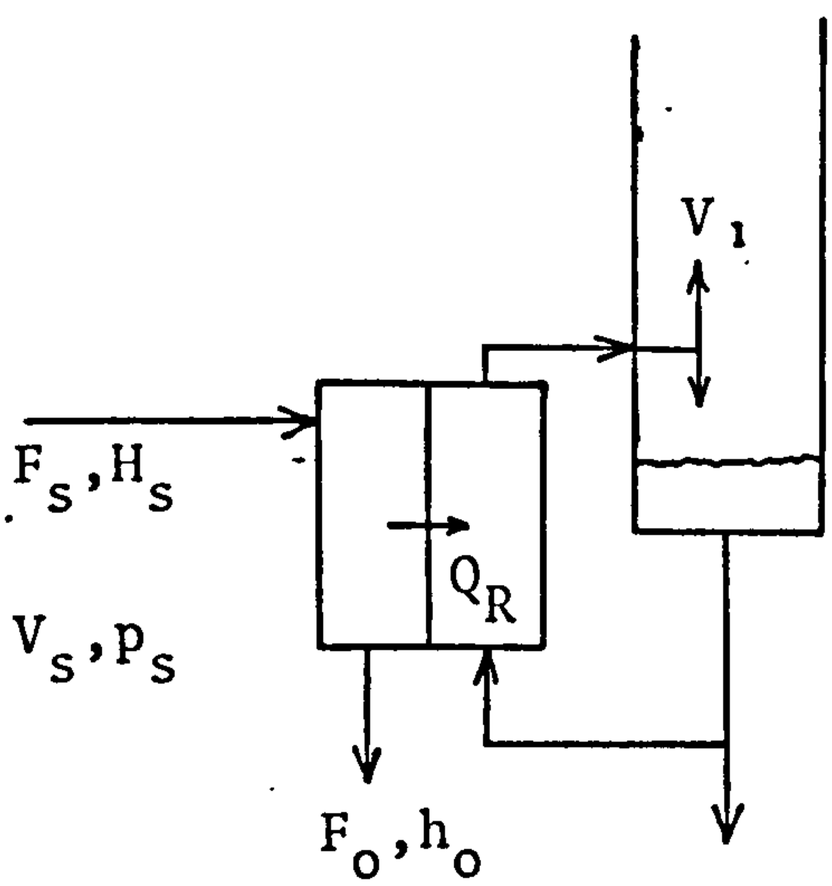


FIG. 3.3(a) REBOILER

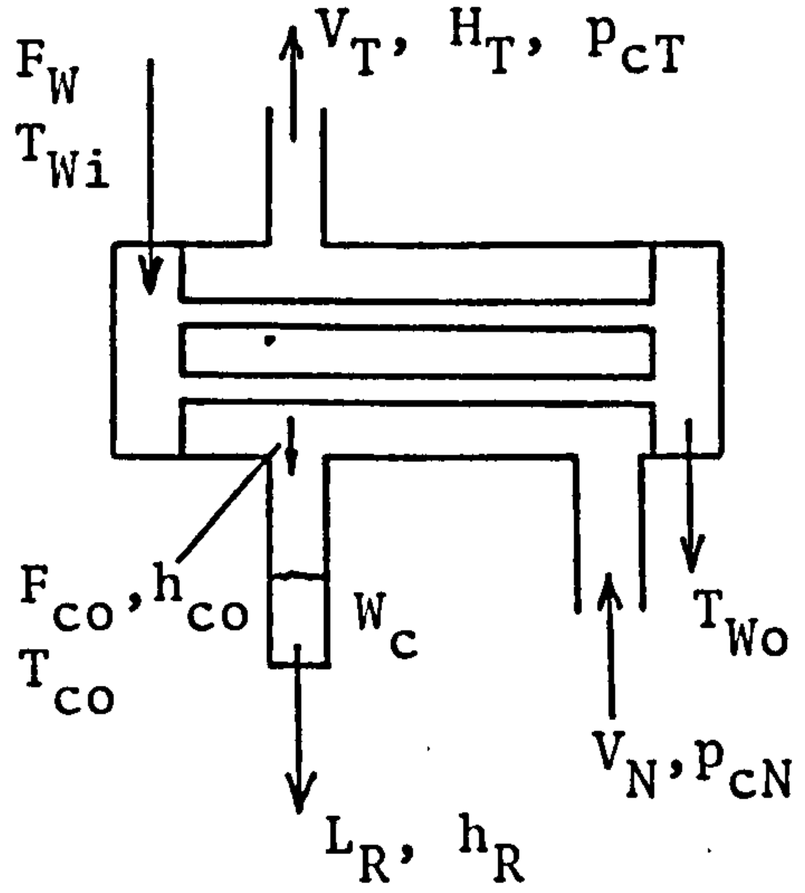


FIG. 3.3(b) CONDENSER

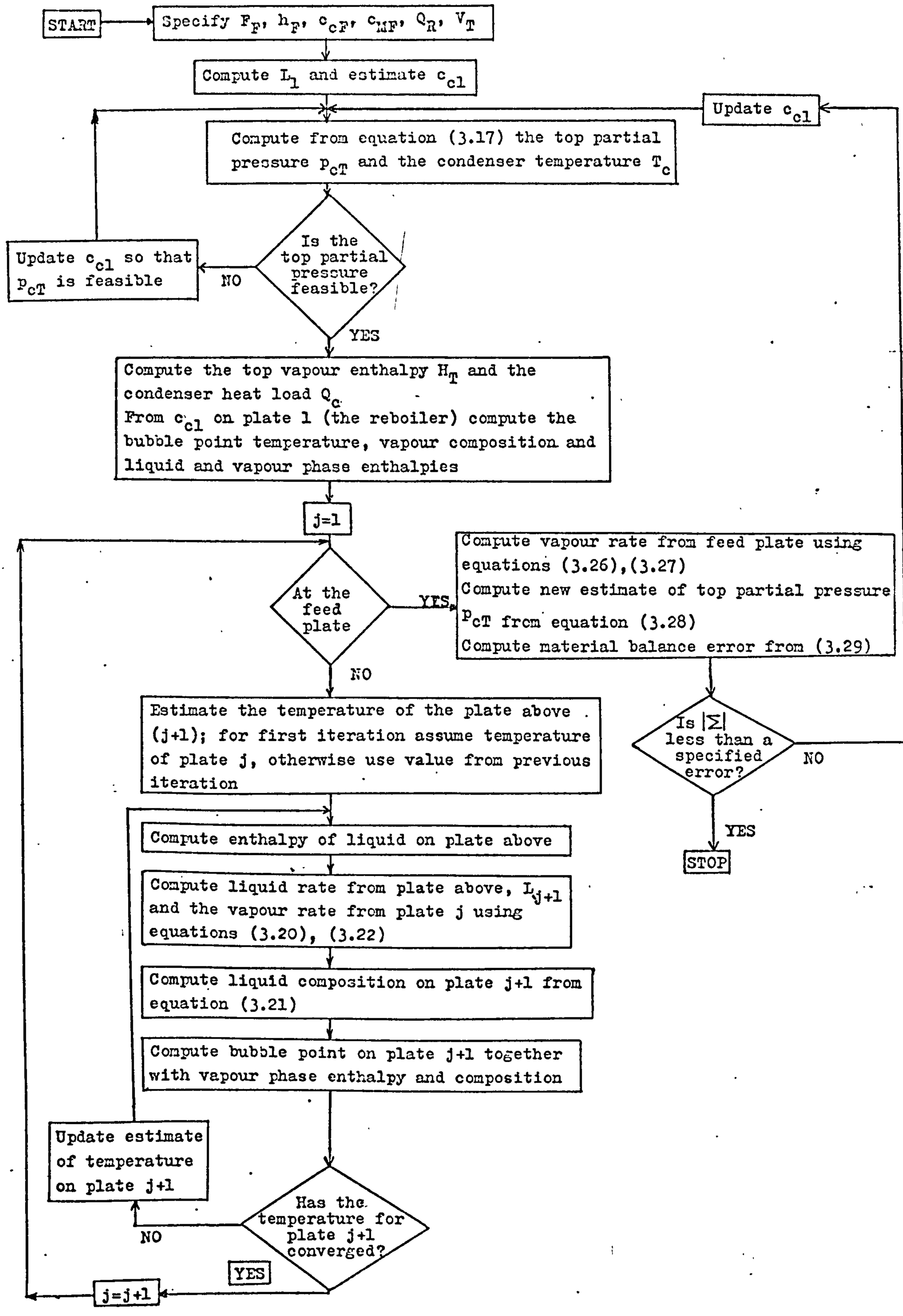


FIG.3.4. COMPUTATIONAL PROCEDURE FOR STEADY STATE

not initially known. An estimate of the liquid enthalpy is made and later refined following computation of the composition and bubble point on plate j+1. The vapour rate from the feed plate is calculated to satisfy the equations for the condenser and then at the top of the column the top partial pressure is recalculated. This is then substituted into equation (3.17) which is written in the form:

$$\Sigma = F_F c_{cF} - \frac{V_T p_{cT}(T_c)}{\pi} - L_1 c_{c_1} \qquad (3.29)$$

The carbon dioxide composition c_{c_1} is updated by a false position technique until the material balance error around the column, represented by the right hand side of equation (3.29), is less than a specified value (usually 10^{-7}).

The procedure proved to be robust in practice and generally required less than ten iterations to converge.

3.3.3. Steady State Results

The particular column considered has twenty plates and can accept the feed on the top plate or three plates lower down. This latter configuration is used with the condenser return flow onto the top plate in order to minimise the loss of trace quantities of amine. Under these conditions essentially no further separation is made over these plates and they act as part of the condenser in cooling the rising vapour.

The result of a typical calculation for the case of the feed entering on the top plate is shown in Table 3.1. The majority of the separation occurs over the top few plates where the equilibrium partial pressure of

TABLE 3.1. STEADY STATE LIQUID AND VAPOUR COMPOSITIONS

Feed flow = $.3 \times 10^{-3}$ m^3/s

Feed carbon dioxide concentration = 1.0 kmole/m^3

Feed MEA concentration = 2.5 kmole/m^3

Feed carbonation ratio = 0.40

Feed temperature = 90°C

Plate Number	Carbonation ratio of liquid	Partial pressure of CO_2 leaving plate mm. of mercury	Temperature of liquid °C	Vapour rate leaving plate kmole/s
21	0.3403	67.96	97.52	$.178 \times 10^{-2}$
17	0.2803	31.74	99.13	$.181 \times 10^{-2}$
13	0.2632	24.85	99.41	$.181 \times 10^{-2}$
9	0.2510	20.84	99.57	$.182 \times 10^{-2}$
5	0.2363	16.65	99.73	$.183 \times 10^{-2}$
1	0.1873	8.12	100.00	$.184 \times 10^{-2}$

Separation rate = 0.159×10^{-3} kmole/s

Top partial pressure of CO_2 = 393.2 mm

Condenser temperature = 76.2°C

Condenser heat load = 62.8 kW

Reboiler heat load = 88.9 kW

Heat for desorption of CO_2 = 12 kW

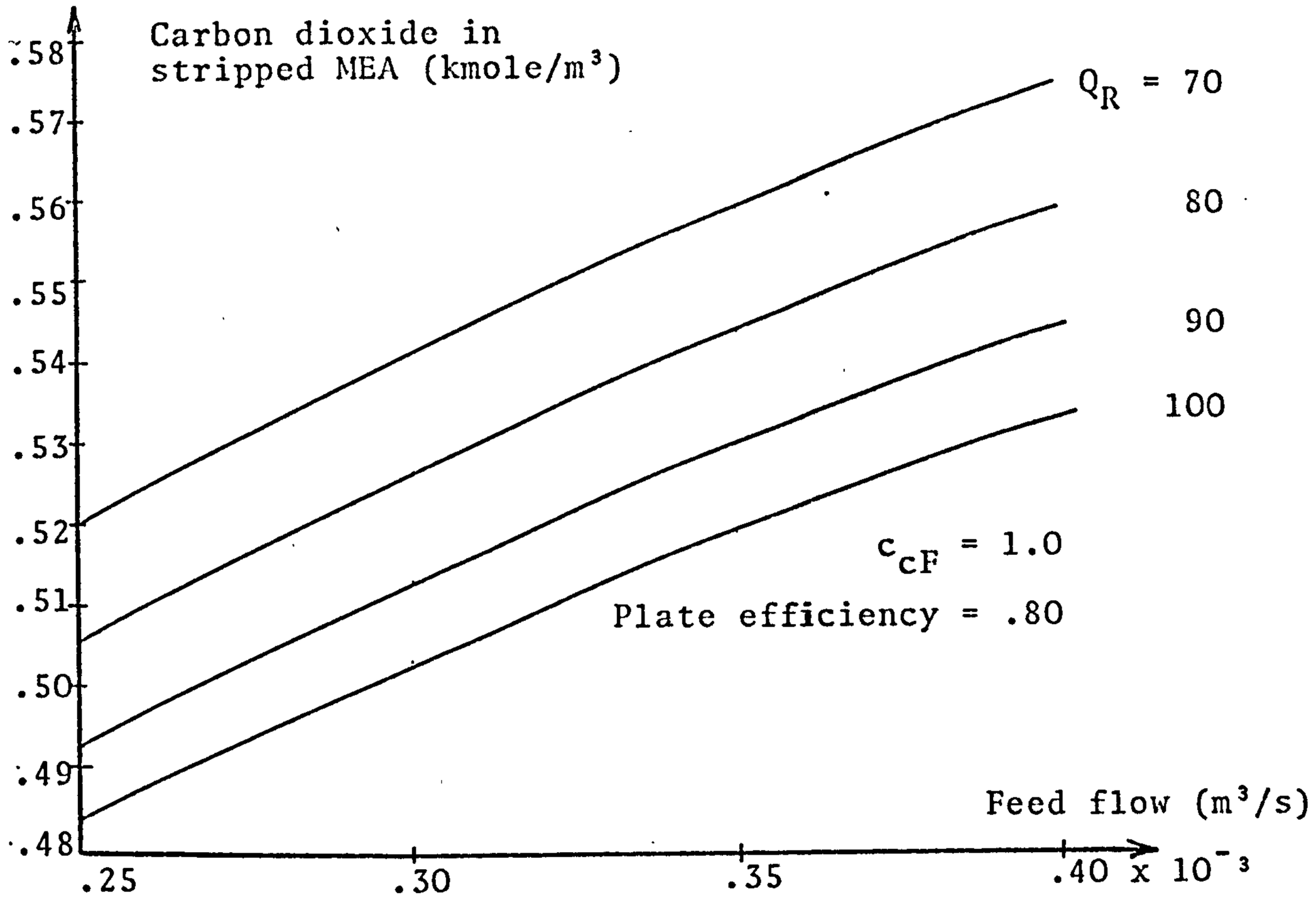


FIG.3.5. CARBON DIOXIDE CONTENT OF STRIPPED MEA

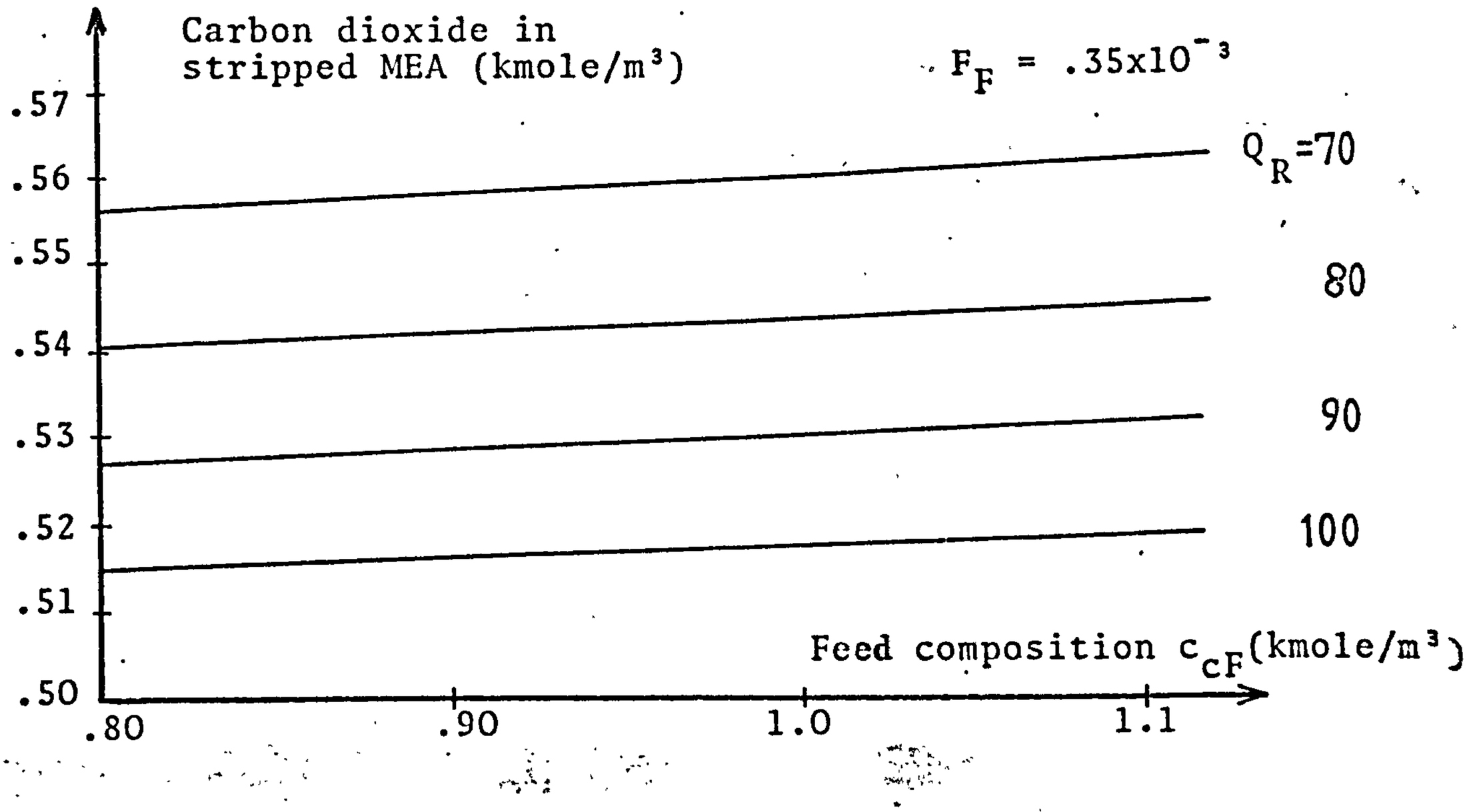


FIG. 3.6. CARBON DIOXIDE CONTENT OF STRIPPED MEA

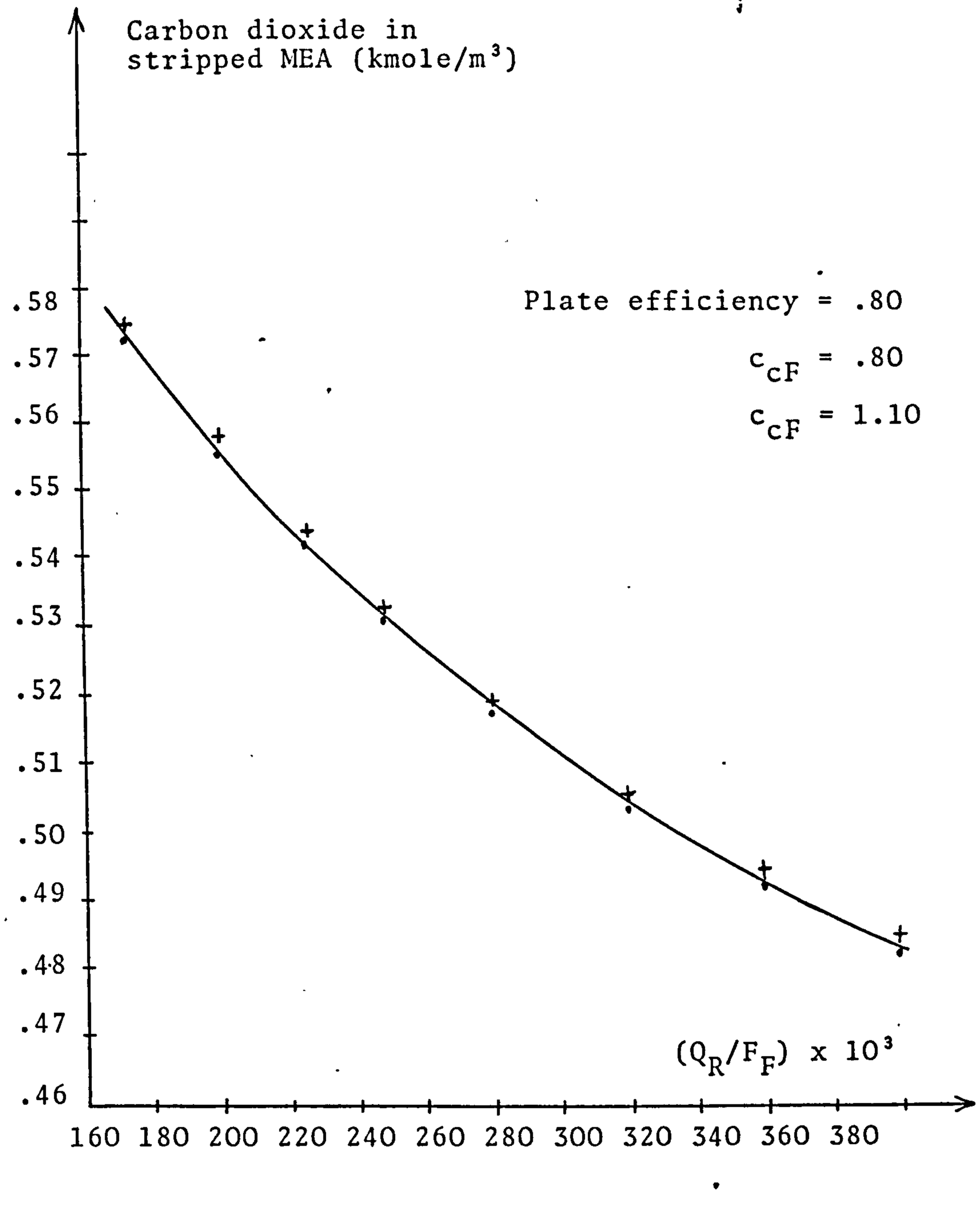


FIG. 3.7. RELATIONSHIP BETWEEN FEED RATE, HEAT LOAD AND STRIPPED MEA CONCENTRATION

carbon dioxide increases rapidly with the liquid composition. The carbon dioxide partial pressure is low even above the feed plate, and consequently there is only a small temperature difference between the feed plate and the bottom of the column. Furthermore, as the separation achieved by each plate is small the change in vapour rate to provide the heat of decomposition is also quite small and so the vapour rate remains almost constant from the reboiler to the top plate.

The variation of the carbon dioxide content of the stripped MEA with feed flow rate and heat load is shown in Fig. 3.5. Of greater importance is the fact that for a given feed flow rate and heat load the composition of the stripped MEA is virtually insensitive to the quantity of carbon dioxide in the feed as can be seen from Fig. 3.6.

A convenient means for representing the results obtained is shown in Fig. 3.7. Points were calculated for the four feed compositions considered and all were found to be within the extreme values shown in Fig. 3.7. The relationship could be adequately represented by a linear form

$$c_{c_1} = k_1 + k_2(Q_R/F_F) \qquad (3.30)$$

If this could be verified experimentally it would be useful in setting the heat load on the reboiler in order to obtain a specified carbon dioxide content of the stripped MEA:

$$Q_R = (F_F/k_2)(k_1 - c_{c_1}) \qquad (3.31)$$

Furthermore, it would be useful in a feed forward control system for the reboiler.

The majority of the heat supplied by the reboiler is in fact extracted by the condenser, as shown in Table 3.1. The efficiency of the desorption or regeneration is considered in terms of the separation rate per unit of reboil heat. The separation rate S is defined:

$$S = V_T p_{cT}/\pi \qquad (3.32)$$

The variation of the efficiency with reboil heat and feed flow is shown in Fig. 3.8. The decrease in efficiency for an increase in heat load is due to the increasing difficulty of producing a lower carbon dioxide content in the stripped MEA. The increase of efficiency with feed flow rate is due to the fact that the results were calculated for a fixed flow rate of top product. The flow rate of steam in the top product reduces as the feed flow rate and the separation rate increase and consequently the efficiency improves. The efficiency was also found to increase with feed composition for a given feed flow rate and reboil heat load. The separation rate increases with the feed composition because the carbon dioxide content of the stripped MEA remains virtually constant. These figures for efficiency compare with values of about 3 to 4.8×10^{-6} kmole/kJ obtained by Benson et al[6]. Their data were obtained using a packed desorption column of similar size but with lower flow rates of both absorbent and carbon dioxide. Their original figures were given in terms of the quantity of carbon dioxide per unit flow rate of steam. They did not specify the steam enthalpy so 2800 kJ/kg was assumed to obtain the figures given here.

The parameters which can be used to calibrate the model against plant data are the efficiency E and those in

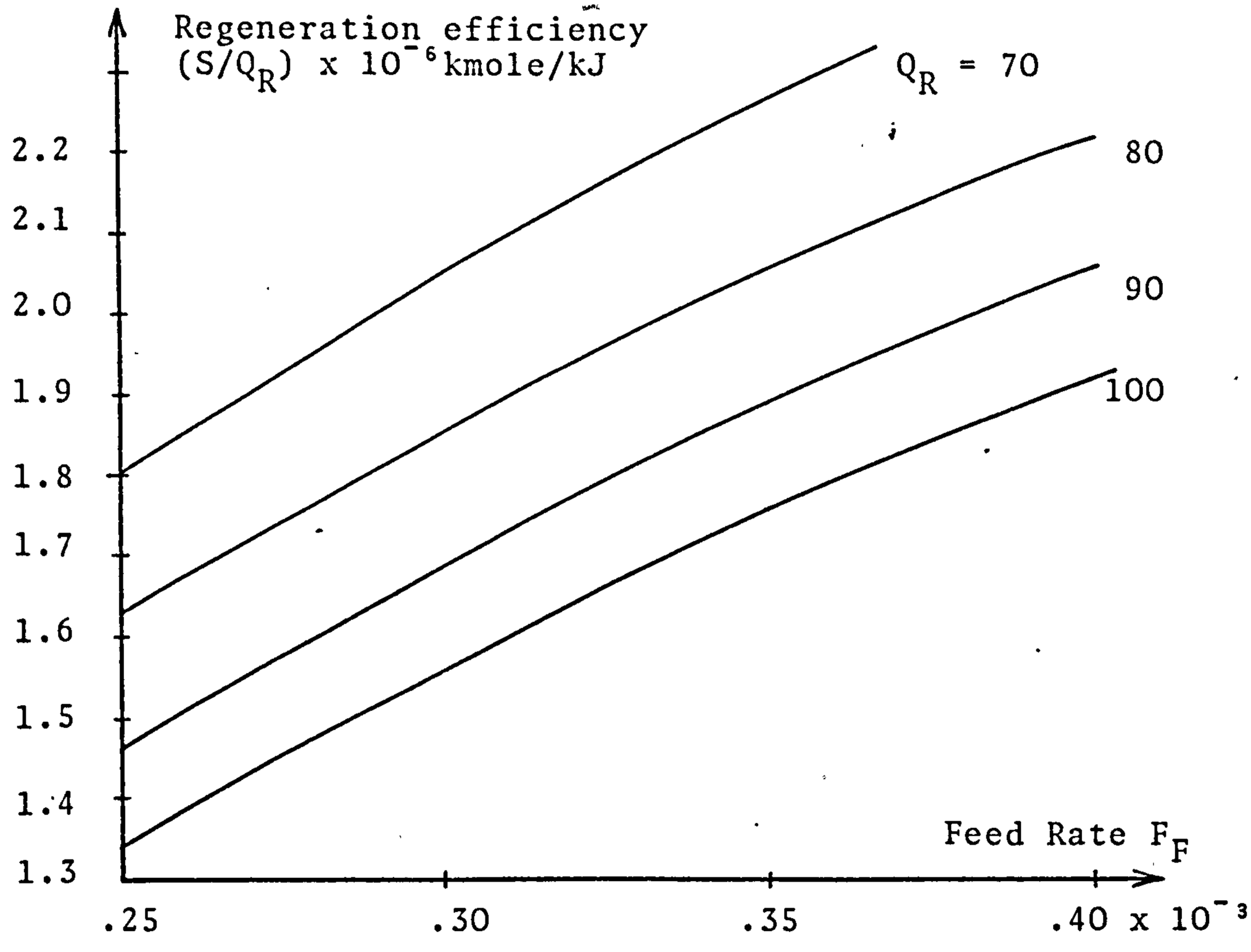


FIG. 3.8. REGENERATION EFFICIENCY

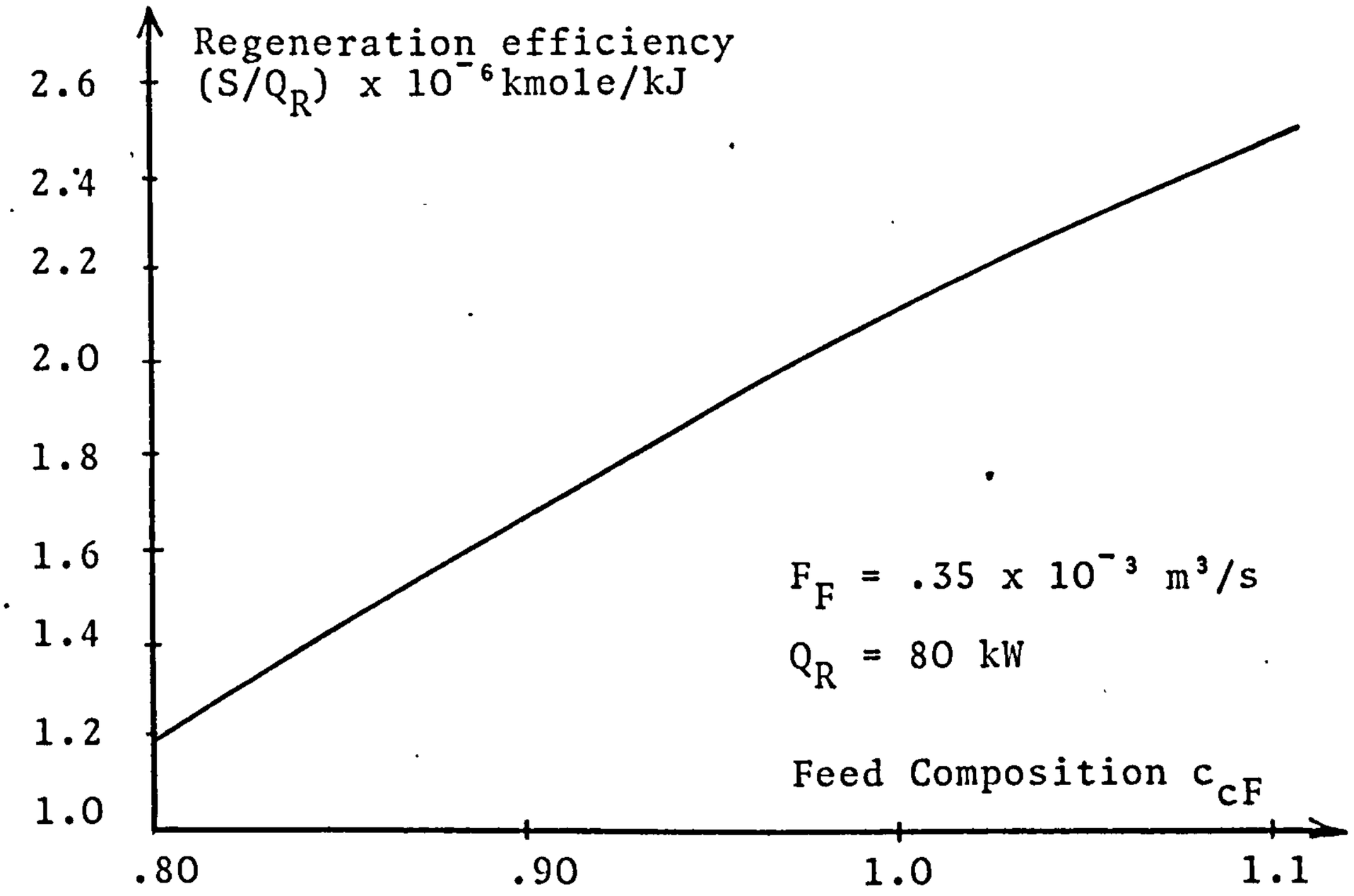


FIG. 3.9. REGENERATION EFFICIENCY

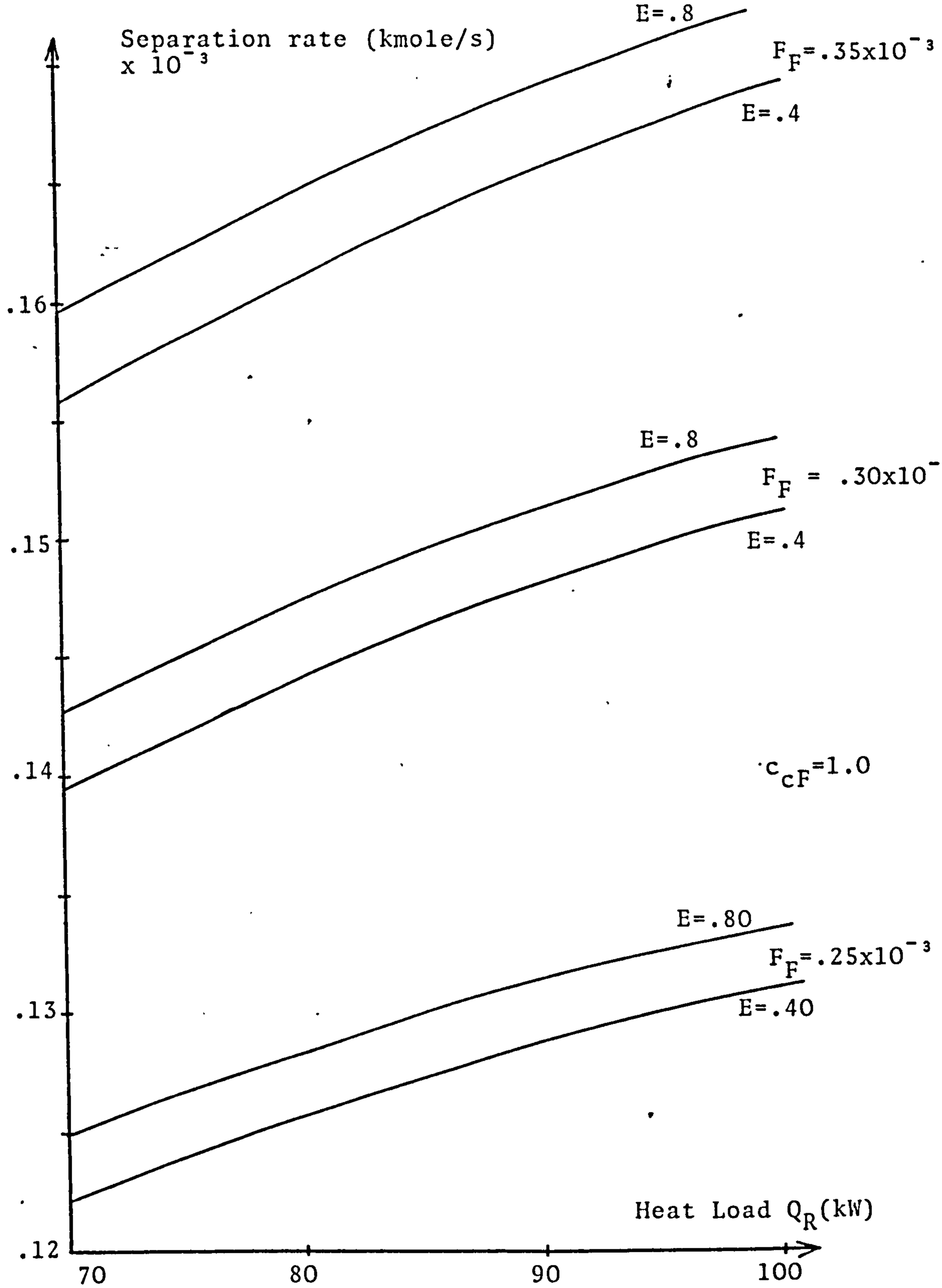


FIG. 3.10. VARIATION OF SEPARATION RATE WITH REBOIL HEAT AND PLATE EFFICIENCY

equations (3.12) and (3.13) defining the equilibrium carbon dioxide partial pressure. The estimation problem is considered in Chapter 5 following a simplification of the equilibrium relationship in Section 3.6.

The effect of a variation in efficiency on the separation rate is shown in Fig. 3.10 and is seen to be relatively small. The separation rate is more sensitive to the parameters in the equilibrium relationship.

3.4. Equations of Full Dynamic Model

3.4.1. Introduction

A dynamic model of the desorption system is derived by considering dynamic material and energy balances around each of the elements in the system. In addition to the equations for the plate hold up and compositions, further equations are included to represent the reboiler and condenser. The relationship between the material and energy balance differential equations is considered in Secion 3.4.4. and used to obtain an expression for the vapour rate leaving a plate.

3.4.2. Equations for Liquid Hold Up

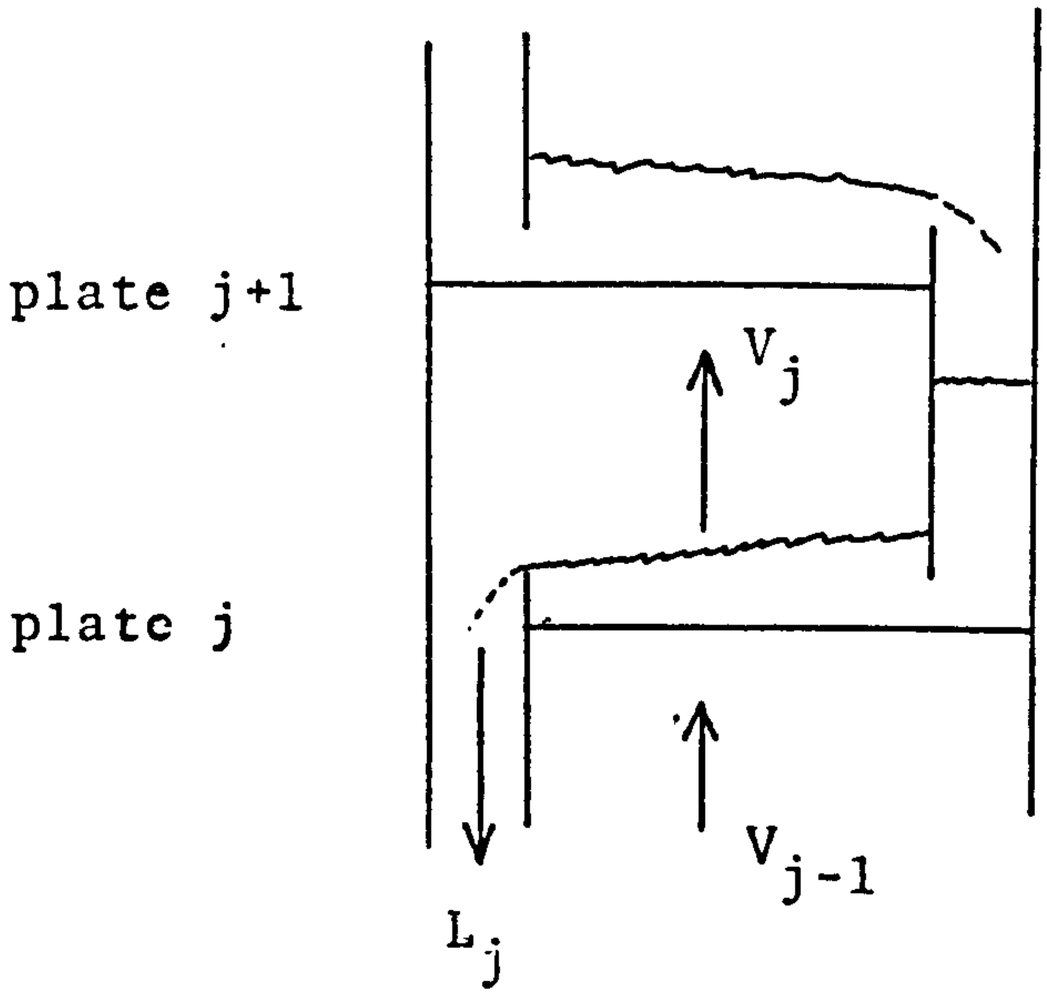
The liquid in the column is distributed on the trays and in the downcomers as shown in Fig. 3.11. Because the column is operated in the neighbourhood of atmospheric pressure, gas phase hold up is not considered. A dynamic description of liquid phase hold up is derived by considering the relationship between liquid flow rate off the tray, pressure drop across the tray and liquid heights on the tray and downcomer. Weeping of liquid from one plate to the next lower is not considered as this has no effect on the plate compositions which are assumed to be perfectly mixed. The flow rate of liquid off a tray has been correlated by a number of formulae, almost all of which give only a qualitative description. The relationship is complex because the liquid may exist as a foam or spray both of which vary with operating conditions and are difficult to analyse. For the system considered a foam is expected and for these conditions Bernard and Sargent[77] showed the Francis formula to be the best of the proposed descriptions:

$$L_j = k^1 \ell_w (z_F - z_W)^{1.5} \qquad (3.33)$$

where the variables are as defined in Fig. 3.11. The foam height is related to the equivalent clear liquid height by the foam density ϕ which may be approximated as a linear function of vapour rate:

$$z_{Lj} = \phi z_{Fj} \qquad (3.34)$$

$$\phi = e\text{-}fV_{j-1} \qquad (3.35)$$



z_W = weir height

z_{Lj} = Height of clear liquid on tray j

z_{Fj} = height of foam on tray j

ϕ = z_{Lj}/z_{Fj} = foam density

ℓ_W = weir length

Z_j = height of clear liquid in downcomer

L_j = volumetric flow rate of liquid off tray j

V_j = molar flow rate of vapour from tray j

W_{Tj} = hold up on tray j

$W_{pj} = W_{Dj} + W_{Tj}$ = total hold up on plate j

FIG. 3.11. DEFINITION OF VARIABLES FOR MODELLING OF PLATES

At steady state the equivalent height of clear liquid in the downcomer is given by the sum of the pressure drops:

$$Z_j = z_{Lj} + \Delta P_{Tj+1} + z_d \tag{3.36}$$

where ΔP_{Tj} is the total pressure drop across plate j expressed as a clear liquid height and z_d is the head loss due to flow resistance under the downcomer.

Bernard and Sargent found this relationship to be satisfactory. The total pressure drop across a plate is the sum of the liquid head on the tray and the dry plate pressure drop z_{vj} which is calculated from the expression given by Kolodzie and van Winkle[49]:

$$\Delta P_{Tj} = z_{Lj} + z_{vj} \tag{3.37}$$

$$\text{where } z_{vj} = \frac{(V_{j-1}M_{j-1})^2}{2gC_d\rho_L A_H^2 \rho_{gj-1}} \tag{3.38}$$

The term plate is used to refer to the tray and downcomer as an entity, so the total plate hold up is the sum of the volumetric hold ups on the tray and in the downcomer:

$$W_{pj} = W_{Tj} + W_{Dj}$$

$$= z_{Lj}A_T + Z_jA_D \tag{3.39}$$

A dynamic material balance is made for each plate

$$\frac{d}{dt} W_{pj} = L_{j+1} - L_j + \frac{1}{\rho_L}[V_{j-1}M_{j-1} - V_jM_j] + F_j \tag{3.40}$$

$$j = 2,N$$

where F_j is the feed to plate j and is non-zero only for the feed plate.

Because the resistance to flow under the downcomer is very small it is assumed that the total plate hold up distributes instantaneously according to equations (3.36) to (3.39). The individual downcomer and tray hold ups are

computed from the total plate hold up by solving the following equations sequentially down the column from the top plate:

$$W_{Dj} = \frac{A_D}{A_T} (W_{Tj} + W_{Tj+1} + A_T z_{vj+1}) \qquad (3.41)$$

$$W_{pj} = W_{Tj} + W_{Dj} \qquad (3.42)$$

starting with $W_{Dj} = 0$ and $W_{pj} = W_{Tj}$ for $j = N$

The vapour rates in the column are determined by the procedure described later in Section 3.4.4. and the liquid flow rates are obtained from equation (3.33).

The hold up model is completed by inclusion of equations for the condenser, column bottoms and reboiler:

$$\frac{d}{dt} W_c = F_c - F_R \qquad (3.43)$$

where F_R is the flow of reflux condensate and is under level control from the condensate leg hold up W_c.

$$\frac{d}{dt} W_{p_1} = L_2 - L_1 - (V_1 M_1 / \rho_L) \qquad (3.44)$$

where W_{p_1} is the combined hold up in the column bottoms and the reboiler; the bottom liquid flow L_1 is under control from the bottom level.

3.4.3. Composition and Enthalpy Equations

The differential equations representing dynamic material, and energy balances for each plate are derived with the following assumptions:-

i) the hold up of liquid in the downcomer and on the tray can be considered as one entity, to be

consistent with the formulation in the previous section;

ii) the liquid is well mixed so that the concentrations are uniform;

iii) the gas phase entering a plate is uniformly mixed and consists of carbon dioxide and water vapour only; the amine is assumed to be non-volatile;

iv) gas phase hold up is negligible;

v) the temperature of the liquid and vapour leaving a stage are assumed equal and are given by the equilibrium expression (3.15); departure from equilibrium is represented by the stage efficiency shown in equation (3.10);

vi) the pressure is constant throughout the column for the purpose of calculating the equilibrium compositions;

vii) there is no heat loss from the column;

viii) reduction of separation due to entrainment of liquid in the gas can be included in the stage efficiency if necessary.

A dynamic material balance for the carbon dioxide around a plate gives:

$$\frac{d}{dt} W_{pj} c_{cj} = L_{j+1} c_{cj+1} + \frac{V_{j-1} p_{cj-1}}{\pi} - L_j c_{cj} - \frac{V_j p_{cj}}{\pi} + F_j c_{cF} \qquad (3.45)$$

$$j = 1, N$$

$$F_j = 0 \text{ for } j \neq \text{feed plate}$$

$$V_0 = 0$$

The monoethanolamine is assumed involatile so a material balance for the total amine, including that combined with the carbon dioxide, is:

$$\frac{d}{dt}W_{pj}c_{Mj} = L_{j+1}c_{Mj+1} - L_j c_{Mj} \qquad (3.46)$$

$$j = 1, N$$

The carbonation ratio α_j on a plate is calculated from

$$\alpha_j = c_{cj}/c_{Mj} \qquad (3.47)$$

An energy balance gives:

$$\frac{d}{dt}W_{pj}h_j = L_{j+1}h_{j+1} + V_{j-1}H_{j-1} - L_j h_j - V_j H_j + F_j h_F + Q_j \qquad (3.48)$$

$$j = 1, N$$

$$Q_j = 0 \text{ for } j \neq 1$$

The partial pressure of carbon dioxide over each plate is calculated from the procedure described in Section 3.2 and the reboiler is assumed to behave as a theoretical plate as a consequence of the rapid recirculation and violent boiling. The liquid flow rates and plate hold ups are known from the equations in the previous section. The composition derivatives are computed from:

$$\frac{d}{dt}c_{cj} = \frac{1}{W_{pj}}\left(\frac{d}{dt}W_{pj}c_{cj} - c_{cj}\frac{d}{dt}W_{pj}\right) \qquad (3.49)$$

$$\frac{d}{dt}c_{Mj} = \frac{1}{W_{pj}}\left(\frac{d}{dt}W_{pj}c_{Mj} - c_{Mj}\frac{d}{dt}W_{pj}\right) \qquad (3.50)$$

where the hold up derivative is obtained from the equations in Section 3.4.2.

The only variables in the derivatives remaining to be

defined are the vapour rates and this problem is considered in the next section.

3.4.4. Solution for the vapour rates

The composition and energy balance differential equations are not independent if the liquid and vapour enthalpies can be expressed in terms of the liquid composition. With the assumption that the liquid is always boiling the required relationship is provided by equations (3.10) and (3.15). An expression for the vapour rate leaving a plate can then be derived to simultaneously satisfy the composition and energy balance equations.

Although the development given here is specific to the desorption column the principle is also applicable to distillation.

The liquid phase enthalpy (in kJ/m^3) is expressed as:

$$h_j = c_p T_j \qquad (3.51)$$

and the vapour phase enthalpy (in kJ/kmole) is written as the sum of the liquid phase enthalpy together with the appropriate fractions of the latent heat of water and the heat of desorption:

$$H_j = c_{pv} T_j + \frac{1}{\pi}(p_{Hj}\lambda_H + p_{cj}\lambda_D) \qquad (3.52)$$

where $c_{pv} = (c_p\ 18.0)/\rho_L$

λ_D is the heat of desorption of carbon dioxide and is assumed independent of α

and λ_H is the latent heat of water.

The left hand side of the energy balance differential equation can be re-written as:

$$\frac{d}{dt}W_{pj}h_j = h_j\frac{d}{dt}W_{pj} + W_{pj}\frac{dh_j}{dt}$$

$$= h_j\frac{d}{dt}W_{pj} + W_{pj}c_p\frac{dT_j}{dt} \qquad (3.53)$$

The temperature derivative in (3.53) can be related to composition:

$$\frac{dT_j}{dt} = \frac{dT_j}{d\alpha_j}\cdot\frac{d\alpha_j}{dt} = \frac{m_\alpha}{c_{Mj}}\frac{dc_{cj}}{dt} - m_\alpha\frac{c_{cj}}{c_{Mj}^2}\frac{dc_{Mj}}{dt}$$

$$= \frac{m_\alpha}{c_{Mj}}\left[\frac{1}{W_{pj}}\left(\frac{d}{dt}W_{pj}c_{cj} - c_{cj}\frac{d}{dt}W_{pj}\right)\right]$$

$$- \frac{m_\alpha}{c_{Mj}^2}c_{cj}\left[\frac{1}{W_{pj}}\left(\frac{d}{dt}W_{pj}c_{Mj} - c_{Mj}\frac{d}{dt}W_{pj}\right)\right]$$

where $m_\alpha = dT_j/d\alpha_j$ (3.54)

The sensitivity of temperature to composition is obtained from equation (3.15) which is differentiated implicitly assuming the total pressure remains constant:

$$d\pi = 0 = \left(\frac{dp_{Hj}}{dT_j} + \frac{\partial p^*_{cj}}{\partial T_j}\right)dT_j + \frac{\partial p^*_{cj}}{\partial \alpha_j}d\alpha_j$$

$$\text{so} \quad m_\alpha = \frac{dT_j}{d\alpha_j} = \frac{-\partial p^*_{cj}/\partial\alpha_j}{\frac{dp_{Hj}}{dT_j} + \frac{\partial p^*_{cj}}{\partial T_j}} \qquad (3.55)$$

The derivatives in (3.55) can be obtained from the equations used for the partial pressures of the carbon dioxide and water vapour.

The right hand side of equation (3.53) can therefore be expanded in terms of liquid, vapour rates and compositions using equation (3.54). This expanded equation can then be solved for the vapour rate leaving the plate. The result is written more neatly with the definition of the following variables which are the terms independent of

the vapour rate in differential equations (3.40), (3.45), (3.46) and (3.48):

$$S_{Hj} = \frac{d}{dt}(W_{Tj}h_j) + V_jH_j \qquad (3.57)$$

$$S_{cj} = \frac{d}{dt}(W_{Tj}c_{cj}) + (V_jp_{cj}/\pi) \qquad (3.58)$$

$$S_{Mj} = \frac{d}{dt}(W_{Tj}c_{Mj}) \qquad (3.59)$$

$$S_{Fj} = \frac{d}{dt}W_{Tj} + (V_jM_j/\rho_L) \qquad (3.60)$$

The vapour rate from plate j can then be written:

$$V_j = \frac{h_jS_{Fj} - S_{Hj} + m_\alpha \frac{c_p}{c_{Mj}}(S_{cj} - \alpha_jS_{Mj})}{h_j\frac{M_j}{L} - H_j + c_p\frac{m_\alpha}{c_{Mj}}\frac{p_{cj}}{\pi}} \qquad (3.61)$$

With the vapour rate known the derivatives are conveniently computed from rearrangement of equations (3.57) to (3.60).

For the particular system studied the variation of the boiling temperature with composition was found to be small, and for the limiting case of a zero value of m_α equation (3.61) reduces to:

$$V_j = \frac{h_jS_{Fj} - S_{Hj}}{h_j\frac{M_j}{\rho_L} - H_j} \qquad (3.62)$$

Although the plate remains isothermal a change in energy hold up on a plate can occur if the plate hold up changes.

Both equation (3.61) and (3.62) are a neat solution to the problem of solving for the vapour rates and can easily be incorporated in the complete computational procedure.

3.4.5. The Reboiler

The reboiler on the particular column under consideration is of the natural circulation type and uses steam which is condensed in the shell of the exchanger. The modelling of its dynamics could be a complex problem in itself if the processes of heat transfer and two phase flow were considered in detail. Under certain conditions the boiling, recirculation rate and heat transfer can become unstable as a consequence of the violent and continual switching between nucleate and film boiling, although under normal operation the system should be stable with perhaps some rapid fluctuation in the recirculation rate about a steady mean. As part of an overall column model it is considered justifiable to consider the use of a simple model, and it is assumed that the heat transfer can be characterised by constant coefficients. The model consists of equations for the steam side, the column side, and an equation for the thermal capacity of the reboiler tube walls. The equations for the steam side consist of differential mass and energy balances:

$$V_s \frac{d}{dt}\rho_s = F_s - F_o \tag{3.63}$$

$$V_s \frac{d}{dt}\rho_s H_o = F_s H_s - F_o h_o - (h_c A_R)(T_s - T_{WR}) \tag{3.64}$$

where the variables are as shown in Fig. 3.3.

The condensation temperature T_s is related to the density and enthalpy of the steam:

$$T_s = T_s(\rho_s, H_o) \tag{3.65}$$

The rate of condensation and the condensate enthalpy are

given by:

$$F_o = (h_c A_R)(T_s - T_{WR})/(H_o - h_o) \qquad (3.66)$$

$$h_o = h_o(T_s) \qquad (3.67)$$

The reboiler tubes are assumed to offer no resistance to the heat transfer so that the temperature is uniform throughout and given by:

$$H_R c_{pR} \frac{dT_{WR}}{dt} = (h_c A_R)(T_s - T_{WR}) - (h_v A_R)(T_{WR} - T_1) \qquad (3.68)$$

where T_1 is the temperature of the liquid in the bottom of the column.

The liquid in the column and reboiler circulates naturally as a consequence of the hydrostatic head set up, and at a sufficiently fast rate to justify the assumption that it is well mixed. The composition equations are therefore those derived in Section 3.4.3. and the vapour rate is calculated from equation (3.61) with the heat transfer Q_R obtained from:

$$Q_R = Q_1 = (h_v A_R)(T_{WR} - T_1) \qquad (3.69)$$

3.4.6. Modelling of the Condenser

The function of the condenser is to lower the partial pressure of the water vapour in the top product, which is also cooled, and to guard against the loss of trace quantities of amine in the top product. The water vapour is condensed in the shell of the exchanger, falls into the condensate leg and then flows into the column feed under level control, see Fig. 3.3. The cooling water makes eight passes through the tube bundle and has a residence time of

a few minutes. The condenser could therefore be considered as a distributed system. However, a complex model is not justifiable as the condenser can only influence the column separation through the return of condensate and the effect of this is small.

A very simple model can be derived by assuming that the vapour is in equilibrium with the condensate in the condenser leg and that the heat load can be specified as an independent function of time. Differential heat and energy balances around the condenser give:

$$\frac{d}{dt}W_c h_R(T_c) = V_N H_N - V_T H_T(T_c) - F_R h_R - Q_c(t) \qquad (3.70)$$

$$\frac{d}{dt} W_c = \frac{1}{\rho_L}(V_N M_N - V_T M_T) - F_R \qquad (3.71)$$

where F_R is the condensate return rate which is controlled from the condensate reservoir level represented by W_c.

The partial pressure of water vapour in the top product is evaluated at saturation conditions and the top product rate is calculated from:

$$\pi = p_{cT} + p_H(T_c) \qquad (3.72)$$

$$V_T = V_N \, p_{cN}/p_{cT} \qquad (3.73)$$

This model is physically unrealistic because the dynamics of the exit vapour are determined by those of the condensate in the liquid leg, which are relatively slow. The behaviour of this model, referred to as model 1, is compared in Section 3.5 with that of the more realistic models which follow.

A more realistic representation is obtained by realising that the temperature of the vapour can change

rapidly and independently of the temperature of the liquid in the condensate leg. The vapour is assumed to be always in equilibrium with the condensate on the tubes, and the quantity of this condensate is assumed negligible. The equilibrium temperature can therefore be calculated from an instantaneous heat and mass balance. As before it is assumed that the heat load Q_c can be specified independently:

$$V_N H_N = V_T H_T(T_v) + Q_c + F_c h_c(T_v) \tag{3.74}$$

$$V_N p_{cN} = V_T[\pi - p_H(T_v)] = V_T p_{cT} \tag{3.75}$$

$$V_N = V_T + (F_c \rho_L / 18.01) \tag{3.76}$$

where T_v is the temperature of the vapour and condensate at equilibrium conditions

and F_c is the condensation rate

These equations are easily solved in an iterative manner by repeated substitution in the equation:

$$T_v^{n+1} = -c_H + b_H/(\ln(\pi - p_{cT}) - a_H) \tag{3.77}$$

where

$$p_{cT} = V_N p_{cN}[H_T(T_v^n) - c_p T_v^n]/[V_N(H_N - c_p T_v^n) - Q_c] \tag{3.78}$$

The dynamics of the system are associated with the condensate only, and the equations are:

$$\frac{d}{dt} W_c h_R = F_c h_c - F_R h_R \tag{3.79}$$

$$\frac{d}{dt} W_c = F_c - F_R \tag{3.80}$$

This representation is referred to as model 2.

To represent the heat load in terms of the vapour temperature and the flow and temperature of the cooling water a more complex formulation is required. A partial differential equation to represent the time and spatial variation of the cooling water would require a complex solution, such as by the method of characteristics considered in Chapter 2. This degree of complexity is not justifiable. A great simplification is made if a mean cooling water temperature is assumed. Changes in cooling water flow and temperature would then have to be represented in terms of a change in the mean temperature. A pseudo-steady state relationship would have to be formulated from plant measurements.

With the assumption of a mean cooling water temperature T_W and a uniform vapour temperature, an overall heat transfer coefficient can be used. Furthermore, the total heat transfer can be expressed as the sum of the sensible and condensation heat transfer:

$$\lambda_H k_G A_c [p_H(T_v) - p_i(T_c)] + h_c A_c (T_v - T_c)$$

$$\doteq U_c A_c (T_v - T_W) = Q_c \qquad (3.81)$$

This equation is solved iteratively for T_c and T_v in association with the heat and mass balance equations for the vapour, (3.74) to (3.76). As before the dynamics of the system are associated with the condensate leg, equations (3.79) and (3.80). The values of the parameters representing condensation and sensible heat transfer would have to be fitted from plant data, but approximate values for this work were estimated from Kern[46], see

Appendix 4. This representation is referred to as model 3.

3.4.7. Computational Procedure

The computational procedure to obtain the derivatives from the state vector is shown in Fig. 3.12. Integration of the equations by a Runge Kutta procedure showed them to be very stiff, a step length of a tenth of a second or less being used for the simulation of a period of 100 seconds or more. This stiffness was attributed to the equations describing the column hold up and liquid flow rates.

A computational economy was made by partitioning the equations into two groups: the hold up equations which are integrated with a short time step of the order of a tenth of a second, and the composition equations which are integrated with a step length of one or two seconds. By this means the computation time was reduced by about a third, and a further economy was made by excluding the integration of the hold up differential equations when the hold up and flows are steady. An additional significant economy was made by linearising the Francis equation for the flow of liquid off a plate and avoiding the evaluation of the exponent:

$$L_j = a + bW_{Tj} + cV_{j-1} \qquad (3.82)$$

This provides an excellent approximation to the original equation.

These economies reduced the computation time to approximately one half of the original, and permitted the use of the model off-line for investigation of responses.

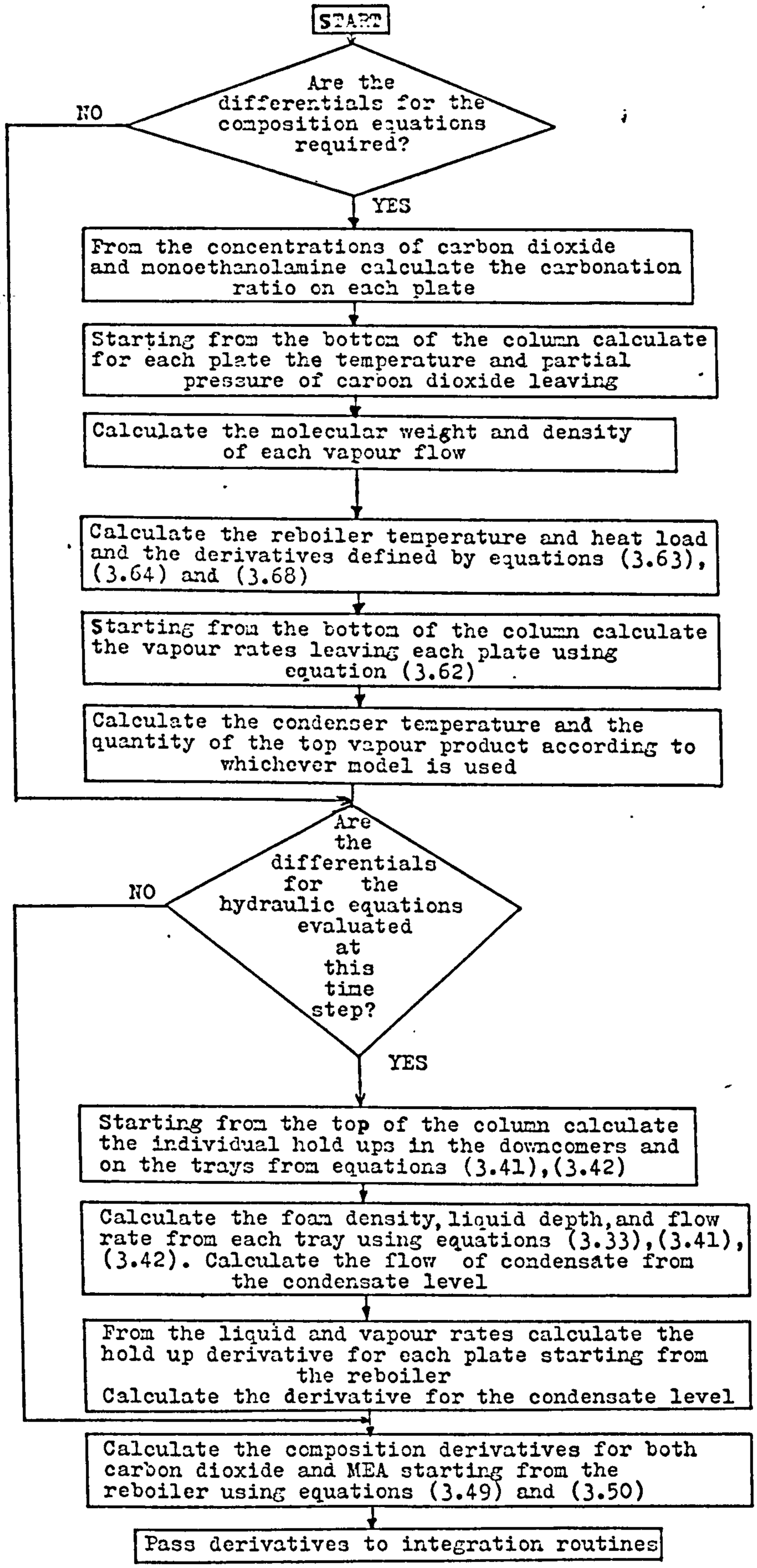


FIG.3.12. COMPUTATION OF DERIVATIVES

However, further economies and advantages could be gained by using an integration method specially suited for stiff systems. Such a method would be necessary if optimisation calculations with this model were envisaged as integration and storage of the state vector is a significant problem. This, therefore, prompted the work on integration methods for stiff systems reported in Chapter 4.

3.5. Responses of the Full Model

The response of the full model to a variety of input disturbances was investigated. As a first test a simulation was made of a start up of the column which initially contains no carbon dioxide, and the responses of the plate compositions are shown in Fig. 3.13. The composition of the plates near the top of the column are established quite rapidly together with the separation rate. The slow response in the lower part of the column is due to the small composition gradients and the large hold up in the reboiler. The plate temperatures changed only slightly from the initial value of about 100°C and the final values range from 96°C to 100°C in agreement with the steady state model.

A simulation was made of the response to a change in feed flow rate using the model equations already stated and then repeated with the alternative assumption that the liquid flow change passes through the column immediately. The difference between composition responses was very small and virtually negligible in practice. This again is

due to the fact that the majority of the stripping occurs near the top of the column. A further consequence of the small composition gradient near the bottom of the column is that the bottom composition does not show an inverse response to a change in steam heat load.

The relatively slow response of the composition of the stripped MEA to a change in heat load indicates that there could be potential for feedforward control of the steam flow. This would be beneficial when the flow rate of carbon dioxide entering the absorber increases and it is necessary not only to increase the recirculation rate of the MEA but also to decrease the carbon dioxide content of the stripped absorbent.

A comparison is shown in Fig. 3.14 of the responses to a change in reboiler heat load predicted by the three condenser models. The separation is only slightly influenced by the condenser and consequently the three models predict an identical response. The first model shows a significantly slower vapour temperature response than the other two due to the assumption that the condensation temperature is equal to the condensate temperature in the reservoir. The other two models are more realistic and show that the condensation temperature and consequently the partial pressure of the water vapour can change rapidly. The response predicted by the third model differs from that predicted by the second because it does not assume the heat load to remain constant and can also represent both latent heat and sensible heat transfer. For most applications the second model is probably adequate and if necessary could easily be modified to make

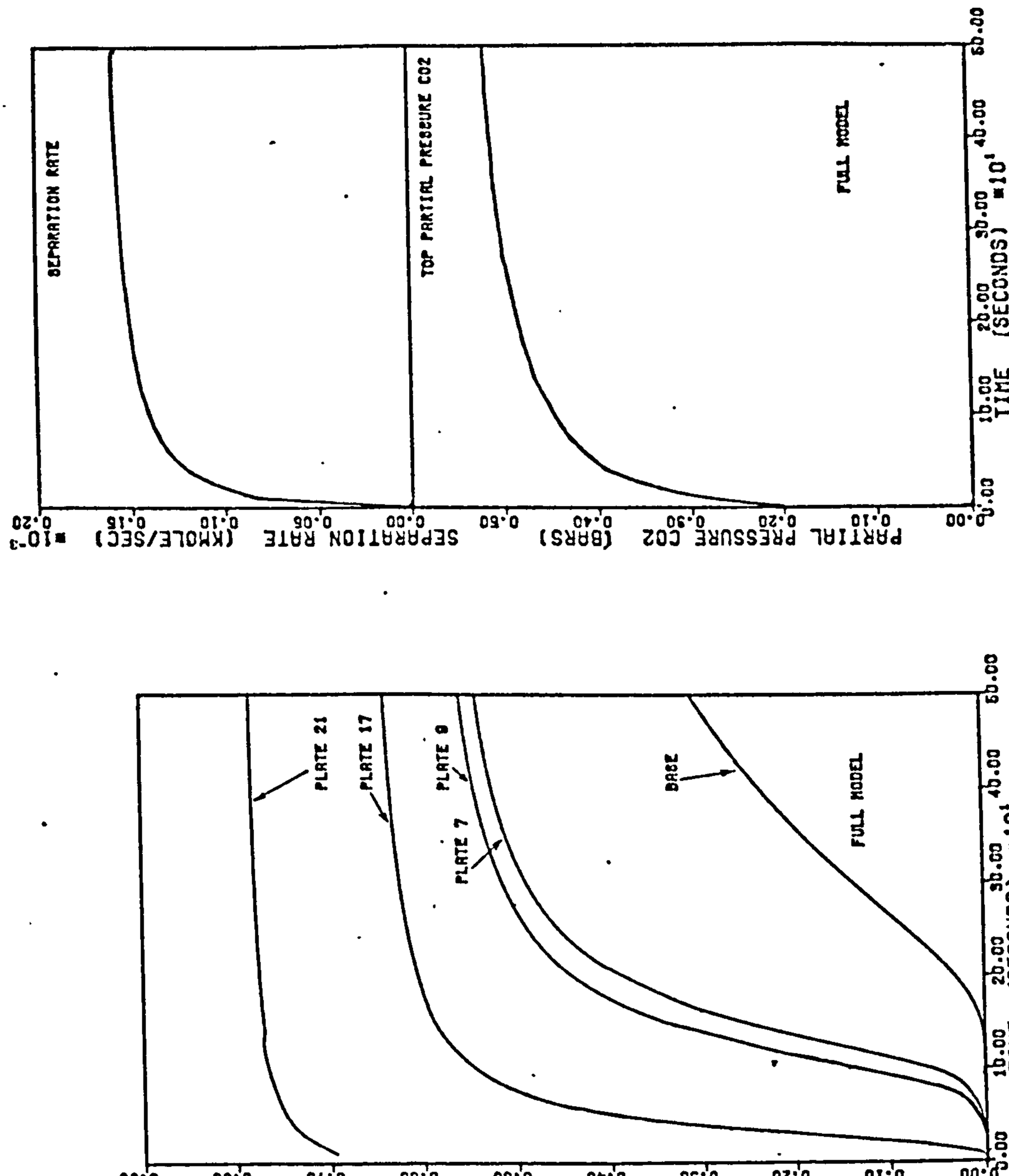


FIG.3.13. SIMULATION OF START UP: FULL MODEL

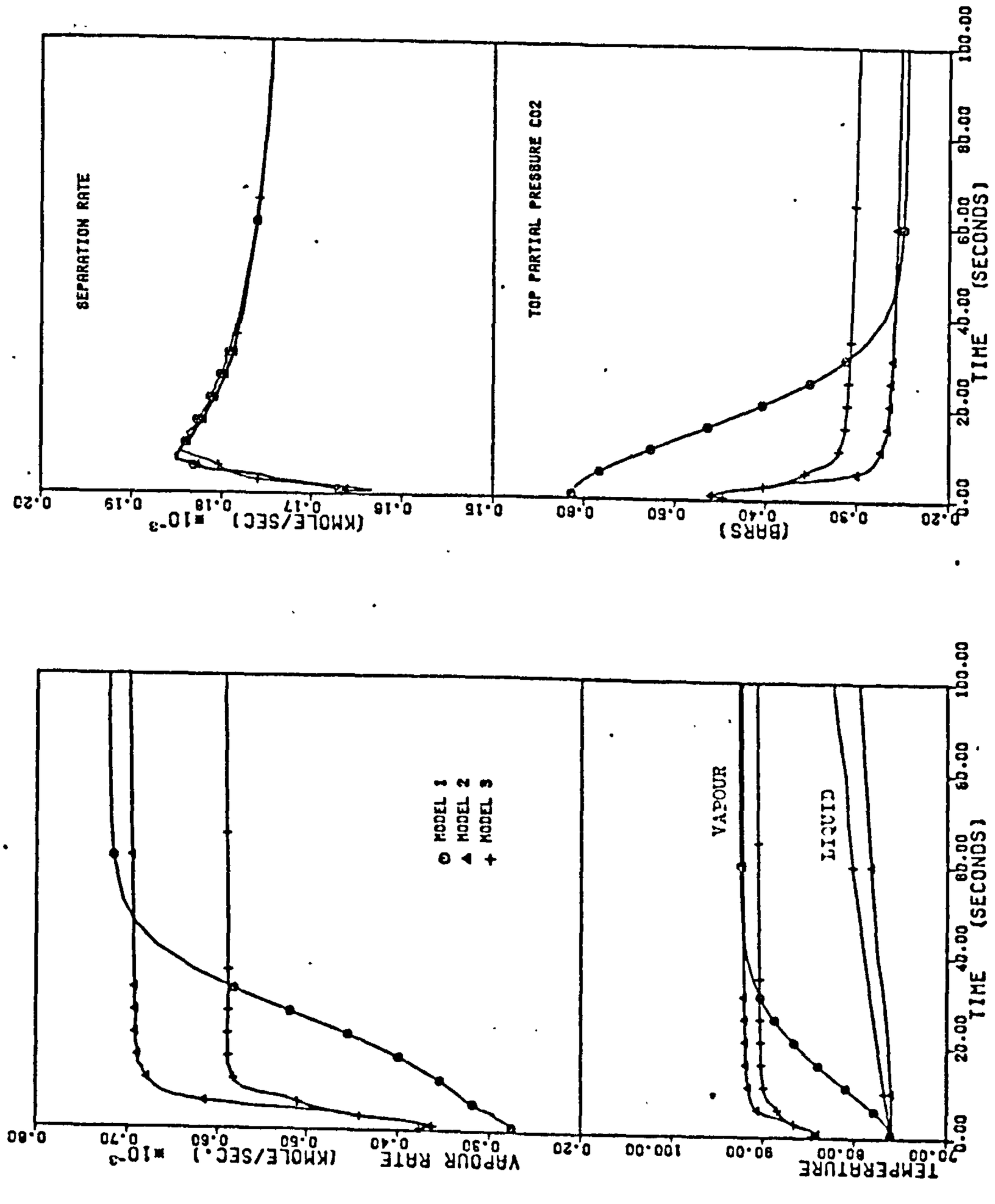


FIG.3.14. COMPARISON OF CONDENSER MODELS

the heat load dependent upon the cooling water temperature as in the third model.

3.6. Proposal and Statement of Simplified Model

The solution of the full model is a complex procedure and although feasible for off-line applications could not be used advantageously on-line. A far simpler model is required for on-line simulation, particularly for prediction.

The full model was simplified in the steady state and dynamic aspects in order to reduce both the state vector and the amount of computation for the derivatives.

The first simplification made was to assume that the column is isothermal; the equilibrium partial pressure of carbon dioxide can then be computed directly without the use of an iterative procedure and equation (3.12) simplifies to:

$$p^*_{cj} = \exp\ (a + b\ c_{cj}/c_{Mj}) \qquad (3.83)$$

where the parameters a and b could be calculated from the assumed temperature and the parameters given earlier. However, as a consequence of the small temperature changes predicted by the original model the values of the parameters a and b have to be adjusted slightly to ensure agreement between the two models. This seems reasonable as they are to be estimated in the future from plant data. The use of a stage efficiency is retained in the simple model so that the separation in the column is defined by three parameters.

Liquid flow transients are assumed to propagate through the column immediately, and the liquid flow rates are assumed constant, given by:

$$L_j = F_F + F_R \qquad j = 2, N_p \tag{3.84}$$

$$L_1 = L_2 - (V_1 M_1 / \rho_L) \tag{3.85}$$

The complex representation of the reboiler in the full model was simplified to a simple first order lag between the vapour rate and the steam flow rate:

$$\frac{d}{dt} V_1 = \frac{1}{\tau_{RS}} (K'' F_s - V_1) \tag{3.86}$$

where the parameters τ_{RS} and K'' are easily found from the results given by the full model or from plant data.

An expression for the vapour rate leaving all other plates is obtained from a steady state heat balance:

$$V_j = L_j \left(\frac{h_{j+1} - h_j}{H_j - (h_{j+1} M_j / \rho_L)}\right) + V_{j-1} \left[\frac{H_{j-1} - (h_{j+1} M_{j-1} / \rho_L)}{H_j - (h_{j+1} M_j / \rho_L)}\right] \tag{3.87}$$

Substituting for the liquid and vapour enthalpies, neglecting the first term and rearranging:-

$$V_j = V_{j-1} \left[\frac{\pi(\lambda_H + c_{pv} T_{j-1} - c_p T_{j+1} M_{j-1} / \rho_L) + p_{cj-1}(\lambda_D - \lambda_H)}{\pi(\lambda_H + c_{pv} T_j - c_p T_{j+1} M_j / \rho_L) + p_{cj}(\lambda_D - \lambda_H)}\right] \tag{3.88}$$

With the exception of the top plate, where the feed is subcooled and equation (3.88) has to be used, an approximation can be made:

$$V_j = V_{j-1} \left[\frac{p_{cj-1}(\lambda_D - \lambda_H) + B}{p_{cj}(\lambda_D - \lambda_H) + B}\right] \tag{3.89}$$

where the constant B is evaluated once and used for all plates except the top.

The technique used to reduce the dimension of the state vector is that of plate lumping which has been described by Coggan and Noton[14]. Instead of considering

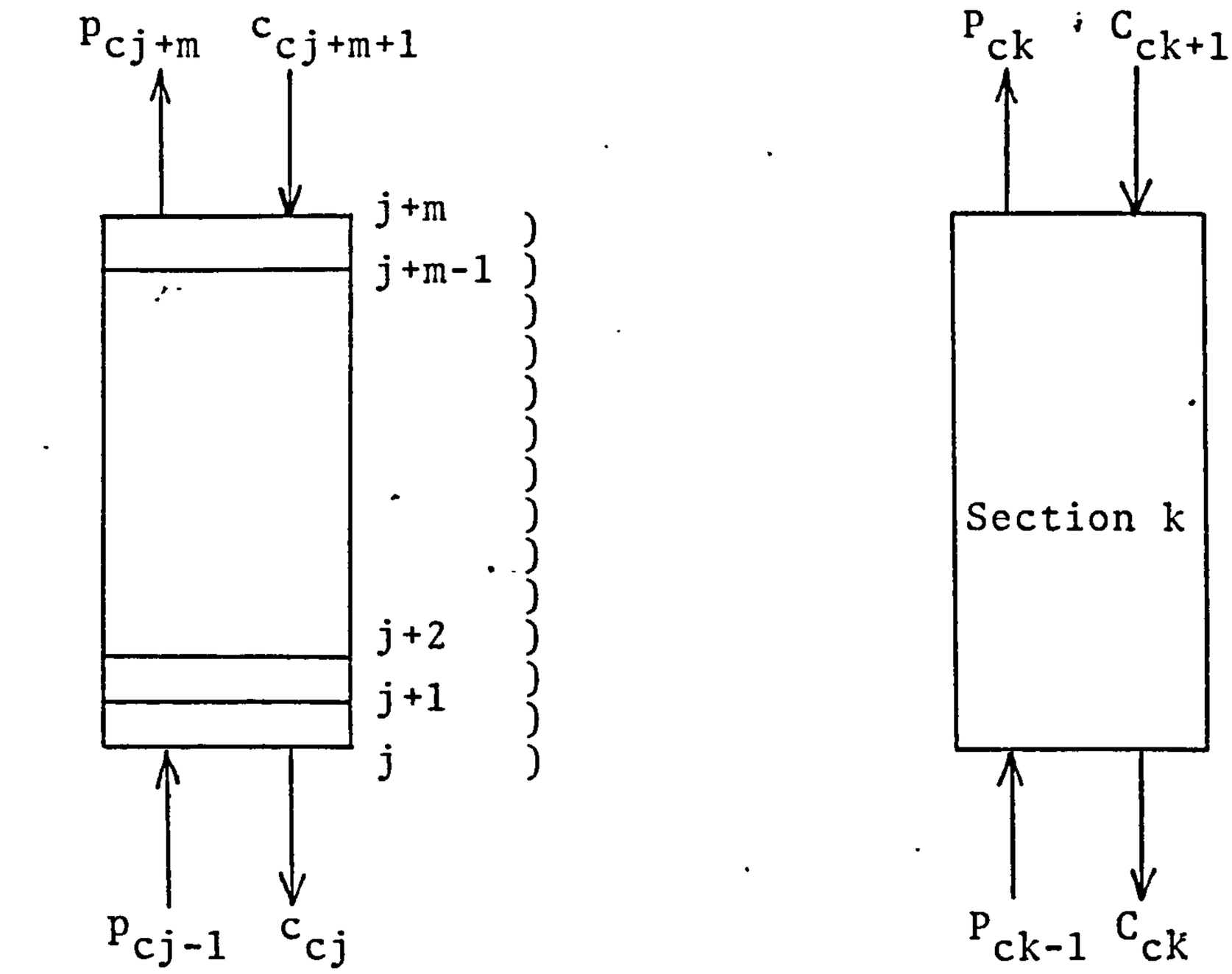


FIG.3.15 SIMPLE MODEL: PLATE LUMPING

TABLE 3.2 SECTION CONFIGURATIONS

Configuration	Total number of sections	Number of plates per sections Base ... Top
A	7	1, 5, 5, 5, 2, 2, 1
B	9	1, 3, 2, 3, 2, 3, 2, 3, 2
C	4	5, 5, 5, 6
D	5	1, 5, 5, 5, .5
E	4	1, 10, 5, 5

a single plate as a unit for dynamic balances, the technique considers a group of plates, as shown in Fig.3.15. Referring to the figure, the section shown would be described in the full model by the set of equations:

$$W_T \frac{d}{dt} c_{cj+\ell} = (Lc_c)_{j+\ell+1} + \left(\frac{Vp_c}{\pi}\right)_{j+\ell+1} - \left(\frac{Vp_c}{\pi}\right)_{j+\ell} - (Lc_c)_{j+\ell}$$

$$0 \leq \ell \leq m \qquad (3.90)$$

In the plate lumped model, the differential equation for this section is written:

$$W_{Tk} \frac{d}{dt} C_{cK} = L_{k+1} C_{ck+1} + \left(\frac{VP_c}{\pi}\right)_{k-1} - \left(\frac{VP_c}{\pi}\right)_k - L_k C_{ck} \qquad (3.91)$$

where the total hold up W_{Tk} which is assumed constant is given by:

$$W_{Tk} = \sum_{i=0}^{m} W_{Ti} \qquad (3.92)$$

A similar equation is written for the amine concentration:

$$W_{Tk} \frac{d}{dt} C_{MK} = L_{k+1} C_{Mk+1} - L_k C_{Mk} \qquad (3.93)$$

The concentration of amine on all the plates in the section is equal to the exit concentration C_{Mk}. For the calculation of the exit vapour composition from the liquid composition Coggan and Noton were able to use a Fenske Underwood equation because they were dealing with a binary mixture. However, a numerical procedure can be used equally well, and in this work the exit partial pressure, P_{ck} is computed from the C_{ck} by a steady state plate to plate procedure using the flow rates, equilibrium relationship (3.83), plate efficiency and the inlet partial pressure P_{ck-1}. It is therefore obvious that the technique of plate lumping preserves perfectly the steady state behaviour of the original non-lumped model.

3.7. Comparison of the full and simplified models

The start up problem was considered first as this allows comparison of both the dynamics and the final steady state predicted by the two models. To assess the effect on the dynamics of the column configuration selected for the simple model, the different configurations shown in Fig. 3.15 and Table 3.2 were used. The parameters used in equation (3.95) for the equilibrium partial pressure of carbon dioxide were evaluated assuming a temperature of 100°C. A comparison of the final steady states of the two models, given in Table 3.3., showed that the simple model predicted compositions significantly different from those given by the full model, particularly near the top of the column. This is due to the assumption of an isothermal column, which changes the relative positions of the equilibrium and operating lines, the effect being particularly accentuated near the top of the column where the gradient of the equilibrium line is increasing rapidly. Better agreement between the two models is obtained by adjusting the parameters in the simple model as shown in Table 3.3. The solution of the start up problem using the fitted model is shown in Fig.3.16; the final steady state is improved and adjustment of the parameters has had very little effect on the dynamics.

The effect of different plate configurations upon the dynamics of the simple model is also shown in Fig. 3.16. The most significant error with all the configurations is seen to be the representation of the base concentration, and

TABLE 3.3. COMPARISON OF STEADY STATES

Section Number (Simple Model Arrgnmt.A.	Simple Model unfitted exit compositions c_c	p_c	Full Model exit compositions c_c	p_c	Simple Model fitted exit compositions c_c	p_c
7	.7550	68.23	.7844	67.96	.7820	67.41
6	.6561	45.29	.6872	48.87	.6880	48.14
5	.6196	31.71	.6472	35.02	.6510	35.28
4	.5785	26.69	.5992	29.41	.6078	30.19
3	.5496	21.04	.5637	22.74	.5764	24.25
2	.4830	17.07	.4920	17.85	.4976	19.95
1	.4740	7.74	.4815	8.12	.4804	8.92

		Simple Model unfitted	Full Model	Simple Model fitted
Separation rate		$.1620 \times 10^{-3}$	$.1595 \times 10^{-3}$	$.1597 \times 10^{-3}$
Equilibrium parameters	a	-.864	-	-.356
	b	15.7751	-	13.603
	E	.80	-	.85

Operating conditions as in Table 3.1.

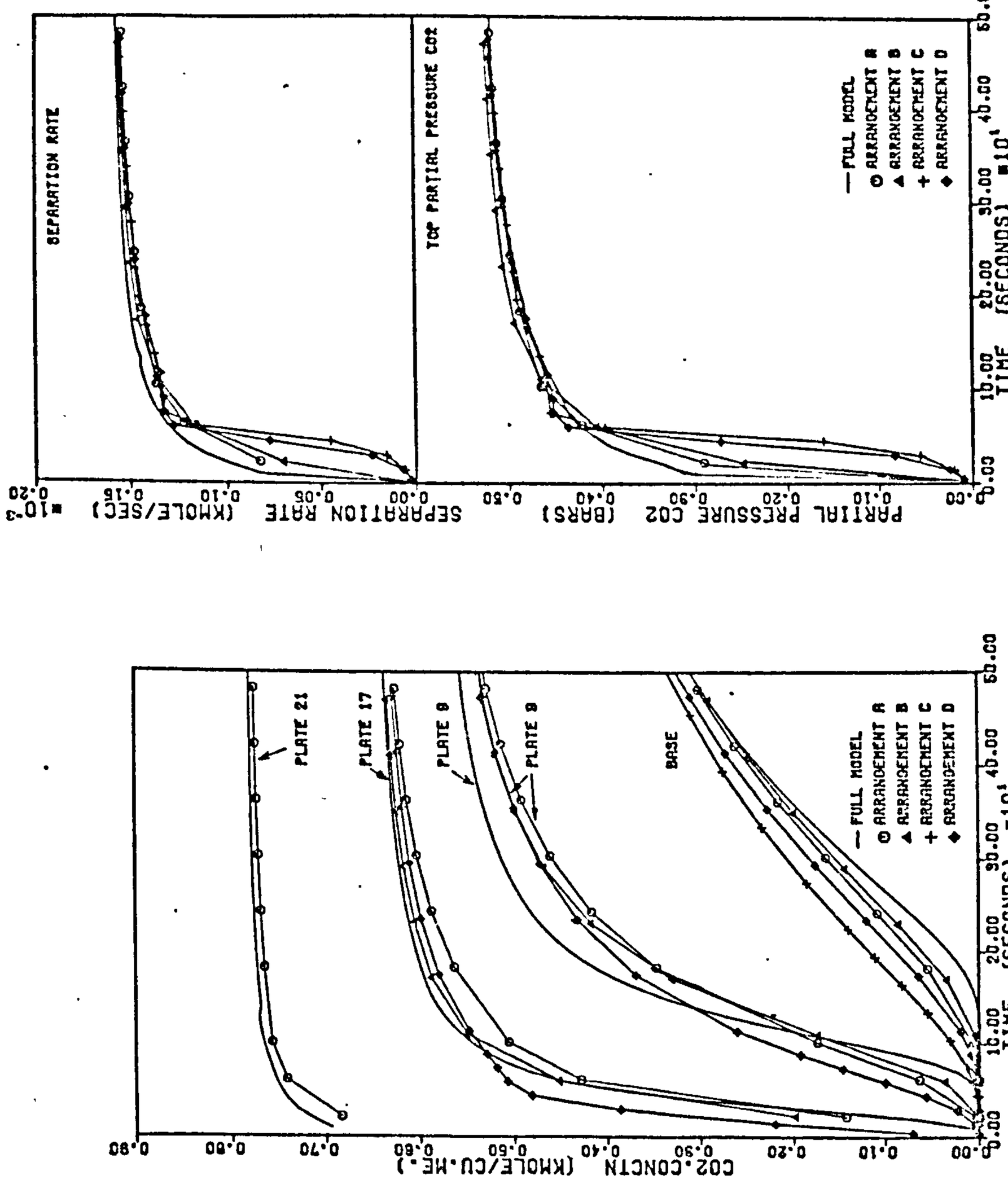


FIG.3.16. SIMULATION OF START UP: FITTED SIMPLE MODEL

lumping the base with adjacent plates gives a poorer approximation than if the base were considered separately as shown by configurations C and D. Both arrangements A and B give a good approximation to the full model and it is likely that the difference between them would be acceptably small compared with the errors in fitting the model to plant responses. The approximation could be further improved by adjustment of the hold up which in the responses shown was obtained from the full model by summing the hold up in each of the lumped sections.

The responses of the full and simple models to positive and negative changes in feed concentration are compared in Fig. 3.17. As may be expected the simple model tends to give more sluggish responses although this could be improved by reducing the hold up.

Other disturbances for which the model could be called upon to simulate the response include changes in the condenser heat load, the feed flow rate and the steam supply to the reboiler. Changes in the condenser heat load have negligible effect on the column separation and so are not considered.

The response to a change in inlet liquid flow rate obtained using the full model with liquid dynamics included is compared in Fig. 3.18 with that obtained using the simple model. Two solutions are given for the simple model, both using configuration A: the first assumes that the liquid flow transient passes through immediately and the second that the liquid flow rate within and out of each section has first order dynamics with respect to the entry liquid flow rate:

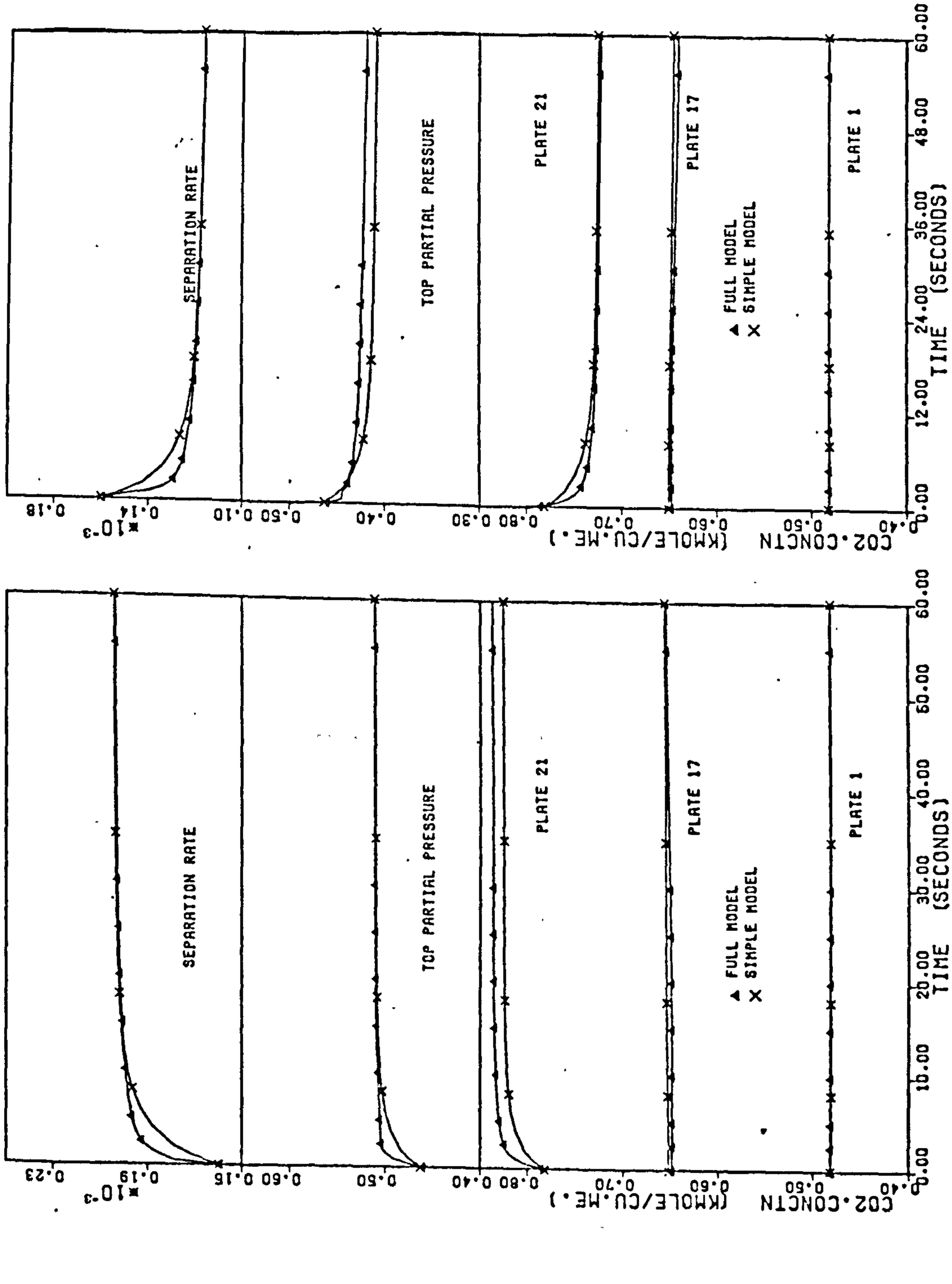


FIG.3.17. RESPONSES TO FEED COMPOSITION CHANGES

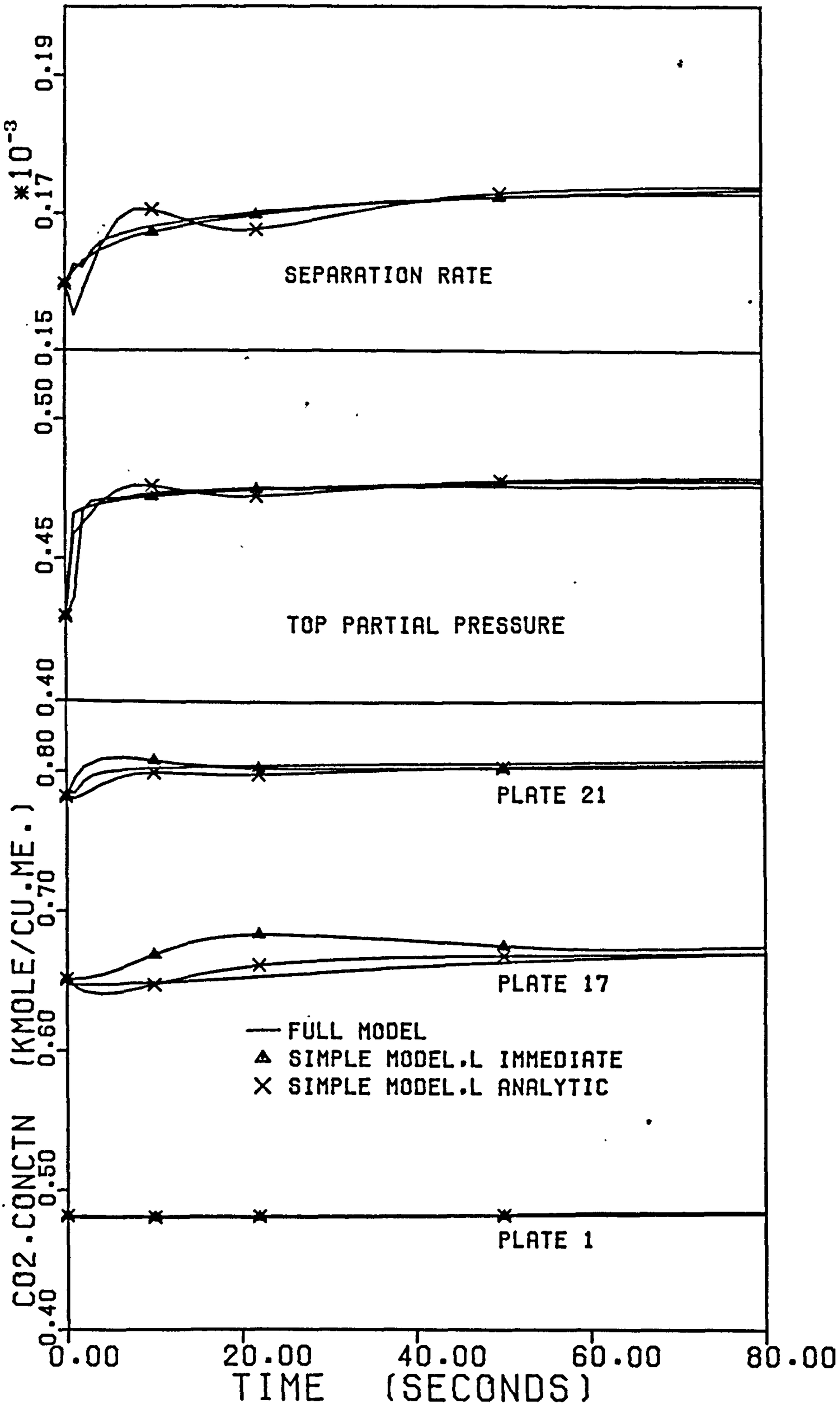


FIG.3.18. RESPONSE TO CHANGE IN FEED FLOW RATE FROM .30 TO .35x10^{-3} m^3/s

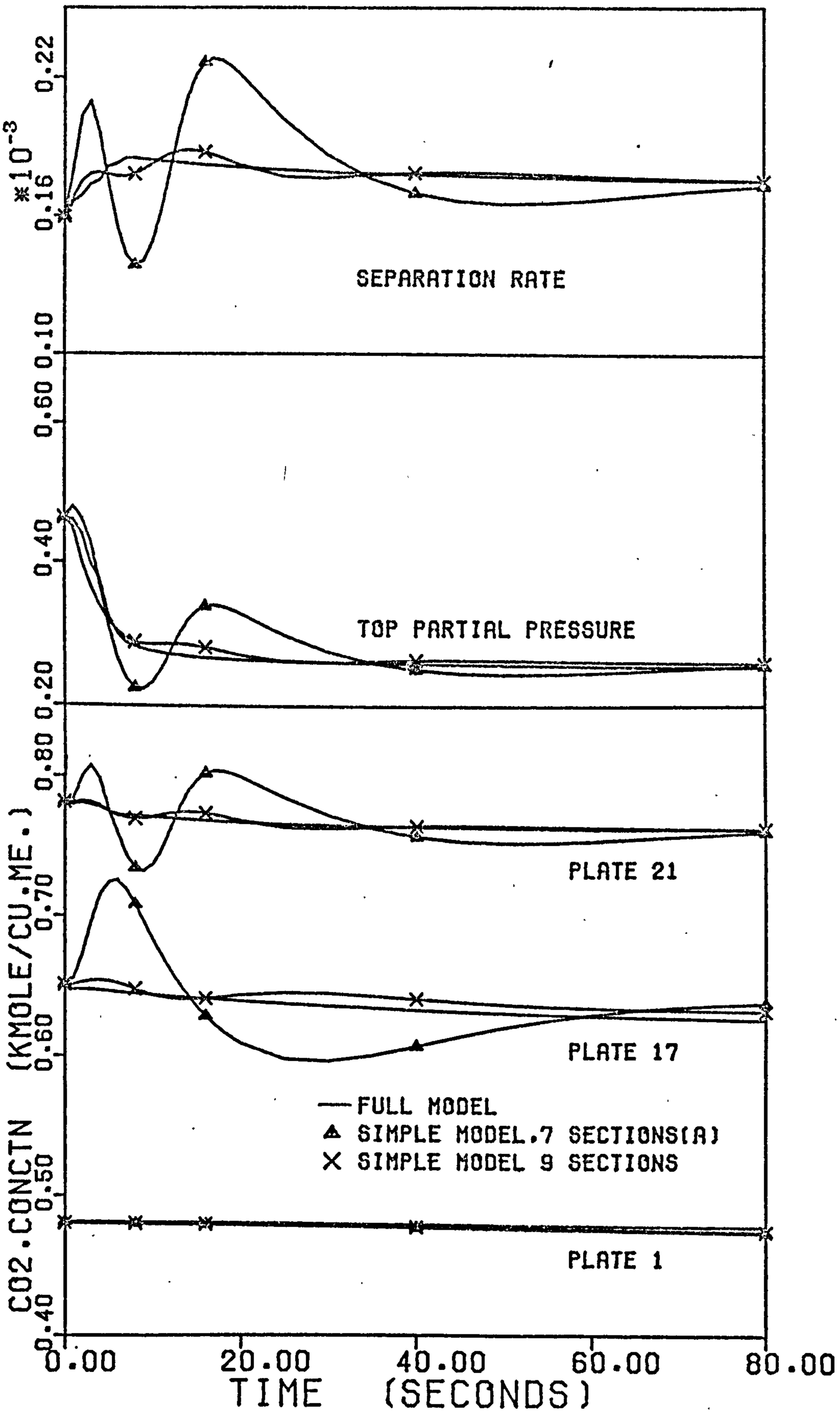


FIG.3.19. RESPONSE TO CHANGE IN STEAM INPUT FROM .03 TO .04 KG/S USING FULL AND TWO SIMPLE MODELS

$$\left.\begin{aligned} \frac{d}{dt}L_N &= \frac{1}{\tau_k}\,[F_F - L_k] \qquad k = N \\ \frac{d}{dt}L_k &= \frac{1}{\tau_k}\,[L_{k+1} - L_k] \qquad k = 1,\ N-1 \end{aligned}\right\} \tag{3.94}$$

where τ_k is a hydraulic response time constant for section k.

This equation can be easily solved numerically and if all the time constants τ_k are equal it can be solved analytically for simple disturbances in the feed flow rate.

The assumption that the liquid flow rate transmits immediately gave a reasonable approximation to the response of the full model. It was surprising to find that instead of improving the response the use of the second assumption introduced oscillation in the separation rate and the top partial pressure. The two responses are compared in Fig. 3.18 and it was concluded that the original assumption generally gave a better approximation.

Finally the response to a change in inlet steam rate was considered. The vapour rate leaving the reboiler was computed from equation (3.86) and the time constant was estimated from the dynamics of the full model. The plate arrangement A selected for the simple model gave considerable oscillation in all the components of interest in the response, see Fig. 3.19. The cause of the oscillation is the same as in the case of a response to a change in liquid flow rate and is due to the assumption that the plate lump is internally at steady state. A change in the liquid or vapour rates in the section causes a change in the operating line for the section, and because the section is

assumed to be at steady state the exit compositions calculated are not representative of those which exist at that point in the real situation. The discrepancy increases as the number of plates in a lump increases, and the oscillation is more severe for the case of a vapour rate change because the partial pressures are computed sequentially up the column and so any disparity in the lower sections is increased as it passes up the column. Repetition of the problem with a nine section arrangement, also shown in Fig.3.19., gave a considerable reduction in the magnitude of the oscillation to a level which is acceptable. Consideration of these responses shows that sections with large numbers of plates should be avoided, and although this may appear to compromise the plate lumping technique it has to be said that despite these difficulties the state vector has been reduced in magnitude by a factor of two or more from that of the original model. If only composition responses are of interest the lumped sections can be made larger with a corresponding saving in time and reduction of the state vector.

The saving in computation time as a consequence of using the simple model is considerable: the solution of the start up problem using arrangement A with Runge Kutta integration required 13 seconds of computation compared with about 40 for the full model. With the use of the integration techniques considered in Chapter 4, the computation time for this problem using the simple model can be further reduced to about 2 seconds which therefore represents a very considerable saving.

3.8. Conclusions

A steady state model using a simple desorption mechanism has been proposed together with a suitable method of solution. The heat load required to achieve a given stripping rate was found to be in reasonable agreement with the data of Benson et al, and the model showed generally feasible behaviour.

The model requires only a few parameters to be estimated and this could be done using the on-line computer.

In the comprehensive model the representation of the condenser was considered in greater detail than previous works and a reasonably simple yet realistic form was found. However, there remains to be investigated on the plant how changes in the heat load can be related to changes in the inlet temperature and flow rate of the cooling water.

The full model initially proposed was considerably simplified by physical assumptions arising from analysis of the model and also by the technique of plate lumping. Combined with the integration techniques described in Chapter 4 the simple model should be sufficiently rapid to employ on-line or for the prediction of optimal control actions off-line.

Practical work on the plant is clearly required in order to understand the desorption process in detail and the plant obviously provides an opportunity for original work. However, the aim of the work reported in this chapter was not the detailed explanation of the desorption process but the development of a model which can simply and adequately represent the column.

3.9. Nomenclature for Chapter 3

a	parameter in expression for equilibrium partial pressure of carbon dioxide	
a′	interfacial area	m^2
a_H	parameter in Antoine equation	
A_C	heat transfer area of condenser	m^2
A_D	downcomer area	m^2
A_H	bubbling area	m^2
A_R	heat transfer area of reboiler	m^2
A_T	tray area	m^2
b	parameter in expression for equilibrium partial pressure of carbon dioxide	
b_H	parameter in Antoine equation	
c*	equilibrium concentration of free carbon dioxide in solution	$kmole/m^3$
c_{cj}	total concentration of carbon dioxide in solution on plate j	$kmole/m^3$
C_{ck}	total concentration of carbon dioxide in section k of the simple model	$kmole/m^3$
c_{cF}	total concentration of carbon dioxide in feed	$kmole/m^3$
c_d	discharge coefficient in expression for dry plate pressure drop	
c_H	parameter in Antoine expression	kJ/Kmole°C
c_i	interfacial concentration of carbon dioxide	$kmole/m^3$
c_{Mj}	concentration of MEA on plate j	$kmole/m^3$
c_{Mk}	concentration of MEA in section k of the simple model	$kmole/m^3$

c_{MF}	concentration of MEA in feed	kmole/m^3
c_o	concentration of carbamate in the bulk solution	kmole/m^3
c_p	specific heat of liquid phase	kJ/m^3°C
D	diffusion coefficient	m^2/s
E	plate efficiency	
F_c	flow of condensate from the condenser	kmole/s
F_F	feed flow to the desorption column	m^3/s
F_o	flow of steam condensate from the reboiler	kg/s
F_R	flow of condensate reflux from condensate reservoir	m^3/s
F_s	flow of steam to the reboiler	kg/s
g	gravity	m/s^2
h	liquid enthalpy	kJ/m^3
h_c	condensation heat transfer coefficient in the reboiler	kW/m^2°C
h_o	enthalpy of steam condensate	kg/s
h_v	column side heat transfer coefficient in the reboiler	kW/m^2°C
H	vapour enthalpy	kJ/kmole
H′	solubility coefficient for carbon dioxide in solution	kmole/m^3bar
H_s	enthalpy of steam to reboiler	kJ/kg
k_G	gas phase mass transfer coefficient	kmole/m^2s bar
k_L	liquid phase mass transfer coefficient	m/s
K_{oG}	overall gas phase mass transfer coefficient	kmole/m^2s bar
k_r	rate constant for decomposition reaction	m^3/kmole.s

k'	constant in Francis Weir formula	
K''	constant relating vapour rate to steam flow rate, equation (3.86)	kmole/kg.
L_j	liquid flow rate off plate j	m^3/s
M_j	molecular weight of vapour leaving plate j	
m_α	sensitivity of bubble point to change in carbonation ratio	°C
N	number of plates in column	
ΔP	total plate pressure drop, expressed as clear liquid height	m
p_{cj}	partial pressure of carbon dioxide leaving plate j	bars or mm. of mercury
p_{Hj}	partial pressure of water vapour leaving plate j	
p_i	interfacial partial pressure of carbon dioxide	
p^*	equilibrium partial pressure of carbon dioxide	
q	heat transfer per unit length in the condenser	
Q_C	heat transfer in the condenser	kW
Q_R	heat transfer in the reboiler	kW
R	specific desorption rate	$kmole/m^2s$
S	separation rate for the column, defined by equation (3.32)	kmole/s.
S_{cj}, S_{Fj}, S_{Hj}, S_{Mj}	quantities defined by equations (3.40), (3.45), (3.46), (3.48)	
T	temperature	°C

T_C	temperature of condensate in condenser	°C
T_V	temperature of vapour in condenser	°C
T_W	temperature of cooling water in condenser	°C
T_{WR}	temperature of reboiler wall	°C
U_C	overall heat transfer coefficient for condenser	$kW/m^2°C$
U_R	overall heat transfer coefficient for reboiler	$kW/m^2°C$
v_j	vapour rate from plate j	kmole/s
W_{Dj}	hold up in downcomer j	m^3
W_{pj}	hold up on tray j	m^3
W_{Tj}	total hold up on plate j	m^3
z_{Fj}	height of foam on tray j	m
z_{Lj}	height of clear liquid on tray j	m
Z_j	height of clear liquid in downcomer on plate j	m
z_W	height of weir	m
α	carbonation ratio	
ϕ	foam density	
ρ_{Gj}	density of gas from plate j	kg/m^3
ρ_L	liquid density	kg/m^3
ρ_s	density of steam in steam chest	kg/m^3
λ_D	heat of decomposition of carbamate	kJ/kmole
λ_H	latent heat of water	kJ/kmole
π	total pressure	bars
τ_K	hydraulic time constant for section k of simple model	s
τ_{RS}	time constant of reboiler	s

Indices and subscripts

j plate number, numbered upwards from reboiler = 1

k index for section in simplified model

T top of the column

N top plate

CHAPTER FOUR

NUMERICAL INTEGRATION METHODS

4.1. Introduction and Literature Survey

The simulation and study of chemical engineering or control systems often requires the solution of a set of ordinary differential equations:

$$\dot{x} = f(x,t) \tag{4.1}$$

Generally this set of equations may be large and contain non-linear components requiring the use of numerical integration techniques. The time constants for the rate processes represented, and consequently the eigenvalues associated with (4.1), may vary over a wide range, especially if the model is comprehensive. The equations are then termed stiff and integration methods such as Runge Kutta require the use of a short step length compared with the response time of the slowest component. Model simplification can generally be expected to reduce the stiffness of equations, but the experience of the simplification made in Chapter 3 suggests that the stiffness may not always be reduced appreciably.

Restriction of the integration step length is inconvenient when integrating plant models on-line for filtering or control. Under such circumstances a rapid method is required rather than one which is highly accurate. Furthermore, in off-line simulation a rapid but approximate integration method would be adequate for many purposes. The aim of this chapter is to assess and develop suitable stiff integration methods.

Distefano[26] compared the performance of a variety of classical integration methods for distillation column simulation. He concluded that the fourth order Runge Kutta and Adams Moulton methods represented the best compromise between accuracy, speed and stability. The stability properties for multistep and Runge Kutta methods are well presented by Lapidus and Seinfeld[54] and Henrici[37].

Consider the linear homogeneous equation:

$$\dot{z} = -\lambda z \tag{4.2}$$

the exact solution of which is

$$z(t) = z(0)\exp(-\lambda t) \tag{4.3}$$

An integration procedure will approximate the exact solution by a computed solution:-

$$z_c(nh) = [M'(h\lambda)]^n z(0) \tag{4.4}$$

The fourth order Runge Kutta procedure generates

$$M'(h\lambda) = 1-\lambda h + \tfrac{1}{2}\lambda^2 h^2 - (1/6)\lambda^3 h^3 + (1/24)\lambda^4 h^4 \tag{4.5}$$

and absolute stability requires that

$$|M'(h\lambda)| \leq 1 \tag{4.6}$$

For Runge Kutta this places a bound on the magnitude of h:

$$\lambda h \leq 2.78 \tag{4.7}$$

Distefano found that this theoretical limit cannot always be achieved. This is attributed to the variation in eigenvalues of a non-linear system.

Dahlquist[17] introduced the important concept of A-stability: a method is A-stable if the numerical approximation (4.4) to the solution of (4.2) tends to zero as $n\to\infty$ with a fixed positive h and $Re(\lambda) > 0$.

He showed that the order of an A-stable linear multistep method cannot exceed two, and also that explicit linear multistep methods are not A-stable. For an integration method to be fast, A-stability is a very desirable property as it allows the step length to be made arbitrarily large, restricted only by the accuracy required or by the convergence of the corrector.

The concept of A-stability is restrictive: Runge Kutta and high order multistep methods are not A-stable, so there is a problem of constructing methods which have accuracy as well as stability. Rosenbrock[76] and Calahan[13] have developed methods based on the Runge Kutta formulae by introducing the Jacobian matrix of the system into the computation of the coefficients k:

$$J = \frac{\partial f}{\partial x} \tag{4.8}$$

$$\left.\begin{aligned} k_1 &= h[I-hc_1J(x_n)]^{-1}f(x_n,t_n) \\ k_2 &= h[I-hc_2J(x_n+c_3k_1)]^{-1}f(x_n+c_4k_1) \\ x_{n+1} &= x_n + c_5k_1 + c_6k_2 \end{aligned}\right\} \tag{4.9}$$

Although these methods are A-stable and explicit, the amount of computation per step is large. Methods have been devised based upon a weakening of the concept of A-stability.

Widlund[97] introduced the concept of A(α) stability, the result of observing that stability is required only in the regions of the $h\lambda$ plane occupied by the $h\lambda_j$. If the eigenvalues λ_j of the equations vary, then stability is required only in the associated wedges of the $h\lambda$ plane. Widlund then proceeds to construct A(α) stable multistep methods of order less than four.

Another weakening of A-stability has been proposed by Gear[33]: a method is said to be stiffly stable if, within the region of the hλ plane close to the origin it is accurate, and for the region to the left of a specified limit it is absolutely stable. Multistep methods are then constructed to meet these conditions.

An alternative approach to the problem of combining accuracy with A-stability has been given by Liniger and Willoughby[56], who have developed the concept of exponential fitting. They consider a class of implicit single step methods, and fit the parameters such that the computed solution satisfies the ordinary differential (4.2) at the discrete values computed. This method will be described in more detail later.

The methods proposed by Calahan, Gear, Liniger and Willoughby all make use of the Jacobian matrix J of the system equations. A method which does not make use of J has been developed by Fowler and Warten[30], who propose an integration formula which accounts for the stiff components directly by using exponential terms rather than polynomial approximations.

4.2. Integration Methods

4.2.1. Runge Kutta Methods

The most frequently used Runge Kutta formula is of fourth order and uses the following explicit procedure for computing x_{n+1} from x_n:-

$$\left.\begin{aligned} k_0 &= hf(x_n, t_n) \\ k_1 &= hf(x_n + \tfrac{1}{2}k_0,\ t + \tfrac{1}{2}h) \\ k_2 &= hf(x_n + \tfrac{1}{2}k_1,\ t + \tfrac{1}{2}h) \\ k_3 &= hf(x_n + k_2, t + h) \end{aligned}\right\} \qquad (4.10)$$

$$x_{n+1} = x(t_n+h) = x_n(t_n) + (1/6)(k_0+2k_1+2k_2+k_3) \qquad (4.11)$$

4.2.2. Gear's Method

Gear's method is based on the use of predictor-corrector formulae up to a maximum order of 6. However, in place of working with the dependent variables stored at the current and previous time points, Gear follows Nordsieck[62] and employs a vector normal form, a_n, which consists of the dependent variable and all known derivatives at the current time point:

$$\underline{a}_n = [x_n, h\dot{x}_n, \frac{h^2\ddot{x}_n}{2!}, \ldots, \frac{h^k x_n(k)}{k!}]$$

$$= [a_0, a_1, \ldots. a_{k+1}] \qquad (4.12)$$

where k denotes the order of the method used at time point n. Using this form the scalar differential equation $\dot{x} = f(x)$ can then be written:

$$F(\underline{a}) = hf(a_0) - a_1 = 0 \qquad (4.13)$$

The prediction step is written as:

$$\underline{a}^0_{n+1} = A\underline{a}_n \qquad (4.14)$$

where A is a coefficient matrix, and the correction step as

$$\underline{a}^{m+1}_{n+1} = \underline{a}^{m}_{n+1} + \underline{b}\ F(\underline{a}^m_{n+1}) \qquad (4.15)$$

where $\underline{b}$ is a vector of coefficients.

The corrector equation is solved by the use of Newton's method, so that (4.13) is satisfied:-

$$\underline{a}_{n+1}^{m+1} = \underline{a}_{n+1}^{m} - \underline{b}\ UF(\underline{a}_{n+1}^{m}) \tag{4.16}$$

where the scalar gradient U is:

$$U = [\frac{\partial F}{\partial \underline{a}} . \underline{b}]^{-1} = [-b_1 + hb_0 \frac{\partial f}{\partial x}]^{-1} \tag{4.17}$$

The coefficients b_0 and b_1 are selected to satisfy the criteria of stiff stability; details regarding their selection and the stability of the resulting methods are given by Gear[32]. The coefficients of the vector b depend upon the order of the method used, and can be changed at any step with relative ease as a consequence of the use of the vector normal form. The method is applicable to vector differential equations and a Fortran listing is available[32].

4.2.3. Fowler-Warten Method

The method is non-linear, explicit and approximates the solution by considering the true solution, z_T, to consist of the sum of two functions:

(i) an asymptotic function, z_A, based upon current and past values: and

(ii) a perturbation function, z_P, to be determined by the local variation.

Considering a scalar case, these functions are assumed to have the form:

$$z_T(t) = z_A(t) + z_P(t) \tag{4.18}$$

$$z_A(t+\theta) = z_A(t) + \theta \dot{z}_A(t) \tag{4.19}$$

$$z_P(t+\theta) = z_P(t) + (\exp(\lambda_P \theta) - 1)(1/\lambda_P)\dot{z}_P(t) \tag{4.20}$$

$$0 \leq \theta \leq h$$

The asymptotic function is a linear function fitted through

the previous and current points (t-h), t:

$$z_A(t) = 0 \tag{4.21}$$

$$\dot{z}_A(t) = [z_T(t)-z_T(t-h)]/h \tag{4.22}$$

The constant λ_p is related to the second differential by:

$$\lambda_p \dot{z}_p(t) = \ddot{z}_T(t) \tag{4.23}$$

If the second differential is not available analytically, as is usually the case, an Euler step is taken and an approximation to the differential made:-

$$\ddot{z}_p(t) = (\dot{z}_p(t+\delta) - \dot{z}_p(t))/\delta \tag{4.24}$$

where $\delta < h$

The approximate solution is then computed from

$$z_c(t+h) = z_T(t) + h\dot{z}_A(t) + hc_1\dot{z}_p(t) \tag{4.25}$$

where $c_1 = (\exp(\lambda_p h) - 1)/\lambda_p h$ (4.26)

If $\dot{z}_p(t) = 0$; then $\lambda_p = 0$, $c_1 = 0$

The authors show that the method is second order, and develop a relation giving an estimate of the truncation error:

$$e = h(\dot{z}_c(t+h) - \dot{z}_A(t) - c_2\dot{z}_p(t)) \tag{4.27}$$

where $c_2 = \exp(\lambda_p h)$ (4.28)

The authors propose a number of modifications to the basic method, one of the most important being due to the reason that the equations presented here are not exact for a non-homogeneous linear ordinary differential equation. They also give a scheme for controlling both the main step and Euler step lengths according to absolute or relative errors.

The authors state that for a system of equations the procedure is applied to each component individually.

4.2.4. Low Order Methods and Exponential Fitting

For an implicit linear multistep method to be A-stable Dahlquist[17] showed that the order must be less than or equal to two; the method with lowest truncation error is the trapezoidal method:-

$$x_{n+1} = x_n + \frac{h}{2}(f(x_n,t_n) + f(x_{n+1},t_{n+1})) \qquad (4.29)$$

There are two problems associated with employing (4.29) for numerical integration:

(i) because the equation is implicit, there is the problem of solving a set of non-linear equations at each step;

(ii) to achieve reasonable accuracy the step length must be small.

To overcome the problem of accuracy, Liniger and Willoughby propose a more general form of (4.29):-

$$x_{n+1} = x_n + h[\beta f(x_n,t_n) + (1-\beta) f(x_{n+1},t_{n+1})] \qquad (4.30)$$

where β is a parameter. They show that, given the correct initial condition, equation (4.30) will predict the exact solution of the scalar differential equation (4.2) at discrete time points h, 2h, 3h ...nh provided the parameter β is selected as:

$$\beta = \left(\frac{1}{q}\right) - [\exp(q)-1]^{-1} \qquad (4.31)$$

where $q = \lambda h$

The method is then said to be exponentially fitted at $q = \lambda h$.

The method simply generalises to the solution of a vector differential equation, and the value of β is then

selected from the eigenvalue of largest magnitude because it is the simulation of the stiffest component which determines the stability of the integration.

4.2.5. Solution of the Non-linear Implicit Equations

The solution of equation (4.30) is a non-trivial task and so the success of an implicit integration method is critically dependent upon the performance of the corrector method employed.

The method of direct substitution can be rejected without further consideration because the convergence condition for the corrector would make large values of λh inadmissible. Parameter relaxation can be used to offset this problem to some extent. A relaxation scheme is defined:

$$x_{n+1}^{\ell+1}=(1-\omega)x_{n+1}^{\ell}+\omega[x_n+h\beta f(x_n,t_n)+h(1-\beta)f(x_{n+1}^{\ell},t_{n+1})] \qquad (4.32)$$

Successive approximations to the solution x_{n+1}^{*} are related by:-

$$(x_{n+1}^{\ell+1} - x_{n+1}^{*}) = M(x_{n+1}^{\ell} - x_{n+1}^{*}) \qquad (4.33)$$

where the matrix M, usually called the iteration matrix, is

$$M = [(1-\omega)I + \omega h(1-\beta)J] \qquad (4.34)$$

The rate of convergence of (4.32) is determined by the spectral radius, or maximum eigenvalue of M, which can be adjusted by varying ω. However, the spectral radius cannot be made arbitrarily small. Suppose J has eigenvalue λ_1 to λ_n in order of decreasing magnitude, then the corresponding eigenvalues of the matrix M are

$$\lambda_1^M = 1 - \omega(1 - h(1-\beta)\lambda_1)$$

$$= 1 - \omega d_1 \qquad (4.35)$$

and $$\lambda_n^M = 1 - \omega(1 - h(1-\beta)\lambda_n)$$

$$= 1 - \omega d_n \qquad (4.36)$$

The spectral radius will be equal to the larger of λ_1^M and λ_n^M which will depend on the value of ω chosen. The minimum value of the spectral radius is obtained when $-\lambda_1^M = \lambda_n^M$ with ω chosen as:

$$\omega = \frac{2}{(d_n+d_1)} = \frac{2}{2-h(1-\beta)(\lambda_1+\lambda_n)} \qquad (4.37)$$

The spectral radius then becomes:

$$|\lambda_1^M| = |\lambda_n^M| = \left|\frac{h(1-\beta)(\lambda_1-\lambda_n)}{2-h(1-\beta)(\lambda_1+\lambda_n)}\right|$$

$$= \left|\frac{h(1-\beta)\left(\frac{\lambda_1}{\lambda_n} - 1\right)}{\frac{2}{\lambda_1} - h(1-\beta)\left(\frac{\lambda_1}{\lambda_n} + 1\right)}\right| \qquad (4.38)$$

It is clear from equation (4.38) that the minimum spectral radius that can be achieved is dependent upon the ratio of the maximum to the minimum eigenvalue, as well as the maximum eigenvalue itself. As the ratio of the eigenvalues increases the minimum spectral radius tends to unity and consequently the rate of convergence becomes worse.

An alternative to the problem of estimating the relaxation parameter has been given by Sumner[94] who shows that an iterative relaxation scheme can be set up with the relaxation parameter chosen at each step to minimise the error between the current and next vector function. Assuming that the vector function can be expanded by a Taylor series to first order terms, the method can be initiated with a

relaxation parameter ω_0.

Define

$$F(x^{\ell}_{n+1}) = x_n + h\beta f(x_n,t_n) + h(1-\beta)f(x^{\ell}_{n+1},t_{n+1}) \qquad (4.39)$$

Then if the initial estimate is $x^{(1)}_{n+1}$:-

$$x^{(2)}_{n+1} = (1-\omega_0)x^{(1)}_{n+1} + \omega_0 F(x^{(1)}_{n+1}) \qquad (4.40)$$

$$x^{(3)}_{n+1} = (1-\omega)x^{(2)}_{n+1} + \omega F(x^{(2)}_{n+1}) \qquad (4.41)$$

where ω is chosen by:-

$$g = x^{(2)}_{n+1} - x^{(1)}_{n+1} \qquad (4.42)$$

$$h = F(x^{(2)}_{n+1}) - 2x^{(2)}_{n+1} + x^{(1)}_{n+1} \qquad (4.43)$$

$$\omega = -h^T g/h^T h \qquad (4.44)$$

then put $x^{(2)}_{n+1} = x^{(3)}_{n+1}$ and repeat until $\|x^{(3)}_{n+1} - x^{(2)}_{n+1}\| < \varepsilon$

Equation (4.30) may also be solved by computing corrections according to Newton's technique:

$$\Delta x^{\ell+1}_{n+1} = [I-(1-\beta)hJ^{\ell}_{n+1}]^{-1}$$

$$\times [x_n + h\beta f(x_n,t_n) + h(1-\beta)f(x^{\ell}_{n+1},t_{n+1}) - x^{\ell}_{n+1}] \qquad (4.45)$$

The estimate is updated until the correction is less than a specified error:

$$x^{\ell+1}_{n+1} = x^{\ell}_{n+1} + \Delta x^{\ell+1}_{n+1} \qquad (4.46)$$

An initial estimate is required; Liniger and Willoughby propose that the final value of the previous step be used:

$$x^{0}_{n+1} = x_n \qquad (4.47)$$

The Newton corrector has good convergence properties; indeed for a linear homogeneous system, the exact solution is obtained in one step.

4.2.6. A modification to the Liniger and Willoughby method

Liniger and Willoughby propose an integration method based upon exponential fitting of the integration coefficients as described in 4.2.4., coupled with the use of the Newton corrector. Although developed primarily for homogeneous equations, they show that exponential fitting can be used for the general non-homogeneous system. With x^0_{n+1} selected as in (4.47), equation (4.45) simplifies considerably provided f is independent of time, and so the first estimate of the solution x_{n+1} can be written

$$x_{n+1} = x_n + h[I-(1-\beta)hJ_n]^{-1}f(x_n) \qquad (4.48)$$

They suggest that this equation itself should be used as an integration formula, implying just one Newton correction per step, with the correction matrix re-evaluated at each step. This is a surprising recommendation, as the amount of computing required for the correction matrix vastly exceeds that required for each iteration of the corrector. In this work the correction matrix is computed and stored, then used with repeated iteration of the corrector at each time step, until convergence as assessed by a weighted Euclidean norm, is attained:-

$$\sum_j (\Delta x_j/x_j)^2 \leq \varepsilon_2 \qquad (4.49)$$

The correction matrix is re-evaluated at a set integral number of steps, or when the corrector fails to converge. If the dimension of the state vector is m, and the Jacobian matrix is calculated by finite difference methods, re-computation of the Jacobian and correction matrices every m

steps does not add much of an overhead to the method.

The step size is controlled by the number of corrector iterations used: the step size is doubled if fewer than a set number of corrector iterations are used at each step over a specific number of steps. The step is halved if the corrector fails to converge, although this is given a lower priority than re-evaluation of the Jacobian matrix. The step length is controlled to be less than a maximum, although an alternative would be to control the step length according to the truncation error which could be estimated from

$$e_n = h(\beta-\tfrac{1}{2})[f(x_n,t_n)-f(x_{n-1},t_{n-1})] \qquad (4.50)$$

A further refinement is to introduce a simple method for estimating the coefficient β which is related to the maximum eigenvalue of the Jacobian matrix by (4.31). For a non-linear system the maximum eigenvalue will vary with the state and it is therefore convenient to have a simple method for estimating it. To compute the eigenvalues from the Jacobian matrix would be excessive, so it is proposed that the largest eigenvalue be estimated using Gerschgorin's theorem[34]:

$$\lambda_{max} \leq \max_i \sum_j |J_{ij}| \qquad (4.51)$$

The row sums of the Jacobian matrix are quickly calculated and the method can be safely used as it over-estimates the maximum eigenvalue.

This method will be referred to as the Euler-Newton method.

4.2.7. Quasi-Newton correction

The Euler-Newton method requires more computation per step than Runge Kutta and has to be used with large step lengths to achieve a reduction in total computation time. When smaller step lengths are required, for example with data supplied at discrete intervals, the Euler-Newton method will show less of a saving in computation. Under these circumstances there is a case for a method which has a smaller amount of computation per step than Euler-Newton, and which is capable of step lengths larger than Runge Kutta. A further economy can be achieved by exploiting the sparseness of the matrices, and this is of particular importance for large systems.

The key to the problem is in the convergence of the corrector, so consider an iteration scheme for the solution of the equation:-

$$x_{n+1}^{\ell+1} = (I-W)x_{n+1}^{\ell} + W[x_n+h\beta f(x_n,t_n)] \qquad (4.52)$$

where W is an arbitrary relaxation matrix.

Assuming that the matrix W remains invariant over the iteration, the convergence condition for (4.52) is:

$$||M|| \leq 1 \qquad (4.53)$$

where

$$M = I + W\,[(1-\beta)hJ - I] \qquad (4.54)$$

To minimise the norm of the iteration matrix M the best choice of W is:

$$W = [I-(1-\beta)hJ]^{-1} \qquad (4.55)$$

As may have been expected from the form of equation (4.52), the matrix W is seen to be an approximation to the

Newton correction matrix in equation (4.45). The excellent convergence properties of the Newton method can thus be attributed to the consequence of making the iteration matrix M the null matrix. The scalar relaxation procedure as given by equation (4.32) can be seen to be a special case of equation (4.55). It was shown in section 4.2.5 that the scalar relaxation parameter can be used to move the eigenvalues of the iteration matrix, although the weakness is that the eigenvalues cannot be adjusted independently. An integration method is therefore proposed using the principle that the relaxation matrix has a simple form consistent with retaining good convergence properties. The form of the relaxation matrix is clearly dependent upon that of the Jacobian matrix. In many chemical engineering applications, particularly absorption or distillation it is simply a band or tridiagonal matrix; or alternatively the dominant elements are restricted to this form. Under such circumstances, the matrix W has a correspondingly simple tridiagonal form, and can be calculated very rapidly. Therefore, for such systems it should be possible to employ a computationally simple but very efficient method for solving the implicit equations.

A very simple method based upon the assumption of a diagonally dominant Jacobian matrix is proposed in order to investigate how well simple approximations can perform. The elements of the matrix W are chosen to ensure that the diagonal elements in the iteration matrix are zero:-

$$W_{jj} = \frac{1}{1-(1-\beta)h\ J_{jj}} \qquad (4.56)$$

Unfortunately for the general case it is not possible to adjust all the eigenvalues of the iteration matrix independently simply by the use of a diagonal relaxation matrix. If the diagonal approximation to the correction matrix fails to reduce the spectral radius sufficiently then a more complex form of the relaxation matrix would have to be considered. The remaining details concerning the integration procedure are as described for the Euler-Newton method.

4.3. Problem Definition

To compare the integration methods described in the previous section, the problem of simulating the start up of the stripping column was considered. The simplified model described in Chapter 3 was used with suitable boundary conditions and model coefficients. The Jacobian matrix was computed by finite difference methods because analytical expressions for the elements are not obtainable.

The stiffness of the system was assessed by computing the eigenvalues of the Jacobian matrix at a few points along the solution.

4.4. Results and Discussion

The solutions were computed initially by use of the Runge Kutta method with a step length of 1 second, then checked by repeating with the step length halved, showing that the initial step length gave four figure accuracy. The ratio of the maximum to the minimum eigenvalue is about 500 to 1, as shown in Table 4.1. With a step length of 1.5 seconds Runge Kutta was unstable, therefore showing that the

TABLE 4.1. EIGENVALUES OF THE JACOBIAN MATRIX

Time from start (sec)	Maximum Eigenvalue	Minimum Eigenvalue	Maximum Eigenvalue / Minimum Eigenvalue	Sum of Eigenvalues
40	2.49	$.44 \times 10^{-2}$	565.9	5.604
200	2.24	$.44 \times 10^{-2}$	509.1	5.916
500	2.40	$.44 \times 10^{-2}$	545.4	6.727

step length of 1 second was quite close to the stability limit. The advantages of Runge Kutta are its high accuracy within a sharply defined stability limit, and its explicit form combined with low storage requirement. The computing times and number of derivative evaluations for the methods used are shown in Tables 4.2 and 4.3.

The methods using parameter relaxation required considerable computation despite their simplicity. The maximum step length for both methods had to be restricted to two seconds to obtain stability and even when using a one second step length the variable parameter technique became unstable in the final part of the solution. Both methods required more derivative evaluations and computation time than Runge Kutta and are, therefore, not suitable for integrating stiff systems. This is not really surprising as there is only one free parameter available to adjust the spectral radius of the iteration matrix and this was shown to be ineffective for stiff systems.

The only explicit method used, that due to Fowler and Warten, had reasonable performance in terms of computing time, although the step lengths used were rather smaller than the other methods. The control of the step length by the approximation to the truncation error was erratic, with multiple step halving a surprisingly common occurrence. The method relies upon using the pseudo-eigenvalue for each component achieved by computing an approximation to the second derivative. The fact that this approximation has a truncation error which increases with decreasing step length implies that the control of the Euler and main step lengths

can be very critical. As can be seen from Fig. 4.1., the stiff components have been approximated well, but the non-stiff component shows considerable error. The reason for this may be traced to error in the second derivative for this component due to use of an insufficiently large Euler step. The accuracy of the method decreases rapidly as the step length increases, and as such, the method could not be reliably used with large steps for this problem. Due to this difficulty of step length and error control, although this method has favourable storage and speed, it is not robust enough to be considered for general use.

Gear's method did not give as much saving in time as expected, although the method is the most accurate of the stiff methods used. The achievement of four figure accuracy throughout the solution is possible provided the maximum error norm is correctly set. The computing time to 200 seconds were in all cases in excess of that used by Runge Kutta. However, the maximum step length set was reached either just before or soon after 200 seconds and as a result the computation time for the remaining 300 seconds was extremely small, indeed the shortest of all the methods. In an attempt to test the method and try to reduce the computation time the effect of the maximum error norm and step length was investigated. As may be expected, increasing the maximum step length did not greatly reduce the computing time, because large steps are not used over the first 150 seconds. However, it was not possible to reduce the computing time to the times typical of those achieved with the Euler-Newton method.

Gear only allows three correction iterations per step, before re-evaluation of the Jacobian matrix; the step size is halved if a further failure occurs. In the simulations where the requested accuracy was high, this lead to frequent re-evaluation of the Jacobian matrix and consequently rather poor performance during the initial transients up to 100 seconds. Other methods, even Runge Kutta were found to be superior over this period.

In this problem the Jacobian matrix was computed by finite difference, and so required m derivative evaluations. In these simulations, more than half of the derivative evaluations were used in evaluating the Jacobian matrix. There is therefore a very definite incentive to compute the Jacobian matrix directly from the system equations. The computation of the Jacobian matrix from analytic relations would in most cases be far more efficient than calculation by finite difference, so it is possible that this method could be more effective in such circumstances.

As a general integration method for stiff and non-stiff systems, Gear's method has the advantages of yielding good accuracy if desired, an excellent error control scheme, and very large steps in the presence of stiff components, provided their transients are reasonably small. However, the computing time for general applications does not offer as great an economy as the Euler-Newton method, especially if accuracy is required only to 2 or 3 figures.

Considering the methods based upon exponential fitting, the computing times for the Euler-Newton method clearly indicate that this method is the quickest. The effectiveness

of exponential fitting was assessed by comparing a solution obtained using the exponentially fitted method with one computed by the trapezoidal rule. It can be seen from Fig. 4.2. that the trapezoidal rule gave oscillations in the stiff components as well as being less accurate when large step lengths were used; in one computation the computed solution failed due to divergence of the corrector. In comparison, the Euler-Newton method gave a solution, shown in Fig. 4.3., which is smooth and sufficiently accurate for most simulation purposes. For the whole problem the Euler-Newton method is approximately four times faster than Runge Kutta, and for the last 300 seconds of simulation is almost an order of magnitude faster. This shows that exponential fitting to the largest eigenvalue as estimated by Gerschgorin's theorem is a sound procedure. The theorem overestimates the largest eigenvalue: this is not a serious problem as higher values of q confer greater stability on the method. When using short step lengths as in runs 8, 9 and 10 the advantage to be gained over the trapezoidal rule by employing exponential fitting is not significant.

Comparison of runs 6 and 7 shows that more frequent evaluation of the Jacobian and correction matrices can lead to faster computation due to more rapid convergence of the corrector. Over the initial transients the more frequent evaluation of the correction matrix in run 6 enabled the corrector to converge in one or two iterations compared with two or three for run 7. After 200 seconds, the corrector in most cases converged in one iteration only, so no saving was possible. Obviously, a compromise exists between the saving of corrector iterations and cost of Jacobian evaluations. No

generalisations are possible as this is likely to be problem dependent.

Integration was attempted using one Newton iteration with a relatively small time step, as given by equation (4.48). However, even with an initial step of 2.0 seconds, the method became unstable after the second or third step. It is therefore logical to use the corrector as many times as required to achieve convergence as measured by the error norm. Over the first 100 seconds, the corrector required approximately 3 iterations per step, with step lengths as large as 8 seconds, so there is little to be gained from using the corrector once per step if the step length has to be reduced to ensure stability as in this case. After 200 seconds, the method was generally converging in one iteration with the maximum step length used.

The Quasi-Newton method was used with a fixed step length of 2 seconds, and although requiring a relatively large number of derivative evaluations was significantly quicker than Runge Kutta. Because of the small step length, the accuracy achieved was in general better than the Euler-Newton methods. Step lengths as large as those used with the Euler-Newton method caused problems with convergence of the corrector. For larger-step lengths to be used a better approximation than a simple diagonal matrix is required. However, for a system as stiff as this it is encouraging that use of a very simple approximation to the Newton correction matrix should give such reasonable results. The method requires little storage, is simple to employ and is therefore ideal for on-line applications.

TABLE 4.2. COMPARISON OF METHODS

Method	Run	Step Length		Error norm for corrector	NSTEP	At 200 secs			At 500 secs.		
		Initial	Max.			h	ND	CP	h	ND	CP
Runge Kutta	1	1.0	1.0	-	-	1.0	800	5.37	1.0	2000	13.58
Fowler-Warten	2	1.0	-	-	-	8.0	304	2.92	2.0	526	5.03
Euler-Newton	3	2.0	10.0	$.1x10^{-3}$	15	8.0	191	3.10	10.0	301	4.68
	4	2.0	10.0	$.1x10^{-3}$	30	8.0	192	2.99	10.0	272	4.24
	5	2.0	10.0	$.1x10^{-3}$	60	10.0	176	2.83	10.0	271	4.32
	6	2.0	10.0	$.1x10^{-2}$	16	10.0	128	2.06	10.0	220	3.29
	7	2.0	10.0	$.1x10^{-2}$	30	10.0	156	2.33	10.0	232	3.44
Quasi-Euler Newton	8	2.0	4.0	$.1x10^{-3}$	15	2.0	430	3.46	2.0	1040	8.61
Fixed Parameter relaxation	9	2.0	4.0	$.1x10^{-3}$	-	1.0	911	6.96	1.0	2422	18.94
Variable Parameter relaxation	10	2.0	4.0	$.1x10^{-3}$	-	1.0	855	7.81	UNSTABLE		

h, ND and CP defined beneath TABLE 4.3

TABLE 4.3. GEARS METHOD

Run	Initial Step length (sec.)	Maximum Step length (sec.)	Error norm for corrector	At 200 secs.				At 500 secs.			
				h	ND	NJ	CP	h	ND	NJ	CP
11	.1	20	$.2\times10^{-3}$	18.25	583	22	12.37	20	646	24	13.86
12	.1	20	$.2\times10^{-2}$	16.52	482	17	9.44	20	539	19	10.76
13	.1	20	$.2\times10^{-1}$	20.0	419	17	7.65	20	444	17	8.51
14	.1	40	$.2\times10^{-2}$	16.52	482	17	9.39	40	536	19	10.59

h: current step length (seconds)
ND: number of derivative evaluations
NJ: number of jacobian evaluations
CP: computing time (CDC 6400) seconds
NSTEP: number of steps between jacobian evaluations

Time for one derivative evaluation = .053 seconds (CDC 6400)

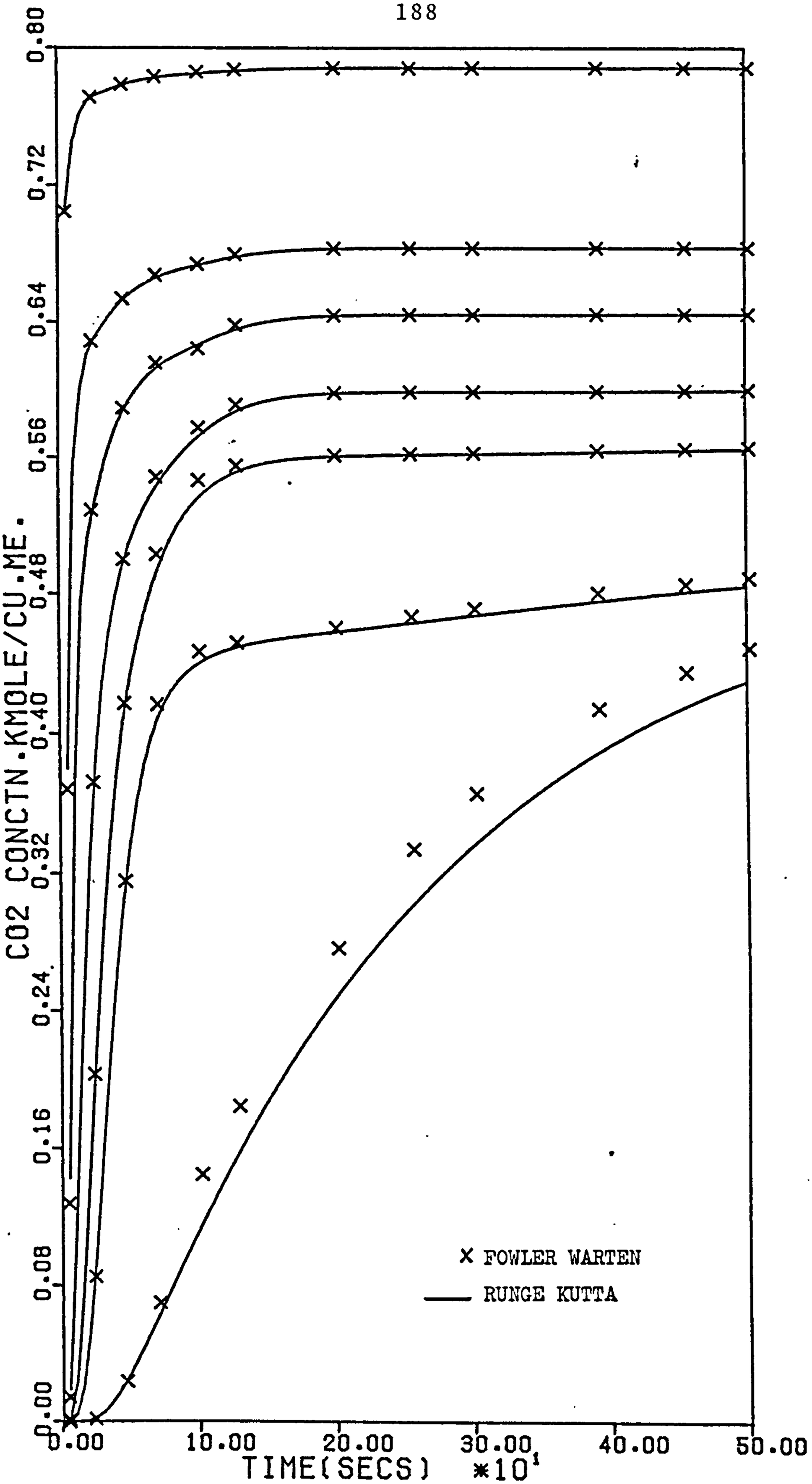


FIG. 4.1 INTEGRATION BY FOWLER WARTEN

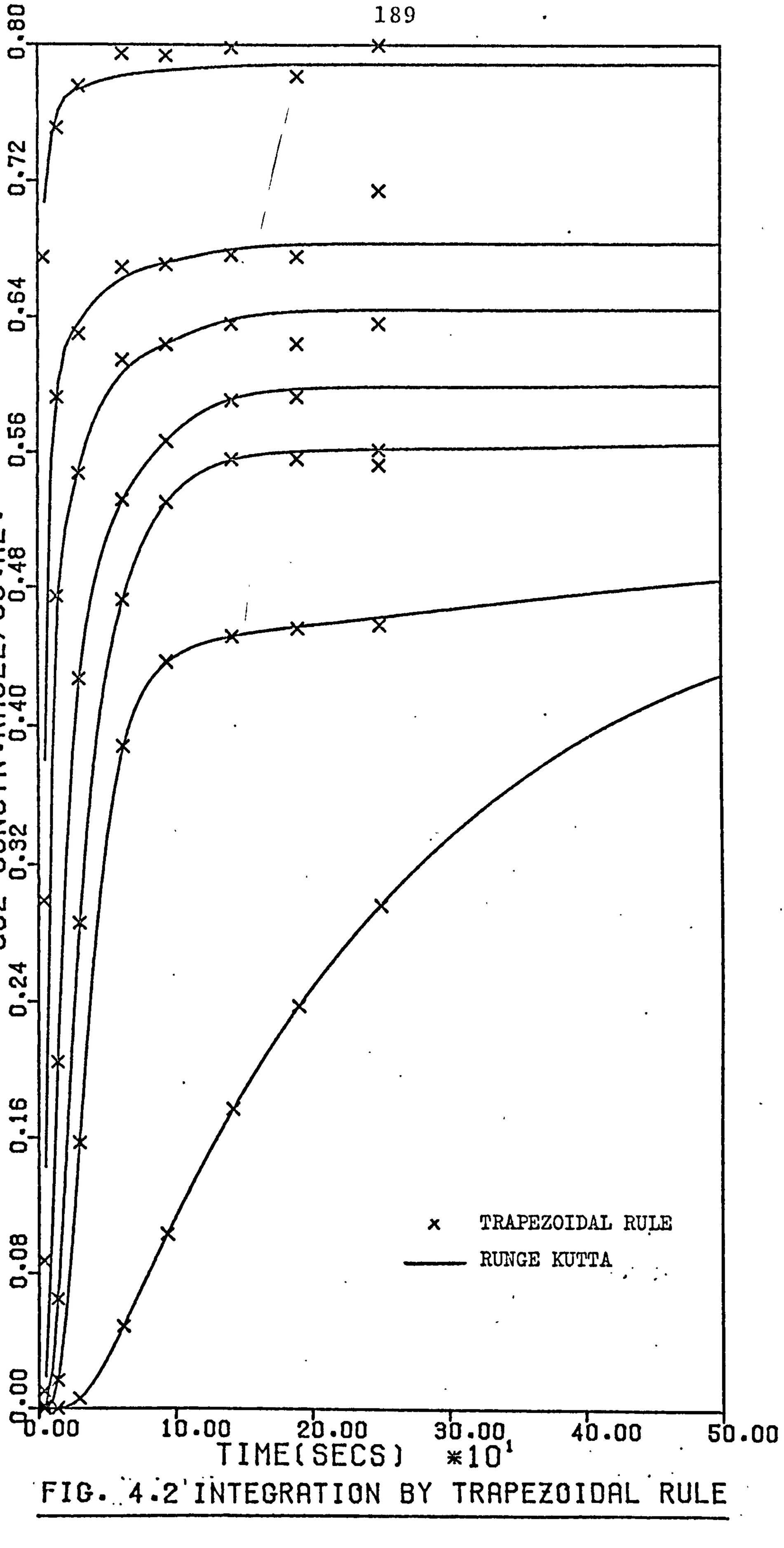


FIG. 4.2 INTEGRATION BY TRAPEZOIDAL RULE

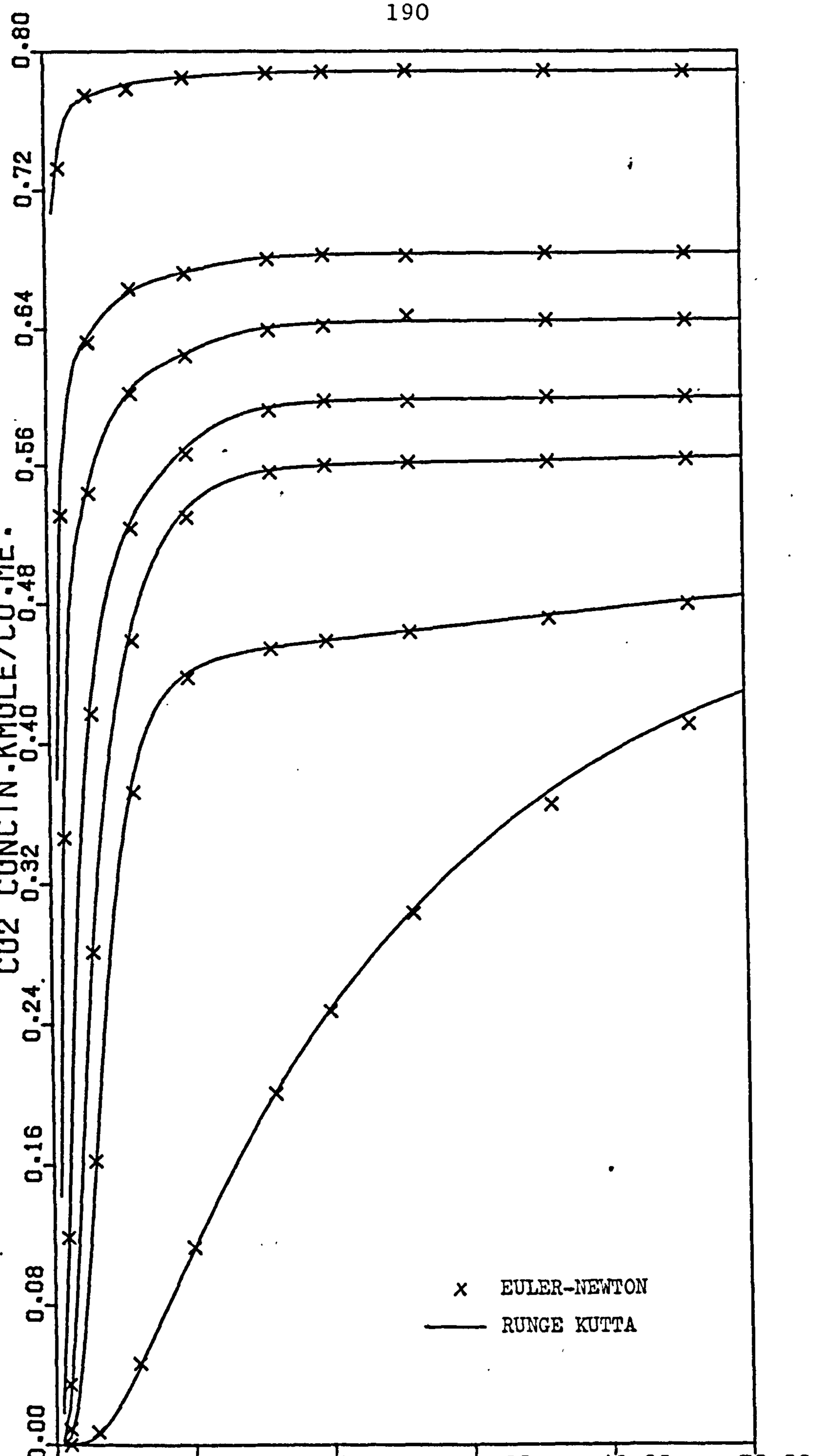


FIG. 4.3 INTEGRATION BY EXPONENTIALLY FITTED EULER-NEWTON, RUN NO. 4

4.5. Conclusions and Recommendations for future work

It has been shown that methods suitable for rapid integration or simulation either exist or can be developed. The Euler-Newton method with exponential fitting is an economical and robust method, suitable for general use. Gear's method was also found to be very good, offering greater accuracy but sometimes requiring more computation. The most effective methods require the evaluation and storage, either analytically or from finite difference, of the Jacobian matrix, as well as the implicit solution of a set of equations. The time required to integrate a set of equations is often of importance in the computation of optimal controls for a dynamic system, and in many cases limits the complexity of the problem that can be considered. Computation of the Jacobian matrix in these situations would be particularly advantageous as it can be used to define an adjoint system as well as being used to integrate the system equations efficiently. The adjoint system could be integrated very rapidly to give the gradients of the objective function which could be conveniently used in a gradient optimisation technique.

For large systems of equations, the amount of computation and storage rises rapidly with the size of the state vector. For this reason and others, the concept of an approximation to the full Newton matrix was considered. The results for the simple approximation used are very encouraging and indicate that it would be worthwhile to investigate the use of an approximate relaxation matrix where

possible. In addition, for most systems it would appear worthwhile to see if the form of the differential equations suggest the use of a simple relaxation matrix. If a suitably simple form is found, as with systems having a tridiagonal Jacobian, then it is possible to construct a very rapid and robust integration procedure.

4.6. Nomenclature for Chapter 4

a_n	vector of dependent variables and derivatives in Gear's method
A,b	matrix and vector of integration coefficients in Gear's method
e_n	truncation error
$f(x_n,t_n)$	vector of first order derivatives at time t_n
h	step length
I	Identity matrix
J	Jacobian matrix of derivatives with respect to state
M	Iteration matrix defined by (4.33)
q	product λh defined in equation (4.31)
t	time
W	relaxation matrix
x_n	state vector at time t_n
x_j	jth element of state vector x
$\Delta x_{n+1}^{\ell+1}$	correction to x_{n+1}^{ℓ} at iteration ℓ
z,z_c	exact and computed solutions to equation (4.2)
z_A,z_P	asymptotic and perturbation functions in the Fowler-Warten method
β	coefficient in exponentially fitted methods, defined by (4.31)
δ	Euler step length in Fowler-Warten method
ε	error norm
λ	an eigenvalue of the Jacobian matrix J
λ_{max}	maximum eigenvalue
λ_p	Constant in Fowler-Warten method
ω	relaxation parameter

CHAPTER FIVE

PARAMETER ESTIMATION

5.1.1. Introduction

The mathematical models derived in the previous chapters require the estimation of parameters defining the steady and unsteady states. Because these parameters will be estimated from noisy measurements with the on-line computer it is natural to consider using a recursive least squares or Kalman filter. The simple plate column model is an example of the situation where the parameters will have to be updated on-line to ensure model accuracy. The model is non-linear and requires the measurement of at least three independent quantities. There is the possibility of using approximately forty measurements although it is obvious that not all of these could be used simultaneously or frequently due to the restrictive availability of instrumentation. The objective of this chapter is, therefore, to find a policy for selecting measurement points which will give the best parameter estimates and enable the filter to converge rapidly. This is clearly of importance when parameters in an approximate model are updated to account for changes in operating conditions. In addition the application of a linear filter to a non-linear estimation problem is examined.

5.1.2. Literature Survey

The pioneering work of modern filtering theory was made by Kalman[43,44] and Bucy[45] who derived algorithms

for linear systems with Gaussian statistics. These algorithms yield estimates which simultaneously satisfy the least squares, mean and maximum likelihood criteria and Kalman showed the very desirable properties of convergence, stability and consistency which are inherent in the application to linear systems. Linear filtering theory has received a stimulus through applications met in the aerospace industry, particularly to linearized problems, some examples of which are to be found in Jazwinski[41] and Sorenson[90].

The problems encountered with the application of a linear filter to a non-linear problem stem from the fact that the desirable properties of the filter are no longer assured, as the filter equations are then only approximations to the propagation of the first two moments of the true state probability density functions. The problem of bias when non-linearity is comparable with measurement error has been demonstrated by Denham and Pines[25]. They propose iterating the corrector to convergence, and showed that this reduced the bias in the estimate.

A further problem is filter divergence due to model errors. To overcome this a number of techniques have been proposed, including overweighting the most recent data, or conditioning the estimate on a restricted number of measurements. However, despite these problems linearized filtering theory has been used successfully in chemical engineering to measure catalyst activity and decay rates[31,80] reaction rate parameters[95] and the parameters in blending and heat transfer systems[14].

Despite the large amount of literature concerned with linear filtering, there is very little concerned with the

problem of measurement selection to achieve an improved estimate. The reason is undoubtedly that in many cases freedom of choice of measurements is either very restricted or non-existent. However, Aström[5] has shown the dependence of the variance of an estimate on the number of observations in the application of a minimum variance filter. A similar dependence for the covariance matrix of the Kalman filter has been shown by Sorenson[91].

Denham and Speyer[24] consider the problem of measurement selection to minimise the terminal uncertainty in a lunar space mission. They derive perturbation equations to describe the variation in objective function with initial uncertainty, control gain matrix and measurement policy. Although their computation of an optimal policy shows an improvement in the objective function over the initial measurement policy chosen, the paper is not clear in showing how the combinatorial nature of the problem was overcome.

A problem closely related to that of measurement selection is the selection of an experimental procedure to discriminate between models. Hunter and Reiner[39] develop a criterion to select the next experimental point such that the difference in prediction between the two rival models, with parameters based on the observations so far, is maximised. Because the discrimination process ultimately depends upon the mean and variance of the measurement residuals, the criterion indicates replication of experiments in order to establish these statistics. Box and Draper[8] and Box and Hill[9] formulate a discrimination function from the posterior probability densities associated with each model, of which there may be more than two. Their

criterion discriminates by use of the posterior probabilities as opposed to measurement residuals, and therefore in the examples they give, experiments are not repeated so frequently as with the criterion of Hunter and Reiner, although the criterion does select measurements at the boundary of the operating region so that the differences between model predictions are increased. However, the problem considered in this chapter is different because the system cannot be freely manipulated, as Box and Hunter assume, and the choice is between measurements and not models.

5.2. Statement of Equations for Extended and Iterated Filters

The recursive Kalman filter gives an estimate of the state of a linear dynamic system conditioned on current and previous measurements. There are numerous derivations of the Kalman filter in the literature, and Jazwinski[41] presents a good derivation and full discussion.

The extended filter is simply the linearized filter with the linearization made about the previous estimate. A discrete time formulation of the filter is:-

$$x_{K+1} = f(x_K, t) + u_K \tag{5.1}$$

$$y_K = h(x_K, t) + v_K \tag{5.2}$$

where u_K, v_K are random processes with zero mean and

$$E(u_i u_j^T) = \delta_{ij} Q_i \tag{5.3}$$

$$E(v_i v_j^T) = \delta_{ij} R_i \tag{5.4}$$

$$E(u_i v_j^T) = 0 \tag{5.5}$$

If $\hat{x}_{K/K}$ is the optimal estimate of x_K conditioned on observations y_1, $y_2 \ldots y_K$,

and $P_{K/K} = E[(x_K - \hat{x}_{K/K})(x_k - \hat{x}_{K/K})^T]$ (5.6)

then the filter equations defining the evolution of the estimate and covariance are:-

$$\hat{x}_{K+1/K} = f(\hat{x}_{K/K}, t) \tag{5.7}$$

$$P_{K+1/K} = \phi P_{K/K} \phi^T + Q_K \tag{5.8}$$

where ϕ is the state transition matrix associated with (5.1):

$$x_{K+1} = \phi x_K == \phi(K+1, K) x_K \tag{5.9}$$

At an observation the state is updated by

$$\hat{x}_{K+1/K+1} = \hat{x}_{K+1/K} + K_{K+1}[y^0_{K+1} - h(\hat{x}_{K+1/K})] \tag{5.10}$$

$$P_{K+1/K+1} = [I - K_{K+1} G_{K+1}] P_{K+1/K} [I - K_{K+1} G_{K+1}]^T + K_{K+1} R_{K+1} K^T_{K+1} \tag{5.11}$$

where G is the Jacobian matrix between the predicted measurement and the state:

$$G_{K+1} = \frac{\partial h_{K+1}}{\partial x} (x_{K+1/K}) \tag{5.12}$$

and K_{K+1} = Kalman gain

$$= P_{K+1/K} G^T_{K+1} [G_{K+1} P_{K+1/K} G^T_{K+1} + R_{K+1}]^{-1} \tag{5.13}$$

y^0_{K+1} = observed measurement vector at K+1.

The filter is initialised with $P_{o/o}$, $\hat{x}_{o/o}$.

For the particular case of a system in steady state, the prediction equations simplify to:

$$\hat{x}_{K+1/K} = \hat{x}_{K/K} \tag{5.14}$$

$$P_{K+1/K} = P_{K/K} + Q_K \tag{5.15}$$

Using the well known Sherman-Morrison-Woodbury formulae, (5.11) can be re-written:

$$P^{-1}_{K+1/K+1} = P^{-1}_{K+1/K} + G^T_{K+1} R^{-1}_{K+1} G_{K+1} \qquad (5.16)$$

In some cases (5.16) is preferable to (5.11).

The iterated filter replaces equations (5.10) to (5.13) with:

$$\eta_{i+1} = \hat{x}_{K+1/K} + K(\eta_i)[y^0_{K+1} - h(\eta_i) - G(\eta_i)(\hat{x}_{K+1/K} - \eta_i)] \qquad (5.17)$$

$$\text{where } G(\eta_i) = \frac{\partial y}{\partial x} k+1(\eta_i) \qquad (5.18)$$

$$K(\eta_i) = P_{K+1/K} G^T(\eta_i)[G(\eta_i) P_{K+1/K} G^T(\eta_i) + R_{K+1}]^{-1} \qquad (5.19)$$

Equations (5.17) to (5.19) are solved recursively for η_{i+1} with:

$$\eta_i = \hat{x}_{K+1/K} \qquad (5.20)$$

$$\text{until } \|\eta_{i+1} - \eta_i\| < \varepsilon \qquad (5.21)$$

$$\text{then } x_{K+1/K+1} = \eta_{i+1} \qquad (5.22)$$

and the covariance is updated:

$$P_{K+1/K+1} = [I - K(\eta_{i+1}) G(\eta_{i+1})] P_{K+1/K} [I - K(\eta_{i+1}) G(\eta_{i+1})]^T + K(\eta_{i+1}) R_{K+1} K^T(\eta_{i+1}) \qquad (5.23)$$

5.3. Concept of an Optimal Measurement Set

The accuracy of the model parameters obtained in an estimation process depends upon the accuracy of the measurements made, and for models with more than one parameter, the relationship between the measurements. It is clear that a two parameter model cannot be completely fitted from two measurements which are linearly dependent, no matter how many times they are repeated. The aim of this section is to analyse how the accuracy of the parameters depends upon

the measurement accuracy and the choice of measurements, in order to develop a criterion which can be used to select the best measurement set.

The assumption is made that the model is a good reprcsentation of the data so that the problem of model error or bias does not occur. If all possible measurements are defined as a vector y, then the Jacobian matrix G^1 is defined as:

$$G^1 = \frac{\partial \underline{y}}{\partial \underline{x}} \tag{5.24}$$

A subset of measurements can be selected from y, and the matrix of G used in the estimation algorithm then consists of the appropriate rows from the matrix G^1, obviously with repetition of a row if there is more than one observation of the corresponding measurement. A least squares estimate $\hat{x}$ is given by:

$$\hat{x} = (G^T G)^{-1} G^T \underline{y} \tag{5.25}$$

where the dimension of the vector $\hat{x}$ is n. The estimate exists if the rank of the matrix G is greater than or equal to n, which implies that G contains at least n linearly independent rows, and ensures that the generalised matrix inverse exists. If the rank of G is less than n then the matrix $(G^T G)$ is singular, the inverse does not exist and the measurements do not define all components of the vector $\hat{x}$. It can therefore be expected that the quality of an estimate depends upon the linear independence of the rows of the G matrix, or alternatively, the proximity to singularity of the matrix. The problem is to select what criterion or measure of proximity to singularity should be used, and how

this is related to the quality of the estimate. The basis of the concept has been introduced here with reference to estimation by least squares, the development of it will now be considered with the Kalman filter.

The quality of an estimate and the performance of an estimation algorithm may be assessed in a variety of ways: the confidence limits of the estimate, the noise in the estimate, or the statistics of the measurement residuals. If there are no problems of biased measurement residuals, which should be so if the model is an adequate representation, then the confidence limits of the estimate may be used as a criterion of optimality. When a Kalman filter is used for the estimation of the state of a linear system, as proposed here, the covariance matrix gives a statistical measure of the accuracy of the estimate. This may be assessed by the magnitude of the elements of the covariance matrix, or more rigorously through the concept of the error ellipsoids as described by Cramer[16].

If the estimate has a multivariable gaussian distribution, as is the case here, then surfaces of constant probability density are defined by:

$$x^T P^{-1} x = c^2 \tag{5.26}$$

For the case of c set equal to unity the surfaces are usually referred to specifically as the error ellipsoids, which have principal semi-axes equal to the square root of the eigenvalues of the covariance matrix. An example of a two dimensional situation is shown in Fig. 5.1; the size of the error ellipsoid for c = 1 gives an indication of the accuracy of the estimate $\hat{x}_1$, $\hat{x}_2$. Obviously, it is desirable

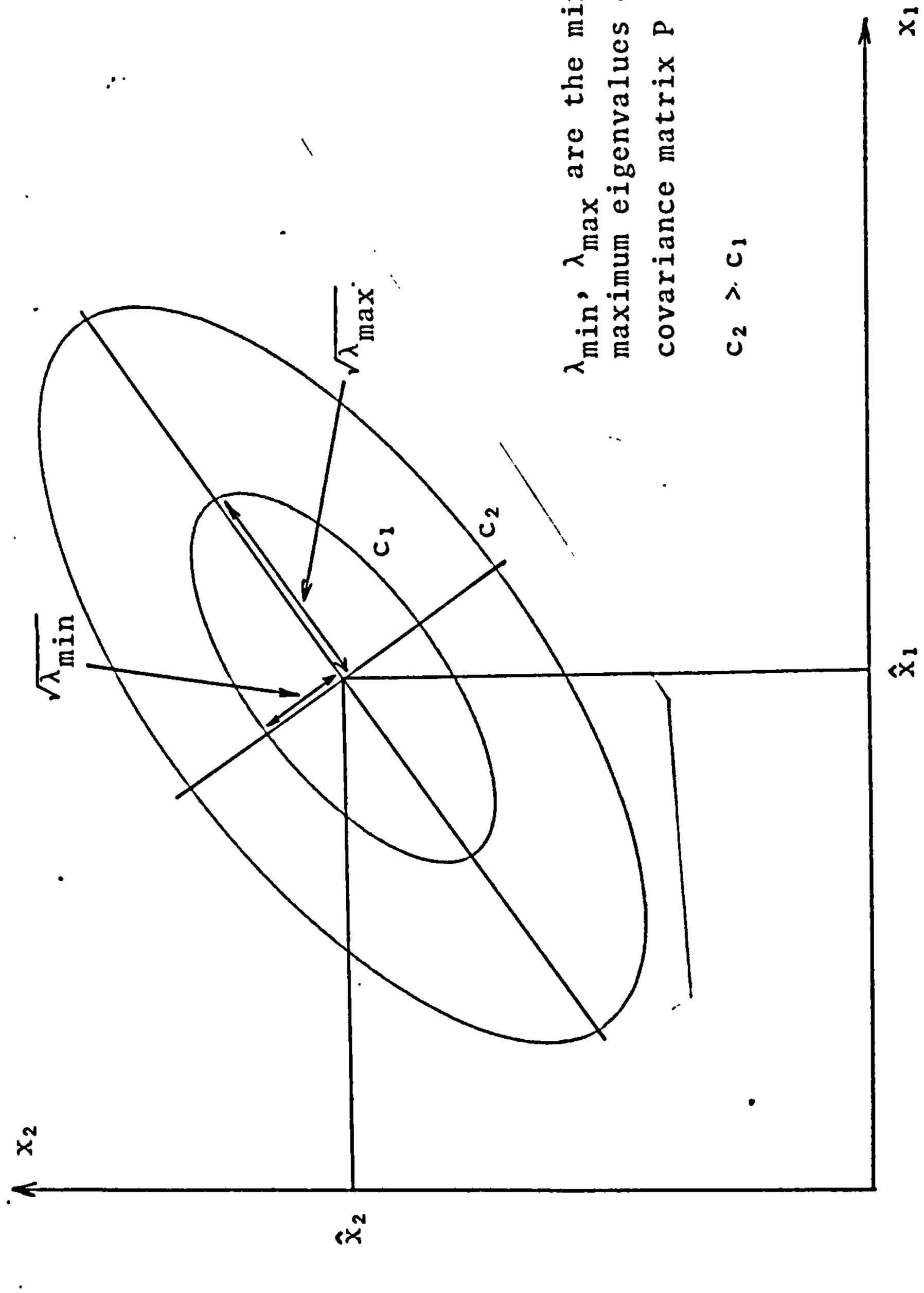


Fig.5. Error ellipsoids for the two dimensional problem

λ_{min}, λ_{max} are the minimum and maximum eigenvalues of the covariance matrix P

$c_2 > c_1$

that the error ellipsoid for c = 1 should be as small as possible, and therefore it is apparent that the quantity of interest is the maximum eigenvalue of the covariance matrix P which should be minimised. It is now necessary to relate the covariance matrix, and consequently the error ellipsoids, to the rows selected from the matrix G^1.

The condition for complete observability of the state of a linear system after K observations is that the information matrix $I'(K,1)$ be positive definite, i.e. non-singular:-

$$I'(K,1) = \sum_{i=1}^{K} \phi^T(K,i) G_i^T R_i^{-1} G_i \phi(i,K)$$

$$= \sum_{i=1}^{K} G_i^T R_i^{-1} G_i \qquad (5.27)$$

for the case of a stationary system. This condition corresponds to that illustrated earlier for the least squares estimate given by (5.25).

To prove the stability and convergence of the linear estimator, Kalman[44] obtained upper and lower bounds for the covariance matrix:-

$$\|[I'(K,1) + C^{-1}(K,0)]^{-1}\| \leq \|P_{K/K}\| \leq \|[I'(K,1)]^{-1}\| + \|C(K,0)\| \qquad (5.28)$$

where C(K,0) = controllability matrix

$$= \sum_{i=1}^{K} \phi(K,i) Q_{K+1} \phi^T(K,i) \qquad (5.29)$$

For a stationary system with no state noise, the state covariance matrix can be related directly to the information matrix:-

$$P_{K/K}^{-1} = P_{o/o}^{-1} + I'(K,1)$$

$$\text{or} \quad P_{K/K} = [P_{o/o}^{-1} + I'(K,1)]^{-1} \qquad (5.30)$$

Now if the initial covariance matrix, $P_{o/o}$, is very large, then in the limit,

$$P_{K/K}^{-1} = [I'(K,1)]$$

$$= [\sum_{i=1}^{K} G_i^T R_i^{-1} G_i]$$

$$\text{or} \quad P_{K/K} = [\sum_{i=1}^{K} G_i^T R_i^{-1} G_i]^{-1} \qquad (5.31)$$

Equation (5.31) defines the relationship desired earlier.

To achieve the desired condition of making the error ellipsoids for c = 1 as small as possible the information matrix should be so constructed that its minimum eigenvalue is maximised. If this is done, and the minimum eigenvalue of $I'(K,1)$ is non-zero and as large as possible, then the condition for observability is clearly satisfied.

Other matrix attributes which can express non-singularity, the determinant and condition number, were also investigated for developing a useful criterion. Both were rejected because neither restrict the maximum size of the error ellipsoids. If a determinant were maximised it would still be possible to have a very long, but thin elongated ellipsoid because the determinant is the product of the matrix eigenvalues. The condition number is the ratio of maximum to minimum eigenvalue, so this would only effectively measure the departure of the ellipsoids from a circular or spherical condition. Maximising the minimum eigenvalue of $I'(K,1)$ is therefore the best criterion.

The conclusion above was made with the assumption of zero state noise and infinitely large initial covariance matrix. It is difficult to see how, if at all, the presence of state noise would affect a measurement policy, because maximising the minimum eigenvalue of the information matrix does ensure that the upper bound in (5.28) is reduced the most rapidly.

The selection of a measurement policy clearly involves integer programming at some stage, a process which is complicated by dimensionality and procedural problems. Therefore, some insight can be gained by closer examination of the information matrix.

If n_m is the dimension of the measurement vector at each observation, and there are k observations in total, then there are kn_m measurements in total, and to try to specify all these would be a formidable task, especially if k were large.

A simpler problem of greatly reduced dimensionality could be posed if the measurement subset taken at each and every observation was assumed to be the same. Then,

$$I'(K,1) = \sum_{i=1}^{K} G_i{}^T R_i G^{-1} = KH \qquad (5.32)$$

where $H = G^T R^{-1} G$

It would then be a relatively simple problem to select n_m measurements from G to constitute the matrix H, so as to maximise the minimum eigenvalue of H. The eigenvalues of $I'(K,1)$ are then given by

$$\lambda I'(K,1) = K\lambda_i H \qquad (5.33)$$

This would be a relatively simple problem to set up, solve and then put in practice. The alternative of solving the full problem is formidable, and even if it were achieved, could possibly be difficult to employ in practice. The foregoing applies to linear systems where the eigenvalues of the information matrix are independent of the estimate, whereas for a non-linear system, this is no longer true.

Therefore, the dependence of the measurement set on the state should be investigated, as if this proved to be too great the policy proposed would not be as effective as a policy where the measurement set were updated according to the changes in state. Such a policy would be far more complex to consider. However, because the filter is essentially linear, and the properties described above refer specifically to the filter, it is reasonable to look for the existence of an optimal measurement policy as outlined above.

5.4. Application to the estimation of the parameters in the desorption column model

5.4.1. Introduction

The steady state plate column model described in Chapter 3 was used and the state vector for estimation was:

$$x = \begin{pmatrix} A \\ B \\ E \end{pmatrix} \tag{5.34}$$

where A,B are parameters in the equilibrium function.

E is the Murphree gas phase efficiency.

Nominally true measurements were computed from the model using a particular value of the state, see Table 5.1,and

TABLE 5.1 NOMINAL TRUE STATE

Conditions: $F = .35 \times 10^{-3} m^3/s$
$c_F = 1.0$ kmole/m^3
$Q = 70$ kW

True State Parameters: $A = -.864$
$B = 15.7751$
$C = .40$

Plate No.	Liquid Concentration c kmole/m^3	Gas Partial Pressure p mm.Hg.
1	.5733	16.17
2	.6179	18.29
3	.6295	20.21
4	.6399	22.01
5	.6497	23.71
6	.6589	25.37
7	.6679	27.03
8	.6769	28.71
9	.6860	30.47
10	.6956	32.35
11	.7057	34.43
12	.7169	36.78
13	.7297	39.54
14	.7446	42.95
15	.7630	47.38
16	.7869	53.58
17	.8202	63.24
18	.8721	81.20

Condenser Heat Load = 50.40 kW
Top Partial Pressure of Carbon Dioxide = 355.5 mm.Hg.
T = Top Temperature = 83.51°C
Reflux rate = $.2 \times 10^{-3} m^3/s$.

TABLE 5.2.(A) MEASUREMENT STATISTICS

Measurement	Standard Deviation for noise	Assumed Deviation for Filter Matrix R	
		low	high
Top gas temperature $T_{c'}$ °C	.25	.50	1.0
Partial pressures P_{cj} mm.Hg.	2.0	2.5	5.0
Concentration c'_{cj} kmole/m^3	.0125	.015	.030

TABLE 5.2.(B) STATE NOISE, Q Matrix

Component	Standard Deviation
1	.04
2	.05
3	.025

the Jacobian matrix for the filter equations was computed by finite difference. The compositions predicted by the model are significantly non-linear with respect to the state because the parameters A and B appear in an exponential term.

The noise statistics were considered to be from a normal distribution with zero mean and variance as shown in Table 5.2(A). The noise to be added to the measurements was produced by a random number generator in order to be reproducible for comparison purposes. The noise produced was checked for consistency with the desired statistics: over fifty measurements, the means were reproduced within one tenth of a standard deviation, and the variances within twenty per cent. The initial choice of measurement sets was arbitrary, although the top gas temperature was included as this is a readily available plant measurement.

To establish firm results from the following comparisons, particularly regarding the relation between the covariance matrix and the estimate, Monte Carlo simulations are required; however, due to the model complexity, this could not be contemplated. Notwithstanding this, particular comparisons can be made, and can be taken as an indication of the general trend to be expected from a full Monte Carlo simulation.

5.4.2. Comparison of iterated and extended filters

The results of comparative computations using both the filters on two measurement sets are shown in Tables 5.3 and 5.4, and the estimates given in the second case are shown in Fig. 5.2.

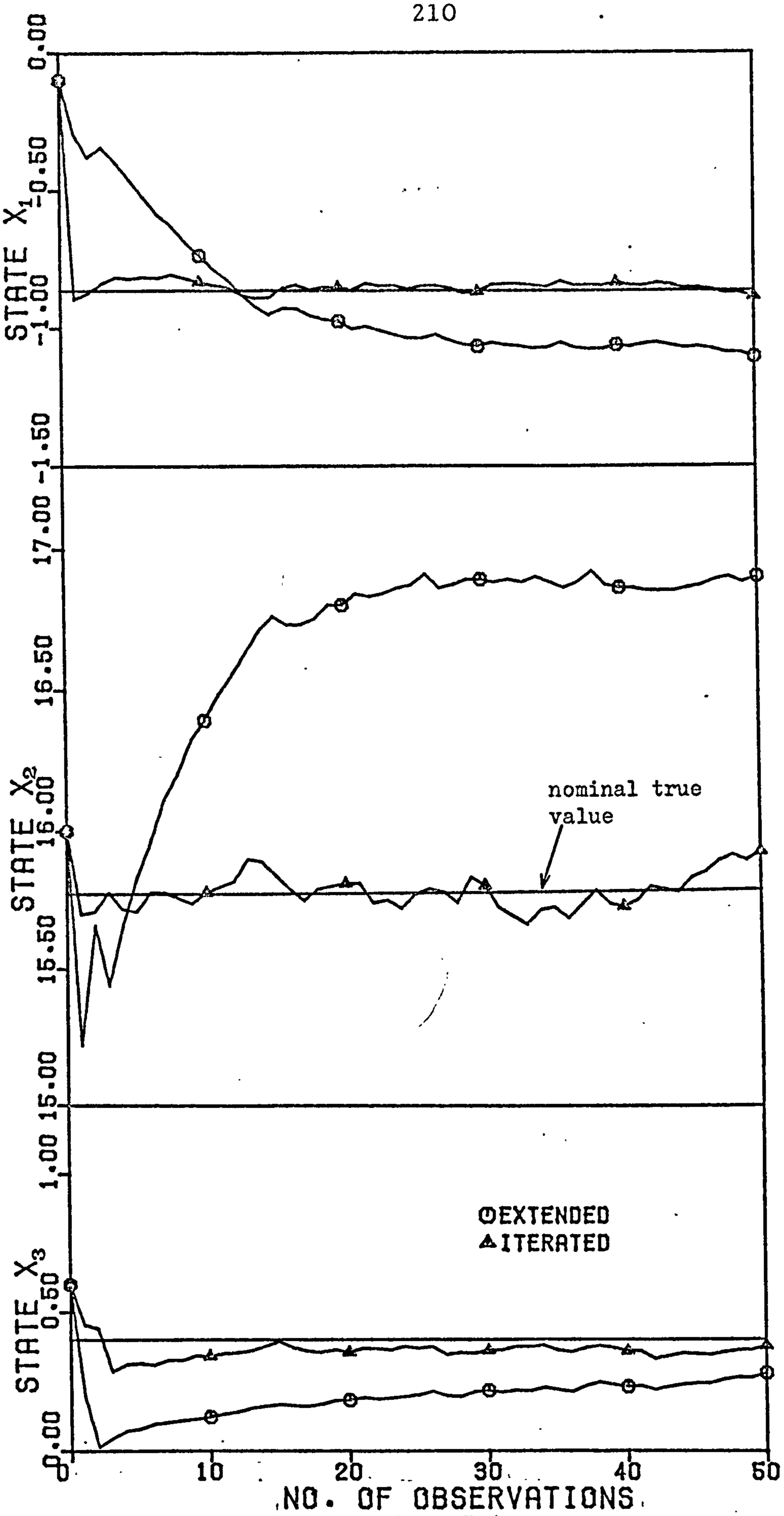


FIG. 5.2 COMPARISON OF EXTENDED, ITERATED FILTERS

TABLE 5.3 COMPARISON OF ITERATED AND EXTENDED FILTERS USING MEASUREMENT SET A (see Table 5.6)

Number of Observations	EXTENDED						ITERATED					
	State Estimate			Covariance Matrix			State Estimate			Covariance Matrix		
	x_1	x_2	x_3	P_{11}	P_{22}	P_{33}	x_1	x_2	x_3	P_{11}	P_{22}	P_{33}
0	- .10	16.0	.60	1.5	1.5	1.5	-.10	16.0	.60	1.5	1.5	1.5
10	-1.419	18.43	.1631	.147E-01	.2720	.1105E-02	-.894	15.88	.342	.2177E-01	.4321	.1191E-01
20	-1.375	18.28	.1718	.137E-01	.2769	.1732E-02	-.787	15.37	.467	.1437E-01	.2434	.1072E-01
30	-1.401	18.29	.1880	.1414E-01	.2847	.1772E-02	-.864	15.69	.392	.1039E-01	.1806	.966E-02
40	-1.388	18.26	.1600	.1435E-01	.2913	.1977E-02	-.836	15.68	.410	.8858E-02	.1562	.8807E-02

Elements of R matrix set to low values as given in Table 5.2 (A)

Note: .1E-02 ≡ .1 x 10^{-2}

TABLE 5.4 COMPARISON OF ITERATED AND EXTENDED FILTERS USING MEASUREMENT SET C

E X T E N D E D

Number of Observations	State Estimate x_1	x_2	x_3	Filter Covariance P_{11}	P_{22}	P_{33}	Mean Mamnt. Residuals T_c	c_7	c_{18}
0	- .1	16.0	.60	1.5	1.5	1.5	-	-	-
10	- .737	16.39	.1218	.557E-01	.838	.128E-02	2.31	-.183E-01	-.189E-01
20	- .976	16.80	.1826	.507E-01	.7955	.370E-02	.209	-.547E-02	-.164E-01
30	-1.06	16.89	.2173	.488E-01	.790	.561E-02	.957E-01	.197E-02	-.935E-02
40	-1.06	16.86	.2307	.483E-01	.790	.728E-02	-.711E-01	.504E-02	-.443E-02
50	-1.09	16.88	.2633	.482E-01	.794	.861E-02	.441E-01	-.388E-02	-.568E-02

I T E R A T E D

Number of Observations	State Estimate x_1	x_2	x_3	Filter Covariance P_{11}	P_{22}	P_{33}	Mean Mamnt. Residuals T_c	c_7	c_{18}
0	-.1	16.0	.60	1.5	1.5	1.5	-	-	-
10	-.832	15.78	.340	.672E-01	1.032	.196E-01	-.718E-01	.117E-03	-.124E-02
20	-.851	15.81	.355	.572E-01	.899	.181E-01	.141E-01	-.538E-03	-.109E-02
30	-.866	15.79	.362	.513E-01	.817	.176E-01	.228E-01	.125E-02	-.146E-02
40	-.834	15.72	.360	.470E-01	.747	.175E-01	-.541E-01	.262E-02	.322E-03
50	-.885	15.91	.377	.441E-01	.703	.167E-01	.804E-01	-.659E-02	-.305E-02

Mean of measurement residuals taken over previous 10 measurements.
Elements of R matrix set to high values as given in Table 5.2(A)

TABLE 5.5. NUMBER OF ITERATIONS FOR CONVERGENCE OF THE ITERATED FILTER

Number of Observations	Number of iterations over last 10 observations	Cumulative Number of Iterations
10	57	57
20	26	83
30	30	113
40	27	140
50	25	165

Figures taken from example presented in Table 5.4.

In both cases the superiority of the iterated filter is clearly evident. The extended filter produced an estimate which was severely biased in all the components, and in some cases apparently converged, although reference to the measurement residuals shows this to be false. The extended filter produces a rapid initial decrease of the covariance matrix, and this is then followed in both cases by an increase in one or more of the diagonal elements. In comparison, the covariance matrix given by the iterated filter decreases less rapidly initially, and final values are in many instances smaller than those for the extended filter. The problem of divergence of the covariance matrix was not encountered in any of the computations made with the iterated filter. Considering the behaviour of the estimate of the iterated filter, this is seen to have very little bias in any of the cases, and as a result converges far more rapidly.

The improvement can also be seen through the mean measurement residuals as shown in Table 5.4. As may be expected, with a better estimate of the state given by the iterated filter, the measurement residuals are generally lower.

The increase in computation associated with the iterated filter may be assessed from Table 5.5. Considering the on-line application, if measurement processing time is not critical, as is likely to be true in this case then the increase in computational load is easily justified. The number of iterations is dependent upon the conditioning of the equations and on the convergence criterion which was in

this case:

$$|(\eta_{j,i+1}-\eta_{j,i})/\eta_{j,i+1}| \leq .0001 \quad 1 \leq j \leq n \qquad (5.35)$$

In the computations with measurement sets A and B there were instances of ill-conditioning with very slow convergence particularly during the initial updates; the maximum number of iterations was therefore arbitrarily restricted to twenty. A further advantage of a well conditioned or optimal measurement set was shown by the rapid convergence of this iteration when such a set was used.

In summary, the iterated filter has produced a considerable improvement in the estimation process, at the cost of extra computation which should not be prohibitive in the on-line situation.

5.4.3. Optimal Measurement Set Selection

Initially measurement subsets of dimension four were considered, and with a set of assumed measurement variances the information matrix for one observation could be computed by specifying the elements of the measurement subset.

An integer branch and bound procedure was used to maximise the minimum eigenvalue of the matrix $G^TR^{-1}G$, with the Jacobian matrix evaluated at the true state, and suitable values selected for the diagonal of the matrix R. A sufficient number of starting points were considered to ensure a reasonable search pattern and the set of measurements giving the optimum was found repeatedly. It was of interest that the particular measurement subset found consisted of three measurements with one repeated. Furthermore, when measurement subsets of dimension three were considered the

optimal subset found consisted of the same three measurements, although naturally with a lower eigenvalue than previously. Details of the optimal subsets and others selected are given in Table 5.6.

Because of the non-linearity of the system as evidenced by the poor performance of the extended filter, the optimisation was repeated for six different values of the state. With the same measurement statistics assumed, it was found that for all but two of the states, the measurement subset previously found as optimal at the nominal state was again selected as optimal, although with different values for the minimum eigenvalue, see Table 5.7. This is a very encouraging result, although it is clearly dependent not only upon the problem, but also upon the size of the region of state in which the filter is working.

5.4.5. Comparison of Measurement Subset Policies

Only the iterated filter was used for this comparison because of the poor performance of the extended filter.

The estimates made with different measurement subsets were analysed for mean and variance and are presented with the results in Tables 5.8 to 5.11. Two initial state estimates were used, and some runs were repeated with assumed measurement variances four times larger than the nominal values. Considering the performance of the four element measurement subsets, the increase in performance given by use of the optimal subset is evident in all the respects mentioned earlier to characterise the performance of an estimation process. With the assumption of a low

measurement variance the optimal subset, see Figs. 5.4 and 5.5, gives a very marked improvement in estimate: by comparison, in run A2, see Fig. 5.3, the filter is slow to converge, and even then to a rather poor estimate. Furthermore, in run A1, the filter is showing signs of bias. With higher values for the measurement variances, as in runs A3 and A4, the performance is better in terms of the estimate produced, but the values of the covariance matrices are not as low. The use of higher measurement variances reduces the filter gain and tends to mask non-linear effects, thereby allowing a less biased estimate, albeit with reduced certainty and the requirement of more measurements to achieve a specified accuracy.

Considering the performance of the filter with the three element measurement subsets, as a result of measurement subset C being less ill-conditioned than either A or B, the improvement given by use of the optimal subset is less than in the previous cases. For high values for the assumed measurement variances, the estimates given by subset C and the optimal are similar, although the covariance matrix for the optimal subset has distinctly smaller diagonal elements. At the lower assumed measurement variance the estimate given by the optimal subset is generally better in terms of the estimate noise, and again the covariance matrix has distinctly lower values.

It is interesting to compare the filter performance when using the three and four element subsets: considering the two optimal subsets, the four element subset gives a lower covariance matrix, as was expected, and after the

first ten observations, lower values of the estimate noise. Despite the smaller measurement vector dimension, the performance of the three element optimal subset is significantly better than that given by use of either A or B. It is also noted that the initial filter gain increases with the dimension of the measurement vector, and is greatest with the optimal measurement subsets. However, this decreases more rapidly than with the non-optimal subsets as a result of the more rapid decrease in the covariance matrix.

If the covariance matrices computed are representative of the statistics of the estimate, as has been the experience of Denham, Pines and Jazwinski when using the iterated filter, then the improvement given by use of the optimal subsets is clearly established. The improvement can also be seen through the noise in the estimate, although because these are only particular results, conclusions drawn from the estimate noise are not as decisive as conclusions drawn from the covariance matrix, which is meant to represent an ensemble of results.

These results indicate two points:-

(i) with careful selection of a minimal subset of measurements, i.e. one of dimension equal to the state vector, according to the criterion given, the state may be estimated more rapidly and accurately than by use of a larger measurement subset selected on an ad hoc basis.

(ii) with the selection of a well-conditioned, or optimal subset, the assumed measurement variance

can be decreased further than with an ill-conditioned subset without the problems of filter instability or divergence.

Both of these points are of importance in the practical situation and therefore it may be concluded that employment of the selection criterion developed would be worthwhile.

5.5. Conclusions

The superiority of the iterated over the extended filter in the fitting of the plate column model has been demonstrated and the advantages gained justify the small increase in computation. The use of different measurement sets has shown some measurement combinations to be preferable to others and advantage should be taken of this where freedom of choice is possible. To assess the merit of a particular combination, the criterion of the size of the maximum eigenvalue of the covariance matrix appears preferable to the others considered because it bounds the size of the error ellipsoids associated with the estimate. However, to find a sequence of measurements which will, after a certain fixed number, optimize this criterion is a very large problem. If the viewpoint is taken that the measurement vector to be used at each observation is the same, as it well may have to be due to constraints on the use of instrumentation, then the policy proposed here would be a sensible one to adopt. The results show that the criterion developed makes an improvement upon measurement sets selected at random. The fact that an optimally chosen

three dimensional vector was found to be better than some with four elements shows that measurement sets should not be selected randomly. Furthermore, ill-conditioned sets give slow convergence and can lead to biased results. Ill-conditioning can be avoided by employing a greater variety of measurements, but is best avoided by using the criterion developed.

The results and conclusions reached justify the continuation of this work in steady state identification and the extension to the dynamic state.

TABLE 5.6 MEASUREMENT SUBSETS

Measurement subset	Measurements	Minimum eigenvalue of matrix H (eqtn.5.32)at nominal true state
A	c_1, P_{10}, P_{17}, T_c	.0994
B	P_{15}, P_{17}, c_{17}, T_c	.0105
C	c_7, c_{18}, T_c	.1042
Optimal 3msmnt	P_7, c_{18}, T_c	.2064
Optimal 4msmnt	P_7, P_7, c_{18}, T_c	.3954

TABLE 5.7 VARIATION OF OPTIMAL SUBSET WITH STATE

State	Measurements	Minimum eigenvalue of matrix H (eqtn.5.32)
-.1,16.0,.60	c_6, c_{10}, T_c	.545
-.1,16.0,.60	P_7, c_{18}, T_c	.401
-.1,15.0,.80	P_6, P_{11}, T_c	1.03
-.1,15.0,.80	P_7, c_{18}, T_c	.644
-.8,15.0,.50	P_7, c_{18}, T_c	.389
-.8,15.0,.30	P_7, c_{18}, T_c	.136
-.8,16.0,.50	P_7, c_{18}, T_c	.293
-.8,16.0,.30	P_7, c_{18}, T_c	.097

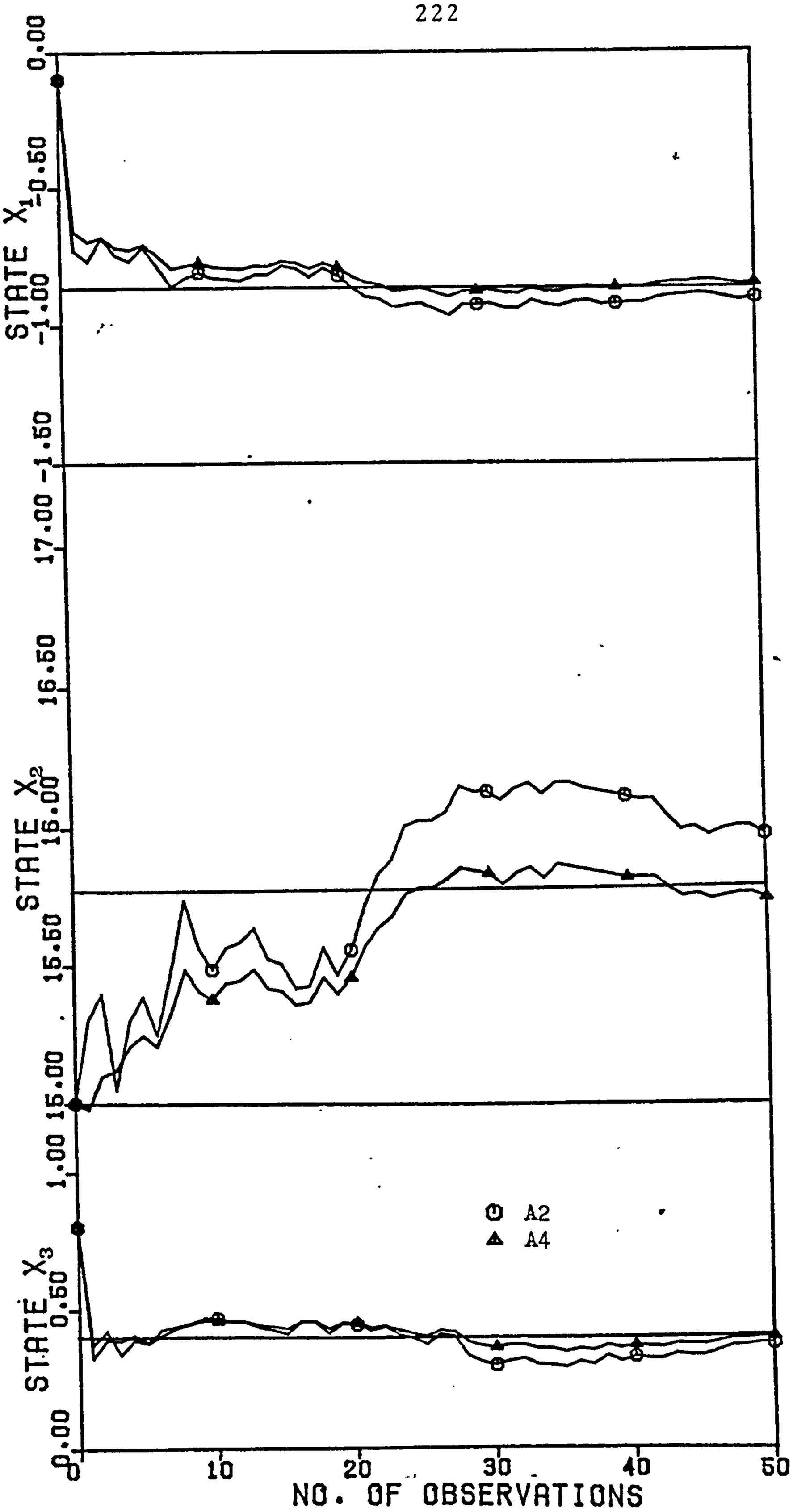


FIG. 5.3 EFFECT OF ASSUMED MEASUREMENT VARIANCE, RUNS A2,A4

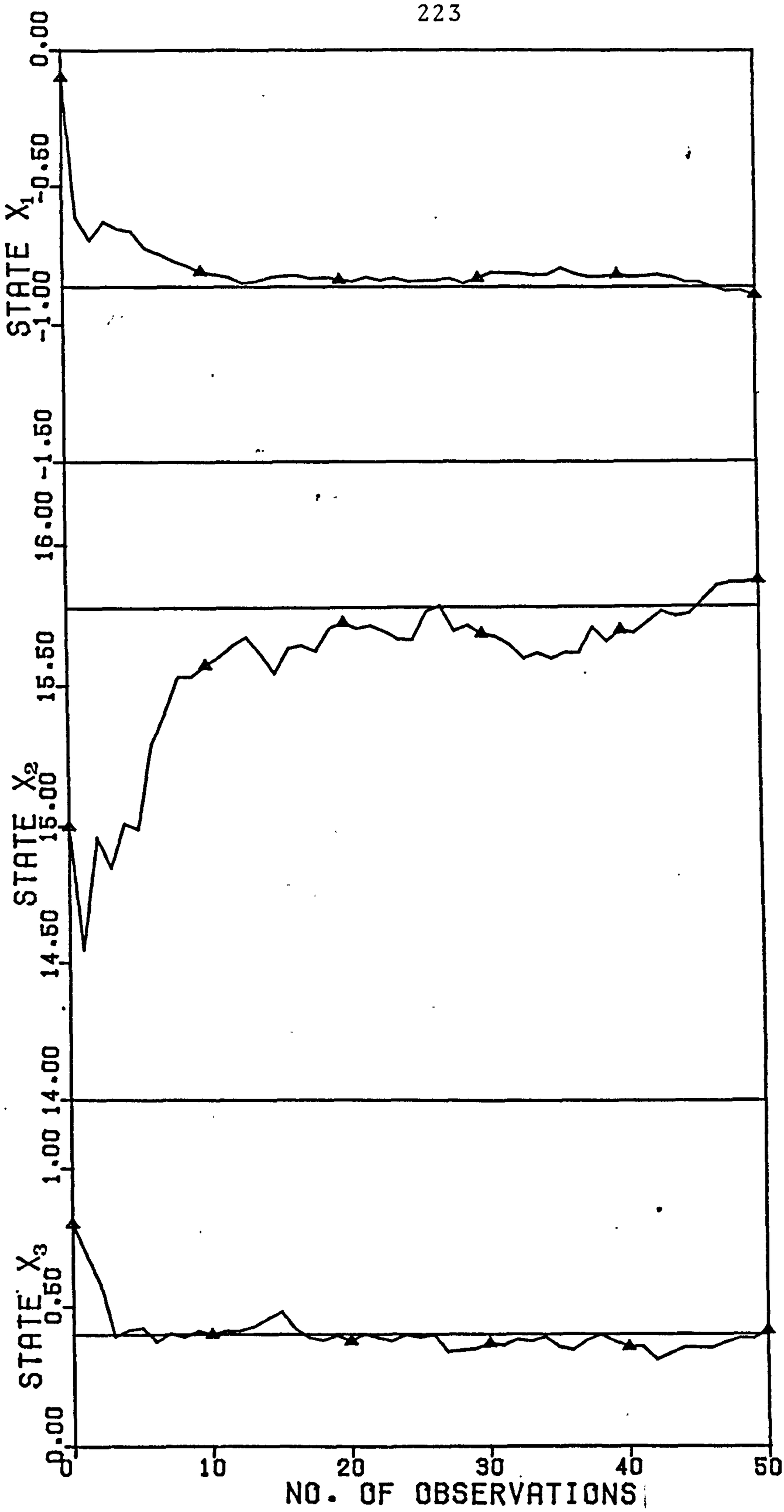


FIG. 5.4 FILTERING USING OPTIMAL MEASUREMENT SET, RUN 0.6
4 MEASUREMENTS AT EACH OBSERVATION

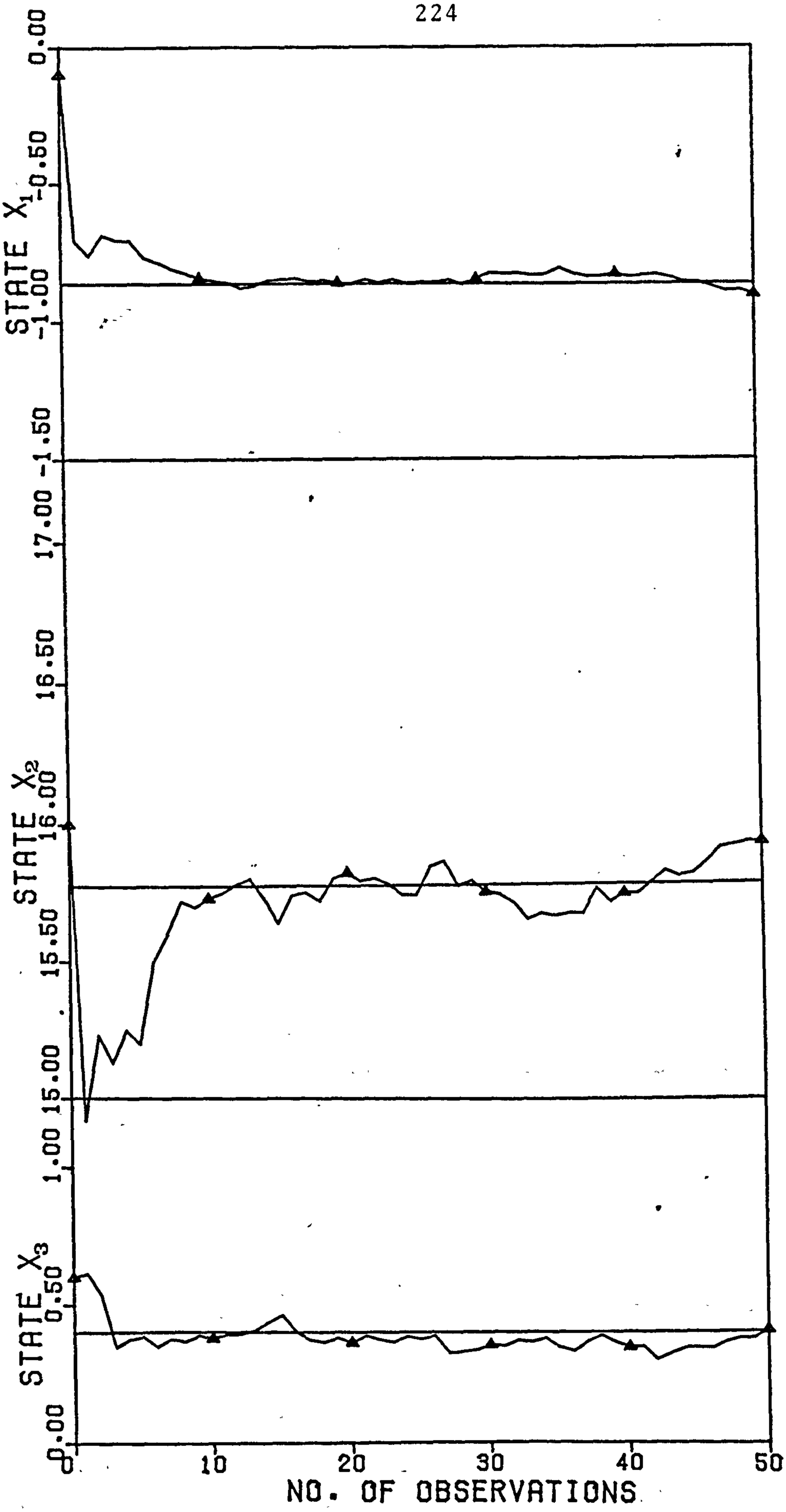


FIG. 5.5 FILTERING USING OPTIMAL MEASUREMENT SET, RUN 0.5
4 MEASUREMENTS AT EACH OBSERVATION

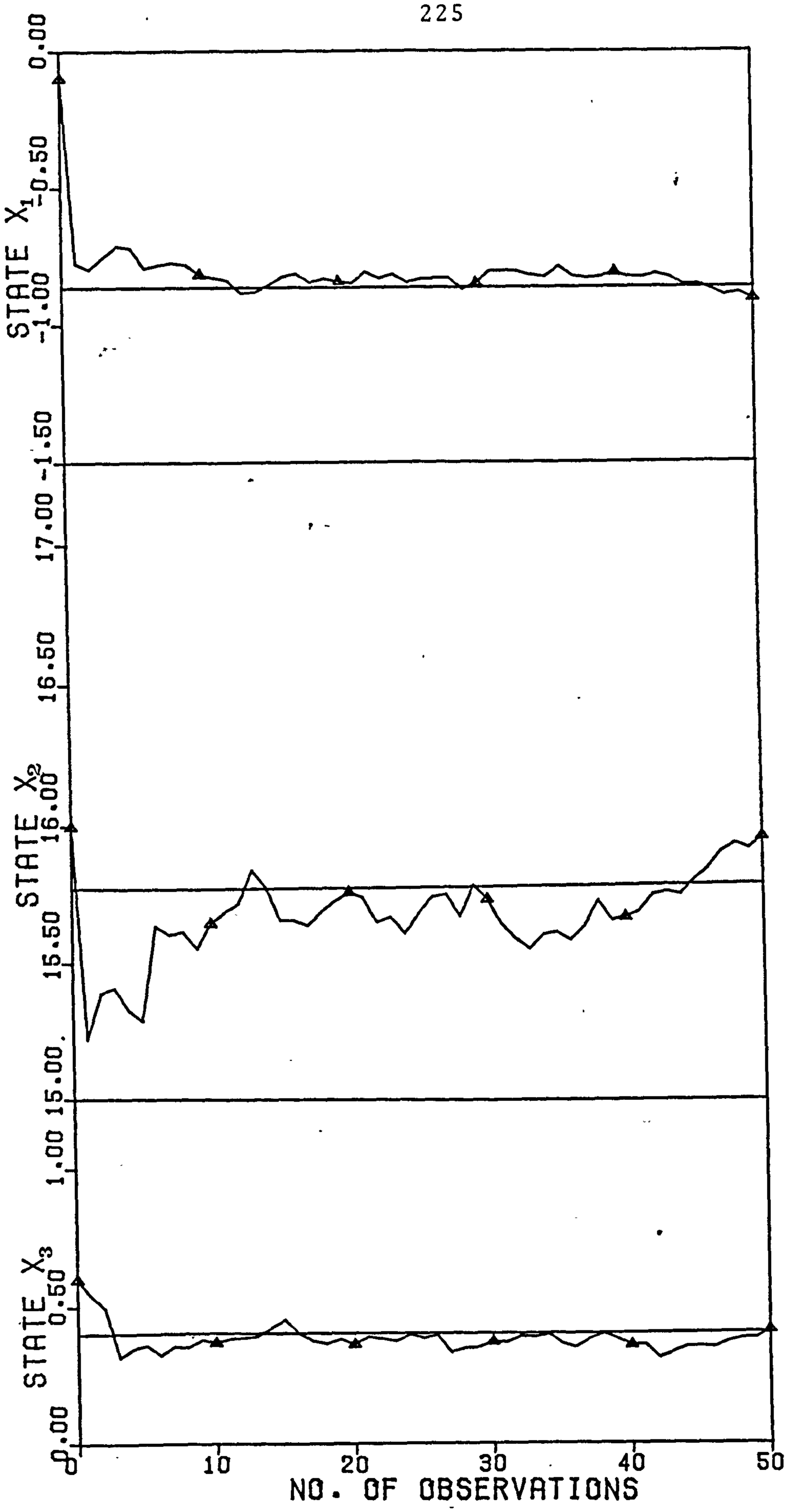


FIG. 5.6 FILTERING USING OPTIMAL MEASUREMENT SET, RUN 0.1
3 MEASUREMENTS AT EACH OBSERVATION

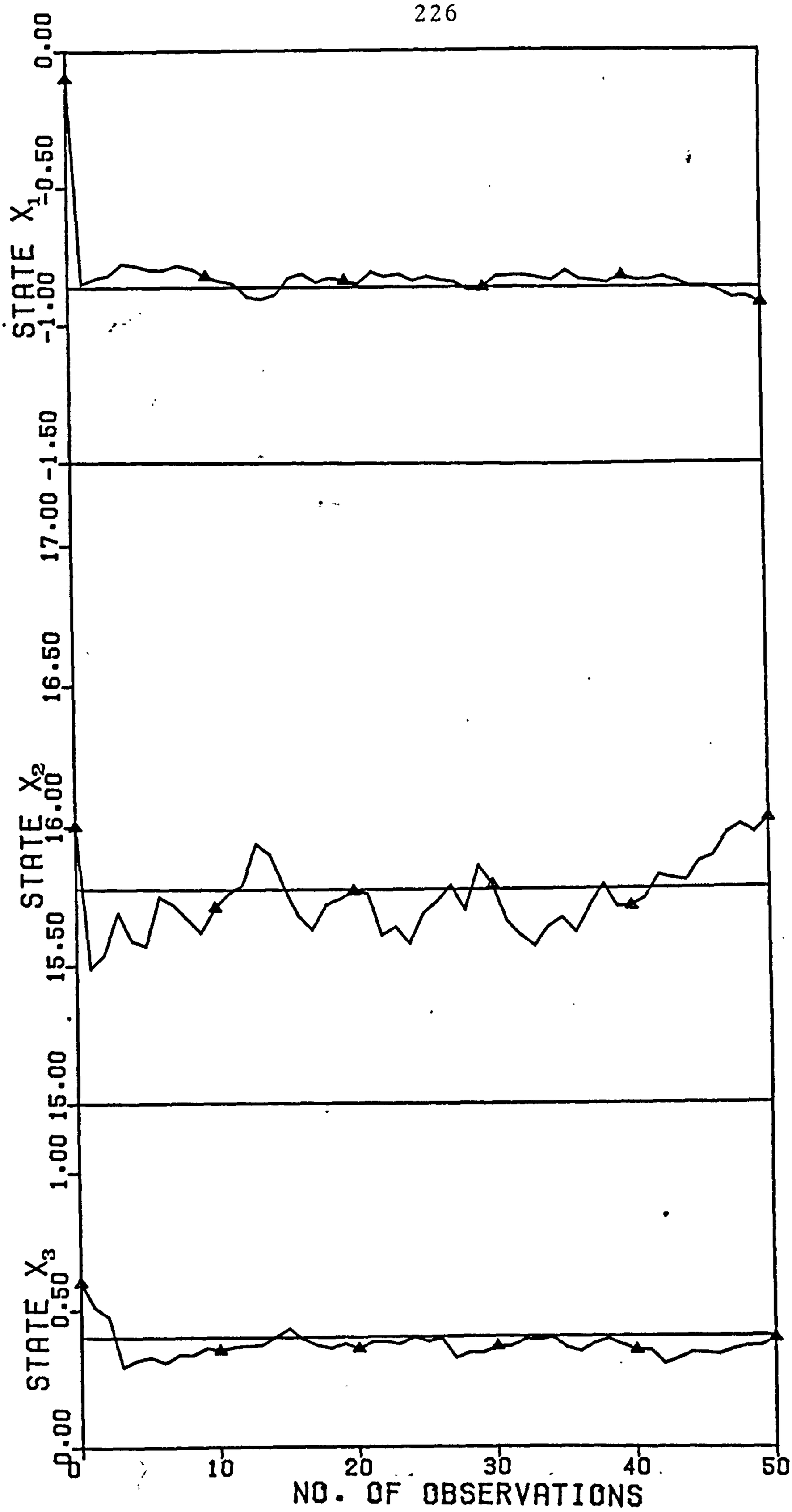


FIG. 5.7 FILTERING USING
MEASUREMENT SET C, RUN C.1
3 MEASUREMENTS AT EACH OBSERVATION

TABLE 5.8 FILTER RESULTS USING MEASUREMENT SETS A & C

Run	Set	Values for R	Number of Observations	State Estimate x_1	x_2	x_3	Mean of Estimates x_1	x_2	x_3	Filter Covariance P_{11}	P_{22}	P_{33}	Std. Devtn. of Estimates σ_{11}	σ_{22}	σ_{33}
A1	A	low	0	- .10	16.0	.60				1.5	1.5	1.5			
			10	-1.08	16.79	.287	-1.03	16.67	.253	.289E-01	.587	.732E-02	.668E-02	.996E-01	.126E-02
			20	-1.03	16.59	.307	-1.05	16.66	.286	.217E-01	.443	.751E-02	.548E-03	.698E-02	.253E-03
			30	-1.14	17.23	.195	-1.14	17.00	.273	.148E-01	.337	.337E-02	.751E-03	.286E-01	.212E-02
A2	A	low	0	- .10	15.0	.80				1.5	1.5	1.5			
			10	- .806	15.49	.467	- .767	15.40	.413	.211E-01	.377	.167E-01	.296E-02	.362E-01	.200E-02
			20	- .818	15.56	.447	- .812	15.53	.442	.126E-01	.226	.117E-01	.339E-03	.499E-02	.326E-03
			30	- .925	16.12	.299	- .92	15.99	.381	.906E-02	.188	.666E-02	.761E-03	.191E-01	.242E-02
			40	- .924	16.10	.329	- .926	16.12	.311	.963E-02	.182	.582E-02	.100E-03	.507E-03	.195E-03
			50	- .901	15.95	.373	- .902	16.00	.348	.944E-02	.168	.667E-02	.141E-03	.247E-02	.439E-03
A3	A	high	0	- .1	16.0	.60				1.5	1.5	1.5			
			10	- .943	16.17	.335	- .906	16.10	.294	.517E-01	.998	.202E-01	.166E-02	.157E-01	.117E-02
			20	- .926	16.08	.355	- .932	16.11	.342	.413E-01	.795	.199E-01	.210E-03	.408E-02	.786E-04
			30	- .995	16.38	.297	- .994	16.34	.334	.332E-01	.692	.168E-01	.332E-03	.565E-02	.430E-03
			40	- .977	16.34	.304	- .987	16.38	.297	.312E-01	.645	.145E-01	.106E-03	.513E-03	.639E-04
A4	A	high	0	- .1	15.0	.80				1.5	1.5	1.5			
			10	- .774	15.38	.459	- .728	15.25	.412	.437E-01	.777	.383E-01	.206E-02	.251E-01	.167E-02
			20	- .79	15.46	.452	- .784	15.42	.449	.314E-01	.562	.292E-01	.949E-04	.175E-02	.116E-03
			30	- .876	15.82	.364	- .866	15.75	.409	.243E-01	.476	.219E-01	.460E-03	.878E-02	.735E-03
			40	- .864	15.81	.371	- .871	15.83	.363	.227E-01	.436	.181E-01	.674E-04	.419E-03	.884E-04
			50	- .849	15.74	.396	- .849	15.76	.381	.219E-01	.396	.174E-01	.667E-04	.837E-03	.136E-03

Mean and standard deviations of estimates computed over previous 10 observations.

TABLE 5.8 continued

Run	Set	Values for R	Number of Observations	State Estimate x_1	x_2	x_3	Mean of Estimates x_1	x_2	x_3	Filter Covariance P_{11}	P_{22}	P_{33}	Std. Devtn.of Estimates σ_{11}	σ_{22}	σ_{33}
C1	C	low	0	-.1	16.0	.60				1.5	1.5	1.5			
			10	-.824	15.71	.354	-.807	15.63	.363	.363E-01	.583	.981E-02	.577E-03	.735E-02	.516E-02
			20	-.840	15.77	.359	-.856	15.77	.381	.264E-01	.431	.919E-02	.101E-02	.905E-02	.512E-03
			30	-.866	15.79	.365	-.841	15.72	.369	.219E-01	.352	.816E-02	.432E-03	.774E-02	.638E-03
			40	-.825	15.71	.349	-.830	15.67	.373	.189E-01	.305	.786	.162E-03	.418E-02	.324E-03
			50	-.921	16.02	.391	-.867	15.89	.346	.182E-01	.282	.734E-02	.100E-02	.918E-02	.650E-03
C2	C	low	0	-.1	15.0	.80				1.5	1.5	1.5			
			10	-.722	15.26	.412	-.673	15.05	.442	.290E-01	.443	.120E-01	.576E-03	.263E-01	.817E-02
			20	-.776	15.49	.393	-.776	15.42	.427	.205E-01	.320	.959E-02	.689E-03	.582E-02	.700E-03
			30	-.812	15.55	.395	-.786	15.47	.401	.173E-01	.268	.834E-02	.391E-03	.657E-02	.625E-03
			40	-.783	15.51	.375	-.784	15.47	.401	.153E-01	.236	.789E-02	.149E-03	.420E-02	.355E-03
C3	C	high	0	-.1	16.0	.60				1.5	1.5	1.5			
			10	-.832	15.78	.340	-.833	15.75	.345	.672E-01	1.032	.196E-01	.818E-03	.931E-03	.323E-02
			20	-.851	15.81	.355	-.861	15.82	.364	.572E-01	.899	.181E-01	.312E-03	.213E-02	.181E-03
			30	-.866	15.79	.362	-.853	15.77	.363	.513E-01	.817	.176E-01	.119E-03	.139E-02	.103E-03
			40	-.834	15.72	.360	-.841	15.71	.369	.470E-01	.747	.175E-01	.365E-04	.107E-02	.726E-04
			50	-.885	15.91	.377	-.856	15.83	.353	.441E-01	.703	.167E-01	.256E-03	.374E-02	.165E-03

Mean and standard deviations of estimates computed over previous 10 observations.

TABLE 5.9 FILTER RESULTS USING OPTIMAL MEASUREMENT SETS.

Run	Set	Values for R	Number of Observations	State Estimate x_1	x_2	x_3	Mean of Estimates x_1	x_2	x_3	Filter Covariance P_{11}	P_{22}	P_{33}	Std. Devtn. of Estimates σ_{11}	σ_{22}	σ_{33}
01	0	low	0	-.1	16.0	.60				1.5	1.5	1.5			
			10	-.817	15.65	.366	-.770	15.47	.383	.183E-01	.306	.916E-02	.112E-02	.262E-01	.549E-02
			20	-.842	15.76	.361	-.845	15.72	.390	.120E-01	.797	.746E-02	.526E-03	.398E-02	.737E-03
			30	-.849	15.73	.370	-.837	15.70	.370	.100E-01	.158	.663E-02	.335E-03	.307E-02	.470E-03
			40	-.812	15.65	.355	-.816	15.62	.376	.881E-02	.135	.641E-02	.182E-03	.229E-02	.306E-03
			50	-.908	15.93	.406	-.858	15.82	.357	.856E-02	.125	.621E-02	.100E-02	.822E-02	.761E-03
02	0	low	0	-.1	15.0	.80				1.5	1.5	1.5			
			10	-.753	15.35	.408	-.681	15.07	.447	.149E-01	.235	.104E-01	.198E-02	.587E-01	.915E-02
			20	-.801	15.57	.386	-.796	15.49	.423	.100E-01	.157	.776E-02	.426E-03	.356E-02	.921E-03
			30	-.818	15.59	.391	-.803	15.55	.393	.874E-02	.131	.681E-02	.337E-03	.293E-02	.492E-03
			40	-.789	15.55	.371	-.791	15.51	.394	.792E-02	.116	.653E-02	.183E-03	.238E-02	.318E-03
03	0	high	0	-.1	16.0	.60				1.5	1.5	1.5			
			10	-.837	15.79	.338	-.820	15.71	.339	.481E-01	.802	.200E-01	.609E-03	.524E-02	.270E-02
			20	-.860	15.84	.351	-.861	15.82	.362	.359E-01	.596	.171E-01	.238E-03	.184E-02	.220E-03
			30	-.863	15.78	.361	-.853	15.78	.360	.297E-01	.408	.157E-01	.164E-03	.133E-02	.955E-04
			40	-.828	15.70	.360	-.832	15.69	.369	.256E-01	.412	.151E-01	.567E-04	.921E-03	.749E-04
			50	-.886	15.89	.382	-.857	15.82	.355	.233E-01	.369	.142E-01	.331E-03	.392E-02	.199E-03
04	0	high	0	-.1	15.0	.80				1.5	1.5	1.5			
			10	-.709	15.18	.433	-.665	14.97	.467	.387E-01	.576	.322E-01	.705E-03	.230E-01	.725E-02
			20	-.765	15.39	.417	-.754	15.32	.444	.272E-01	.410	.216E-01	.276E-03	.275E-02	.454E-03
			30	-.787	15.43	.414	-.771	15.39	.420	.224E-01	.337	.178E-01	.216E-03	.165E-02	.180E-03
			40	-.767	15.42	.404	-.767	15.38	.418	.197E-01	.292	.162E-01	.660E-04	.122E-02	.970E-04
			50	-.825	15.62	.417	-.797	15.54	.393	.183E-01	.268	.148E-01	.323E-03	.455E-02	.163E-03
05	0	low	0	-.1	16.0	.60				1.5	1.5	1.5			
			10	-.844	15.72	.377	-.760	15.40	.410	.104E-01	.171	.848E-02	.315E-02	.820E-01	.798E-02
			20	-.861	15.82	.362	-.858	15.75	.397	.723E-02	.112	.657E-02	.114E-03	.280E-02	.103E-02
			30	-.847	15.75	.355	-.857	15.79	.362	.648E-02	.981E-01	.570E-02	.509E-04	.165E-02	.596E-03
			40	-.830	15.74	.345	-.829	15.70	.361	.609E-02	.897E-01	.563E-02	.801E-04	.159E-02	.306E-03
			50	-.903	15.92	.406	-.863	15.85	.353	.608E-02	.860E-01	.572E-02	.663E-03	.422E-02	.908E-03
06	0	low	0	-.1	15.0	.80				1.5	1.5	1.5			
			10	-.810	15.57	.400	-.709	15.17	.448	.924E-02	.142	.907E-02	.470E-02	.119	.105E-01
			20	-.839	15.72	.376	-.833	15.64	.415	.661E-02	.980E-01	.671E-02	.967E-04	.264E-02	.115E-02
			30	-.833	15.67	.368	-.839	15.70	.375	.606E-02	.879E-01	.584E-02	.490E-04	.147E-02	.591E-03
			40	-.819	15.68	.355	-.817	15.64	.372	.577E-02	.822E-01	.574E-02	.818E-04	.158E-02	.307E-03
			50	-.893	15.87	.413	-.851	15.79	.361	.581E-02	.805E-01	.579E-02	.673E-03	.462E-02	.876E-03

Runs 01 to 04 use 3 measurements, 05 and 06 use 4 measurements.

TABLE 5.10 MEAN MEASUREMENT RESIDUALS USING SETS A AND C

Run	Number of Observations	Mean Measurement Residuals			
		$-c_1$	p_{10}	p_{17}	T_c
A1	10	.108E-02	.277	-1.36	-.898E-01
	20	-.793E-03	.729	- .569	-.145E-01
	30	.127E-02	-.293	.382	-.604E-02
A2	10	.114E-02	-.431	- .754	-.689E-01
	20	.557E-03	.407E-01	.128E-01	.476E-02
	30	.146E-02	-.912	.671	.959E-02
	40	.305E-02	.518	- .637	-.754E-01
	50	-.648E-02	.198	- .409	.706E-01
A3	10	.807E-03	-.993E-01	-1.366	-.113
	20	-.710E-03	.374	- .438	-.846E-02
	30	.150E-02	-.641	.513	.200E-01
	40	.208E-02	.790	.506	-.815E-01
A4	10	.958E-03	-.707	- .944	-.100
	20	.586E-03	-.206	- .798E-01	.215E-02
	30	.165E-02	-.113	.688	.240E-01
	40	.309E-02	.437	- .284	-.726E-01
	50	-.651E-02	.958E-02	- .298	.681E-01
		c_7	c_{13}		T_c
C1	10	-.652E-04	-.628E-03		-.326E-01
	20	-.833E-03	-.753E-03		.833E-02
	30	.712E-03	-.157E-02		.974E-02
	40	.245E-02	.298E-03		-.419E-01
	50	-.625E-02	-.316E-02		.912E-01
C2	10	-.348E-02	.349E-04		.846E-02
	20	-.277	.152E-03		.302E-01
	30	-.587E-03	-.118E-02		.243E-01
	40	.136E-02	.710E-03		-.300E-01
C3	10	.117E-03	-.124E-02		-.718E-01
	20	-.538E-03	-.109E-02		.141E-01
	30	.125E-02	-.146E-02		.228E-01
	40	.262E-02	.322E-03		-.541E-01
	50	-.659E-02	-.305E-02		.304E-01

Residuals are mean values over previous 10 observations

TABLE 5.11 MEAN MEASUREMENT RESIDUALS USING OPTIMAL MEASUREMENT SETS

Run	Number of Observations	Mean Measurement Residuals			
		p_7	c_{18}	p_7	T_c
01	10	- .285	-.486E-03		-.229E-01
	20	- .238	-.147E-03		-.273E-02
	30	.168	-.154E-02		.166E-01
	40	.368	.305E-03		-.987E-02
	50	-1.23	.324E-02		.198E-01
02	10	- .804	.247E-03		-.278E-01
	20	- .506	.253E-03		.581E-02
	30	- .140E-02	.119E-02		.146E-01
	40	.241	.638E-03		-.121E-01
03	10	- .529E-01	-.177E-02		-.444E-01
	20	- .161	-.124E-02		.974E-02
	30	.255	-.153E-02		.344E-01
	40	.450	.279E-03		-.228E-01
	50	-1.23	-.338E-02		.139E-01
04	10	- .919	.572E-03		-.619E-01
	20	- .744	.167E-03		.228E-02
	30	- .175	-.549E-03		.268E-01
	40	.104	.112E-02		-.284E-01
	50	-1.53	-.289E-02		.101E-01
05	10	- .346	.677E-03	-1.02	-.310E-01
	20	- .172	.614E-03	- .247	-.875E-02
	30	.259	.151E-02	.385	.146E-01
	40	.428	-.234E-03	- .246	-.639E-02
	50	-1.21	.336E-03	- .878E-01	.216E-01
06	10	- .655	.110E-02	-1.33	-.334E-01
	20	- .304	.915E-03	- .379	-.106E-01
	30	.182	-.121E-02	.307	.133E-01
	40	.374	.106E-03	- .301	-.644E-02
	50	-1.26	-.319E-02	- .137	.203E-01

Runs 01,02,03 & 04 are 3 measurement, 05 & 06 are 4 measurement.

5.6. Nomenclature for Chapter 5

A,B	parameters in equilibrium function for desorption column
C	controllability matrix defined by (5.29)
c	parameter associated with error ellipsoids, defined (5.26)
E	parameter in desorption column model: Murphree gas phase efficiency
G	measurement matrix: Jacobian of predicted measurements with respect to the model parameters
h	functional relationship between predicted measurements and model parameters
H	matrix defined by (5.32)
I	Identity matrix
I'	Information matrix defined by (5.27)
K	Kalman gain matrix defined by (5.13)
n_m	dimension of the measurement vector
n	dimension of parameter vector
$P_{K+1/K}$	matrix of covariance of x_{K+1} with x_K
Q_K	state noise covariance matrix
R	measurement noise covariance matrix
u	state noise vector
v	measurement noise vector
$\hat{x}_{K+1/K}$	best estimate of state at stage K+1 based upon observations up to and including stage K
y_K^0	observed measurement vector at stage K
ε	error norm for iterated filter
η_i	variable at iteration i: converged value becomes $x_{K+1/K+1}$
$\phi(K+1/K)$	state transition matrix between K+1 and K

CHAPTER SIX

C O N C L U S I O N S

The objectives described in the introduction have in general been achieved. The dynamic simulation of an absorption column with second order reaction together with the development of an efficient solution technique represent an advance on previous work. Of the two absorption models studied the theoretical reaction model was shown to be more generally applicable and preferable to the Kohl correlation. For the particular column considered the absorption rate should approximate that obtained for pseudo-first order conditions and a correspondingly simple absorption model has been proposed together with a method for updating the model parameters from plant measurements. The dynamic simulations showed the importance of the liquid phase dynamics which dominate those of the column, the gas phase hold up being negligible. In addition the significance of liquid and gas phase dispersion, of isothermal conditions, and of static liquid hold up is discussed.

A steady state model for the desorption column has been described and, as may have been expected, is of a more empirical nature than the absorption column model. Nevertheless, the model has a theoretical basis and gives feasible results. However, it is clear that a considerable amount of work remains to be done before the desorption

of carbon dioxide from MEA is adequately understood and the pilot plant therefore offers a good opportunity for original work.

The typical problem for control of this plant is to maintain the carbon dioxide content of the absorber exit gas below a specified level and to achieve this it may be necessary to alter the carbonation ratio of the stripped MEA. A feedforward control to set the reboiler heat load would be beneficial in reducing the delay in changing the stripped MEA concentration. The steady state model showed that a simple relation may exist between the reboil heat load, stripped MEA concentration and the circulation rate.

The comprehensive dynamic model for the desorption column was simplified by a number of techniques. For staged columns of any type plate lumping offers a means of simplification that is easy to use and has the advantage of retaining the original model steady state. No problems were encountered with simulating composition responses, but for responses which changed the internal flow rates the simplification that could be achieved was less.

This work also contributes to the field of numerical techniques and integration in particular. It has shown that special techniques for stiff systems offer significant advantages and that simple approximations to the Jacobian matrix can give very good results. Furthermore, the example of the transformation of the partial pressure differential equation for the absorption column shows the value of analysing equations.

In the field of parameter estimation this work has posed the new problem of selecting the best measurements to use for fitting a multi-parameter model. This is of particular significance where the number of measurements which can be made is limited by instrumentation. The concept of an optimal measurement subset was formulated and application of the criterion was shown to improve the performance of the filter. This is an interesting area of work and one of practical significance. Future work should aim at extending the analysis to dynamic systems.

In conclusion this work provides the basis for the future research work on the pilot plant. The simple models proposed here should be verified and modified if necessary. Following this the problem of selecting the liquid circulation rate should be studied. A control system which minimises the stripping steam consumption whilst maintaining a specified partial pressure of carbon dioxide in the absorber exit gas should then be developed. In the pursuit of these aims new problems and solutions will be found which will increase the knowledge of chemical plant, processes, and the means of controlling them.

R E F E R E N C E S

1. ABBOT, M.B., "An Introduction to the Method of Characteristics",Thames and Hudson (1966)

2. AMUNDSON, N.R., COSTE, J., and RUDD, D., "Taylor Diffusion in Tubular Reactions", Canadian Journal of Chem.Eng. 39, 149 (1961)

3. ARIS, R., and AMUNDSON, N.R., "Some Remarks on Longitudinal Mixing or Diffusion in Fixed Beds", A.I.Ch.E.J, 3,280 (1957)

4. ARMSTRONG, W.D., and WILKINSON, W.L., "Plant and Process Dynamics", Trans.Instn.Chem.Engrs. 35, 352-67 (1967)

5. ASTROM, K.J., "On the Achievable Accuracy in Identification Problems", Proceedings 1st IFAC Symposium on Identification, Prague (1967)

6. BENSON, H.E., FIELD, J.H., and JIMESON, R.M., "Carbon dioxide absorption employing hot potassium carbonate", Chem. Eng. Prog. 50, 365 (1954)

7. BENSON, H.E., FIELD, J.H., and HAYNES, W.P., "Improved Processes for CO_2 Absorption" Chem. Eng. Prog., 52, 433 (1956)

8. BOX, G.E.P., and DRAPER, N.R., "The Bayesian Estimation of Common Parameters", Biometrika 52, 355, (1965)

9. BOX, G.E.P., and HILL, W.J., "Discrimination among Mechanistic Models", Technometrics 9, 57 (1967)

10. BRIAN, P.L.T., HURLEY, J.F., HASSELTINE E.H., "Penetration Theory for Gas Absorption Accompanied by a Second Order Chemical Reaction", A.I.Ch.E.J.,7, 226, (1961)

11. BRIAN, P.L.T., VIVIAN, J.E., MATIATOS, D.C. "Interfacial Turbulence during the absorption of carbon dioxide into monoethanolamine", A.I.Ch.E.J., 13, 28, (1967)

12. BURKETT, R.J., FORTESCUE, T.R., KERSHENBAUM, L.S., and SARGENT, R.W.H., "On-line estimation and control of a carbon dioxide absorption plant", presented at the A.I.Ch.E.J. Symposium on Advances in Chemical Engineering Computing, Philadelphia (1973)

13. CALAHAN, D.A., Proc. I.E.E.E. (Letters) 56, 744, (1968)

14. COGGAN, G.C., and NOTON, A.R.M., "Discrete Time Sequential State and Parameter Estimation in Chemical Engineering", Trans.Instn.Chem.Engrs. 48, 255. (1970)

15. COURANT, R., and HILBERT, D., "Methods in Mathematical Physics" Interscience, (1961)

16. CRAMER, H. "Higher Mathematical Methods of Statistics", Princeton University Press, New Jersey, (1961)

17. DAHLQUIST, G., "A Special Stability Problem for Linear Multistep Methods", BIT.3, 27 (1963)

18. DANCKWERTS, P.V., "Gas Liquid Reactions", McGraw Hill (1970)

19. DANCKWERTS, P.V., and SHARMA, M.M., "The Absorption of Carbon Dioxide into Solutions of Alkalis and Amines", Chem.Engnr., No.202, p.244 (1966)

20. DANCKWERTS, P.V., and McNEIL, K.M., "The absorption of carbon dioxide into aqueous amine solutions and the effects of catalysis" Trans.Instn.Chem.Engrs., 45, 32 (1967)

21. DANCKWERTS, P.V., and McLACHLAN, "Desorption of carbon dioxide from aqueous potash solutions with and without the addition of arsenite as catalyst", Trans Inst.Chem.Engrs., 50. 300 (1972)

22. DAY, R.L., "Dynamic Characteristic of the Distillation Column Reboiler", Plant Process Dynamic Characteristics, Butterworths, (1957)

23. DE MARIA, F., and WHITE, R.R., "Transient Response Study of Gas Flowing Through Irrigated Packing", A.I.Ch.E.J., 6, 473 (1960)

24. DENHAM, W.F., and SPEYER, J.L., "Optimal Measurement and Velocity Correction Programmes for Midcourse Guidances", A.I.A.A. Jnl,2, No.5., 896 (1964)

25. DENHAM, W.F., and PINES, S., "Sequential Estimation when Measurement Function Non-linearity is Comparable to Measurement Error", A.I.A.A. Jnl.4, No.6, 1071 (1966)

26. DISTEFANO, G.P., "Stability of Numerical Integration Techniques", A.I.Ch.E.J., 14, 946, (1968)

27. DUTKAI, E., and RUCKENSTEIN, E., "New Experiences Concerning the Distribution of Liquid in a Packed Column", Chem.Eng.Sci. 25, 483 (1970)

28. DUYFJES, G., and VAN DER GRINTEN, P.M.E.M., "Application of a Mathematical Model for the Control and Optimisation of a Distillation Plant" I.F.A.C. Conference, Paris (1972)

29. ECKERT, J.S., "Pall Rings - New type of tower packing", Chem.Eng.Prog. 54, 71 (1958)

30. FOWLER, M.E., and WARTEN, R.M., IBM Journal of Research 537 (1967)

31. GAVALAS, G.R., and SEINFELD, J.H., "Sequential Estimation of State and Kinetic Parameters in Tubular Reactor with Catalyst Decay", Chem.Eng. Sci. 24, 625 (1969)

32. GEAR, C.W., "Information Processing, 68th Edn. A.J.H. Morrel, North Holland Publishing Co., Amsterdam, pp. 187-193 (1968)

33. GEAR, C.W., "Numerical Initial Value Problems in Ordinary Differential Equations", Prentice Hall, New Jersey (1971)

34. GERSCHGORIN, S., Izv.Akad.Nauk, SSSR Ser.Mat.7, 749-754, 1b,22,25 (1931)

35. GILATH, C., NAPTHALI, L.M., and RESNICK, W., "Transient Response of a Packed Column to Changes in Liquid and Gas Flow Rate", Ind.Chem.Eng.Process Design and Development, Vol.8, No.3, p.324 (1969)

36. GRAY, R.J., and PRADOS, J.W., "The Dynamics of a Packed Gas Absorber by Frequency Response Analysis", A.I.Ch.E.J. 9, 211, (1963)

37. HENRICI, P., "Discrete Variable Methods in Ordinary Differential Equations" John Wiley, N.Y. (1962)

38. HOLLAND, C.D., TETLOW, N.J. and GROVES, D.M., "A Generalised Model for the Dynamic Behaviour of a Distillation Column", A.I.Ch.E.J. 13, 476 (1967)

39. HUNTER, W.G., and REINER, A.M., "Designs for Discriminating Between Two Rival Models", Technometrics 7, p.307, (1965)

40. JASWON, M.A., and SMITH, W., "Countercurrent Transfer Processes in the Non-Steady State", p.226 A 225; Proc.R.Soc. (1954)

41. JAZWINSKI, A.H., "Stochastic Processes and Filtering Theory" Academic Press, New York, (1970)

42. JONES, J.H., FRONING, H.R., and CLAYTON, E.E., "Solubility of Acidic Gases in Aqueous Monoethanolamine" J.Chem.Eng.Data 4, 85 (1959)

43. KALMAN, R.E., "A New Approach to Linear Filtering and Prediction Problems", Trans. A.S.M.E., Ser.D: J. Bas. Eng. 82, 35 (1960)

44. KALMAN, R.E., "New Methods in Wiener Filtering Theory" Proc.Symp.Eng.Appl., Random Function Theory and Probability, Wiley, New York (1963)

45. KALMAN, R.E., and BUCY, R.S., "New Results in Linear Filtering and Prediction Theory", Trans.A.S.M.E., Ser.D. J.Bas.Eng. 83, 95 (1961)

46. KERN, D.Q., "Process Heat and Mass Transfer", New York, McGraw-Hill, (1950)

47. KOHL, A.L, "Plate efficiency with chemical reaction - absorption of carbon dioxide in monoethanolamine solutions", A.I.Ch.E.J., 2, 264, (1956)

48. KOHL, A.L, and RIESENFELD, F.C., "Gas Purification", New York, McGraw-Hill Book Co. (1960)

49. KOLODZIE, P.A., and van WINKLE, M. "Discharge coefficients through perforated plates", A.I.Ch.E.J. 3, 305 (1957)

50. KRAMERS, H., and ALBERDA, G., "Frequency Response Analysis of Continuous Flow Systems", Chem.Eng.Sci., 2, 173, (1953)

51. van KREVELEN, D.W., and HOFTYZER, P.J., "Graphical design of gas-liquid contactors", Chem.Eng.Sci. 2, 145 (1953)

52. LAMB, D.E., PIGFORD, R.L., and RIPPIN, D.W.T., "Dynamic Characteristics and Analogue Simulation of Distillation Columns", Chem.Eng.Prog. - Symp.Series No.36., 57, 132 (1961)

53. LANGLEY, P.E. and HASELDEN, G.G., "The desorption of carbon dioxide from hot potassium carbonate solutions" Proceedings of the Symposium on Mass Transfer with Chemical Reaction, Montreal, p.61 (1968)

54. LAPIDUS, L., and SEINFELD, J.M., "Numerical solution of partial differential equations", Academic Press (1971)

55. LEES, F.P., "Frequency Response of a Packed Gas Absorption Column", Chem.Eng.Sci, 23, 97 (1968)

56. LINIGER, W., and WILLOUGHBY, R.A., "Efficient Integration Methods of stiff systems of ordinary differential equations", S.I.A.M. J.Numer.Anal. 7, 47 (1970)

57. LUPFER, D.E., and PARSONS, J.R., "A Predictive Control System for Distillation Columns", Chem.Eng.Prog. 58, 37 (1962)

58. LUYBEN, W.L., VERNEUIL, V.S., and GERSTER, J.A., "Experimental Transient Response of a Pilot Plant Distillation Column", A.I.Ch.E.J., 10, 357 (1964)

59. MUHLBAUER, H.G. and MONAGHAN, P.R., "Sweetening Natural Gas with Ethanolamine Solutions", Oil and Gas Journal, 55, April 139 (1957)

60. McHENRY, K.W., and WILHELM, R.H., "Axial Mixing of Binary Gas Mixtures Flowing in a Random Bed of Spheres", A.I.Ch.E.J., 3, 83 (1957)

61. McWHIRTER, J.R., and LLOYD, W.A. "Controlled cycling in distillation and extraction", Chem.Eng.Prog.59, 58, (1963)

62. NORDSIECK, A., "On Numerical Integration of Ordinary Differential Equations", Mathematics of Computation (1962)

63. NORMAN, W.S., "Absorption, Distillation and Cooling Towers", Longmans, (1962)

64. PIESER, A.M., and GROVER, S.S., "Dynamic Simulation of a Distillation Tower", Chem.Eng.Prog.58,65 (1962)

65. PORTER, K.E., "The Effect of Contact Time Distribution on Gas Absorption with Chemical Reaction", Trans. Instn.Chem.Engrs. 44, T25 (1966)

66. PORTER, K.E., "Liquid Flow in Packed Columns Part I: The Rivulet Model", Trans.Instn.Chem.Engrs. 46,69 (1968)

67. PORTER, K.E., and JONES, M.C., "A Theoretical Prediction of Liquid Distribution in a Packed Column with Wall Effect", Trans.Instn.Chem.Engrs. 41, 240 (1963)

68. PORTER, K.E., and TEMPLEMAN, J.J., "Experimental determination of wallflow in packed columns", Chem. Eng.Sci. 20, 1139 (1965)

69. PORTER, K.E., BARNET, V.D., and TEMPLEMAN, J.J., "Liquid Flow in Packed Columns. Part II: Spread of Liquid over Random Packings", Trans.Instn.Chem. Engrs. 46, 74 (1968)

70. PORTER, K.E., and CANTWELL, D.C., and McDERMOTT, C., "Absorption and Desorption accompanied by a reversible chemical reaction", A.I.Ch.E.J. 17, 536 (1971)

71. PRADOS, J.W. and SAKATA, N. "Dynamics of a Packed Gas Absorber by Pulse Response Techniques" A.I.Ch.E.J. 18, 572 (1972)

72. RADEMAKER, D., RIJNSDORP, J.E., and MAARLEVELD, A. "Dynamics and Control of Continuous Distillation Units", Elsevier Scientific Publishing Company, Amsterdam (1975)

73. RIJNSDORP, J.E., Birmingham University Chemical Engineer, 12, S14, (1961)

74. ROSENBROCK, H.H., "Distinctive problems of process control", Chem.Eng.Prog. 58, 43, (1962)

75. ROSENBROCK, H.H., "The Control of Distillation Columns" Trans.Instn.Chem.Engrs. 40, 35 (1962)

76. ROSENBROCK, H.H., "Some general implicit processes for the numerical solution of differential equations", Computer Journal 5, 320, (1963)

77. SARGENT, R.W.H., and BERNARD, J.D.T., "Hydrodynamics of Sieve Plates, Trans.Instn.Chem.Engrs., 44, 314 (1966)

78. SARGENT, R.W.H., and MURTAGH, B.A., "The Design of Plate Distillation Columns for Multicomponent Mixtures", Trans.Instn.Chem.Engrs., 47, 85 (1969)

79. SARGENT, R.W.H., and POLLARD, G., "Off Line Computation of Optimum Controls for a Plate Distillation Column", Automatica Vol. 6, 59, (1970)

80. SARGENT, R.W.H., and JOFFE, B.L., "The Design of an On-line Control Scheme for a Tubular Catalytic Reactor", Trans.Instn.Chem.Engrs. 50, 270 (1972)

81. SATER, V.E., and LEVENSPIEL, O., "Two Phase Flow in Packed Beds", Ind.Eng.Chem.Fund., 5, 87, (1966)

82. SEINFELD, J.H., LAPIDUS, L., and HWANG, M., "Review of Numerical Integration Techniques for Stiff Ordinary

Differential Equations", Ind. Eng. Chem. Fund., Vol. 9., No. 2. (1970)

83. SEINFELD, J.H., and LAPIDUS, L., "Numerical Solution of Ordinary Differential Equations", Academic Press, N.Y. and London, (1971)

84. SCHMALZER, D.K. and HOELSCHER, H.E., "Stochastic Model of Packed Bed Mixing and Mass Transfer", A.I.Ch.E.J., 17, 104, (1976)

85. SHAH, Y.T., and SHARMA, M.M., "Desorption with or without chemical reaction", Trans.Instn.Chem. Engrs. 54, 1 (1976)

86. SHULMAN, H.L., ULRICH, C.F., and WELLS,N., "Performance of Packed Columns" A.I.Ch.E.J. 1, 247, (1955)

87. SHULMAN, H.L., ULRICH, C.F., PROULX, A.Z., and ZIMMEMAN, J.O., "Performance of Packed Columns", A.I.Ch.E.J. 1, 253 (1955)

88. SHULMAN, H.L., ULRICH, C.F., WELLS, W., and PROULX,A.Z., "Performance of Packed Columns", A.I.Ch.E.J. 1, 259, (1955)

89. SHULMAN, H.L., MELLISH, W.G., and LYMAN, W.H., "Simulation of a Packed Column", A.I.Ch.E.J., 17, 631, (1971)

90. SORENSON, H.W., "Advances in Control Systems", Vol.3, Ch.5. Academic Press, New York, (1966)

91. SORENSON, H.W., "Advances in Control Systems", Vol.6. Ch.2. Academic Press, New York, (1968)

92. SORENSON, H.W., and STUBBERUD, A.R., "Recursive Filtering for Systems with small but non-negligible non-linearities" Int.J.Control, 7, 271 (1968)

93. STAFFORD, T.J., "A Comparison of Complete and Simplified Models for Dynamic Optimisation of Steam Raising Plant", A.I.Ch.E. I.Chem.E. Symp. Series No.4. "Application of Mathematical Models in Chemical Engineering Research, Design and Production", London, (1965)

94. SUMNER, H.M., Report No. AEEW-R. 453 (1965)

95. WEILAND, R.H. and TRASS, O. "Absorption of Carbon Dioxide in EDA Solutions", Can.J.Chem.Eng. 49, 767, (1971)

96. WELLS, C.H., "Application of Modern Estimation and Identification Techniques to Chemical Processes", A.I.Ch.E.J. 17, 967, (1971)

97. WIDLAND, O., B.I.T., 7. pp.65-70, (1967)

APPENDIX 1 PARAMETERS FOR ABSORPTION COLUMN MODEL

Column Details

The packing is arranged in 5 sections of 1.22m each,

total height $z = 6.1m$

Column diameter $= .254$ m

Cross section area $= .0507$ m^2

Packing : pall rings : $1\frac{1}{4}$ inch (.0318m)

Reaction Rate Constant

Danckwerts[19] has given the reaction rate constant at various temperatures and this data can be fitted by

$$\log_{10} k_c = 11.46 - \frac{2250}{T+273} \qquad (A.1.1)$$

where k_c is in m^3/kmole.s.

and T is the liquid temperature in degrees centigrade.

Henry coefficient H

The Henry coefficient is assumed to be equal to the coefficient for the solubility of carbon dioxide in water:

$$\log_{10} H = -5.30 + \frac{1140}{T+273} \qquad (A.1.2)$$

where H is in kmole/m^3 bar.

Diffusivities

The data for the diffusivity of carbon dioxide in water can be fitted by (19)

$$D_c = (.66 + .0437T)x10^{-8} \text{ m}^2/\text{s} \qquad (A.1.3)$$

Assuming the same temperature variation as for the diffusivity of carbon dioxide in water, the following expression is used for MEA diffusivity at the MEA concentration used (2.48 kmole/m^3):

$$D_M = (.77 + .0437(T-25))x10^{-8} \ m^2/s \qquad (A.1.4)$$

Interfacial Area and Mass Transfer Coefficients

Over the range of superficial liquid flow rate concerned (.002 to .010 m/s) Danckwerts[19] found the following variation for the liquid phase mass transfer coefficient and interfacial area on 1" ceramic pall rings:-

$$k_L = (700(L/A) + 9.6)x10^{-5} \ m/s \qquad (A.1.5)$$

$$a = 180 + 5000((L/A) - .010) \ m^{-1} \qquad (A.1.6)$$

There appears to be no data in the literature for the gas phase mass transfer coefficient so an approximation is made by use of the dimensionless relation:-

$$\frac{k_G p_T}{G} = f(Sc, Re) \qquad (A.1.7)$$

where Sc = Schmidt number = $(\mu_G/\rho D_G)$

Re = Reynolds number = (Gd_p/μ_G)

and the dependence on the Schmidt number is usually assumed to be

$$(\frac{k_G p_T}{G}) \ \alpha Sc^{-2/3}$$

The volumetric gas phase mass transfer coefficient for the absorption of ammonia into water from an ammonia air mixture at atmospheric pressure on 1" Raschig rings has been correlated by Norman[63]:

$$(k_G a) = 9.05x10^{-4}(G')^{.77}(L')^{.20} \ g.moles/cm^3 s.atm \qquad (A.1.8)$$

where G' and L' are the superficial flows in $gm/cm^2 s$.

Under the conditions stated the Schmidt number for the ammonia air mixture is .65 compared to 1.1 for that of the

nitrogen carbon dioxide mixture. The difference in interfacial area for the absorption on 1" Raschig rings and 1¼" pall rings also has to be taken into account; at the nominal design liquid flow rate the interfacial areas are 120 and 180 m^{-1} respectively. The volumetric mass transfer coefficient for the absorption of carbon dioxide on 1¼" pall rings is therefore given approximately by:

$$k_G a = 9.05 \times 10^{-4} (G')^{.77} (L')^{.20} \left(\frac{1.8}{1.2}\right) \left(\frac{1.1}{.65}\right)^{-2/3} \left(\frac{1}{p_T}\right) \qquad (A.1.9)$$

Under the nominal design condition this gives:-

$$k_G a = .097 \quad \text{kmole/m}^3\text{s.bar.}$$

and so the gas phase mass transfer coefficient is

$$k_G = 5.4 \times 10^{-4} \text{ kmole/m}^2\text{s.bar.}$$

Heat of Reaction

The heat of reaction or absorption at a carbonation ratio of .4 and at 40°C has been measured by Kohl and Reisenfeld[48] as approximately 74,000 kJ/kmole.

Equilibrium of the primary amine-carbon dioxide reaction

The primary reaction, equation (2.1), is not completely irreversible and the quantity of free carbon dioxide in the bulk solution is given by:

$$c_A = (CO_2) = \frac{1}{K_e} \left(\frac{\alpha}{1-2\alpha}\right)^2 \qquad (A.1.10)$$

where K_e is the equilibrium constant.

Danckwerts and McNeil[20] measured the equilibrium constant and the values given by (A.1.10) are shown in Table A.1.1. In the lower part of the column where the carbonation ratios can be 0.45 and higher, the interfacial concentration of carbon dioxide is of the order of 2×10^{-3}

TABLE A.1.1. QUANTITY OF FREE CARBON DIOXIDE IN SOLUTION

Carbonation ratio α	$(\frac{\alpha}{1-2\alpha})^2$	(CO_2) kmole/m^3
.45	20.25	$.054 \times 10^{-3}$
.46	33.06	$.088 \times 10^{-3}$
.47	61.36	$.163 \times 10^{-3}$
.48	144.	$.383 \times 10^{-3}$
.49	600.	1.595×10^{-3}

$K_e = 3.76 \times 10^5$ kmole/m^3 at 18°C

kmole/m^3. Therefore for carbonation ratios higher than .46 the presence of free carbon dioxide could influence the absorption rate. The absorption rate equations (2.5), (2.6) and (2.16) are modified to:

$$\psi' = \frac{R}{k_L(c^* - c_A)} \qquad \text{(A.1.11)}$$

$$\psi = 1 + \frac{c_o}{2(c^* - c_A)} \sqrt{\frac{D_M}{D_c}} \left[1 - \sqrt{\frac{c_A}{c^*}}\right] \qquad \text{(A.1.12)}$$

$$R = \frac{\psi k_L H P_c - c_A}{1 + (\psi H k_L / k_G)} \qquad \text{(A.1.13)}$$

These were the equations used in the programme and clearly if c_A is negligible they reduce to equations given earlier.

Liquid phase hold up

The linear relationship used was obtained by linearising an expression due to Shulman[88]:

$$L = (-.115 + 5.15\phi_L)x10^{-3} \qquad \text{(A.1.14)}$$

Gas phase hold up and residence time

Assuming that the voidage of pall rings is 85% and that the liquid phase occupies 10% of the total column volume:

gas volume = (6.1)(.0507)(.75) = .232m^3

The gas flow is nominally $3.3x10^{-3}$ kmole/s at 3.32 bars and 30°C, so the volumetric flow rate is .025m^3/s. The gas phase residence time is then calculated to be 9.3 seconds.

Column Pressure Drop

Below the column loading point the pressure drop for pall rings has been correlated by Eckert[29] using an

equation of the form

$$\Delta p = a10^{bL''} \frac{(G'')^2}{\rho''_G} \qquad (A.1.15)$$

where L'', G'' are flows in lb/ft^2s, ρ''_G is the gas density in lb/ft^3 and Δp is the pressure drop expressed in inches water guage per foot of packing.

For 1" pall rings a = .35, b = .16

For the nominal design conditions

$L'' = 1.61\ lb/ft^2s$, $G'' = .37\ lb/ft^2s$.

and equation (A.1.15) gives $\Delta p = 1.48$ inches water per foot of packing

total column pressure drop = 28.6 inches

= .075 bar

APPENDIX 2. COMPUTATIONAL PROCEDURES FOR THE ABSORPTION COLUMN

1. Solution by characteristics with inclusion of gas phase hold up

The model which employs a plug flow description for both liquid and vapour phases can be conveniently solved by the use of characteristics. Both liquid and vapour rates are assumed to be constant so that the grid used is invariant, with characteristic directions given by:

$$\left.\frac{dz}{dt}\right)_I = -\frac{L}{\phi_L A} = -\frac{Z}{\tau_L} \quad \text{for the liquid phase} \qquad (A.2.1)$$

and

$$\left.\frac{dz}{dt}\right)_{II} = \frac{v_I R' T_G}{A\phi_G P_T} = \frac{Z}{\tau_G} \quad \text{for the vapour phase} \qquad (A.2.2)$$

where τ_L and τ_G are the liquid and gas phase residence times respectively. Because the characteristic directions remain invariant the problem of storage within the computer programme is considerably simplified. The number of lines, N_L, used for the liquid phase is specified according to the accuracy required, and the grid is then laid out as shown in Fig. A.2.1(a). The time step is specified as $\Delta t = (\tau_L/N_L)$ which ensures that the storage used by the programme remains constant throught the solution. The differential equations have already been derived, but for convenience are repeated here:-

$$\left.\frac{dc}{dz}\right)_I = -\frac{N}{L} \qquad (A.2.3)$$

$$\frac{d}{dz}\ell n p_c = -\frac{NP_T}{v_I p_c} \qquad (A.2.4)$$

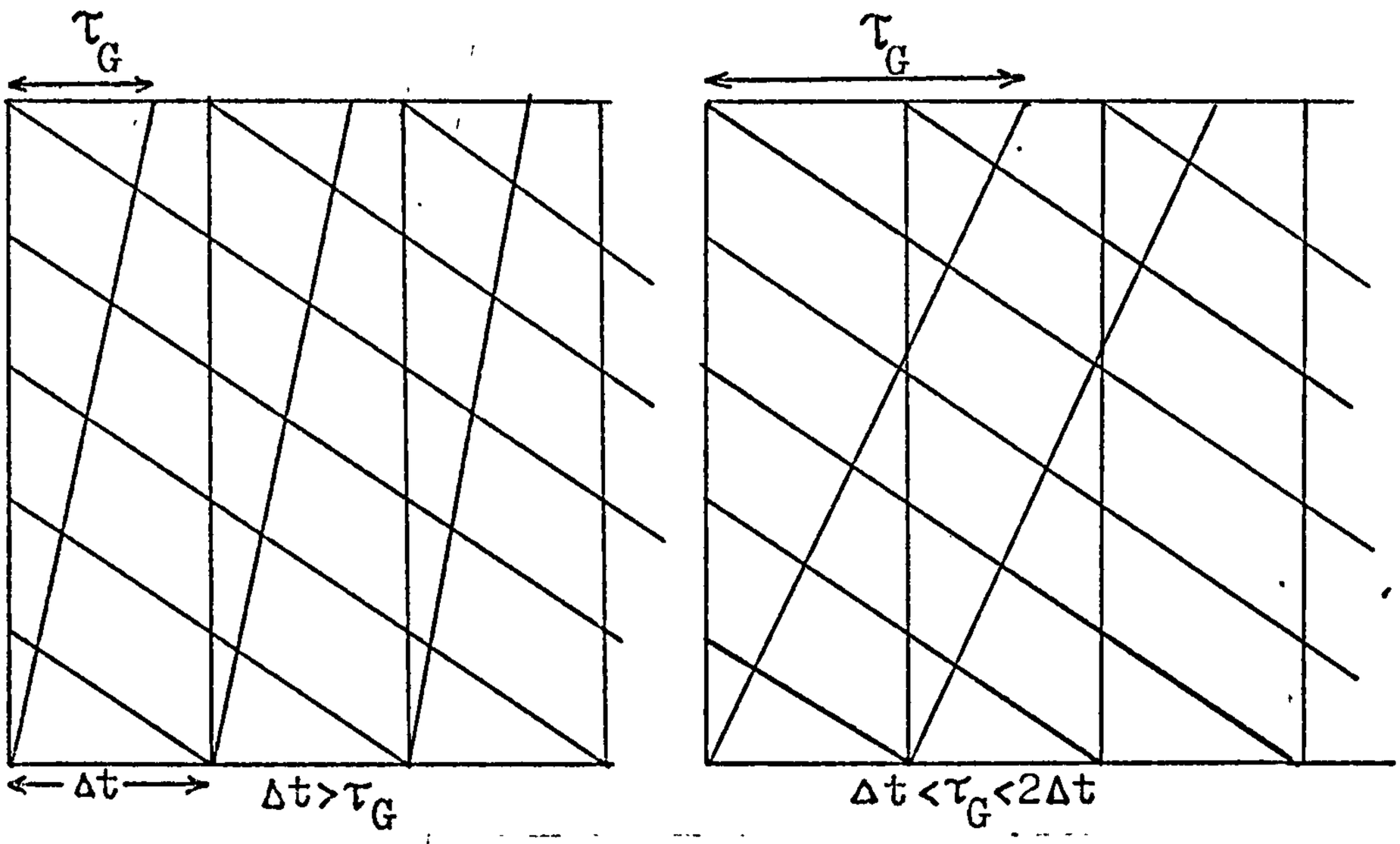


FIG.A.2.1.(A) LAYOUT OF GRID

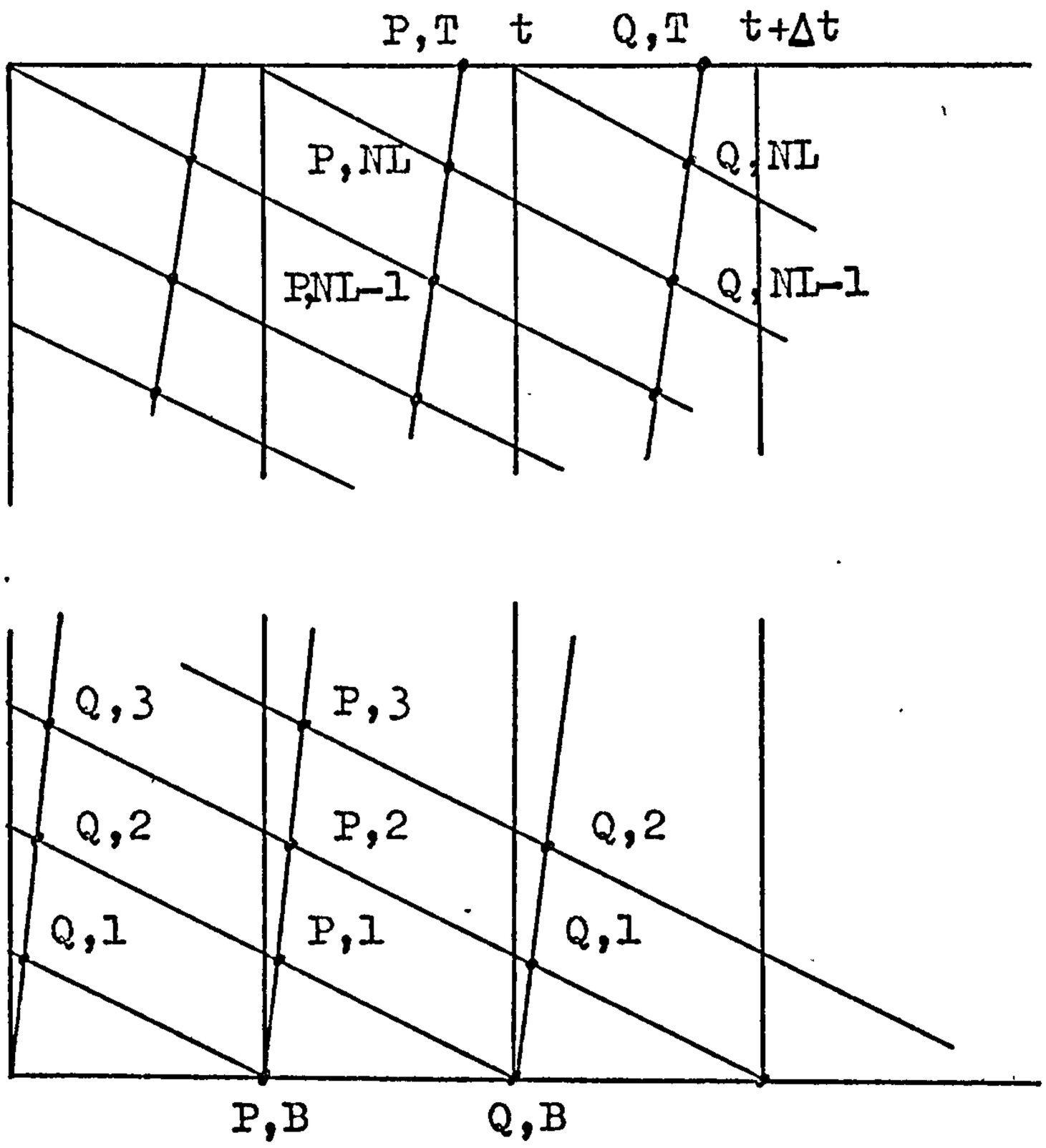


FIG.A.2.1.(B) USE OF SUBSCRIPTS

Values for the liquid and vapour composition are computed and stored along the gas phase characteristics at the points of intersection with the characteristics of the liquid phase. Simpson integration is used, wherever possible, along both sets of characteristics and this requires the storage of the two phase compositions along both the current and previous gas phase characteristics. The procedure used generally is to start at the bottom of a gas phase characteristic and to successively compute values for the two independent variables such that they both satisfy a Simpson integration formula along their relevant directions. Referring to the notation in Fig. A.2.1(b) this procedure involves the iterative solution of the two following equations:-

$$\ell np_c(Q,i) = \ell np_c(Q,i+2) + \frac{\Delta z'}{3}\{f_1(Q,i) + 4f_1(Q,i+1) + f_1(Q,i+2)\} \quad (A.2.5)$$

where $f_1(Q,i) = \frac{d}{dz}\ell np_c(Q,i)$

$$= -\frac{p_T}{v_I}\,\frac{N(p_c(Q,i),\ c(Q,i))}{p_c(Q,i)}$$

$$c(Q,i) = c(Q,i+2) + \frac{\Delta z'}{3}\{f_2(Q,i) + 4f_2(P,i+1) + f_2(Q,i+2)\} \quad (A.2.6)$$

where $f_2(Q,i) = \frac{d}{dz}\,c(Q,i) = -N(p_c(Q,i),c(Q;i))/L$

The height increment $\Delta z'$ used in (A.2.5) and (A.2.6) is given by

$$\Delta z' = \frac{\Delta z}{1-(\tau_G/\tau_L)} \quad (A.2.7)$$

where $\Delta z = Z/NL$

Direct substitution was tried and the solution always converged without problems, normally in one or two iterations. At the bottom of the gas phase characteristic the partial pressure is specified by the boundary condition, and so it is only ncessary to employ equation (A.2.6) to compute the exit liquid concentration. When a Simpson formula cannot be used because of an insufficient number of points before the one being calculated, a trapezoidal rule is used. This is the case for the calculation of the partial pressure at the first point within the column, and so equation (A.2.5) is replaced by:

$$\ell np_c(Q,1) = \ell np_c(Q,B) + \frac{\Delta z'}{2}\{f_1(Q,1) + f_1(Q,B)\} \qquad (A.2.8)$$

A similar procedure is used for the calculation of the liquid composition at the highest point:-

$$c(Q,NL) = c(t) + \frac{\Delta z'}{2}\{f_2(c(t),p_c(t)) + f_2(Q,NL)\} \qquad (A.2.9)$$

where $\Delta z' = Z - NL\Delta Z$ and $p_c(t)$ is found by extrapolation from the two previous values of the top partial pressure.

The exit partial pressure is calculated by solving:

$$\ell np_{cT} = \ell np_c(Q,NL) + \frac{\Delta z'}{2}\{f_1(c(t'),p_{cT}) + f_1(Q,NL)\} \qquad (A.2.10)$$

where $\Delta z'$ is the same as in (A.2.9) and the entry liquid composition $c(t')$ is obtained by interpolation from the entry liquid compositions at times t and $(t+\Delta t)$.

The whole procedure is initiated from the initial conditions which are specified as the phase compositions at time zero at the heights $i\Delta z$, $i = 0, N_L$. The first two steps are therefore to establish both the phase compositions along the first two gas phase characteristics, and a

trapezoidal formula is used for the liquid phase. Once these first two lines have been established the computation proceeds as described earlier.

The procedure can be conveniently programmed such that the elements of the arrays used for storage are correctly overwritten as the the computation proceeds.

2. Characteristic grid with varying liquid flow rate and zero gas phase hold up

The comprehensive model in section 2.8.1. employs for the solution of the liquid phase compositions a grid of characteristics which is dependent upon the liquid flow rate. There are no gas phase characteristics because of the assumption of zero gas phase hold up.

The layout of the grid is determined by the equation for hold up

$$\left(\frac{k_2}{A}\right) \frac{\partial L}{\partial z} = \frac{\partial L}{\partial t} \qquad \text{(A.2.11)}$$

and the characteristic direction arising from the transformation of the composition partial differential equation:

$$\left.\frac{dz}{dt}\right)_I = - \frac{L}{\phi_L A} = S \qquad \text{(A.2.12)}$$

together with the relevant initial and boundary conditions for equation (A.2.11) which are:

$$\left.\begin{aligned} L(z,0) &= L^0(z) \qquad t = 0 \\ L(Z,t) &= L_T(t) \qquad 0 \leq t < t_f \end{aligned}\right\} \qquad \text{(A.2.13)}$$

The fractional hold up is related to the flow rate by:

$$L = k_1 + k_2 \phi_L \qquad \text{(A.2.14)}$$

The parameter k_2 expresses the variation of liquid flow rate with hold up and consequently determines the rate of propagation of a change in liquid flow rate. The solution of equation (A.2.11) subject to the conditions (A.2.13) is

$$\left.\begin{aligned} &L(z,t) = L(Z,t') \text{ if } t' = t - (zA/k_2) > 0 \\ &L(z,t) = L(z',0) \text{ if } t' < 0 \\ &\text{and where } z' = z+(tk_2/A) \end{aligned}\right\} \quad (A.2.15)$$

The slope of the liquid phase characteristic, given by (A.2.12), can therefore be obtained at any point in the (z,t) plane.

The number of lines in the grid at any time instant is selected according to the accuracy required and the computational procedure is so arranged that this number remains constant throughout the solution. Because the grid is used in association with the analytic solution developed in 2.8.1. where the partial pressures and liquid compositions are numbered from the top downwards the same convention is adopted here. The programme computes and stores at each time instant in the solution the liquid flow rate, characteristic gradient and height for each of the characteristics. Fig. A.2.2. shows the simple case of a response to a step change in the inlet liquid flow rate; initially the lines are spaced at equal height increments, but as the solution proceeds the spacing of the lines changes as the disturbance propagates down the column.

For the calculation of the heights of each line at the end of a time step, the mean of the gradients at the start and finish of the time step is used. The step is selected such that a line leaves the grid at the end of the

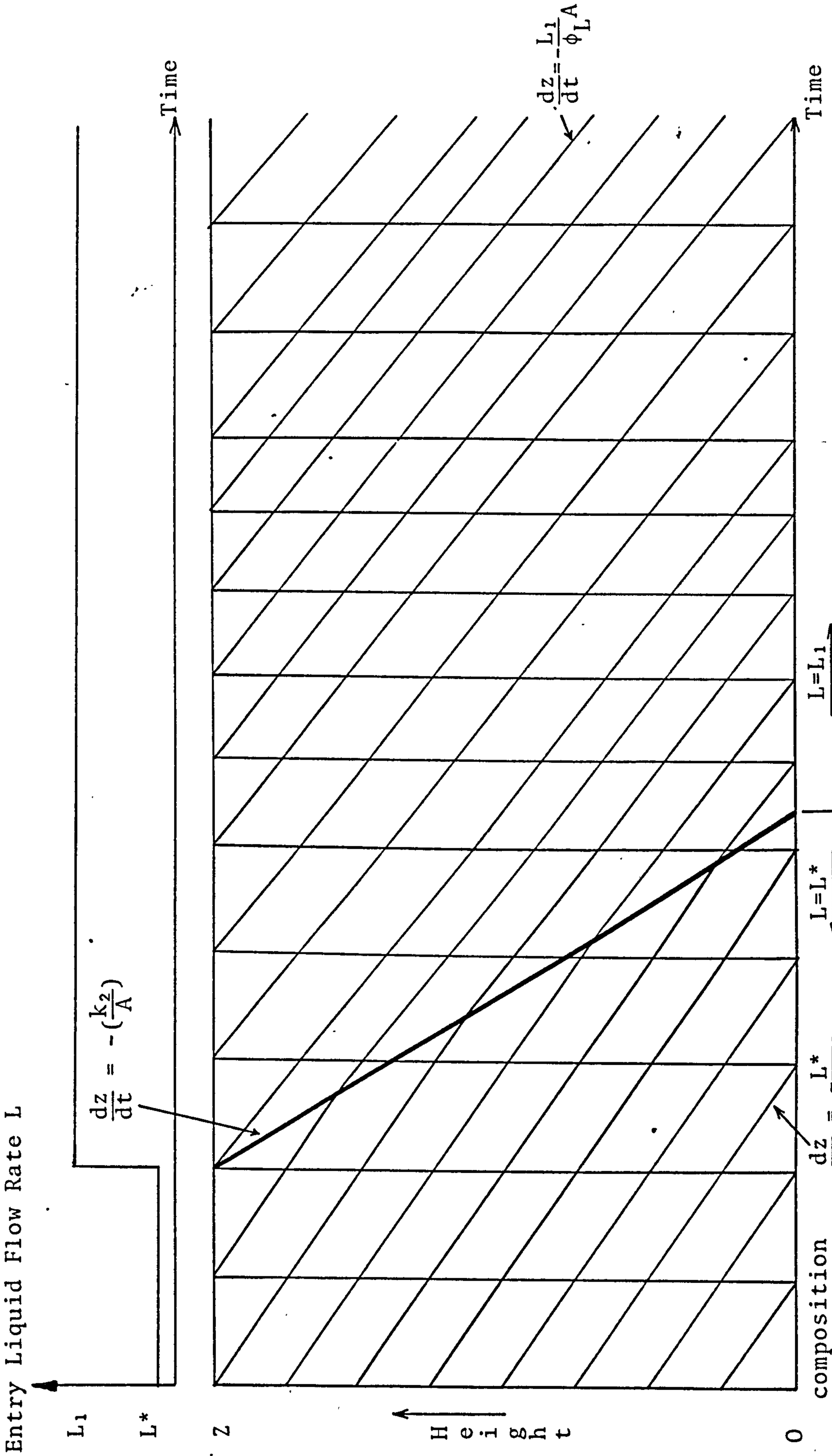


FIG.A.2.2. CONSTRUCTION OF CHARACTERISTIC GRID

time step, and because the gradient at this point is not initially known, an iteration is employed until the following equation is satisfied:

$$h_{NL}(t_0+\Delta t) = \tfrac{1}{2}(S_{NL}(t_0)+S_{NL}(t_0+\Delta t))\Delta t = 0 \qquad (A.2.16)$$

where $S_{NL}(t_0+\Delta t)$ is found by reference to equation (A.2.12) and the subscript NL denotes the characteristic line that leaves the solution at the end of the time step.

With the time step fixed the heights for each line at the end of the time step are calculated according to:

$$h_i(t_0+\Delta t) = h_i(t_0) + \tfrac{1}{2}(S_i(t_0) + S_i(t_0+\Delta t))$$

$$i = 1, NL-1 \qquad (A.2.17)$$

and again $S_i(t_0+\Delta t)$ is found by reference to (A.2.12)

The use of a mean gradient proved in practice to be satisfactory and the iteration used in equation (A.2.16) and (A.2.17) always converged very rapidly without problem.

Employment of this procedure implies that the time step is not altered until the disturbance reaches the bottom of the column, as shown in Fig. A.2.2. In practice this proved to be a good policy, even when more complex input disturbances were used.

It is interesting to consider the significance of the parameters k_1 and k_2 in relation to the propagation rates of flow and composition disturbances. Solving the linear flow hold up relationship for zero liquid flow rate gives

$$\phi_L = -(k_1/k_2) \qquad (A.2.18)$$

which is the static hold up: as a consequence it would be expected that the parameter k_1 is negative. Furthermore, a negative value of k_1 is obtained if the flow hold up

relationship (2.21) is linearised. The propagation rate of flow disturbances is dependent upon the variation of the operating hold up with liquid flow rate as expressed by the parameter k_2, and is independent of the static hold up. However, the propagation rate of composition disturbances is dependent upon the total hold up and therefore both parameters:

$$\frac{dz}{dt} = -\frac{L}{\phi_L A} = -\left(\frac{k_1 + k_2 \phi_L}{\phi_L A}\right) \qquad (A.2.19)$$

If the parameter k_1 is zero, implying no static hold up then both flow and composition disturbances propagate at the same rate, determined by (k_2/A). Under these conditions the characteristic grid is very simply constructed with a fixed time step and lines of gradient $-(k_2/A)$, and along each line the hold up remains constant at the initial value specified by the boundary condition at the top of the column. Obviously this is very simple to use, requiring only a very slight increase in computation from the case with constant liquid flow rate. In practice it may be found that the static hold up is either small or does not significantly affect the column dynamics in which case the propagation rates would be similar and the use of such a simple model would be justified.

3. Solution of the liquid and gas phase compositions in the general model

The general model uses the time instantaneous solution for the gas phase, described in Section 2.8.1, together with the partial differential equations for hold up and

composition which define the characteristic grid described in the previous section. The ordinary differential equation for composition that is integrated along each characteristic is:-

$$\left(\frac{dc}{dt}\right) = \frac{N}{A\phi_L}(p_c, c, T) \qquad (A.2.20)$$

A Runge Kutta procedure is employed, and the equation above is convenient to use because the time step is the same for all the equations at a particular instant; the alternative of using the differential equation written in terms of height would require extra computation. At a particular time instant the liquid composition and temperature profiles in the column are used by the time instantaneous gas phase solution to find the partial pressure and absorption rate at each of the heights required.

Because the height difference between points does not generally remain constant, the height increment Δs used in equation (2.91) has to be calculated from the respective points in the grid. At each point the absorption rate and liquid flow rate define the derivative to be used for the composition differential equation, and so the Runge Kutta procedure can be applied without difficulty. The Runge Kutta procedure requires the evaluation of derivatives at a mid-point, and for this purpose a mid-point in time is constructed as shown in Fig. A.2.3. The inlet boundary conditions at the top and bottom of the column are known, and appropriate mean height increments and liquid phase compositions are used in the solution for the gas phase.

The entire procedure at each time step for solution

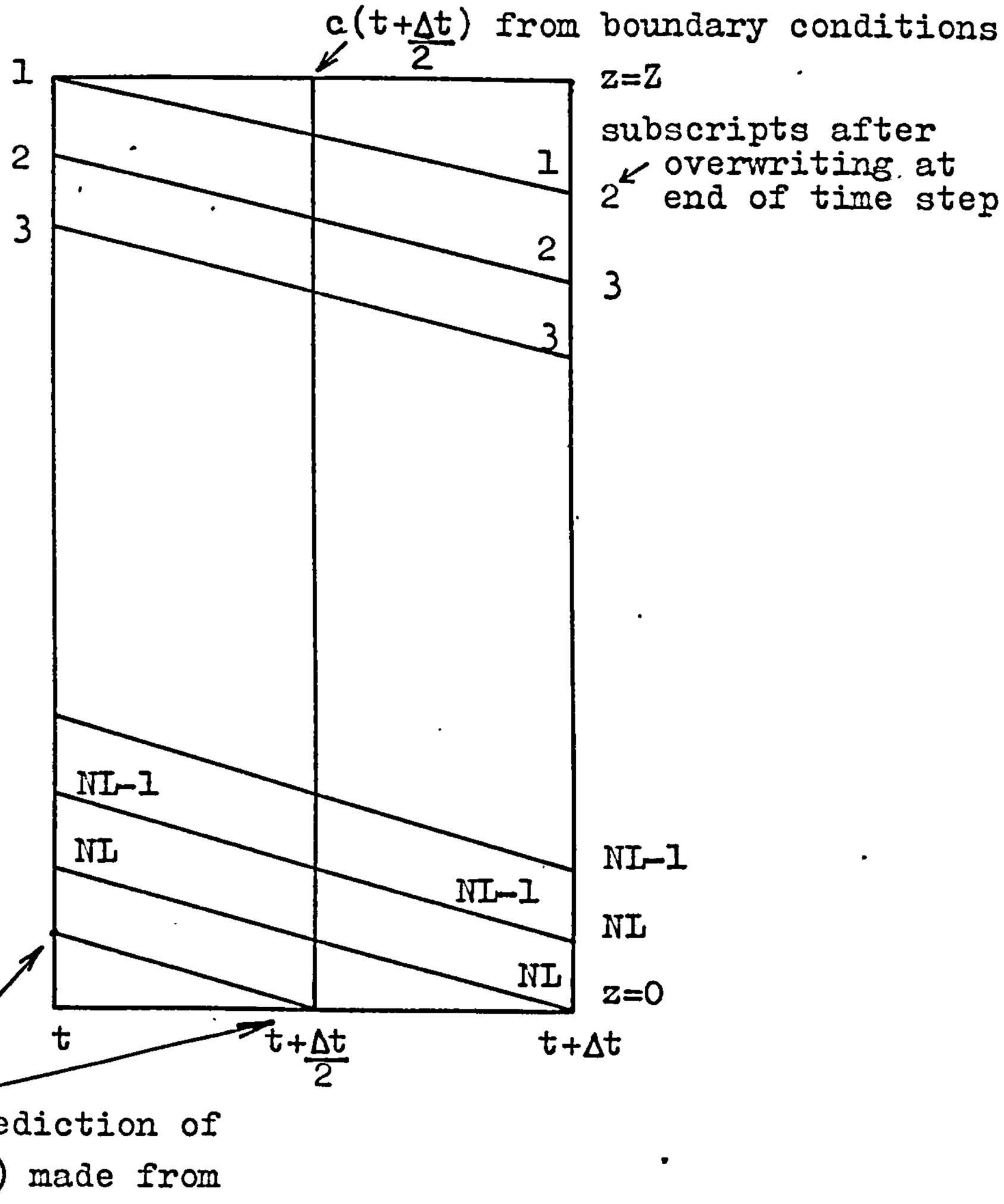


FIG.A.2.3. CONSTRUCTION OF GRID FOR GENERAL MODEL

of the general model, including the layout of the grid, is shown in flow chart form in Fig. A.2.4. The gas phase solution employed can be with or without dispersion, and using either the Kohl or reaction models. The procedure for calculating the liquid phase compositions is explicit, contrary to the case described in the first section of this Appendix.

Start of new time step t=t
Composition, temperature and absorption rate profiles known.
Height and gradient of characteristic known at each grid point.

↓

Layout of grid for current time step:

1. Compute time step Δt using equation A.2.16.
2. From heights at t and with reference to the entry liquid flow rate compute heights and gradient of liquid characteristics at $t + \Delta t$.
3. Compute height increments Δs to be used in the time instantaneous gas phase solution at times $t+(\Delta t/2)$, $t+\Delta t$

↓

Runge Kutta integration of equation (A.2.20) along each characteristic from t to $t+\Delta t$:

1. Find entry liquid and gas phase compositions at $t+(\Delta t/2)$ from boundary conditions.
2. Predict composition and temperature profile at $t+(\Delta t/2)$.
3. Solve for partial pressure profile and absorption at each grid point at time $t+(\Delta t/2)$; equation (2.91).
4. Repeat steps 2,3 with new prediction of composition profile at $t+(\Delta t/2)$ by standard Runge Kutta procedure.
5. Predict composition and temperature profile at time $t+\Delta t$.
6. Solve for partial pressure profile at $t+\Delta t$ using (2.91).
7. Runge Kutta prediction of final values for temperature and composition at $t+\Delta t$.
8. Solve for partial pressure and absorption rate profile at $t+\Delta t$, using equation (2.91).
9. Overwrite arrays for liquid composition and temperature with new values computed at $t+\Delta t$

FIG. A.2.4 COMPUTATIONAL PROCEDURE

APPENDIX 3. PROCEDURE FOR ON-LINE ESTIMATION OF THE ABSORPTION RATE PARAMETERS

The proposed procedure employs a Kalman or suitable recursive filter to estimate the absorption rate parameters from the following plant measurement:-

i) liquid and vapour flow rates;

ii) inlet partial pressure of carbon dioxide and the total pressure in the column; it is assumed that the inlet partial pressure is always measured.

iii) inlet (or outlet) liquid carbonation ratio

iv) the liquid temperature profile which consists of the temperature at the inlet and those below each packing section;

v) a partial pressure of carbon dioxide; the gas analyser can be used to analyse a sample taken at the top of any of the five packing sections.

The model parameters are updated by comparison of the predicted and observed values of the partial pressures and liquid temperatures leaving each packing section. With only one gas analyser available for use on the column only one partial pressure comparison can be made at each observation; the complete partial pressure profile may be built up over several observations. The measurement vector to be used at each observation is:

$$\underline{Y} = (T_i, p_j)^T \qquad i = 1,5 \text{ and } j \text{ can be selected from 1 to 5} \qquad \text{(A.3.1)}$$

The remaining measurements such as the flow rates and inlet conditions are taken in order to make the model

predictions, and it is sensible that these should be filtered or smoothed by some suitable procedure before being used.

The model parameters are elements of the state vector $\underline{x}$ which, for the single parameter absorption rate model proposed in Section 2.6.5. is:-

$$\underline{x} = (K', \Delta E) \qquad (A.3.2.)$$

It is assumed here, for generality, that the absorption within the column is determined by a model incorporating gas phase dispersion and that the dispersion coefficient is known from other experiments. The model equations are:

$$-\left(\frac{DA}{RT_G'}\right)\frac{d^2p_c}{ds^2} - \left(\frac{v_I}{p_T}\right)\frac{dp_c}{ds} + N = 0 \qquad (A.3.3)$$

$$\text{where } N = A\,K'\sqrt{M_m - 2c}\;p_c \qquad (A.3.4)$$

$$\text{and} \quad c = \left(\frac{v_I}{LP_T}\right)(p_c - p_{cT}) + c_T \qquad (A.3.5)$$

$$T = \left(\frac{\Delta E}{\rho c_p}\,\frac{v_I}{Lp_T}\right)(p_c - p_{cT}) + T_T \qquad (A.3.6)$$

with boundary conditions:

$$\frac{dp_c}{ds} = 0 \quad p_c = p_{cT} \quad \text{at } s = 0 \qquad (A.3.7)$$

$$p_{cB} = p_c + \left(\frac{DA}{RT_G'}\right)\left(\frac{p_T}{v_I}\right)\frac{dp_c}{ds} \quad \text{at } s = S \qquad (A.3.8)$$

At each update equation (A.3.3) is solved with the current model parameters subject to the measured inlet liquid and gas compositions to give the predicted values of partial pressure and liquid temperature at the discrete heights corresponding to those of the measurements. The technique for solving this problem is described in Section 2.8.1.

In addition the filter requires the Jacobian matrix $\partial \underline{Y}/\partial \underline{x}$ and the equations for computing the elements of this matrix are now derived. A finite difference technique could be used, but this would require repeated integration to solve the boundary condition problem and the accuracy of the technique is questionable. Instead a variational analysis is carried out and a set of differential equations derived to describe the first order variation in the liquid and vapour composition profiles with the model parameters. The variation of the partial pressure profile with the top partial pressure is also required as the latter is varied to satisfy the boundary condition (A.3.8) at the bottom of the column.

The second order differential equation is transformed to two first order equations:

$$\underline{V} = \begin{pmatrix} U \\ p_c \end{pmatrix} \qquad \text{where } \frac{dp_c}{ds} = U \tag{A.3.9}$$

$$\text{so } \frac{d}{ds}\underline{V} = \frac{d}{ds}\begin{pmatrix} U \\ p_c \end{pmatrix} = \begin{pmatrix} \frac{R'T_G}{DA}\left\{-\left(\frac{v_I}{p_T}\right)U + N\right\} \\ U \end{pmatrix} = \underline{f} \tag{A.3.10}$$

$$\text{with boundary conditions } \underline{V} = \underline{V}_o = \begin{pmatrix} 0 \\ p_{cT} \end{pmatrix} \quad s = 0 \tag{A.3.11}$$

$$p_{cB} = p_c(S) + \left(\frac{DA}{R'T_G}\right)\left(\frac{p_T}{v_I}\right) U(S) \quad s = S \tag{A.3.12}$$

Equation (A.3.10) is differentiated with respect to a model parameter x_j to obtain a differential equation defining the first order variation of $\underline{V}$ at any particular height. This differentiation is carried out with the top partial pressure held constant:

$$\frac{d}{ds}\frac{\partial}{\partial x_j}\underline{V} = \frac{\partial}{\partial \underline{V}}\underline{f}\,\frac{\partial}{\partial x_j}\underline{V} + \frac{\partial}{\partial x_j}\underline{f} \qquad \delta p_{cT} = 0 \qquad \text{(A.3.13)}$$

Similarly, equation (A.3.10) is differentiated with respect to the top partial pressure p_{cT} with the model parameters held constant to give a second equation:

$$\frac{d}{ds}\frac{\partial}{\partial p_{cT}}\underline{V} = \frac{\partial}{\partial \underline{V}}\underline{f}\,\frac{\partial}{\partial p_{cT}}\underline{V} + \frac{\partial}{\partial p_{cT}}\underline{f} \qquad \delta \underline{x} = 0 \qquad \text{(A.3.14)}$$

The Jacobian matrix of the system common to both (A.3.13) and (A.3.14) is:

$$\frac{\partial}{\partial \underline{V}}\underline{f} = \begin{pmatrix} -\frac{R'T_G}{DA}\frac{v_I}{p_T}, & -\left(\frac{R'T_G}{DA}\right)\frac{v_I}{p_T}AK'\sqrt{M_m-2c} \\ 1, & 0 \end{pmatrix} \qquad \text{(A.3.15)}$$

For the single parameter model the solution of the differential equation (A.3.10) is independent of the heat of reaction ΔE so that there is only one equation of type (A.3.13). The partial derivatives of partial pressure with respect to the heat of reaction are consequently zero. The final term in equation (A.3.13) is in this case:

$$\frac{\partial f}{\partial K'} = \begin{pmatrix} -\left(\frac{R'T_G}{DA}\right)A\sqrt{M_m-2c}\;p_c \end{pmatrix} \qquad \text{(A.3.16)}$$

and the boundary condition for (A.3.13) is $(0,0)^T$.

The final term in equation (A.3.14) is

$$\frac{\partial}{\partial p_{cT}}\underline{f} = \begin{pmatrix} -\left(\frac{R'T_G}{DA}\right)\left(\frac{v_I}{p_{cT}}\right)\,A\,K'\frac{\partial}{\partial p_{cT}}\sqrt{M_m-2c} \\ 0 \end{pmatrix} \qquad \text{(A.3.17)}$$

and employing equation (A.3.4)

$$\frac{\partial}{\partial p_{cT}}\sqrt{M_m-2c} = \frac{v_I}{Lp_T}\,\frac{1}{\sqrt{M_m-2c}} \qquad \text{(A.3.18)}$$

The initial condition for (A.3.14) is:

$$\frac{\partial}{\partial p_{cT}} \quad V_o = \begin{pmatrix} 0 \\ 1 \end{pmatrix}$$

Equations (A.3.13) and (A.3.14) are integrated to give the derivatives $(\partial p_c/\partial x_j)_{p_{cT}}$ and $(\partial p_c/\partial p_{cT})_x$ at the required column heights; the subscripts denoting the quantities held constant. At a particular height in the column the change in partial pressure due to changes in a model parameter x_j and the top partial pressure is :

$$\delta p_c = \left(\frac{\partial p_c}{\partial x_j}\right)_{p_{cT}} \delta x_j + \left(\frac{\partial p_c}{\partial p_{cT}}\right)_x \delta p_{cT} \qquad \text{(A.3.19)}$$

where the derivatives are the solutions to (A.3.13) and (A.3.14) at height z. The relationship between δx_j and δp_{cT} is obtained from the boundary condition (A.3.12) which must still be satisfied so:

$$0 = \left(\frac{\partial p_c}{\partial x_j}\right)_{p_{cT}} \delta x_j + \left(\frac{\partial p_c}{\partial p_{cT}}\right)_x \delta p_{cT}$$

$$+ \left(\frac{DA}{RT_G}\right)\left(\frac{p_T}{v_I}\right)\left[\left(\frac{\partial U}{\partial x_j}\right)_{p_{cT}} \delta x_j + \left(\frac{\partial U}{\partial p_{cT}}\right)_x \delta p_{cT}\right] \qquad \text{(A.3.20)}$$

where all the derivatives are the solution values at s = S.

The variation in top partial pressure is eliminated between (A.3.19) and (A.3.20) and the limit taken to give

$$\left(\frac{\partial p_c}{\partial x_j}\right) = \left(\frac{\partial p_c}{\partial x_j}\right)_{p_{cT}} - \left(\frac{\partial p_c}{\partial p_{cT}}\right) \frac{\left[\frac{\partial p_c}{\partial x_j}(S) + \left(\frac{DA}{RT_G}\frac{p_T}{v_I}\right)\frac{\partial U}{\partial x_j}(S)\right]}{\left[\frac{\partial p_c}{\partial p_{cT}}(S) + \left(\frac{DA}{RT_G}\frac{p_T}{v_I}\right)\frac{\partial U}{\partial p_{cT}}(S)\right]} \qquad \text{(A.3.21)}$$

where the differential on the left hand side is the one required as an element of the matrix $\partial \underline{Y}/\partial \underline{x}$.

The partial derivative of the liquid temperatures with respect to the heat of reaction is obtained from equation (A.3.6):

$$\frac{\partial T}{\partial \Delta E} = \left(\frac{v_I}{\rho c_p L p_T}\right)(p_c - p_{cT}) \qquad (A.3.22)$$

The partial derivative with respect to the absorption rate parameter K' is found by a procedure identical in principle to that just followed for obtaining equation (A.3.21). The variation in temperature with the model parameter x_j and top partial pressure is

$$\delta T = \left(\frac{\Delta E\ v_I}{\rho c_p L p_T}\right)\left\{\left(\frac{\partial p_c}{\partial x_j}\right)_{p_{cT}} \delta x_j + \left(\frac{\partial p_c}{\partial p_{cT}} - 1\right)_x \delta p_{cT}\right\} \qquad (A.3.23)$$

Equation (A.3.20) is again used to eliminate δp_{cT} and the limit taken to give

$$\frac{\partial T}{\partial x_j} = \left(\frac{\Delta E\ v_I}{\rho c_p L p_T}\right)\left[\left(\frac{\partial p_c}{\partial x_j}\right)_{p_{cT}} + \left\{1 - \left(1/\left(\frac{\partial p_c}{\partial p_{cT}}\right)\right)\right\}\left\{\left(\frac{\partial p_c}{\partial x_j}\right) - \left(\frac{\partial p_c}{\partial x_j}\right)_{p_{cT}}\right\}\right] \qquad (A.3.24)$$

where equation (A.3.21) has been used to allow a simpler expression.

In summary, for the single parameter absorption model, the procedure requires the integration of two further differential equations, (A.3.13) and (A.3.14) and then the required elements in the matrix $\partial \underline{Y}/\partial \underline{x}$ are obtained from equations (A.3.21) and (A.3.24). The differential equations have only to be integrated once to give the partial derivatives at any one or all of the points in the column.

In section 2.6.5. it was stated that the absorption rate model may be extended to the form:

$$N = A \exp(K_5 + \frac{K_6}{T}) \sqrt{c_0}\ p_c \qquad (A.3.25)$$

and the parameter vector is then $\underline{x} = [K_5, K_6, \Delta E]$.

A similar procedure may be used to obtain the elements of the matrix $\partial \underline{Y}/\partial \underline{x}$ except that in this case the heat of reaction will influence the absorption profile and consequently two equations of the form (A.3.13) exist and equation (A.3.15) has to be modified. The modification is obtained from equation (A.3.23) and utilises

$$\delta T = (\frac{v_I}{\rho c_p L p_T})(p_c - p_{cT})\delta\Delta E + (\frac{v_I\ \Delta E}{\rho c_p L p_T})[(\frac{\partial p_c}{\partial E})_{p_{cT}}\ \delta\Delta E + (\frac{\partial p_c}{\partial p_{cT}} - 1)_x \delta p_{cT}] \qquad (A.3.26)$$

The precise form of the filter used and the measurements used will depend upon the application and plant experience. At the outset there are two possible applications: initially simply to find values for the parameters and verify the form of the model, and secondly to update the model parameters so that the model gives a good representation of the column in the neighbourhood of the current operating conditions. In the latter case it will be necessary to decide the location of the gas analyser or a policy for a sequence of different measurements such that its analysis together with the temperature profile gives the best indication of the current model parameters. However, whatever sort of filter is used the equations presented here form the model dependent part of the filter and show that the derivatives required can be obtained fairly simply.

APPENDIX 4. PARAMETERS FOR THE DESORPTION COLUMN MODEL

TABLE A.4.1. COLUMN DETAILS

Column diameter	.252 m
Bubbling (tray area)	0.0245m^2
Hole area	0.00203m^2
Downcomer area	0.0219m^2
Weir height	0.0381m
Weir length	0.212m

TABLE A.4.2. STEADY STATE HOLD UP OF LIQUID (TYPICAL VALUES)

Tray hold up W_T	0.94×10^{-3} m^3
Downcomer hold up W_D	0.24×10^{-2} m^3
Total plate hold up W_p	0.334×10^{-2} m^3
Liquid flow rate off tray	0.33×10^{-3} m^3/s
Depth of clear liquid on tray	0.0384 m
Vapour rate leaving tray	0.18×10^{-3} kmole/s
Reboiler hold up (column side including column bottoms)	0.0748 m^3
Condenser hold up	0.53×10^{-2} m^3

TABLE A.4.3. THERMODYNAMIC PROPERTIES

Heat of decomposition	73400 kJ/kmole
Latent heat of water	45400 kJ/kmole
Specific heat of liquid phase	4200 kJ/m^3°C
Enthalpy of steam	2800 kJ/kg

TABLE A.4.4. PARAMETERS FOR THE REBOILER

Volume of steam chest	0.0724m^3
Heat transfer area A_R	6.86m^2
Tube mass H_R	83.3kg
Condensation heat transfer coefficient h_c	0.7kW/m^2°C
Coefficient for heat transfer to liquid h_v	0.4kW/m^2°C

TABLE A.4.5. PARAMETERS FOR THE CONDENSER

Heat transfer area A_c	3.62m^2
Gas phase mass transfer coefficient k_G	3.78×10^{-5}
Sensible heat transfer coefficient h_c	0.124kW/m^2°C